

Cover Page



Universiteit Leiden



The handle <http://hdl.handle.net/1887/29988> holds various files of this Leiden University dissertation

Author: Wezel, Anouk

Title: Innate immune modulation in atherosclerosis and vascular remodelling

Issue Date: 2014-12-11

INNATE IMMUNE MODULATION IN ATHEROSCLEROSIS AND VASCULAR REMODELLING

Anouk Wezel

Innate immune modulation in atherosclerosis and vascular remodelling

Anouk Wezel

Leiden Academic Center for Drug Research and Department of Surgery,
LUMC, 11 december 2014

Cover design: Dante Tatipata

ISBN: 978-94-6203-693-2

Printing: Wöhrmann Print Service

Proefschrift Leiden

Met literatuur opgave - met samenvatting in het Nederlands

© 2014, Anouk Wezel

No part of this thesis may be reproduced or transmitted in any form or by any means, without permission of the author.

INNATE IMMUNE MODULATION IN ATHEROSCLEROSIS AND VASCULAR REMODELLING

PROEFSCHRIFT

ter verkrijging van
de graad van Doctor aan de Universiteit Leiden,
op gezag van Rector Magnificus prof. mr. C.J.J.M. Stolker,
volgens besluit van het College voor Promoties
te verdedigen op donderdag 11 december 2014
klokke 13.45 uur

door

Anouk Wezel

Geboren te Zaanstad
in 1986

Promotiecommissie

Promotoren: Prof. dr. J. Kuiper
Prof. dr. P.H.A. Quax
Co-promotor: Dr. I. Bot

Overige leden: Prof. dr. P. Kovanen (Wihuri Research Institute)
Prof. dr. A.J. Rabelink (LUMC)
Prof. dr. J.F. Hamming (LUMC)
Prof. dr. P.H. van der Graaf (LACDR)

The research described in this thesis was supported by a grant of the Dutch Heart Foundation (DHF 2010-B029) and was performed at the Division of Biopharmaceutics, Leiden Academic Center for Drug Research, Leiden University, Leiden, The Netherlands, and the department of of Surgery, Leiden University Medical Center, Leiden, The Netherlands. Financial support by the Dutch Heart Foundation for publication of this thesis is gratefully acknowledged.

The realization of this thesis was also financially supported by:

- LACDR
- Leiden University
- Chipsoft
- Greiner Bio-One

Measure what can be measured, and make
measurable what cannot be measured

-Galileo Galilei-

Aan mijn ouders

Table of contents

Chapter 1	General introduction	9
Chapter 2	The role of mast cells in atherosclerosis <i>Hämostaseologie, in press</i>	37
Chapter 3	Complement factor C5a as mast cell activator mediates vascular remodelling in vein graft disease <i>Cardiovasc Res. 2013; 97: 311-20</i>	53
Chapter 4	Complement factor C5a induces atherosclerotic plaque disruptions <i>J Cell Mol Med. 2014; 18: 2020-30.</i>	75
Chapter 5	Mast cells mediate neutrophil recruitment during atherosclerotic plaque progression <i>Submitted for publication</i>	95
Chapter 6	RP105 deficiency aggravates vein graft disease and lesion instability via increased inflammation and mast cell activation <i>Submitted for publication</i>	111
Chapter 7	RP105 deficiency attenuates early atherosclerosis via decreased monocyte influx in a CCR2 dependent manner <i>Conditionally accepted by Atherosclerosis</i>	131
Chapter 8	Inhibition of microRNA-494 reduces atherosclerotic lesion development and increases plaque stability <i>Submitted for publication</i>	153
Chapter 9	General summary and perspectives	179
	Nederlandse samenvatting	189
	Curriculum Vitae	197
	Publications	199

Chapter 1

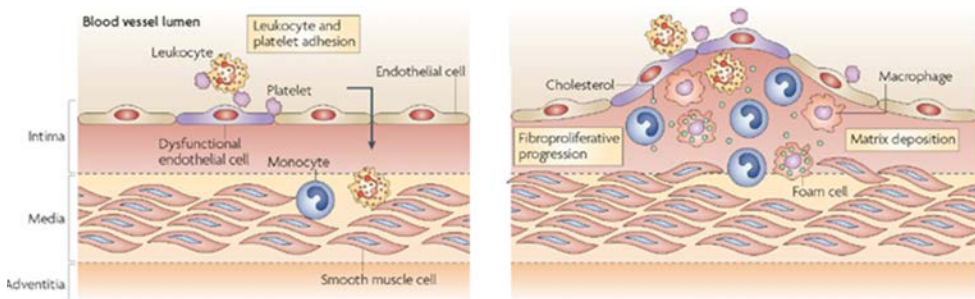
General Introduction

Atherosclerosis

Atherosclerosis is a chronic, multifactorial disease in which multiple inflammatory processes and modifications in cholesterol homeostasis play a key role. The formation of atherosclerotic lesions in the innermost layer of the vessel wall, the intima, occurs at predisposed sites in the arterial tree located near branch points and inner curvatures¹. These asymmetric, focal thickenings in the vessel wall consist of lipids, debris and various inflammatory cells. Rupture of an advanced atherosclerotic plaque can result in thrombus formation, which may occlude the blood vessel and lead to severe cardiovascular complications. In fact, atherosclerosis is the major cause of cardiovascular diseases (CVD) such as peripheral ischemia, myocardial infarction and stroke². Pre-emptive therapeutic options include the use of statins and antihypertensive drugs, also, lifestyle changes such as smoking cessation are recommended, which reflects the multifactorial nature of the disease³. Despite an improved treatment, CVD are still responsible for 1 in every 4 deaths in the Netherlands⁴. It is therefore important to identify new therapeutic targets to prevent the initiation, growth and rupture of an atherosclerotic plaque.

Early atherosclerosis

Already early in life, around the age of 20 to 30, the first signs of atherosclerosis are present in the vessel wall, without any clinical manifestations yet⁵. The initiation of these early atherosclerotic plaques, also referred to as 'fatty streaks', starts at sites of damaged or activated endothelium. Activated endothelial cells up-regulate the expression of several adhesion molecules, such as ICAM-1, VCAM-1 and selectins, thereby causing rolling and subsequent adherence of monocytes and other leukocyte subtypes⁶. These leukocytes are subsequently stimulated to migrate through the endothelial junctions by combined actions of PECAM-1 and various chemokines produced in the intima. Once present in the intima, monocytes differentiate into macrophages, which then take up lipids via their scavenger

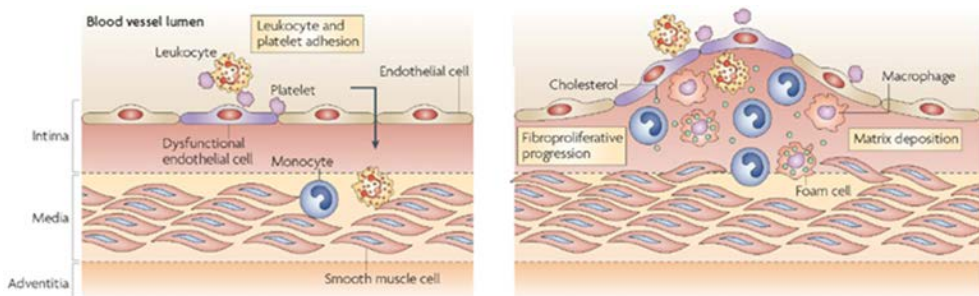


During the initiation of atherosclerosis, leukocytes adhere to the activated endothelium and subsequently migrate into the intima (left panel). Gradual intimal thickening caused by the accumulation of lipid-laden macrophages (foam cells) leads to the formation of fatty streaks (right panel). Adapted and modified from Weber et al. Nat Rev Immunol 2008;8:802-15.

receptors and transform into foam cells. Early fatty streaks may disappear again in time or eventually progress to advanced atherosclerotic lesions⁷.

Advanced atherosclerosis

Growth of a plaque is caused by the continued influx and activation of inflammatory cells such as monocytes, T cells and mast cells. Several endogenous ligands in the lesion, such as oxidized LDL and damage associated molecular patterns (DAMPs) are able to activate immune cells via pattern recognition receptors such as Toll-like receptors (TLRs), causing them to release various cytokines and chemokines thereby amplifying the inflammatory process⁸. In addition, secreted cytokines and growth factors induce a phenotypic switch in smooth muscle cells from the media, from a resting contractile state into a proliferative state^{9,10}. These smooth muscle cells then migrate into the intima where they produce collagen and other extracellular matrix components, which results in the formation of a fibrous cap. Inflammation, hypoxia and excessive protease activity in the plaque can promote cellular apoptosis, leading to the formation of a necrotic core underneath the fibrous cap. These advanced atherosclerotic plaques do not necessarily lead to clinical events, as lesions containing a thick fibrous cap and preserved lumen area may remain stable for years without apparent clinical manifestations¹¹.



Impaired clearance of apoptotic cells results in the formation of a necrotic core, which is covered by a fibrous cap. Multiple immune cells and leaky neovessels present in the plaque contribute to the inflammation (left panel). Rupture of the fibrous cap leads to exposure of the necrotic core to the blood, resulting in thrombus formation (right panel). Adapted and modified from Weber *et al.* Nat Rev Immunol 2008;8:802-15.

Atherosclerotic plaque destabilization

Unstable atherosclerotic lesions have been extensively described based on histology and plaque morphology^{11,12}. A typical unstable lesion consists of a large necrotic core, covered by a thin fibrous cap. A high density of leaky neovessels derived from the adventitial *vasa vasorum* contributes to increased leukocyte infiltration. The inflammatory cell content is high, in particular at the rupture-prone shoulder regions of the plaque¹³. Thinning of the fibrous cap is the result of smooth muscle cell apoptosis, which may be caused by for example chymase derived from the mast cell¹⁴ or by complement component C5a¹⁵. Also, matrix

metalloproteinases (MMPs) impair the integrity of the fibrous cap due to increased breakdown of the collagen content. Eventually, rupture (or erosion) of the cap may occur, leading to exposure of the pro-thrombotic necrotic core to the blood flow¹⁶. Subsequent thrombus formation can result in either distal embolization or in incorporated lesional thrombi, thereby adding to the plaque burden¹⁷.

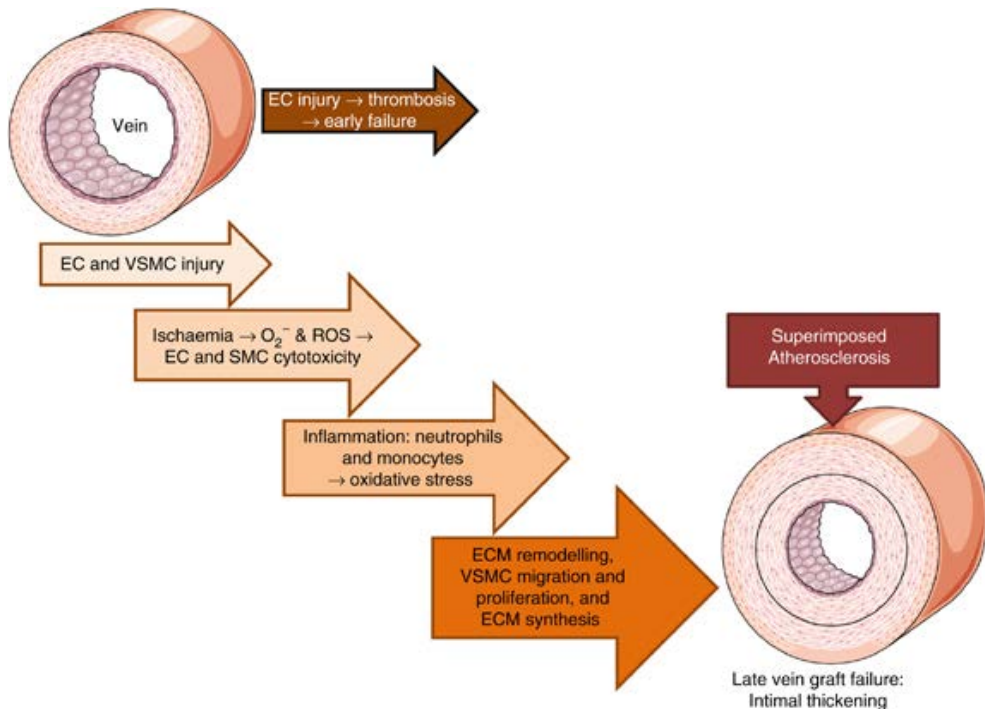
Vascular intervention techniques

Various surgical techniques, such as percutaneous transluminal angioplasty (PTA), stenting, atherectomy and placement of bypass conduits have been developed in order to treat or prevent atherosclerotic complications. During PTA, a balloon is inserted with the use of a catheter into the blood vessel and inflated at the site of the atherosclerotic lesion. The plaque is then compressed into the vessel wall, thereby widening the lumen and increasing blood flow. PTA is often combined with stenting, in which a small metal tube is placed at the site of the narrowed artery in order to maintain the appropriate lumen area. During atherectomy a catheter with a sharp blade is utilized to discard the atherosclerotic plaque from the arteries, this may also be done in an open surgical procedure referred to as endarterectomy. Finally, bypassing the blocked artery with either arterial or venous conduits is also a commonly used surgical treatment for atherosclerosis. Unfortunately, all of the above-mentioned techniques have their drawbacks, severely impairing the success rate of these operations. Damage to the vessel wall induced by atherectomy, balloon angioplasty or stenting generates a local inflammatory reaction, which results in restenosis, caused by accelerated neointimal formation. Also, excessive intimal hyperplasia occurs in bypass segments, which may lead to failure of the graft. Still, venous bypass grafts are commonly used due to their easy accessibility and the advantage of their long length, making it possible to bypass multiple atherosclerotic lesions¹⁸.

Vein graft disease

Vein graft disease (VGD) can be divided in early graft failure, due to thrombosis or technical complications, or in midterm to late failure, caused by atherosclerosis and intimal hyperplasia¹⁹. After one year, already 15-20% of the venous bypass grafts fail, which is increased up to 60% after ten years²⁰⁻²². Placement of a vein in the arterial circulation, with a corresponding high blood pressure, results in immediate endothelial damage of the vein graft. This is followed by fibrin depositions, platelet adhesion and leukocyte transmigration into the vessel wall in the first week after the operation²³. Smooth muscle cells from the media then

start to proliferate and migrate into the intima, which is necessary for the strength of the vein graft. However, excessive smooth muscle cell proliferation contributes to typical hyperplasia of the vessel wall. Complete occlusion of the graft may eventually be caused by intimal hyperplasia, or because rupture of the vein graft lesion results in thrombosis²⁴.



Following endothelial cell damage after vein graft surgery, immediate failure of the graft may be caused by occlusive thrombosis. Late graft failure may be the result of excessive smooth muscle cell proliferation, inflammation and extracellular matrix deposition, leading to decreased blood flow due to intimal thickening. Adapted from Wan *et al.* Gene Ther. 2012;19:630-6.

Murine models for atherosclerosis and vein graft disease

In order to study the mechanisms behind the complex, multifactorial nature of atherosclerosis and vein graft disease, the use of animal models is indispensable. Mice are the most commonly used animals for these experiments due to various advantages, such as their short breeding time and their well-known genetic background. Also, the execution of transgenic studies and specific gene targeting is possible in murine models. However, mice are highly resistant to atherosclerosis, even when they are fed a high cholesterol diet²⁵. Therefore, apoE knockout (apoE^{-/-}) mice have been generated by inactivating the apolipoprotein E gene, which results in high VLDL and LDL plasma levels with early atherosclerotic lesion formation in the aortic root. These mice will develop advanced atherosclerotic

plaques²⁶ when placed on a “western type diet” containing fat and cholesterol. In contrast to the apoE^{-/-} mice, LDL receptor deficient mice (LDLR^{-/-}) do not develop atherosclerosis under basal conditions. However, LDLR^{-/-} mice are very responsive to high cholesterol diet feeding, resulting in the formation of atherosclerotic lesions when fed for example a western type diet^{27,28}.

Collar model

Rapid, site-specific atherosclerotic lesions can be induced by placing perivascular collars in apoE^{-/-} or LDLR^{-/-} mice on a western type diet. In this experimental setup, nonconstrictive collars prepared from silastic tubes are placed around both common carotid arteries. Disturbed flow at the proximal site of the collar coincides with a downregulation of Krüppel-like factor 2 (KLF2), an endothelial transcription factor regulated by shear stress²⁹, while the adhesion molecules ICAM-1 and VCAM-1 are strongly upregulated²⁵. These hemodynamic changes, combined with a western type diet, result in advanced atherosclerotic lesions after 4 weeks.

Vein graft model

The most widely used experimental model for vein graft disease is introduced by Xu³⁰ over 15 years ago. In this model, the vena cava from a donor mouse is interlaced in the carotid artery of the recipient mouse. After harvesting the caval vein, the carotid artery of the recipient mouse is dissected free, ligated, and cut in the middle. The ends of the arteries are inversed around two cuffs, after which they are fixed with a ligature. Finally, the donor caval vein is sleeved over both cuffs and is fixated with two ligatures. A visible pulsatile flow confirms successful engraftment. Immediate endothelial damage of the vein graft due to the high blood pressure in the arterial circulation results in vessel wall thickening as early as 1 week after surgery. After 4 weeks, the intimal hyperplasia is even progressed to a 10-fold increase compared to the original thickness. Vein graft surgery in hypercholesterolemic mice results in an even more aggravated lesion formation with atherosclerotic features such as foam cell accumulation.

Interestingly, lesions induced in a murine vein graft model display a complex morphology including neovascularization, calcifications and disruptions consisting of fibrin depositions and intraplaque hemorrhage³¹. These disruptions are not completely comparable to plaque ruptures in the classical definition, in which a thin cap covering a lipid core ruptures, resulting in atherothrombosis¹⁶. However, investigating plaque rupture in mouse models has always been challenging since there are no mouse models available in which plaque ruptures occur in a similar manner as in the human situation. Therefore, the vein graft model is, besides an interesting model to investigate novel therapeutic strategies in vein graft disease, also a useful tool to study underlying mechanisms of plaque disruptions.

The immune system

Traditionally, the immune system has been divided into innate and adaptive immune responses, both of which play an important role in atherosclerosis. Monocytes, macrophages, dendritic cells, neutrophils, mast cells and NK cells all belong to the innate immune system and act as a first line of defense against common microorganisms and infections. These cells make use of germ line encoded pattern recognition receptors for pathogens or damaged self components, such as TLRs and scavenger receptors³². Pathogens are internalized, degraded and subsequently presented by antigen presenting cells (APCs) such as dendritic cells, which initiates the adaptive immune response. Adaptive immunity comprises clonally diverse lymphocytes with unique antigen recognition receptors, which allows them to recognize almost every possible pathogen and subsequently develop an antigen-specific immune response³³. Activation of the T and B lymphocytes results in cytokine secretion, antibody production and in memory formation, the latter being a typical feature of the adaptive immune system.

Monocytes

Recruitment of monocytes to the site of inflammation is a key mechanism in the initiation of atherosclerosis³⁴. Two distinct monocyte subsets in the blood have been described: classical monocytes (CD14⁺CD16⁻ in human; Ly6C⁺CX3CR1^{low}CCR2⁺ in mice) and non-classical monocytes (CD14^{low}CD16⁺ in human; Ly6C⁻CX3CR1^{high}CCR2⁻ in mice)³⁵. Non-classical monocytes constantly patrol healthy tissue by transient crawling along the endothelium, which allows rapid tissue invasion in case of infection or inflammation³⁶. Following this early response, classical monocytes are primarily recruited to the site of inflamed tissue, where they produce high levels of inflammatory cytokines³⁷. Interestingly, these classical Ly6C^{high} monocytes are markedly increased in hypercholesterolemic apoE^{-/-} mice, where they adhere to activated endothelium and infiltrate into atherosclerotic lesions³⁸. It has previously been shown that suppression of monocyte recruitment in atherogenesis reduces plaque size, however, similar effects were not observed in late stage atherosclerosis, which indicates the importance of monocyte influx in early atherogenesis³⁹.

Different chemokine receptors, amongst which are CCR1, CCR2, CCR5 and CX3CR1, are involved in the influx of monocytes to the atherosclerotic lesion. For instance, several groups have shown that deficiency or inhibition of CCR2 markedly decreases plaque size^{40–42}, stressing the importance of chemokine-receptor signalling pathways in monocyte recruitment. Once infiltrated into the vessel wall, monocytes differentiate into lesional macrophages, which engulf modified LDL, transform into foam cells, and contribute to the ongoing inflammatory process through the excretion of inflammatory mediators.

Macrophages

Macrophages are a heterogenic population of cells with diverse roles in development, homeostasis, tissue repair and immunity. They have the ability to efficiently phagocytose and kill pathogens as well as remove cellular debris in inflamed tissues. Moreover, they can present processed peptides to T cells thereby assisting in the execution of an immunological response⁴³.

The accumulation of macrophages and lipids underneath the endothelial cell layer is the initial hallmark of the atherosclerotic process, leading to the formation of early 'fatty streaks'. These macrophages engulf modified lipids via phagocytosis or via scavenger receptors, such as CD36 or scavenger receptor A1 (SR-A1), which are then digested in the lysosome⁴⁴. The resulting free cholesterol may be effluxed from the cell or it may be esterified and stored in cytosolic lipid droplets. Excessive free cholesterol accumulation increases pro-inflammatory signalling, leading to the activation of nuclear factor- κ B (NF κ B) with subsequent production of proinflammatory cytokines. Translocation of NF κ B to the nucleus may also be induced via TLR mediated activation by ligands such as oxidized LDL or DAMPs⁴⁵. However, not all the macrophages in the atherosclerotic plaque are thought to increase the inflammatory status of the lesion. Initially, a model was proposed in which macrophages were suggested to be of either a pro-inflammatory phenotype (M1, classically activated macrophage), or a wound-healing, anti-inflammatory phenotype (M2, alternatively activated macrophage)⁴⁶. LPS, IFN γ and IL-1 β are capable to induce M1 macrophages while the peroxisome proliferator-activated receptor- γ (PPAR γ) and the Th2 related cytokines IL-4 and IL-13 are able to polarize macrophages towards an M2 phenotype⁴⁷. M1 macrophages may aggravate atherosclerosis by excreting large amounts of inflammatory mediators such as IL-1 β , IL-6, IL-8 and TNF α . Also, the production of reactive oxygen species (ROS) leads to oxidative stress, and various M1 derived MMPs (MMP1, MMP3, MMP9) may contribute to thinning of the fibrous cap by collagen degradation. M2 macrophages on the other hand are thought to resolve the inflammation via secretion of anti-inflammatory cytokines such as IL-10⁴⁸. Since the initial division of macrophages into M1 and M2, other subsets such as Mox or M4 macrophages have been recognized as well, reflecting the highly heterogeneous nature of macrophages^{49,50}. The exact number of macrophage subsets with their corresponding functions is currently still under debate, and it is likely that additional classifications will ensue in the future.

In late stage atherosclerosis, clearance of apoptotic cell debris and lipids by macrophages is impaired, leading to the formation of a necrotic core. A large necrotic core accompanied by a high number of inflammatory macrophages is an important feature of unstable lesions, prone to rupture¹³. Therapeutic approaches have focused on shifting macrophages from an inflammatory M1 to an anti-

inflammatory M2 phenotype, on cholesterol efflux mechanisms and on egress of macrophages from the atherosclerotic lesion.

Mast cells

Mast cells are effector immune cells of the innate immune system capable of excreting a broad spectrum of proteases, chemokines, cytokines and growth factors. These potent inflammatory cells are derived from bone marrow precursor cells and differentiate into mature mast cells upon migration into the tissue where they reside, under the influence of stem cell factor and IL-3⁵¹. Typically, mast cells are present in various mucosal tissues and in the skin; in close proximity to blood vessels, lymphatics and nerves⁵². The typical morphology of the mast cell, caused by the vast amount of granules they contain, led to their name 'Mastzellen', which means well-fed cells⁵³. Mast cell granules are loaded with a vast amount of inflammatory preformed mediators, such as the mast cell specific tryptases, chymases and carboxypeptidase A3 (CPA3) inflammatory cytokines (e.g. TNF α) and histamine⁵⁴. Upon activation, these secretory granules are acutely released into the extracellular environment. Various stimuli are capable to induce mast cell activation, amongst which are IgE and IgG immune complexes; the complement components C5a^{15,55} and C3a⁵⁶ and the neuropeptides substance P⁵⁷ and NPY⁵⁸. Also, mast cells express different TLRs via which they may be activated, however, this route of activation does generally not cause degranulation but instead only induces the release of cytokines and chemokines⁵⁹.

Although it is already 60 years ago that the mast cell has been described in relation to atherosclerosis⁶⁰, it is not until the past 15 years that its importance receives increasing recognition. Interestingly, high numbers of activated mast cells are detected in the rupture-prone shoulder regions of human atherosclerotic plaques⁶¹. An increased amount of mast cells in the plaque of patients suffering from carotid artery stenosis is even found to correlate with intraplaque hemorrhage and the occurrence of future cardiovascular events⁶². Moreover, a causal role is established linking mast cell activation to both atherosclerotic plaque growth and destabilization. Systemic mast cell activation in apoE^{-/-} mice with a DNP hapten results in an increased lesion size in the brachiocephalic artery, while mast cell inhibition with the general stabilizer cromolyn significantly reduces this effect⁶³. One mode of action via which the mast cell is thought to aggravate atherosclerosis is via the potent proteases chymase and tryptase. Inhibition of chymase does not only reduce lesion size, plaque stability is also increased as measured by a decreased necrotic core area, increased collagen content and a reduced number of intraplaque hemorrhages⁶⁴. Moreover, *in vitro* and *in vivo* evidence indicates that mast cell chymase can induce smooth muscle cell apoptosis, leading to plaque destabilization^{14,65}. The importance of mast cell derived tryptase has been shown

after lentiviral overexpression of tryptase in apoE^{-/-} mice, which increases both atherosclerotic plaque size and intraplaque hemorrhages⁶⁶. Mast cell derived inflammatory cytokines are major contributors to the atherosclerotic process as well, in particular IL-6 and IFN γ . This was investigated by the adoptive transfer of IL-6, IFN γ and TNF α deficient mast cells into mast cell deficient LDLr^{-/-}/Kit^{W-sh/W-sh} mice. Interestingly, the reduced lesion size observed in these mice was again increased after the transfer of TNF α deficient mast cells, but not after that of IL-6 or IFN γ deficient mast cells, indicating an important role for these cytokines in atherogenesis⁶⁷. Furthermore, the potent angiogenic mediator basic fibroblast growth factor (bFGF) is stored and secreted by the mast cell. A positive correlation is found between numbers of bFGF positive mast cells and microvessels in the plaque, which is increased with the severity of atherosclerosis⁶⁸. Thus, there are a number of ways via which the mast cell can contribute to the growth and destabilization of atherosclerotic plaques.

Mast cell activation in the context of atherosclerosis may be induced by various ligands. For instance, the bioactive lysophospholipid acid (LPA) is present in atherosclerotic plaques, and local administration of LPA in apoE^{-/-} mice results in increased mast cell activation and plaque destabilization⁶⁹. Other mast cell ligands present in the atherosclerotic plaque include C5a, substance P, neuropeptide Y, and oxidized LDL, which may all contribute to mast cell activation, with subsequent aggravation of atherosclerosis^{55,57,58,70}.

Neutrophils

Neutrophils, the most abundant white blood cells in the circulation, are terminally differentiated cells derived from the bone marrow⁷¹. They are relatively short-lived cells which continuously patrol the blood in search for pathogens and apoptotic cells. Neutrophils can be recruited to the site of inflammation by various chemotactic agents, such as fMLP, C3a, C5a and a number of chemokines (e.g. IL-8)⁷². After transmigration through the endothelium, neutrophils may become activated and release their preformed granules which contain vast amounts of reactive oxygen intermediates, myeloperoxidase (MPO), cytokines, chemokines and the matrix degrading proteases MMP2 and MMP9⁷³. Also, it has been recently described that neutrophils may expel their DNA in order to trap bacteria, in a process called NETosis (neutrophil extracellular traps)^{74,75}.

The role of neutrophils in atherosclerosis has not been extensively studied yet, which may be caused by their rare detection in the lesions due to their short lifespan or because of their ability to undergo phenotypic changes, resulting in the expression of markers normally present on antigen-presenting cells⁷⁶. However, some studies have established a role for neutrophils in different stages of atherosclerosis. Neutrophils are detected in early and advanced lesions, in

particular in rupture-prone shoulder lesions⁷⁷. Also, circulating neutrophils are increased in apoE^{-/-} mice fed a high cholesterol diet, which is directly correlated to an increase in early atherosclerotic lesion size⁷⁸. Moreover, neutrophils are present in human plaques and an increase in their numbers has been shown to correlate with unstable lesions⁷⁹.

Dendritic cells

Dendritic cells (DCs), named for their dendrite-like projections, are professional antigen presenting cells derived from hematopoietic precursors in the bone marrow. They link the adaptive and innate immune system and have the potential to either stimulate or suppress inflammatory responses⁸⁰. Immature dendritic cells (iDCs) patrol the peripheral blood and tissues in search for antigens, which they can efficiently take up and process intracellularly. Uptake of antigens in the presence of “danger” signals, such as LPS or inflammatory cytokines, leads to the maturation of DCs⁸¹. This is accompanied by an upregulation of antigen-presenting molecules and co-stimulatory molecules on their cell surface, while the phagocytic activities are downregulated⁸². The processed antigens are loaded on the cell surface in the context of major histocompatibility (MHC) class I and II; subsequently the DCs will migrate to draining lymph nodes and present these antigens to naïve and memory T cells⁸³. Antigen presentation in combination with the presence of co-stimulatory molecules induces a profound immune response via the activation and clonal expansion of T cells. On the other hand, tolerogenic DCs may suppress inflammation via the induction of regulatory T cells (Treg)⁸⁴. In atherosclerosis, DCs have been detected in the vicinity of neovessels as well as near vasa vasorum in the adventitia, in close proximity to T cells⁸⁵. DCs are involved in both early and late stages of atherosclerosis and have been described to be both detrimental and protective in atherosclerosis. While some groups have reported that CD11c deficiency in mice fed a high cholesterol diet attenuates atherosclerosis^{86,87}, others did not observe any effect on plaque size⁸⁸. Deletion of non-classical DCs in LDLr^{-/-} mice results in exacerbated atherosclerotic lesion formation with reduced numbers of Tregs, indicating a protective role of non-classical DCs in atherosclerosis⁸⁹. Moreover, a beneficial contribution of DCs has been described after the transfer of oxLDL-pulsed mature DCs into LDLr^{-/-} mice, which markedly reduces lesion size⁹⁰.

T cells

T cells are derived from hematopoietic stem cells in the bone marrow; however, they undergo their development in the thymus. After exiting the thymus, naïve T cells travel to secondary lymphoid organs to survey for antigens for which they are specific. In these secondary lymphoid organs DCs present processed

antigens on MHC class I, recognized by CD8⁺ T cells (cytotoxic T cells), or on MHC class II, recognized by CD4⁺ T cells (T helper cells)⁹¹. Activation of the T cell further requires a co-stimulatory signal from the APCs as well as the presence of cytokines. Subsequently, CD4⁺ T cells acquire effector functions, which results in the formation of different subsets depending on the cytokine environment. The classical T helper 1 (Th1) cells are induced by IL-12 and IFN γ , while IL-2 and IL-4 are critical for Th2 differentiation. Development of Th17 cells is mostly initiated by IL-6, TGF β and the master regulator ROR γ t⁹². Another subset comprises regulatory T cells (Tregs), which require the transcription factor Foxp3 for their development and function. Tregs have immunosuppressive functions through secretion of the inhibitory cytokines IL-10 and TGF β ⁹³. Activation of naïve CD8⁺ T cells results in the differentiation of cytotoxic T lymphocytes (CTLs), which may induce apoptosis of target cells (through granzymes and perforin) and promote inflammation via secretion of IFN γ and TNF α ⁹⁴. Following differentiation, effector T cells migrate to non-lymphoid tissues for a second activation by APCs that present the same antigen.

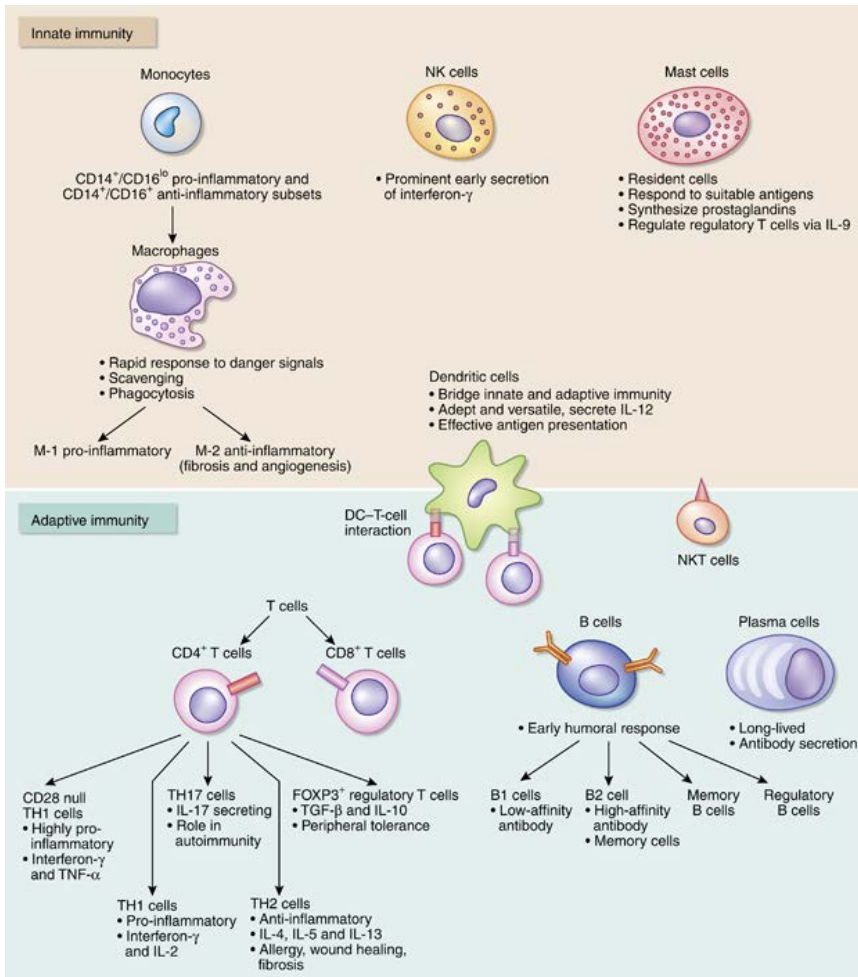
T cells have been detected in both human and mouse atherosclerotic plaques and in general, the majority of plaque T cells are CD4⁺ cells^{95,96}. Interestingly, 10% of all T cells in the plaque were found to recognize oxLDL in an MHC class II restricted manner⁹⁷. A detrimental role for CD4⁺ T cells was observed after transfer of CD4⁺ cells in immunodeficient apoE^{-/-}/scid/scid mice, which develop markedly increased atherosclerotic lesions⁹⁸. The Th1 cell subset is thought to exert pro-atherogenic effects via the excretion of its principal cytokine IFN γ . Mice deficient for IFN γ develop less atherosclerosis⁹⁹, however, it must be mentioned that other cells implicated in atherosclerosis, namely NKT cells and NK cells, also secrete IFN γ . Conversely, Th2 cells are described to have both pro- and anti-atherogenic properties. For instance, Th2 cells secrete IL-4, and deficiency of IL-4 was shown to result in decreased atherosclerosis¹⁰⁰. However, Th2 cells are also an important source of IL-5, which promotes the differentiation of atheroprotective B1 cells¹⁰¹. The subset Th17 cells are postulated to aggravate atherosclerosis, mediated by the secretion of the proinflammatory cytokine IL-17. However, no definite conclusions can be drawn on the effects of IL-17, considering some groups showed that blocking IL-17 reduced lesion formation¹⁰², while others found no effects on plaque burden¹⁰³. Regulatory T cells are important for immune suppression and consequently, they are thought to be beneficial in the context of atherosclerosis. Indeed, depletion of CD4⁺Foxp3⁺ cells in apoE^{-/-} mice results in increased atherosclerotic lesion formation. The effect of depleting CD8⁺ T cells has been under debate, and although it has been previously reported that CD8⁺ cells do not affect lesion size¹⁰⁴, recent data implicate proinflammatory CD8⁺ cells in plaque destabilization¹⁰⁵.

B cells

B cells and the wide variety of antibodies directed against an extensive amount of diverse pathogens produced by these cells form a central part of the humoral immune response. In the bone marrow, B cells are formed from hematopoietic precursor cells after a series of functional rearrangements of immunoglobulin gene segments¹⁰⁶. Eventually, an IgM molecule is expressed on the surface of these cells, which are then named “immature B cells”. Immature B cells migrate to the spleen after they have left the bone marrow, where they differentiate into naïve, follicular or marginal zone B cells¹⁰⁷.

Relatively few B cells are found in the atherosclerotic plaque; however, they are predominantly present in lymphocyte infiltrates in the adventitia called tertiary lymphoid organs¹⁰⁸. In one of the first studies that demonstrated a role for B cells in atherosclerosis, surgical removal of the spleen in apoE^{-/-} mice was found to aggravate lesion formation. Subsequent adoptive transfer of splenic B cells did not only reverse this effect, but even resulted in a mild protection against atherosclerosis¹⁰⁹, indicative of a protective effect of B cells. However, the depletion of mature B cells with the use of a CD20-specific monoclonal antibody unexpectedly reduced atherosclerosis¹¹⁰. These seemingly opposing roles of B cells may be partially explained by the differential role of the functional B cell subsets B1 and B2 cells. B1 cells produce natural antibodies such as IgM in a T cell independent manner, while B2 cells require T cell interaction for activation and antibody production such as IgG and IgE¹¹¹. The transfer of specific B2 cells, but not the transfer of B1 cells, to lymphocyte-deficient triple knockout (TKO) mice was found to aggravate atherosclerosis¹¹². Also, additional evidence for a detrimental role of B2 cells is provided by disruption of B cell activating factor (BAFF) signalling, which is necessary for the survival of B2 cells. Mice deficient for BAFF receptor lack B2 cells but have minor changes in B1 cells, which leads to reduced atherosclerotic lesion formation¹¹³.

On the other hand, protective effects of the subset B1a cells have been demonstrated, which is thought to be caused by IgM deposits in the lesions¹¹⁴. Natural IgM may limit plaque burden by preventing uptake of oxLDL, inhibiting accumulation of apoptotic cells, and neutralizing inflammatory gene expression in response to oxidized lipids¹¹⁵. An additional third B cell subset, called the B10 cell, acts as negative regulator of the inflammatory response by producing IL-10¹¹⁶. Although a definite role for these regulatory B10 cells is not yet described in atherosclerosis, they are most likely to attenuate atherosclerosis via an immunosuppressive manner.



General overview of innate and adaptive immune cells and some of their key effector functions. Adapted from Swaminathan *et al.* *Kidney Int.* 2011;80:453-63.

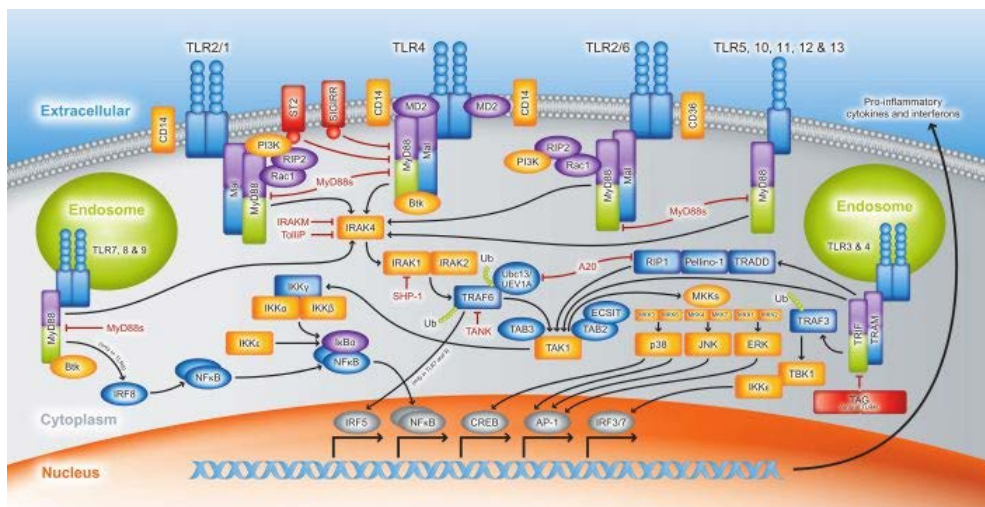
Toll-like receptor signalling

Toll-like receptors (TLRs) are a type of pattern recognition receptors (PRRs) that play a central role in the initiation of the innate and adaptive immune response. They are able to recognize conserved motifs on pathogens called pathogen-associated molecular patterns (PAMPs) or danger-associated molecular patterns (DAMPs) from endogenous damaged tissue¹¹⁷. In humans, 10 different TLRs have been identified (TLR1 to TLR10), whereas 12 distinct TLRs exist in mice (TLR1 to TLR9 and TLR11 to TLR13)¹¹⁸. TLR1 and TLR2, both expressed on the plasma membrane, can heterodimerize and subsequently sense bacterial triacylated lipopeptides. TLR2 is also able to heterodimerize with TLR6, which can recognize bacterial diacylated lipopeptides¹¹⁹. TLR3 is localized in the endolysosomal

compartment and recognizes double stranded RNA. TLR4 and TLR5, both present on the cellular membrane, can be activated respectively by lipopolysaccharide (LPS) and flagellin from bacteria¹²⁰. TLR7, TLR8 and TLR9 are, similar to TLR3, located intracellularly. TLR7 and TLR8 sense single stranded RNA while TLR9 binds unmethylated bacterial CpG DNA¹²¹.

Upon binding of a ligand to the TLR, adaptor proteins are recruited to the cytoplasmic domain of the receptor. All TLRs, with exception of TLR3, interact with MyD88 via their TIR domain, which results in a series of intracellular signalling events leading to translocation of NFκB to the nucleus¹²². TLR4 and the intracellular TLRs may also signal via an MyD88 independent pathway, which ultimately results in type I Interferon (IFN) production¹²¹.

In one of the earliest studies investigating the role of TLRs in atherosclerosis, lesions were induced in MyD88 deficient mice. These mice developed reduced atherosclerotic plaques, caused by decreased macrophage recruitment to the lesion due to lower chemokine levels¹²³. These findings were confirmed by Michelsen *et al.*¹²⁴, who also demonstrated that lack of TLR4 decreases atherosclerosis. TLR4 is the most extensively studied TLR regarding atherosclerotic research, and will be discussed into more detail in the next section. Similar to TLR4, inactivation of TLR2 results in less macrophage recruitment and lipid accumulation to the lesion, thereby attenuating plaque progression¹²⁵. However, not all TLRs exert detrimental effects on lesion formation; for example, functional inactivation of TLR7 has been shown to result in accelerated atherosclerosis¹²⁶. The exact role of other TLRs is still under debate, either due to lack of mechanistic data or due to conflicting evidence¹²⁷.



General overview of the extra- and intra-cellular Toll-like receptors and their signalling pathways. Adapted from Abcam Posters.

TLR4 and its accessory molecule RP105

Signalling via TLR4 requires the presence of the soluble protein MD2, which is associated with the extracellular domain of TLR4. In contrast to other TLRs, TLR4 does not directly bind to its ligand. Instead, MD2 is the primary recognition molecule responsible for the interaction with LPS¹²⁸. The responsiveness to LPS is enhanced by the cell-surface protein CD14; CD14 can bind LPS and mediate its transfer to the TLR4/MD2 complex¹²⁹. A distinct regulatory molecule, radioprotective 105 (RP105), was initially thought to act as an enhancer of TLR4 signalling as well. RP105 was discovered on the cell surface of B cells, in which it was found to drive B cell proliferation and activation^{130,131}. Later, it was discovered that RP105 is not B cell specific, but that it is expressed by all myeloid cells. The structure of RP105 is highly comparable to that of TLR4 and similar to the TLR4/MD2 complex, RP105 associates with an adaptor molecule: MD1. However, the RP105/MD1 complex lacks the intracellular TIR domain, suggesting it may not induce signalling by itself¹³². In contrast to its stimulatory role on B cells, RP105 was found to inhibit TLR4 mediated responses in dendritic cells and macrophages¹³³. Consequently, LPS injection in RP105 deficient mice results in an exaggerated inflammatory response with profoundly increased TNF α plasma levels¹³⁴.

Besides LPS, TLR4 has many other ligands that may induce inflammatory signalling. Interestingly, several of these endogenous ligands are present in the atherosclerotic plaque, such as oxidized LDL, heat shock protein 60 (Hsp60) and the alternatively spliced EDA (extra domain A) of fibronectin^{135,136}. Targeting of TLR4 in atherosclerosis, as well as in vein graft disease, has thus shown some promising results, mostly via inhibition of vascular inflammation^{124,137–139}. The effects of RP105 deficiency in cardiovascular disorders are less straight-forward. In a setting of damage-induced vascular remodelling, lack of RP105 results in increased neointima formation, which is in line with the inhibitory effects RP105 can exert on TLR4 in dendritic cells and macrophages¹⁴⁰. However, reduced atherosclerotic lesion formation is observed in LDLr^{-/-} mice on a high fat diet receiving RP105 deficient bone marrow, due to a reduction in inflammatory B2 cell numbers as well as decreased activation of B2 cells¹⁴¹. These conflicting data reflect the dichotomous effects RP105 can have on different cells types, and future research is aimed at further elucidating the regulatory mechanisms of RP105 in vascular remodelling.

The complement system

The complement system consists of over 30 plasma proteins that are converted into active proteases upon activation. Although complement is considered a part of the innate immune system, it may serve as a functional bridge between innate and adaptive immunity via enhancing antibody responses and immunological memory¹⁴². Complement activation can occur via three major pathways: the

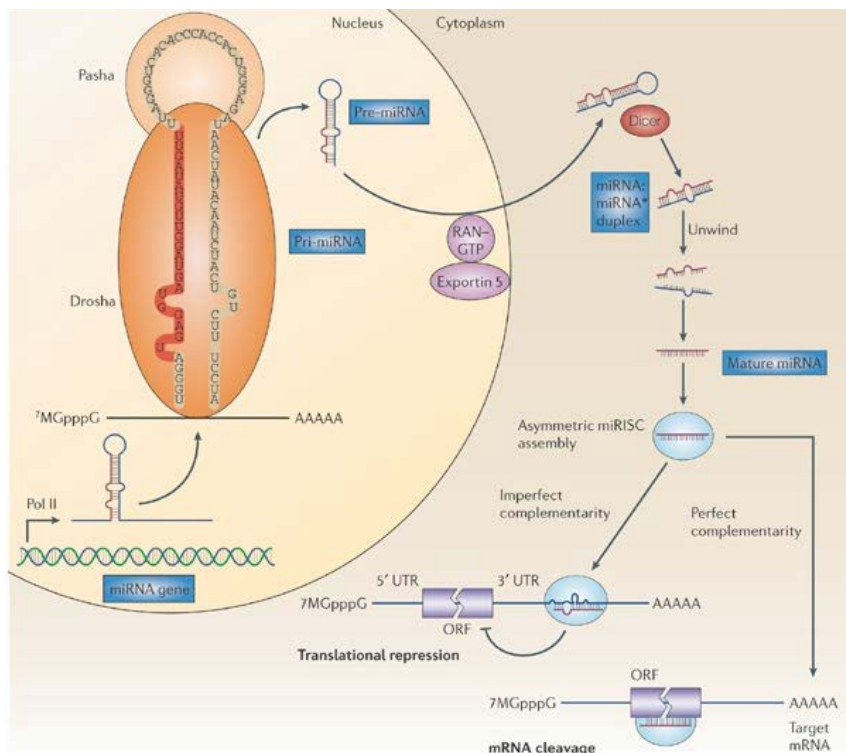
classical, the lectin or the alternative pathway; and also via the 'coagulation' pathway, which all result in the initiation of the complement cascade. The classical pathway is activated by binding of antibodies to their target antigens, while the lectin pathway is induced by binding of mannose-binding lectin to mannose residues on a range of bacteria¹⁴³. The alternative pathway on the other hand is spontaneously activated at a constant low level. Finally, the 'coagulation' pathway is triggered by the cleavage and immediate activation of C3 and C5 by thrombin¹⁴⁴. All major pathways lead to the formation of convertases that cleave the central component C3 into C3b and C3a. C3b is responsible for the amplification reaction of the complement cascade and the anaphylatoxin C3a is a potent chemoattractant that induces proinflammatory signalling after binding to its receptor C3aR. Cleavage of C5 results in the formation of C5b, which initiates the assembly of the terminal complement complex (TCC). Also, C5a is formed, a powerful anaphylatoxin with chemoattractant and inflammatory properties similar to C3a^{145,146}. To prevent excessive activation and damage to healthy tissues, multiple proteins regulate the complement cascade, including factor H, CD59 and DAF¹⁴³.

Complement activation in the context of atherosclerosis may be induced by different mechanisms, for instance via immune complexes, c-reactive protein (CRP), apoptotic cells and modified LDL¹⁴⁷. Also, the expression of receptors for C5a and C3a is significantly upregulated in human coronary plaques compared to normal coronary arteries¹⁴⁸. However, the exact contribution of the complement system to atherosclerosis is not yet elucidated. Deficiency of the central component C3 aggravates aortic lesion development in mice placed on a high fat diet^{149,150}, while the opposite effect was found when targeting of C3 in the setting of vein graft disease¹⁵¹. Other studies point to a protective role for the inhibitory proteins CD59¹⁵² and DAF¹⁵³, while the complement component C6¹⁵⁴ exerts detrimental effects on atherosclerosis. Of particular interest is the anaphylatoxin C5a, which has been shown to associate with future cardiovascular events in patients with advanced atherosclerosis¹⁵⁵. C5a may aggravate plaque formation and destabilization via activation of endothelium, attraction of leukocytes to the site of inflammation and inducing the expression of multiple inflammatory cytokines. Further investigations into the exact role of C5a in atherosclerosis is therefore of high interest.

MicroRNAs

The presence of microRNAs (miRs) in vertebrates was first described by three separate groups in a series of Science papers in 2001^{156–158}. Each of these papers defined miRs as short, noncoding RNA strands approximately 21–25 nucleotides in length, capable of posttranscriptional regulation of specific mRNA targets. The posttranscriptional repression is induced by Watson-Crick base pairing between

the miR seed region and sequences located in the 3' untranslated region (UTRs) of the mRNA targets. Following these first pioneering papers, a burst of studies into the biological actions of miRs in different research areas has ensued.



MicroRNAs are generally transcribed in the nucleus as large pri-miRNA transcripts. Processing by the enzyme Drosha results in the formation of pre-miRNA, which is transported into the cytoplasm and further processed by the Dicer enzyme. The miRNA is loaded into the RNA-induced silencing complex (RISC), where it can bind to the complementary site of the mRNA target, thereby leading to either translational repression or mRNA cleavage, depending on the degree of complementarity. Adapted from Esquela-Kerscher *et al.* Nat rev cancer. 2006;6:259-69.

The distinct characteristic of miRs to regulate the expression of numerous genes makes them interesting targets for interference in complex, multifactorial disease-processes. Indeed, several studies have shown that inhibition of specific miRs in atherosclerosis leads to profound effects on lesion development or progression. One of the most extensively investigated miRs with regard to atherosclerosis is miR-33: a miR encoded by the intron of sterol regulatory element-binding protein 2 (Srebp2), which is important for cholesterol synthesis and uptake. Mice deficient for miR-33 were shown to have increased ABCA1 levels in the liver and higher serum HDL levels¹⁵⁹. These findings were confirmed in primates, in which inhibition of miR-33a/b resulted in increased HDL levels and also reduced VLDL levels¹⁶⁰. However, the exact role of miR-33 in atherosclerosis has recently been under

debate. While several papers showed that antagonism of miR-33 induces plaque regression or prevent lesion progression^{159,161,162}, others have recently claimed that prolonged silencing of miR-33 fails to induce a sustained increase of HDL levels and does not prevent plaque progression¹⁶³. A different miR implicated in atherosclerosis, miR-155, is involved in inflammatory signalling in macrophages, endothelial cells and smooth muscle cells. Deficiency of miR-155 was found to reduce the expression of CCL2 while increasing Bcl6 expression, a transcription factor that represses proinflammatory NFκB signalling, leading to aggravated atherosclerotic lesion formation¹⁶⁴. Conflicting *in vitro* evidence however, shows that miR-155 deficient macrophages stimulated by oxidized LDL display an enhanced inflammatory response¹⁶⁵. Besides miR-33 and miR-155, several other miRs have been described to be either present in lesions or to be able to affect lesion formation.

The above mentioned examples of miR inhibition in the setting of atherosclerosis clearly demonstrate the potential therapeutic value miRs may have. However, it has also become evident that miR research is still a developing field with accompanying shortcomings and contradictory reports. Moreover, the unique ability of miRs to regulate a biological process via a multitude of genes rather than single genes has not been utilized to its full extent yet. Therefore, future research directed towards validating known miRs, as well as identifying miRs not yet described in atherosclerosis, may yield promising results.

Outline of this thesis

The aim of this thesis is to gain more insight into the role of the innate immune system in vascular remodelling, in particular in vein graft disease and atherosclerosis, as well as to identify new therapeutic targets to prevent vascular diseases and acute cardiovascular syndromes. **Chapter 2** encompasses a review which focuses on the role of the mast cell in early and late stage atherosclerosis, with particular emphasis on plaque rupture. Also, the prognostic value of mast cell mediators as well as therapeutic implications of mast cell stabilization are discussed. While mast cells have previously been indicated as important players in atherosclerosis, their role in vein graft disease has not been elucidated yet. In **chapter 3**, we show that mast cell activation results in a marked increase in vein graft thickening and plaque disruptions. Also, we investigated the mechanism via which mast cells are activated in the context of vein graft disease. We found that the complement component C5a, capable of activating mast cells, is upregulated during vein graft disease. Local application of C5a in a gel aggravated vein graft disease, which could be inhibited with the mast cell stabilizer cromolyn, indeed indicating a mast cell dependent mechanism. **Chapter 4** describes the effect of

C5a on advanced vein graft lesions. Application of C5a in these late stage lesions increased plaque disruptions in a mast cell independent manner, since cromolyn was not able to reduce these events. Instead, C5a was seen to directly promote apoptosis of smooth muscle cells and endothelial cells *in vitro* and *in vivo*, which may overrule the effect of the mast cells and lead to the observed increase in disruptions. **Chapter 5** focuses on the role of mast cell derived chemokines in atherosclerosis. Chronic mast cell activation results in a profound increase of neutrophils in the intima and adventitia of atherosclerotic plaques. *In vivo* influx studies using mast cell deficient mice and control mice show indeed that mast cell activation leads to excessive neutrophil migration.

Chapter 6 provides insight in the role of RP105 in vein graft disease. Deficiency of RP105 in mice fed a chow diet exacerbates vessel wall thickening of the vein grafts, as well as the number of plaque disruptions. An additional *in vivo* study shows that LDLr^{-/-}/RP105^{-/-} mice on a high fat diet do not display increased vessel wall thickening compared to control LDLr^{-/-} mice, however more plaque disruptions were still observed. Both studies show that RP105 deficiency increases the number of activated perivascular mast cells, which was more pronounced in mice fed a chow diet, thereby possibly leading to the observed effects of vein graft disease. In **chapter 7**, total body RP105 deficiency in atherosclerosis has been investigated. Opposed to vein graft disease, LDLr^{-/-}/RP105^{-/-} mice on a high fat diet develop reduced early atherosclerotic lesions, accompanied by a decrease in lesional macrophages. We demonstrate that this may be caused by disturbed monocyte migration in RP105 deficient mice, due to a downregulation of the chemokine receptor CCR2.

Chapter 8 describes the use of a Reversed Target Prediction (RTP) method to identify microRNAs that are predicted to affect atherosclerotic lesion development and thus act as a so-called master switch. With this RTP, we singled out miR-494 from the miR-gene cluster 14q32, which has not been previously described in atherosclerosis. Inhibition of miR-494 *in vivo* by means of gene silencing oligonucleotides (GSOs) results in reduced lesion formation, while plaque stability is increased. Also, upregulation of target genes for miR-494 is observed both *in vivo* and *in vitro*.

The results of all the studies described in this thesis, as well as future prospectives, are discussed in **chapter 9**.

References

1. Wentzel JJ, Chatzizisis YS, Gijzen FJ, *et al.* Endothelial shear stress in the evolution of coronary atherosclerotic plaque and vascular remodelling: current understanding and remaining questions. *Cardiovasc. Res.* 2012;96:234–243.
2. Frostegård, J. Immunity, atherosclerosis and cardiovascular disease. *BMC Med.* 2013;11:117.

3. Yusuf, S, Hawken S, Ounpuu S, *et al*; INTERHEART Study Investigators. Effect of potentially modifiable risk factors associated with myocardial infarction in 52 countries (the INTERHEART study): case-control study. *Lancet*. 2004;364:937–952.
4. Go, AS, Mozaffarian D, Roger VL, *et al* ; American Heart Association Statistics Committee and Stroke Statistics Subcommittee. Heart disease and stroke statistics--2014 update: a report from the American Heart Association. *Circulation*. 2014;129:e28–e292.
5. Velican C, Velican D. Progression of coronary atherosclerosis from adolescents to mature adults. *Atherosclerosis*. 1983;47:131–144.
6. Blankenberg S, Barbaux S, Tiret L. Adhesion molecules and atherosclerosis. *Atherosclerosis* 2003;170: 191–203.
7. Hansson GK, Inflammation, atherosclerosis, and coronary artery disease. *N. Engl. J. Med*. 2005;352: 1685–1695.
8. Cole JE, Georgiou E, Monaco C. The expression and functions of toll-like receptors in atherosclerosis. *Mediators Inflamm*. 2010;2010:393946.
9. Van der Veer EP, de Bruin RG, Kraaijeveld AO, *et al*. Quaking, an RNA-binding protein, is a critical regulator of vascular smooth muscle cell phenotype. *Circ. Res*. 2013;113:1065–1075.
10. Saito, Y. Mechanism of phenotype formation of smooth muscle cells. *Ann. N. Y. Acad. Sci*. 1995;748:7–10.
11. Virmani R, Kolodgie FD, Burke AP, *et al*. Lessons from sudden coronary death: a comprehensive morphological classification scheme for atherosclerotic lesions. *Arterioscler. Thromb. Vasc. Biol*. 2000;20:1262–1275.
12. Stary HC. Natural history and histological classification of atherosclerotic lesions: an update. *Arterioscler. Thromb. Vasc. Biol*. 2000;20:1177–1178.
13. Shah PK. Mechanisms of plaque vulnerability and rupture. *J. Am. Coll. Cardiol*. 2003;41:155–225.
14. Den Dekker WK, Tempel D, Bot I, *et al*. Mast cells induce vascular smooth muscle cell apoptosis via a toll-like receptor 4 activation pathway. *Arterioscler. Thromb. Vasc. Biol*. 2013;32:1960–1969.
15. Wezel A, de Vries MR, Lagraauw HM, *et al*. Complement factor C5a induces atherosclerotic plaque disruptions. *J. Cell. Mol. Med*. 2014;doi:10.1111/jcmm.12357.
16. Finn AV, Nakano M, Narula J, *et al*. Concept of vulnerable/unstable plaque. *Arterioscler. Thromb. Vasc. Biol*. 2010;30:1282–1292.
17. Bentzon JF, Otsuka F, Virmani R, *et al*. Mechanisms of Plaque Formation and Rupture. *Circ. Res*. 2014;114:1852–1866.
18. Al-Sabti HA, Al Kindi A, Al-Rasadi K, *et al*. Saphenous vein graft vs. radial artery graft searching for the best second coronary artery bypass graft. *J. Saudi Heart Assoc*. 2013;25:247–254.
19. Desai M, Mirzay-Razzaz J, von Delft D, *et al*. Inhibition of neointimal formation and hyperplasia in vein grafts by external stent/sheath. *Vasc. Med. Lond. Engl*. 2010;15:287–297.
20. Fitzgibbon GM, Kafka HP, Leach AJ, *et al*. Coronary bypass graft fate and patient outcome: angiographic follow-up of 5,065 grafts related to survival and reoperation in 1,388 patients during 25 years. *J. Am. Coll. Cardiol*. 1996;28:616–626.
21. Motwani JG, Topol EJ. Aortocoronary saphenous vein graft disease: pathogenesis, predisposition, and prevention. *Circulation* 1998;97:916–931.
22. Campeau L, Enjalbert M, Lespérance J, *et al*. The relation of risk factors to the development of atherosclerosis in saphenous-vein bypass grafts and the progression of disease in the native circulation. A study 10 years after aortocoronary bypass surgery. *N. Engl. J. Med*. 1984;311:1329–1332.
23. Kim FY, Marhefka G, Ruggiero NJ, *et al*. Saphenous vein graft disease: review of pathophysiology, prevention, and treatment. *Cardiol. Rev*. 2013;21:101–109.
24. Shukla N, Jeremy JY. Pathophysiology of saphenous vein graft failure: a brief overview of interventions. *Curr. Opin. Pharmacol*. 2012;12:114–120.
25. Breslow JL. Mouse models of atherosclerosis. *Science* 1996;272:685–688.
26. Hofker MH, van Vlijmen BJ, Havekes LM. Transgenic mouse models to study the role of APOE in hyperlipidemia and atherosclerosis. *Atherosclerosis* 1998;137:1–11.
27. Kapourchali FR, Surendiran G, Chen L, *et al*. Animal models of atherosclerosis. *World J. Clin. Cases* 2014;2:126–132.
28. Fazio S, Linton MF. Mouse models of hyperlipidemia and atherosclerosis. *Front. Biosci. J. Virtual Libr*. 2001;6:D515–525.
29. Dekker RJ, van Thienen JV, Rohlena J, *et al*. Endothelial KLF2 links local arterial shear stress levels

- to the expression of vascular tone-regulating genes. *Am. J. Pathol.* 2005;167:609–618.
30. Zou Y, Dietrich H, Hu Y, *et al.* Mouse model of venous bypass graft arteriosclerosis. *Am. J. Pathol.* 1998;153:1301–1310.
 31. De Vries MR, Niessen HW, Löwik CW, *et al.* Plaque rupture complications in murine atherosclerotic vein grafts can be prevented by TIMP-1 overexpression. *PLoS One* 2012;7:e47134.
 32. Hoebe K, Janssen E, Beutler B. The interface between innate and adaptive immunity. *Nat. Immunol.* 2004;5:971–974.
 33. Cooper MD, Herrin BR. How did our complex immune system evolve? *Nat. Rev. Immunol.* 2010;10:2–3.
 34. Woollard KJ. Immunological aspects of atherosclerosis. *Clin. Sci. Lond. Engl.* 2013;125:221–235.
 35. Strauss-Ayali D, Conrad SM, Mosser DM. Monocyte subpopulations and their differentiation patterns during infection. *J. Leukoc. Biol.* 2007;82:244–252.
 36. Auffray C, Fogg D, Garfa M, *et al.* Monitoring of blood vessels and tissues by a population of monocytes with patrolling behavior. *Science* 2007;317:666–670.
 37. Drechsler M, Soehnlein O. The complexity of arterial classical monocyte recruitment. *J. Innate Immun.* 2013;5:358–366.
 38. Soehnlein O, Swirski FK. Hypercholesterolemia links hematopoiesis with atherosclerosis. *Trends Endocrinol. Metab.* 2013;24:129–136.
 39. Stoneman V, Braganza D, Figg N, *et al.* Monocyte/macrophage suppression in CD11b diphtheria toxin receptor transgenic mice differentially affects atherogenesis and established plaques. *Circ. Res.* 2007;100:884–893.
 40. Bot I, Guo J, Van Eck M, *et al.* Lentiviral shRNA silencing of murine bone marrow cell CCR2 leads to persistent knockdown of CCR2 function in vivo. *Blood* 2005;106:1147–1153.
 41. Dawson TC, Kuziel WA, Osahar TA, Maeda N. Absence of CC chemokine receptor-2 reduces atherosclerosis in apolipoprotein E-deficient mice. *Atherosclerosis* 1999;143:205–211.
 42. Boring L, Gosling J, Cleary M, Charo IF. Decreased lesion formation in CCR2^{-/-} mice reveals a role for chemokines in the initiation of atherosclerosis. *Nature* 1998;394:894–897.
 43. Johnson JL, Newby AC. Macrophage heterogeneity in atherosclerotic plaques. *Curr. Opin. Lipidol.* 2009;20:370–378.
 44. Canton J, Neculai D, Grinstein S. Scavenger receptors in homeostasis and immunity. *Nat. Rev. Immunol.* 2013;13:621–634.
 45. Moore KJ, Sheedy FJ, Fisher EA. Macrophages in atherosclerosis: a dynamic balance. *Nat. Rev. Immunol.* 2013;13:709–721.
 46. Gordon S, Taylor PR. Monocyte and macrophage heterogeneity. *Nat. Rev. Immunol.* 2005;5:953–964.
 47. Murray PJ, Wynn TA. Protective and pathogenic functions of macrophage subsets. *Nat. Rev. Immunol.* 2011;11:723–737.
 48. Butcher MJ, Galkina EV. Phenotypic and functional heterogeneity of macrophages and dendritic cell subsets in the healthy and atherosclerosis-prone aorta. *Front. Physiol.* 2012;3:44.
 49. Erbel C, Tyka M, Helmes CM, *et al.* CXCL4-induced plaque macrophages can be specifically identified by co-expression of MMP7+S100A8+ in vitro and in vivo. *Innate Immun.* 2014;doi:10.1177/1753425914526461.
 50. Kadl A, Meher AK, Sharma PR, *et al.* Identification of a novel macrophage phenotype that develops in response to atherogenic phospholipids via Nrf2. *Circ. Res.* 2010;107:737–746.
 51. Dai H, Korthuis RJ. Mast Cell Proteases and Inflammation. *Drug Discov. Today Dis. Models.* 2011;8:47–55.
 52. Kovanen PT. Mast cells: multipotent local effector cells in atherothrombosis. *Immunol. Rev.* 2007;217: 105–122.
 53. Blank U, Falcone FH, Nilsson G. The history of mast cell and basophil research - some lessons learnt from the last century. *Allergy.* 2013;68:1093–1101.
 54. Wernersson S, Pejler G. Mast cell secretory granules: armed for battle. *Nat. Rev. Immunol.* 2014; 14:478–94.
 55. De Vries MR, Wezel A, Schepers A, *et al.* Complement factor C5a as mast cell activator mediates vascular remodelling in vein graft disease. *Cardiovasc. Res.* 2013;97:311–320.
 56. Thangam EB, Venkatesha RT, Zaidi AK, *et al.* Airway smooth muscle cells enhance C3a-induced mast cell degranulation following cell-cell contact. *FASEB J.* 2005;19:798–800.
 57. Bot, I, de Jager SC, Bot M, *et al.* The neuropeptide substance P mediates adventitial mast cell

- activation and induces intraplaque hemorrhage in advanced atherosclerosis. *Circ. Res.* 2010;106:89–92.
58. Lagraauw HM, Westra MM, Bot M, *et al.* Vascular neuropeptide Y contributes to atherosclerotic plaque progression and perivascular mast cell activation. *Atherosclerosis* 2014;235:196–203.
 59. Sandig H, Bulfone-Paus S. TLR signaling in mast cells: common and unique features. *Front. Immunol.* 2012;3:185.
 60. CONSTANTINIDES P. Mast cells and susceptibility to experimental atherosclerosis. *Science* 1953;117:505–506.
 61. Kaartinen M, Penttilä A, Kovanen PT. Accumulation of activated mast cells in the shoulder region of human coronary atheroma, the predilection site of atheromatous rupture. *Circulation* 1994;90:1669–1678.
 62. Willems S, Vink A, Bot I, *et al.* Mast cells in human carotid atherosclerotic plaques are associated with intraplaque microvessel density and the occurrence of future cardiovascular events. *Eur. Heart J.* 2013;34:3699–3706.
 63. Bot I, de Jager SC, Zernecke A, *et al.* Perivascular mast cells promote atherogenesis and induce plaque destabilization in apolipoprotein E-deficient mice. *Circulation* 2007;115:2516–2525.
 64. Bot I, Bot M, van Heiningen SH, *et al.* Mast cell chymase inhibition reduces atherosclerotic plaque progression and improves plaque stability in ApoE^{-/-} mice. *Cardiovasc. Res.* 2011;89:244–252.
 65. Leskinen M, Wang Y, Leszczynski D, Lindstedt KA, Kovanen PT. Mast cell chymase induces apoptosis of vascular smooth muscle cells. *Arterioscler. Thromb. Vasc. Biol.* 2001;21:516–522.
 66. Zhi X, Xu C, Zhang H, *et al.* Trypsin promotes atherosclerotic plaque haemorrhage in ApoE^{-/-} mice. *PLoS One* 2013;8:e60960.
 67. Sun J, Sukhova GK, Wolters PJ, *et al.* Mast cells promote atherosclerosis by releasing proinflammatory cytokines. *Nat. Med.* 2007;13:719–724.
 68. Lappalainen H, Laine P, Pentikäinen MO, Sajantila A, Kovanen PT. Mast cells in neovascularized human coronary plaques store and secrete basic fibroblast growth factor, a potent angiogenic mediator. *Arterioscler. Thromb. Vasc. Biol.* 2004;24:1880–1885.
 69. Bot M, de Jager SC, MacAleese L, *et al.* Lysophosphatidic acid triggers mast cell-driven atherosclerotic plaque destabilization by increasing vascular inflammation. *J. Lipid Res.* 2013;54:1265–1274.
 70. Meng Z, Yan C, Deng Q, *et al.* Oxidized low-density lipoprotein induces inflammatory responses in cultured human mast cells via Toll-like receptor 4. *Cell. Physiol. Biochem.* 2013;31:842–853.
 71. Von Vietinghoff S, Ley K. Homeostatic regulation of blood neutrophil counts. *J. Immunol.* 2008;181:5183–5188.
 72. Phillipson M, Kubes P. The neutrophil in vascular inflammation. *Nat. Med.* 2011;17:1381–1390.
 73. Nathan C. Neutrophils and immunity: challenges and opportunities. *Nat. Rev. Immunol.* 2006;6:173–182.
 74. Yipp BG, Petri B, Salina D, *et al.* Infection-induced NETosis is a dynamic process involving neutrophil multitasking in vivo. *Nat. Med.* 2012;18:1386–1393.
 75. Cabrini M, Nahmod K, Geffner J. New insights into the mechanisms controlling neutrophil survival. *Curr. Opin. Hematol.* 2010;17:31–35.
 76. Soehnlein O. Multiple roles for neutrophils in atherosclerosis. *Circ. Res.* 2012;110:875–888.
 77. Rotzius P, Thams S, Soehnlein O, *et al.* Distinct infiltration of neutrophils in lesion shoulders in ApoE^{-/-} mice. *Am. J. Pathol.* 2010;177:493–500.
 78. Drechsler M, Megens RTA, van Zandvoort M, Weber C, Soehnlein O. Hyperlipidemia-triggered neutrophilia promotes early atherosclerosis. *Circulation* 2010;122:1837–1845.
 79. Ionita MG, van den Borne P, Catanzariti LM, *et al.* High neutrophil numbers in human carotid atherosclerotic plaques are associated with characteristics of rupture-prone lesions. *Arterioscler. Thromb. Vasc. Biol.* 2010;30:1842–1848.
 80. Steinman RM, Banchereau J. Taking dendritic cells into medicine. *Nature.* 2007;449:419–426.
 81. Chung CYJ, Ysebaert D, Berneman ZN, Cools N. Dendritic cells: cellular mediators for immunological tolerance. *Clin. Dev. Immunol.* 2013;972865.
 82. Gordon JR, Ma Y, Churchman L, Gordon SA, Dawicki W. Regulatory Dendritic Cells for Immunotherapy in Immunologic Diseases. *Front. Immunol.* 2014;5:7.
 83. Figdor CG, de Vries, IJM, Lesterhuis WJ, Melief CJM. Dendritic cell immunotherapy: mapping the way. *Nat. Med.* 2004;10:475–480.
 84. Chistiakov DA, Sobenin IA, Orekhov AN, Bobryshev YV. Dendritic cells in atherosclerotic inflammation: the complexity of functions and the peculiarities of pathophysiological effects. *Front. Physiol.*

- 2014;5:196.
85. Erbel C, Sato K, Meyer FB, *et al.* Functional profile of activated dendritic cells in unstable atherosclerotic plaque. *Basic Res. Cardiol.* 2007;102:123–132.
 86. Wu H, Gower RM, Wang H, *et al.* Functional role of CD11c+ monocytes in atherogenesis associated with hypercholesterolemia. *Circulation* 2009;119:2708–2717.
 87. Paulson, K. E. *et al.* Resident intimal dendritic cells accumulate lipid and contribute to the initiation of atherosclerosis. *Circ. Res.* 106, 383–390 (2010).
 88. Gautier EL, Zhu SN, Chen M, *et al.* Conventional dendritic cells at the crossroads between immunity and cholesterol homeostasis in atherosclerosis. *Circulation* 2009;119:2367–2375.
 89. Choi JH, Cheong C, Dandamudi DB, *et al.* Flt3 signaling-dependent dendritic cells protect against atherosclerosis. *Immunity* 2011;35:819–831.
 90. Habets KLL, van Puijvelde GH, van Duivenvoorde LM, *et al.* Vaccination using oxidized low-density lipoprotein-pulsed dendritic cells reduces atherosclerosis in LDL receptor-deficient mice. *Cardiovasc. Res.* 2010;85:622–630.
 91. Matloubian M, Lo CG, Cinamon G, *et al.* Lymphocyte egress from thymus and peripheral lymphoid organs is dependent on S1P receptor 1. *Nature* 2004;427:355–360.
 92. Luckheeram RV, Zhou R, Verma AD, Xia B. CD4+T cells: differentiation and functions. *Clin. Dev. Immunol.* 2012;2012:925135.
 93. Vignali DAA, Collison LW, Workman CJ. How regulatory T cells work. *Nat. Rev. Immunol.* 2008;8:523–532.
 94. Kaech SM, Cui W. Transcriptional control of effector and memory CD8+ T cell differentiation. *Nat. Rev. Immunol.* 2012;12:749–761.
 95. Frostegård J, Ulfgrén AK, Nyberg P, *et al.* Cytokine expression in advanced human atherosclerotic plaques: dominance of pro-inflammatory (Th1) and macrophage-stimulating cytokines. *Atherosclerosis* 199;145:33–43.
 96. Roselaar SE, Kakkanathu PX, Daugherty A. Lymphocyte populations in atherosclerotic lesions of apoE -/- and LDL receptor -/- mice. Decreasing density with disease progression. *Arterioscler. Thromb. Vasc. Biol.* 1996;16:1013–1018.
 97. Stemme S, Faber B, Holm J, *et al.* T lymphocytes from human atherosclerotic plaques recognize oxidized low density lipoprotein. *Proc. Natl. Acad. Sci.* 1995;92:3893–3897.
 98. Zhou X, Nicoletti A, Elhage R, Hansson GK. Transfer of CD4(+) T cells aggravates atherosclerosis in immunodeficient apolipoprotein E knockout mice. *Circulation* 2000;102:2919–2922.
 99. Buono C, Come CE, Stavrakis G, *et al.* Influence of interferon-gamma on the extent and phenotype of diet-induced atherosclerosis in the LDLR-deficient mouse. *Arterioscler. Thromb. Vasc. Biol.* 2003;23:454–460.
 100. King VL, Szilvassy SJ, Daugherty A. Interleukin-4 deficiency decreases atherosclerotic lesion formation in a site-specific manner in female LDL receptor-/- mice. *Arterioscler. Thromb. Vasc. Biol.* 2002;22:456–461.
 101. Erickson LD, Foy TM, Waldschmidt TJ. Murine B1 B cells require IL-5 for optimal T cell-dependent activation. *J. Immunol.* 2001;166:1531–1539.
 102. Smith E, Prasad KM, Butcher M *et al.* Blockade of interleukin-17A results in reduced atherosclerosis in apolipoprotein E-deficient mice. *Circulation* 2010;121:1746–1755.
 103. Madhur MS, Funt SA, Li L, Vinh A, *et al.* Role of interleukin 17 in inflammation, atherosclerosis, and vascular function in apolipoprotein e-deficient mice. *Arterioscler. Thromb. Vasc. Biol.* 2011;31:1565–1572.
 104. Elhage R, Gourdy P, Bouchet L, *et al.* Deleting TCR alpha beta+ or CD4+ T lymphocytes leads to opposite effects on site-specific atherosclerosis in female apolipoprotein E-deficient mice. *Am. J. Pathol.* 2004;165:2013–2018.
 105. Kyaw T, Winship A, Tay C, *et al.* Cytotoxic and proinflammatory CD8+ T lymphocytes promote development of vulnerable atherosclerotic plaques in apoE-deficient mice. *Circulation* 2013;127:1028–1039.
 106. Baumgarth, N. The double life of a B-1 cell: self-reactivity selects for protective effector functions. *Nat. Rev. Immunol.* 2011;11:34–46.
 107. Pieper K, Grimbacher B, Eibel H. B-cell biology and development. *J. Allergy Clin. Immunol.* 2013;131:959–971.
 108. Campbell KA, Lipinski MJ, Doran AC, *et al.* Lymphocytes and the adventitial immune response in atherosclerosis. *Circ. Res.* 2012;110:889–900.

109. Caligiuri G, Nicoletti A, Poirier B, Hansson GK. Protective immunity against atherosclerosis carried by B cells of hypercholesterolemic mice. *J. Clin. Invest.* 2002;109:745–753.
110. Ait-Oufella H, Herbin O, Bouaziz JD, *et al.* B cell depletion reduces the development of atherosclerosis in mice. *J. Exp. Med.* 2010;207:1579–1587.
111. Van Leeuwen M, Damoiseaux J, Duijvestijn A, Tervaert JWC. The therapeutic potential of targeting B cells and anti-oxLDL antibodies in atherosclerosis. *Autoimmun. Rev.* 2009;9:53–57.
112. Kyaw T, Tay C, Khan A, *et al.* Conventional B2 B cell depletion ameliorates whereas its adoptive transfer aggravates atherosclerosis. *J. Immunol.* 2010;185:4410–4419.
113. Sage AP, Tsiantoulas D, Baker L, *et al.* BAFF receptor deficiency reduces the development of atherosclerosis in mice--brief report. *Arterioscler. Thromb. Vasc. Biol.* 2012;32:1573–1576.
114. Kyaw T, Tay C, Krishnamurthi S, *et al.* B1a B lymphocytes are atheroprotective by secreting natural IgM that increases IgM deposits and reduces necrotic cores in atherosclerotic lesions. *Circ. Res.* 2011;109:830–840.
115. Tsiantoulas D, Diehl CJ, Witztum JL, Binder CJ. B Cells and Humoral Immunity in Atherosclerosis. *Circ. Res.* 2014;114:1743–1756.
116. Bouaziz JD, Yanaba K, Tedder TF. Regulatory B cells as inhibitors of immune responses and inflammation. *Immunol. Rev.* 2008;224:201–214.
117. Mann DL. The emerging role of innate immunity in the heart and vascular system: for whom the cell tolls. *Circ. Res.* 2011;108:1133–1145.
118. Beutler B. Inferences, questions and possibilities in Toll-like receptor signalling. *Nature* 2004;430:257–263.
119. O'Neill LAJ, Bowie AG. The family of five: TIR-domain-containing adaptors in Toll-like receptor signalling. *Nat. Rev. Immunol.* 2007;7:353–364.
120. Lee CC, Avalos AM, Ploegh HL. Accessory molecules for Toll-like receptors and their function. *Nat. Rev. Immunol.* 2012;12:168–179.
121. Kanzler H, Barrat FJ, Hessel EM, Coffman RL. Therapeutic targeting of innate immunity with Toll-like receptor agonists and antagonists. *Nat. Med.* 2007;13:552–559.
122. Watters TM, Kenny EF, O'Neill LAJ. Structure, function and regulation of the Toll/IL-1 receptor adaptor proteins. *Immunol. Cell Biol.* 2007;85:411–419.
123. Björkbacka H, Kunjathoor VV, Moore KJ, *et al.* Reduced atherosclerosis in MyD88-null mice links elevated serum cholesterol levels to activation of innate immunity signaling pathways. *Nat. Med.* 2004;10:416–421.
124. Michelsen KS, Wong MH, Shah PK, *et al.* Lack of Toll-like receptor 4 or myeloid differentiation factor 88 reduces atherosclerosis and alters plaque phenotype in mice deficient in apolipoprotein E. *Proc. Natl. Acad. Sci. U. S. A.* 2004;101:10679–10684.
125. Liu X, Ukai T, Yumoto H, *et al.* Toll-like receptor 2 plays a critical role in the progression of atherosclerosis that is independent of dietary lipids. *Atherosclerosis* 2008;196:146–154.
126. Salagianni M, Galani IE, Lundberg AM, *et al.* Toll-like receptor 7 protects from atherosclerosis by constraining 'inflammatory' macrophage activation. *Circulation* 2012;126:952–962.
127. Cole JE, Kassiteridi C, Monaco C. Toll-like receptors in atherosclerosis: a 'Pandora's box' of advances and controversies. *Trends Pharmacol. Sci.* 2013;34:629–636.
128. Akashi-Takamura S, Miyake K. TLR accessory molecules. *Curr. Opin. Immunol.* 2008;20:420–425.
129. Akashi S, Ogata H, Kirikae F, *et al.* Regulatory roles for CD14 and phosphatidylinositol in the signaling via toll-like receptor 4-MD-2. *Biochem. Biophys. Res. Commun.* 2000;268:172–177.
130. Ogata H, Su I, Miyake K, *et al.* The toll-like receptor protein RP105 regulates lipopolysaccharide signaling in B cells. *J. Exp. Med.* 2000;192:23–29.
131. Miyake K, Yamashita Y, Ogata M, Sudo T, Kimoto M. RP105, a novel B cell surface molecule implicated in B cell activation, is a member of the leucine-rich repeat protein family. *J. Immunol.* 1995;154:3333–3340.
132. Yoon S, Hong M, Wilson IA. An unusual dimeric structure and assembly for TLR4 regulator RP105-MD-1. *Nat. Struct. Mol. Biol.* 2011;18:1028–1035.
133. Divanovic S, Trompette A, Atabani SF, *et al.* Inhibition of TLR-4/MD-2 signaling by RP105/MD-1. *J. Endotoxin Res.* 2005;11:363–368.
134. Divanovic S, Trompette A, Atabani SF, *et al.* Negative regulation of Toll-like receptor 4 signaling by the Toll-like receptor homolog RP105. *Nat. Immunol.* 2005;6:571–578.
135. Geng H, Wang A, Rong G, *et al.* The effects of ox-LDL in human atherosclerosis may be mediated in part via the toll-like receptor 4 pathway. *Mol. Cell. Biochem.* 2010;342:201–206.

136. Hollestelle SCG, De Vries MR, Van Keulen JK, *et al.* Toll-like receptor 4 is involved in outward arterial remodeling. *Circulation* 2004;109:393–398.
137. Lu Z, Zhang X, Li Y, Jin J, Huang Y. TLR4 antagonist reduces early-stage atherosclerosis in diabetic apolipoprotein E-deficient mice. *J. Endocrinol.* 2013;216:61–71.
138. Higashimori M, Tatro JB, Moore KJ, *et al.* Role of toll-like receptor 4 in intimal foam cell accumulation in apolipoprotein E-deficient mice. *Arterioscler. Thromb. Vasc. Biol.* 2011;31:50–57.
139. Karper JC, de Vries MR, van den Brand BT, *et al.* Toll-like receptor 4 is involved in human and mouse vein graft remodeling, and local gene silencing reduces vein graft disease in hypercholesterolemic APOE*3Leiden mice. *Arterioscler. Thromb. Vasc. Biol.* 2013;33:2810–2817.
140. Karper JC, Ewing MM, de Vries MR, *et al.* TLR accessory molecule RP105 (CD180) is involved in post-interventional vascular remodeling and soluble RP105 modulates neointima formation. *PLoS One* 2013;8:e67923.
141. Karper JC, de Jager SC, Ewing MM, *et al.* An unexpected intriguing effect of Toll-like receptor regulator RP105 (CD180) on atherosclerosis formation with alterations on B-cell activation. *Arterioscler. Thromb. Vasc. Biol.* 2013;33:2810–2817.
142. Walport MJ. Complement. First of two parts. *N. Engl. J. Med.* 2001;344:1058–1066.
143. Speidl WS, Kastl SP, Huber K, Wojta J. Complement in atherosclerosis: friend or foe? *J. Thromb. Haemost.* 2011;9:428–440.
144. Huber-Lang M, Sarma JV, Zetoune FS, *et al.* Generation of C5a in the absence of C3: a new complement activation pathway. *Nat. Med.* 2006;12:682–687.
145. Klos A, Tenner AJ, Johswich KO, *et al.* The role of the anaphylatoxins in health and disease. *Mol. Immunol.* 2009;46:2753–2766.
146. Ricklin D, Hajishengallis G, Yang K, Lambris JD. Complement: a key system for immune surveillance and homeostasis. *Nat. Immunol.* 2010;11:785–797.
147. Haskard DO, Boyle JJ, Mason JC. The role of complement in atherosclerosis. *Curr. Opin. Lipidol.* 2008;19:478–482.
148. Oksjoki R, Laine P, Helske S, *et al.* Receptors for the anaphylatoxins C3a and C5a are expressed in human atherosclerotic coronary plaques. *Atherosclerosis.* 2007;195:90–99.
149. Buono C, Come CE, Witztum JL, *et al.* Influence of C3 deficiency on atherosclerosis. *Circulation.* 2002;105:3025–3031.
150. Persson L, Borén J, Robertson AK, *et al.* Lack of complement factor C3, but not factor B, increases hyperlipidemia and atherosclerosis in apolipoprotein E^{-/-} low-density lipoprotein receptor^{-/-} mice. *Arterioscler. Thromb. Vasc. Biol.* 2004;24:1062–1067.
151. Schepers A, de Vries MR, van Leuven CJ, *et al.* Inhibition of complement component C3 reduces vein graft atherosclerosis in apolipoprotein E3-Leiden transgenic mice. *Circulation.* 2006;114:2831–2838.
152. Wu G, Hu W, Shahsafaei A, *et al.* Complement regulator CD59 protects against atherosclerosis by restricting the formation of complement membrane attack complex. *Circ. Res.* 2009;104:550–558.
153. Lewis RD, Perry MJ, Guschina IA, *et al.* CD55 deficiency protects against atherosclerosis in ApoE-deficient mice via C3a modulation of lipid metabolism. *Am. J. Pathol.* 2011;179:1601–1607.
154. Schmiedt W, Kinscherf R, Deigner HP, *et al.* Complement C6 deficiency protects against diet-induced atherosclerosis in rabbits. *Arterioscler. Thromb. Vasc. Biol.* 1998;18:1790–1795.
155. Speidl WS, Exner M, Amighi J, *et al.* Complement component C5a predicts future cardiovascular events in patients with advanced atherosclerosis. *Eur. Heart J.* 2005;26:2294–2299.
156. Lee RC, Ambros V. An extensive class of small RNAs in *Caenorhabditis elegans*. *Science.* 2001;294:862–864.
157. Lagos-Quintana M, Rauhut R, Lendeckel W, Tuschl T. Identification of novel genes coding for small expressed RNAs. *Science.* 2001;294:853–858.
158. Lau NC, Lim LP, Weinstein EG, Bartel DP. An abundant class of tiny RNAs with probable regulatory roles in *Caenorhabditis elegans*. *Science.* 2001;294:858–862.
159. Horie T, Baba O, Kuwabara Y, *et al.* MicroRNA-33 deficiency reduces the progression of atherosclerotic plaque in ApoE^{-/-} mice. *J. Am. Heart Assoc.* 2012;1:e003376.
160. Rayner KJ, Esau CC, Hussain FN, *et al.* Inhibition of miR-33a/b in non-human primates raises plasma HDL and lowers VLDL triglycerides. *Nature.* 2011;478:404–407.
161. Rayner KJ, Sheedy FJ, Esau CC, *et al.* Antagonism of miR-33 in mice promotes reverse cholesterol transport and regression of atherosclerosis. *J. Clin. Invest.* 2011;121:2921–2931.
162. Rotllan N, Ramírez CM, Aryal B, Esau CC, Fernández-Hernando C. Therapeutic silencing of

- microRNA-33 inhibits the progression of atherosclerosis in Ldlr^{-/-} mice--brief report. *Arterioscler. Thromb. Vasc. Biol.* 2013;33:1973–1977.
163. Marquart TJ, Wu J, Lusis AJ, Baldán Á. Anti-miR-33 therapy does not alter the progression of atherosclerosis in low-density lipoprotein receptor-deficient mice. *Arterioscler. Thromb. Vasc. Biol.* 2013;33:455–458.
164. Nazari-Jahantigh M, Wei Y, Noels H, *et al.* MicroRNA-155 promotes atherosclerosis by repressing Bcl6 in macrophages. *J. Clin. Invest.* 2012;122:4190–4202.
165. Huang R, Hu G, Lin B, Lin Z, Sun C. MicroRNA-155 silencing enhances inflammatory response and lipid uptake in oxidized low-density lipoprotein-stimulated human THP-1 macrophages. *J. Investig. Med.* 2010;58:961–967.

Chapter 2

The role of mast cells in atherosclerosis

Hämostaseologie, in press

Anouk Wezel^{1,2}
Paul H. A. Quax²
Johan Kuiper¹
Ilze Bot¹

¹Division of Biopharmaceutics, Gorlaeus Laboratories, Leiden Academic Center for Drug Research, Leiden University, Leiden, The Netherlands

²Department of Surgery, Leiden University Medical Center, Leiden, The Netherlands

Abstract

Rupture of an atherosclerotic plaque is the major underlying cause of adverse cardiovascular events such as myocardial infarction or stroke. Therapeutic interventions should therefore be directed towards inhibiting growth of atherosclerotic lesions as well as towards prevention of lesion destabilization. Interestingly, the presence of mast cells has been demonstrated in both murine and human plaques, and multiple interventional murine studies have pointed out a direct role for mast cells in early and late stages of atherosclerosis. Moreover, it has recently been described that activated lesional mast cells correlate with major cardiovascular events in patients suffering from cardiovascular disease. The current review focuses on the effect of different mast cell derived mediators in atherogenesis and in late stage plaque destabilization. Also, possible ligands for mast cell activation in the context of atherosclerosis are discussed. Finally, we will elaborate on the predictive value of mast cells, together with therapeutic implications, in cardiovascular disease.

Introduction

Atherosclerosis is still among the leading causes of death worldwide, responsible for major cardiovascular events such as myocardial infarction, stroke and peripheral artery disease. Over the recent years, evidence has accumulated in which a detrimental role for mast cells in atherosclerosis is described. Mast cells are long-lived cells commonly present in tissues exposed to the outside environment, such as the skin, the gastrointestinal tract and the lungs, where they play a key role in innate immunity by functioning as sentinels. At these strategic places mast cells reside in close proximity to blood vessels, nerves and lymphatics, allowing them to rapidly act upon an encounter with foreign threats¹. Mast cells are derived from progenitor cells and originate in the bone marrow; they home to tissues in response to locally produced stem cell factor (SCF) by fibroblasts, stromal cells and endothelial cells. The receptor for SCF is c-kit, a tyrosine kinase receptor expressed on the membrane of mast cells. SCF is required for the differentiation and maturation of mast cells, a necessity that becomes evident in mice carrying a mutation in their c-kit gene, which results in complete mast cell deficiency^{2,3}.

After activation, mast cells exert their adverse effects through the excretion of pre-formed granules loaded with a vast array of mediators, including histamine, vascular endothelial growth factor (VEGF), various inflammatory cytokines (for example TNF α and IL-6), and the proteases tryptase, chymase and carboxypeptidase A3 (CPA3)⁴. These stored granules give mast cells their typical morphologic appearance which originally led to their name 'Mastzellen', meaning well-fed cells. Mast cell activation may be triggered by different ligands, including IgE, complement components, neuropeptides and TLR ligands. Although their presence is highly important to combat bacterial and parasitic infections, mast cells are actually commonly known for their contribution to diseases such as allergic asthma and IgE dependent allergic responses.

A role for mast cells in the setting of atherosclerosis has first been described over 60 years ago. It was discovered that heparin attenuates atherosclerotic lesion development in high-cholesterol fed rabbits, and heparin was postulated to be produced by mast cells in the connective tissue surrounding the blood vessels⁵. However, as the important contribution of inflammation to the atherosclerotic process received increasing recognition, mast cells were later in fact discovered to aggravate atherosclerosis. Atherosclerosis is a chronic disease of the middle and large-sized vessels, often occurring at sites of low or oscillatory endothelial shear stress. In early atherogenesis, monocytes enter the vessel wall and differentiate into macrophages, which can scavenge modified LDL and turn into foam cells. Continued inflammation can eventually result in the formation of advanced unstable lesions, consisting of a large necrotic core, a thin fibrous cap, luminal erosions, a high inflammatory cell count and multiple leaky neovessels. Rupture

of the plaque may lead to acute thrombus formation with subsequent adverse cardiovascular events such as myocardial infarction or stroke⁶, for which lesional mast cells have recently been shown to have a predictive value⁷.

This review focuses on the role of the mast cell in both early and late stages of atherosclerosis, with particular emphasis on lesion destabilization with subsequent plaque rupture. Also, we will elaborate on the predictive value of mast cells, as well as on potential therapeutic implications, in cardiovascular disease.

The role of mast cells in atherosclerotic lesion development

The presence of both resting and degranulated mast cells has been established in human coronary arteries and aortas without signs of atherosclerosis and interestingly, mast cell numbers, as well as their activation status, are increased at sites of foam cell accumulation in the vessel wall⁸. The buildup of intimal foam cells is a key event in atherogenesis, caused by excessive uptake of modified LDL particles by macrophages combined with insufficient cholesterol efflux. Mast cells may influence the impaired cholesterol regulation via different pathways. First, it has been demonstrated in *in vitro* studies, that the mast cell releasate strongly enhances uptake of LDL by macrophages. Also, LDL can bind to granule remnants derived from the mast cell, fuse into larger particles, and subsequently be scavenged by macrophages and smooth muscle cells⁹. Second, the mast cell may promote foam cell formation by secreting tryptase, which is capable of degrading pre- β -high-density lipoprotein (HDL). As HDL particles have the ability to remove cholesterol from the macrophage and transport it back to the circulation, inhibition of the production of mature HDL via mast cell tryptase can thus impair reverse cholesterol transport¹⁰ and may aggravate atherosclerotic lesion development.

Upon activation, mast cells release a variety of chemokines, amongst which are CXCL1, CXCL2, CXCL10, CCL2, CCL3 and CCL5 (Figure 1)⁴. CCL2 is one of the chemokines which has been suggested to play a role in leukocyte recruitment to the atherosclerotic lesion¹¹. Also, inhibition of CCR5, the prime receptor for CCL5, was recently shown to decrease atherosclerosis¹². CCL3, CXCL1 and CXCL2 all have the potential to attract neutrophils to the site of inflammation¹³⁻¹⁶ and indeed, we have recently observed a profound influx of neutrophils to the atherosclerotic plaque after chronic mast cell activation¹⁷. Thus, mast cell derived chemokines may exacerbate atherogenesis by attracting multiple inflammatory cells to the lesion.

Most *in vivo* studies investigating mast cell effects in cardiovascular diseases have been performed in mice. Mast cell deficient Kit(W/W^{-v}) mice were first described by Kitamura *et al.* and these mice have, besides a lack of mast cells, impaired melanogenesis, anemia, and sterility³. Although it has been shown that following acute restraint stress, cardiac histamine release is impaired in Kit(W/W^{-v}) mice¹⁸, there is no data available on the effects on atherosclerosis in these mice. More

recently, a mast cell deficient $\text{Kit}^{\text{W-sh/W-sh}}$ mice has been reported², which has been backcrossed on either an LDLr or ApoE deficient background. These mice are also mast cell deficient, but lack the anemia and sterility. It should be taken into account however, that these mice have increased numbers of neutrophils and platelets in the blood that may affect atherosclerosis as well.

Direct *in vivo* evidence for a detrimental role of the mast cell in atherosclerotic lesion development was provided in 2007, when it was established that lesion formation in the brachiocephalic arteries was markedly aggravated after systemic mast cell activation in apolipoprotein E (apoE) knockout mice on a high cholesterol diet. Moreover, treatment with the mast cell stabilizer cromolyn in this experimental setup significantly reduced lesion size back to control level. The observed effects on atherosclerosis were independent of cholesterol metabolism, since no effect on plasma cholesterol levels were reported¹⁹. These findings were confirmed by Sun *et al.*, who demonstrated that mice deficient for mast cells ($\text{Kit}^{\text{W-sh/W-sh}}$), crossbred on an LDLr^{-/-} background, displayed reduced atherogenesis. Interestingly, the observed reduction in lesion size was again increased after the transfer of TNF α deficient mast cells, but not after that of IL-6 or IFN γ deficient mast cells, indicating an important role for these inflammatory cytokines in atherosclerosis. Cholesterol levels were lower in IL-6 deficient mast cell reconstituted mice, but not in mice receiving wild type or IFN γ deficient mast cells²⁰. In a study performed by Heikkilä *et al.*, mast cell function in atherosclerosis was investigated in LDLr^{-/-} $\text{Kit}^{\text{W-sh/W-sh}}$ as well. In line with the previous reports, mast cell deficient mice developed significantly reduced atherosclerotic lesions in the aortic sinuses compared to control LDLr^{-/-} mice²¹. However, serum cholesterol and triglyceride levels were lower in mice lacking mast cells, which was accompanied by a decrease in pre- β -HDL. These data indicate that although mast cells clearly aggravate early atherosclerotic lesion development, the exact contribution of alterations in cholesterol metabolism versus inflammatory actions remains to be further elucidated.

Effects of mast cell derived mediators on plaque destabilization

Advanced atherosclerotic plaques containing a thick fibrous cap and preserved lumen area may remain stable for years without apparent clinical manifestations²². Therefore, it is more compelling to study the mechanisms behind plaque destabilization, in which mast cells are thought to be of importance as well (Figure 1). A potential connection between the mast cell and unstable lesions was first proposed by Kovanen *et al.* who observed increased numbers of degranulated mast cells in ruptured coronary plaques and in plaques displaying erosions, compared to unaffected intimas, in autopsy material from patients who had died from myocardial infarction²³. A causal role for mast cells in plaque destabilization was later demonstrated after perivascular mast cell activation in apoE^{-/-} mice with established atherosclerotic lesions in their carotid arteries. Focal mast cell activation

at the lesion site profoundly increased the incidence of intraplaque hemorrhages, while also the percentage of apoptotic cells in the lesion was increased, both indicative of reduced plaque stability¹⁹. Also, mast cell deficient LDLR^{-/-}Kit^{W-sh/W-sh} mice have been described to contain more stable lesions with decreased apoptosis and increased collagen content and fibrous cap thickness²⁰.

Various mast cell derived mediators are postulated to contribute to plaque destabilization, amongst which are the specific neutral proteases chymase and tryptase. In humans, mast cells are divided into two subtypes according to their protease content, namely MC_T cells (expressing tryptase α and β) or MC_{TC} cells (expressing α and β tryptase, chymase and carboxypeptidase A), both of which have been identified in atherosclerotic plaques²⁴. Also, murine mast cells are classified as either connective tissue type mast cells (expressing chymase mMCP-4 and -5; and tryptase mMCP-6 and -7) and mucosal mast cells (expressing chymase mMCP-1 and -2)²⁵. In the perivascular tissue of murine atherosclerotic plaques, mostly the connective tissue type mast cells are present. Besides the differences in protease content between murine and human mast cells, increased levels of IL-4 and TNF α and a higher expression of the IL-3 receptor have been observed in murine mast cells, which is important to keep in mind when comparing human data to murine data. The potent protease chymase is stored and secreted as a fully active enzyme, involved in a number of pathways that may affect atherosclerotic lesion stability. For instance, chymase acts as an angiotensin converting enzyme generating the potent vasoconstrictor angiotensin II, a potent stimulus for the generation of reactive oxygen species²⁶. Furthermore, chymase facilitates the conversion of pro-matrix metalloproteinases (pro-MMPs) to the active enzymes MMP1 and MMP3, which in turn may activate MMP2 and MMP9, leading to matrix degradation²⁷. Also, chymase itself has the ability to cleave the extracellular matrix proteins vitronectin and procollagen, all possibly contributing to thinning of the fibrous cap. A number of *in vitro* studies have demonstrated that chymase exerts pro-apoptotic effects on smooth muscle cells and endothelial cells via disruption of focal adhesion complexes necessary for cell survival^{28,29}. While smooth muscle cell apoptosis leads to additional impairment of the integrity of the cap, apoptosis of endothelial cells may result in plaque erosions and leaky neovessels. Finally, it has been reported that chymase acts as a chemoattractant, attracting multiple immune cells such as neutrophils to the site of inflammation³⁰. A direct *in vivo* role for chymase was confirmed after inhibition of chymase in apoE^{-/-} mice, which indeed significantly improved atherosclerotic plaque stability by increasing lesional collagen content, decreasing necrotic core size and reducing the incidence of intraplaque hemorrhage³¹.

Similarly to the effector functions of chymase, tryptase released by the mast cell can also induce chemotaxis and matrix degradation. The importance of tryptase in atherosclerosis was demonstrated by Zhi *et al.*, who showed that systemic len-

tiviral overexpression of tryptase in apoE^{-/-} mice aggravated both plaque size as well as the frequency of intraplaque hemorrhages³². The increase in incidence of hemorrhages observed in this study were suggested to be caused by enhanced lesional angiogenesis due to alterations in the expression of plasminogen activator inhibitor-1 (PAI-1) and tissue plasminogen activator (tPA) following tryptase overexpression. However, it is unlikely that tryptase is the sole culprit actor in mast cell induced angiogenesis. In fact, the potent angiogenic mediator basic fibroblast growth factor (bFGF) is known to be stored and secreted by the mast cell as well, and a positive correlation has previously been found between numbers of bFGF positive mast cells and microvessel density in human plaques. Also, the percentage of bFGF positive mast cells was higher in advanced atherosclerotic lesions compared to the unaffected intima³³. Furthermore, mast cells secrete vascular endothelial growth factor (VEGF), which is well-known to induce neovascularization. Although a direct role for mast cell derived VEGF has not been demonstrated yet in atherosclerosis, it is likely that VEGF may also contribute to the formation of intraplaque neovessels. Increased leakage of these intraplaque neovessels may be induced by the mast cell product histamine. Histamine exerts its effects by binding to members of the histamine receptor family, which consists of histamine receptors H1, H2, H3 and H4. Binding of histamine to the H1 receptor on endothelial cells was shown to induce vascular permeability³⁴. Vascular leakage, but also macrophage apoptosis, induced by mast cell derived histamine was shown to be solely dependent on the H1 receptor¹⁹. Smooth muscle cells also express the H1 receptor and are promoted to contract upon binding of histamine, which can generate vasospasms. Rozenberg *et al.* demonstrated a role for the H1 receptor by treating apoE^{-/-} mice with an H1 receptor antagonist, which resulted in reduced lesion formation. Correspondingly, genetic deletion of the H1 receptor decreased lesion size, while no effects were observed after blocking or deleting the H2 receptor³⁵. Mice deficient for H1 receptor displayed reduced vascular permeability for LDL in the aortic wall, which was suggested to account for the observed effects on atherosclerosis.

Mast cell activators in atherosclerosis

Multiple mediators are capable of inducing mast cell activation (Figure 1), the most famous of which is IgE mediated degranulation. Mast cells express the high affinity receptor FcεRI which can bind to IgE in a practically irreversible manner. Each cell carries a range of IgE molecules bound to the FcεRI with varying antigen specificity. Upon encountering the antigen, mast cells are promptly triggered to degranulate. Recently, mice deficient for the FcεRIα on an apoE^{-/-} background were shown to display reduced lipid depositions in the aortic arch when fed a western type diet. Furthermore, lesions contained fewer macrophages, T cells and apoptotic cells, as well as lower levels of inflammatory cytokines. *In vitro*, IgE activa-

tion was seen to affect inflammatory signalling and apoptosis in macrophages, smooth muscle cells and endothelial cells, therefore in this study, mast cell specific effects remain to be identified³⁶.

In order to discover potential therapeutic leads for mast cell stabilization in atherosclerosis, it is crucial to further elucidate the underlying mechanisms of mast cell activation in the setting of atherosclerosis. Ligands present in the lesion or the underlying adventitial tissue, capable of inducing local mast cell activation, may thus be promising targets. For instance, the complement component C5a has been detected in human atherosclerotic plaques in lipid-rich inflammatory regions³⁷, and mast cells are known to express the receptor for C5a. Interestingly, treatment with a C5a receptor antagonist decreased lesion size in a murine vein graft model, while perivascular application of C5a during disease initiation aggravated lesion formation. More importantly, C5a application combined with cromolyn treatment significantly reduced lesion size to control level, indicative of a mast cell dependent effect³⁸. In late stages of vein graft disease, C5a was seen to promote vein graft destabilization in a mast cell independent fashion³⁹. Although mast cells are also known to express the receptor for C3a via which they can be activated, the interactions between C3a, mast cells and atherosclerosis have not yet been elucidated.

Toll-like receptors (TLRs) are pattern recognition receptors widely expressed by cells of the innate immune system. Murine mast cells express TLR 1 to TLR9, with the exception of TLR5, while human mast cells express TLR1 to TLR7, TLR9 and TLR10. Currently, the mechanism of mast cell activation via TLRs is still under debate, in particular the effects on degranulation versus mere cytokine release. While some groups have shown that activation of TLR2 on murine and human mast cells with peptidoglycan results in degranulation, others have been unable to reproduce these results⁴⁰. Also, mast cell degranulation following TLR4 activation with for example LPS has not often been observed; instead, this triggers the release of various pro-inflammatory cytokines and chemokines. With regard to atherosclerosis, TLR4 is of particular interest, for different endogenous ligands present in the plaque are proposed to be able to induce TLR4 signalling, including heat shock protein 60 (hsp60), extra domain A of fibronectin (EDA), oxidized LDL (oxLDL), fibrinogen and HMGB1⁴¹. It should be noted however that endotoxin contamination may also induce TLR4 signalling, complicating this area of research and sometimes leading to the finding of 'false-positive' TLR4 ligands. Den Dekker *et al.* showed that mast cells promote plaque destabilization in a TLR4 dependent manner *in vivo* via chymase-induced smooth muscle cell apoptosis⁴². In contrast to previous reports, mast cell degranulation as measured by chymase release after TLR4 activation was observed. It was postulated that TLR4 signalling induces release of proinflammatory cytokines, including IL-6, which then in an autocrine manner trigger mast cell degranulation with chymase release, thereby causing

smooth muscle cell apoptosis. Since TLR4 in that study was activated by E. Coli lipopolysaccharide (LPS) and inhibited by a general TLR4 antagonist, it remains to be investigated which exact endogenous ligands contribute *in vivo* to mast cell activation in atherosclerosis.

In addition to serving as an endogenous ligand for TLR4, oxLDL may also form antigen-antibody complexes with autoantibodies directed against oxLDL, mainly of the IgG isotype. Immune complexes are present in the circulation of patients with cardiovascular disease⁴³, as well as in the atherosclerotic plaque itself. Mast cells express FcγRs that bind monomeric IgG with low affinity while they can bind to antigen-antibody complexes with a relatively high affinity. *In vitro* studies have shown that oxLDL-IgG immune complexes are capable of inducing mast cell activation, as indicated by increased secretion of tryptase, chymase, histamine, TNFα, IL-6 and CCL2⁴⁴.

One of the major lipid parts of modified LDL is lysophosphatidic acid (LPA). This naturally occurring lysophospholipid has recently been described as a potential mast cell activator in atherosclerosis⁴⁵. With the use of mass spectrometry it was established that several LPA species are present in the plaque, especially in the necrotic core area. Exposure of mast cells to LPA *in vitro* resulted in exacerbated degranulation and cytokine release. Similarly, intraperitoneal injection of LPA increased tryptase levels in the peritoneal fluid, which was absent in mast cell deficient Kit^{W-sh/W-sh} mice. *In vivo*, perivascular application of LPA in established lesions increased the macrophage content and the frequency of intraplaque hemorrhages. These effects were suggested to be mast cells specific, since cromolyn was able to reduce both the number of hemorrhages and the percentage of lesional macrophages. Also, LPA administration in mast cell deficient mice did not significantly increase the percentage of macrophages nor the intraplaque hemorrhages. Adventitial mast cells have been found in close proximity to sensory nerve fibers in human coronary arteries, and the number of mast cell- nerve contacts was seen to increase with lesion progression⁴⁶. These nerves stained positive for the neuropeptides substance P and calcitonin gene-related peptide (CGRP), both capable of stimulating mast cells. Furthermore, mast cell numbers were seen to correlate with the number of neurofilament⁺ nerve fibers in coronary artery specimens⁴⁶. Taken together, these findings led to the hypothesis that neuronal activation may trigger adventitial mast cells in the setting of atherosclerosis. Indeed, it was established that local application of substance P in apoE^{-/-} mice increased both mast cell numbers as well as their activation status and moreover, the frequency of intraplaque hemorrhages was significantly enhanced. These findings were postulated to be mast cell specific, since substance P application in mast cell deficient apoE^{-/-} Kit^{W-sh/W-sh} mice was ineffective⁴⁷. Recently, also neuropeptide Y (NPY) has been detected in human endarterectomy plaques. Its expression was twofold higher in unstable lesions compared to stable plaques and local lentiviral

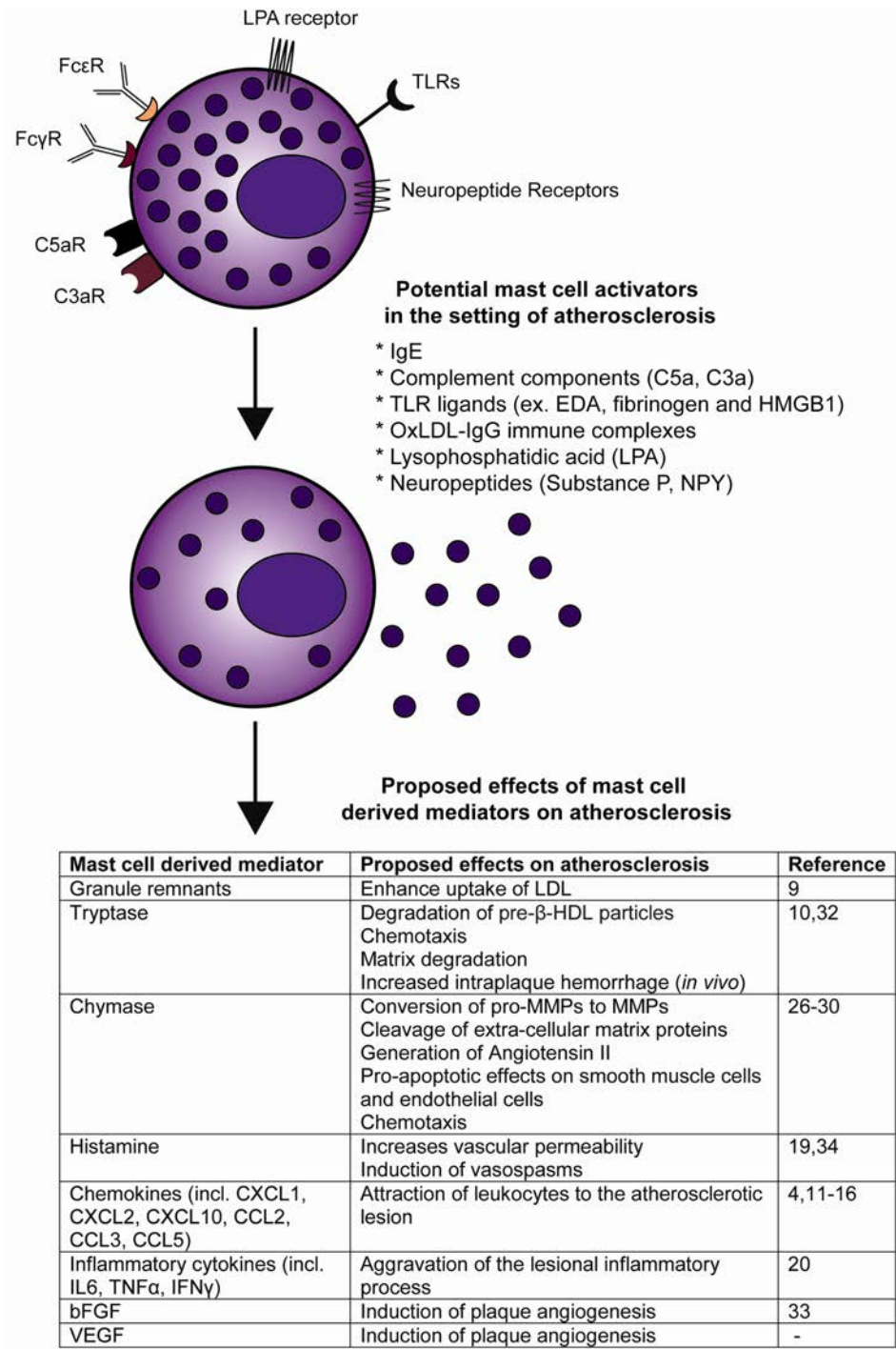


Figure 1. Overview of potential mast cell activators and mast cell derived mediators in atherosclerosis

overexpression of NPY in the carotid artery of apoE^{-/-} mice resulted in increased perivascular mast cell activation, as well as exacerbated atherosclerotic lesion formation⁴⁸. *In vitro* activation of murine mast cells with NPY was shown to induce IL-6 and tryptase release. Since long, it has been suggested that cardiovascular events may be elicited by (chronic) psychological stress. As stress is known to activate sensory nerves with subsequent release of, amongst others, different neuropeptides, it is thus compelling in light of the previous reports to further elucidate the effect of stress-mediated mast cell activation in atherosclerotic plaque destabilization.

Therapeutic implications and conclusions

In addition to the mast cell mediated effects demonstrated in murine experimental models, several case studies in humans reported on a link between acute mast cell activation and cardiovascular events. These findings were first described as the occurrence of an allergic reaction acutely followed by typical angina pectoris, confirmed by clinical and laboratory parameters, now collectively referred to as the 'Kounis syndrome'⁴⁹. It is postulated that mast cell derived mediators such as histamine, proteases and cytokines excreted upon allergic reactions or anaphylactic insults may be responsible for the coronary events. Additional research is required to elucidate whether angina pectoris is caused by vasospasms induced by histamine or by actual plaque destabilization with subsequent embolization. Regardless, the Kounis syndrome clearly illustrates the major impact mast cell activation may have on coronary events.

A few studies have addressed the association between allergic diseases (atopy) and the occurrence of thromboembolism and cardiovascular disease. In a case-control study, the incidence of atopic sensitization and allergic rhinitis were found to be increased in patients with venous thromboembolism⁵⁰. Moreover, in both the Bruneck Study and the ARMY study, enhanced atherosclerosis was observed in patients with allergic diseases⁵¹, suggested to be caused by either a systemic inflammatory response in allergy, or by shared effector pathways in both diseases, such as mast cell activation and leukotriene synthesis. In contrast, a recent study performed by Skaaby *et al.* failed to show a significant association between atopy and the incidence of ischemic heart diseases or stroke⁵². Thus, it remains to be elucidated whether an actual association between allergic diseases and cardiovascular disease exists.

Recently, the atherosclerotic plaques of 270 patients suffering from carotid artery stenosis have been evaluated for the presence of mast cells⁷. In that study, the number of mast cells significantly increased with lesion progression and particularly in unstable lesions, mast cells were seen to accumulate in the rupture-prone shoulder regions. A correlation was observed between mast cell numbers and microvessel density, intraplaque hemorrhages, lesional macrophage and neutrophil

content. Most importantly, during a 3 year follow-up period, adverse events were significantly associated with increased lesional mast cell numbers. Also, higher plasma tryptase levels were observed in patients experiencing a secondary event, indicative of a predictive value for mast cells in cardiovascular disease⁷. However, conflicting evidence prevails in literature regarding the usefulness of tryptase as a biomarker for adverse events. For example, elevated tryptase levels have been observed in patients with significant coronary artery disease⁵³, while a separate study performed by van Haelst *et al.* failed to show differences in serum tryptase levels from patients with acute coronary syndromes as compared to controls⁵⁴. In addition to these studies, several other groups have reported either affirmative or negative findings for the predictive value of tryptase, often limited by a relatively small cohort size. Therefore, future studies are necessary to appoint a definite role for tryptase as a biomarker in cardiovascular disease.

Besides mast cell derived mediators, ligands for mast cell activation have also been investigated as potential biomarkers in cardiovascular disease. Increased levels of the immunoglobulins IgG, IgA and IgE have previously been shown to associate with myocardial infarction and cardiac death in men with dyslipidemia⁵⁵. However, a recent study performed by Willems *et al.* did not show a correlation between plasma oxLDL-IgG, total IgG and total IgE levels and characteristics of a vulnerable plaque in patients which have undergone carotid endarterectomies⁴³. These inconsistencies may be caused by the difference in the location of the atherosclerotic plaques (coronary versus carotid arteries) between the studies. Also, other inflammatory diseases may raise circulating immunoglobulins as well, which in general is a major challenge in the search for predictive markers.

As basophils share some phenotypic similarities with mast cells, such as the FcεR1-expression via which both cell types can be activated, it is interesting to note that some studies have investigated a potential association between blood basophil numbers and the occurrence of cardiovascular disease. However, no correlation was found between the percentage of blood basophils and asymptomatic carotid atherosclerosis⁵⁶, the intima-media thickness of the common carotid artery⁵⁷ or the frequency of restenosis after stenting⁵⁸.

Mast cell stabilization in murine models for atherosclerosis have thus far shown beneficial effects, and taking into account the ample mechanisms via which the mast cell is capable of aggravating atherosclerosis, pharmaceutical mast cell stabilization in patients with cardiovascular disorders may thus yield promising results. As of yet, limited clinical trials in humans suffering from atherosclerosis have been performed using mast cell stabilizers. The antiallergic drug Tranilast has been tested in the PRESTO trial which enrolled over 10.000 patients undergoing percutaneous coronary intervention. No effects were observed in major adverse cardiovascular events or restenosis after a follow-up period of 9 months⁵⁹. It

should be noted that Tranilast also exerts effects on other cell types, such as fibroblasts and endothelial cells, making it difficult to draw any conclusions regarding mast-cell specificity. Interestingly, a patent for the use of mast cell stabilizers in the treatment and prevention of cardiovascular disease has recently been published (US8445437 B2), which may direct further research towards investigating the therapeutic potential of mast cell inhibition in the clinic. However, considering the important role mast cells play as a first line of defense against pathogens, care must be taken with complete systemic mast cell inhibition, and unwanted side-effects such as infections should be tightly monitored.

In conclusion, multiple interventional murine models have demonstrated a direct causal role for mast cell activation in both atherosclerotic lesion development and plaque destabilization. Moreover, increased mast cell activation in humans has been associated with adverse cardiovascular events. Therefore, mast cell stabilization in patients suffering from cardiovascular disease may be a promising therapeutic strategy in order to prevent major complications such as myocardial infarction or stroke.

Acknowledgements

This work was supported by a grant from the Dutch Heart Foundation (A.W.: 2010B029; I.B.: 2012T083). We acknowledge the support from the Netherlands CardioVascular Research Initiative: "the Dutch Heart Foundation, Dutch Federation of University Medical Centres, the Netherlands Organisation for Health Research and Development and the Royal Netherlands Academy of Sciences" for the GENIUS project "Generating the best evidence-based pharmaceutical targets for atherosclerosis" (CVON2011-19).

References

1. Marshall JS. Mast-cell responses to pathogens. *Nat Rev Immunol.* 2004;4:787-99.
2. Grimbaldston MA, Chen CC, Piliponsky AM, Tsai M, Tam SY, Galli SJ. Mast cell-deficient W-sash c-kit mutant Kit W-sh/W-sh mice as a model for investigating mast cell biology in vivo. *Am J Pathol.* 2005;167:835-48.
3. Kitamura Y, Go S, Hatanaka K. Decrease of mast cells in W/W^v mice and their increase by bone marrow transplantation. *Blood.* 1978;52:447-52.
4. Lindstedt KA, Mäyränpää MI, Kovanen PT. Mast cells in vulnerable atherosclerotic plaques--a view to a kill. *J Cell Mol Med.* 2007;11:739-58.
5. Constantinides P. Mast cells and susceptibility to experimental atherosclerosis. *Science.* 1953;117:505-6.
6. Bentzon JF, Otsuka F, Virmani R, Falk E. Mechanisms of plaque formation and rupture. *Circ Res.* 2014;114:1852-66.
7. Willems S, Vink A, Bot I, Quax PH, de Borst GJ, de Vries JP, van de Weg SM, Moll FL, Kuiper J, Kovanen PT, de Kleijn DP, Hoefer IE, Pasterkamp G. Mast cells in human carotid atherosclerotic plaques are associated with intraplaque microvessel density and the occurrence of future cardiovascular events. *Eur Heart J.* 2013;34:3699-706.
8. Kovanen PT. Mast cells in human fatty streaks and atheromas: implications for intimal lipid accumulation. *Curr Opin Lipidol.* 1996;7:281-6.

9. Kovanen PT. The mast cell--a potential link between inflammation and cellular cholesterol deposition in atherogenesis. *Eur Heart J*. 1993;14 Suppl K:105-17.
10. Lee M, Sommerhoff CP, von Eckardstein A, Zettl F, Fritz H, Kovanen PT. Mast cell tryptase degrades HDL and blocks its function as an acceptor of cellular cholesterol. *Arterioscler Thromb Vasc Biol*. 2002;22:2086-91.
11. Boring L, Gosling J, Cleary M, Charo IF. Decreased lesion formation in CCR2^{-/-} mice reveals a role for chemokines in the initiation of atherosclerosis. *Nature*. 1998;394:894-7.
12. Combadière C, Potteaux S, Rodero M, Simon T, Pezard A, Esposito B, Merval R, Proudfoot A, Tedgui A, Mallat Z. Combined inhibition of CCL2, CX3CR1, and CCR5 abrogates Ly6C(hi) and Ly6C(lo) monocytosis and almost abolishes atherosclerosis in hypercholesterolemic mice. *Circulation*. 2008;117:1649-57.
13. De Filippo K, Dudeck A, Hasenberg M, Nye E, van Rooijen N, Hartmann K, Gunzer M, Roers A, Hogg N. Mast cell and macrophage chemokines CXCL1/CXCL2 control the early stage of neutrophil recruitment during tissue inflammation. *Blood*. 2013;121:4930-7.
14. De Jager SC, Bot I, Kraaijeveld AO, Korporaal SJ, Bot M, van Santbrink PJ, van Berkel TJ, Kuiper J, Biessen EA. Leukocyte-specific CCL3 deficiency inhibits atherosclerotic lesion development by affecting neutrophil accumulation. *Arterioscler Thromb Vasc Biol*. 2013;33:e75-83.
15. Döring Y, Soehnlein O, Weber C. Neutrophils cast NETs in atherosclerosis: employing peptidylarginine deiminase as a therapeutic target. *Circ Res*. 2014;114:931-4.
16. Drechsler M, Megens RT, van Zandvoort M, Weber C, Soehnlein O. Hyperlipidemia-triggered neutrophilia promotes early atherosclerosis. *Circulation*. 2010;122:1837-45.
17. Bot I, Wezel A, Lagraauw HM, van der Velden D, de Jager SCA, Quax PHA, Kuiper J. Mast cell mediated neutrophil influx enhances plaque progression. *Cardiovasc. Res*. 2014;103 Suppl 1:S5.
18. Huang M, Pang X, Letourneau R, Boucher W, Theoharides TC. Acute stress induces cardiac mast cell activation and histamine release, effects that are increased in Apolipoprotein E knockout mice. *Cardiovasc Res*. 2002;55:150-60 18.
19. Bot I, de Jager SC, Zernecke A, Lindstedt KA, van Berkel TJ, Weber C, Biessen EA. Perivascular mast cells promote atherogenesis and induce plaque destabilization in apolipoprotein E-deficient mice. *Circulation*. 2007;115:2516-25.
20. Sun J, Sukhova GK, Wolters PJ, Yang M, Kitamoto S, Libby P, MacFarlane LA, Mallen-St Clair J, Shi GP. Mast cells promote atherosclerosis by releasing proinflammatory cytokines. *Nat Med*. 2007;13:719-24.
21. Heikkilä HM, Trosien J, Metso J, Jauhiainen M, Pentikäinen MO, Kovanen PT, Lindstedt KA. Mast cells promote atherosclerosis by inducing both an atherogenic lipid profile and vascular inflammation. *J Cell Biochem*. 2010;109:615-23.
22. Virmani R, Kolodgie FD, Burke AP, Farb A, Schwartz SM. Lessons from sudden coronary death: a comprehensive morphological classification scheme for atherosclerotic lesions. *Arterioscler Thromb Vasc Biol*. 2000;20:1262-75.
23. Kovanen PT, Kaartinen M, Paavonen T. Infiltrates of activated mast cells at the site of coronary atheromatous erosion or rupture in myocardial infarction. *Circulation*. 1995;92:1084-8.
24. Dai H, Korthuis RJ. Mast Cell Proteases and Inflammation. *Drug Discov Today Dis Models*. 2011;8:47-55.
25. Kaartinen M, Penttilä A, Kovanen PT. Mast cells of two types differing in neutral protease composition in the human aortic intima. Demonstration of tryptase- and tryptase/chymase-containing mast cells in normal intimas, fatty streaks, and the shoulder region of atheromas. *Arterioscler Thromb*. 1994;14:966-72.
26. Caughey GH, Raymond WW, Wolters PJ. Angiotensin II generation by mast cell alpha- and beta-chymases. *Biochim Biophys Acta*. 2000;1480:245-57.
27. Johnson JL, Jackson CL, Angelini GD, George SJ. Activation of matrix-degrading metalloproteinases by mast cell proteases in atherosclerotic plaques. *Arterioscler Thromb Vasc Biol*. 1998;18:1707-15.
28. Leskinen MJ, Heikkilä HM, Speer MY, Hakala JK, Laine M, Kovanen PT, Lindstedt KA. Mast cell chymase induces smooth muscle cell apoptosis by disrupting NF-kappaB-mediated survival signaling. *Exp Cell Res*. 2006;312:1289-98.
29. Heikkilä HM, Lätti S, Leskinen MJ, Hakala JK, Kovanen PT, Lindstedt KA. Activated mast cells induce endothelial cell apoptosis by a combined action of chymase and tumor necrosis factor-alpha. *Arterioscler Thromb Vasc Biol*. 2008;28:309-14.
30. Tani K, Ogushi F, Shimizu T, Sone S. Protease-induced leukocyte chemotaxis and activation: roles in

- host defense and inflammation. *J Med Invest.* 2001;48:133-41.
31. Bot I, Bot M, van Heiningen SH, van Santbrink PJ, Lankhuizen IM, Hartman P, Gruener S, Hilpert H, van Berkel TJ, Fingerle J, Biessen EA. Mast cell chymase inhibition reduces atherosclerotic plaque progression and improves plaque stability in ApoE^{-/-} mice. *Cardiovasc Res.* 2011;89:244-52.
 32. Zhi X, Xu C, Zhang H, Tian D, Li X, Ning Y, Yin L. Tryptase promotes atherosclerotic plaque haemorrhage in ApoE^{-/-} mice. *PLoS One.* 2013;8:e60960.
 33. Lappalainen H, Laine P, Pentikäinen MO, Sajantila A, Kovanen PT. Mast cells in neovascularized human coronary plaques store and secrete basic fibroblast growth factor, a potent angiogenic mediator. *Arterioscler Thromb Vasc Biol.* 2004;24:1880-5.
 34. Lu C, Diehl SA, Noubade R, Ledoux J, Nelson MT, Spach K, Zachary JF, Blankenhorn EP, Teuscher C. Endothelial histamine H1 receptor signaling reduces blood-brain barrier permeability and susceptibility to autoimmune encephalomyelitis. *Proc Natl Acad Sci.* 2010;107:18967-72.
 35. Rozenberg I, Sluka SH, Rohrer L, Hofmann J, Becher B, Akhmedov A, Soliz J, Mocharla P, Borén J, Johansen P, Steffel J, Watanabe T, Lüscher TF, Tanner FC. Histamine H1 receptor promotes atherosclerotic lesion formation by increasing vascular permeability for low-density lipoproteins. *Arterioscler Thromb Vasc Biol.* 2010;30:923-30.
 36. Wang J, Cheng X, Xiang MX, Alanne-Kinnunen M, Wang JA, Chen H, He A, Sun X, Lin Y, Tang TT, Tu X, Sjöberg S, Sukhova GK, Liao YH, Conrad DH, Yu L, Kawakami T, Kovanen PT, Libby P, Shi GP. IgE stimulates human and mouse arterial cell apoptosis and cytokine expression and promotes atherogenesis in ApoE^{-/-} mice. *J Clin Invest.* 2011;121:3564-77.
 37. Speidl WS, Kastl SP, Hutter R, Katsaros KM, Kaun C, Bauriedel G, Maurer G, Huber K, Badimon JJ, Wojta J. The complement component C5a is present in human coronary lesions in vivo and induces the expression of MMP-1 and MMP-9 in human macrophages in vitro. *FASEB J.* 2011;25:35-44.
 38. de Vries MR, Wezel A, Schepers A, van Santbrink PJ, Woodruff TM, Niessen HW, Hamming JF, Kuiper J, Bot I, Quax PH. Complement factor C5a as mast cell activator mediates vascular remodelling in vein graft disease. *Cardiovasc Res.* 2013;97:311-20.
 39. Wezel A, de Vries MR, Lagraauw HM, Foks AC, Kuiper J, Quax PH, Bot I. Complement factor C5a induces atherosclerotic plaque disruptions. *J Cell Mol Med.* 2014;18:2020-30.
 40. Sandig H, Bulfone-Paus S. TLR signaling in mast cells: common and unique features. *Front Immunol.* 2012;3:185.
 41. Hollestelle SC, De Vries MR, Van Keulen JK, Schoneveld AH, Vink A, Strijder CF, Van Middelaar BJ, Pasterkamp G, Quax PH, De Kleijn DP. Toll-like receptor 4 is involved in outward arterial remodeling. *Circulation.* 2004;27:109:393-8.
 42. Den Dekker WK, Tempel D, Bot I, Biessen EA, Joosten LA, Netea MG, van der Meer JW, Cheng C, Duckers HJ. Mast cells induce vascular smooth muscle cell apoptosis via a toll-like receptor 4 activation pathway. *Arterioscler Thromb Vasc Biol.* 2012;32:1960-9.
 43. Willems S, van der Velden D, Quax PH, de Borst GJ, de Vries JP, Moll FL, Kuiper J, Toes RE, de Jager SC, de Kleijn DP, Hoefer IE, Pasterkamp G, Bot I. Circulating immunoglobulins are not associated with intraplaque mast cell number and other vulnerable plaque characteristics in patients with carotid artery stenosis. *PLoS One.* 2014;9:e88984.
 44. Lappalainen J, Lindstedt KA, Oksjoki R, Kovanen PT. OxLDL-IgG immune complexes induce expression and secretion of proatherogenic cytokines by cultured human mast cells. *Atherosclerosis.* 2011;214:357-63.
 45. Bot M, de Jager SC, MacAleese L, Lagraauw HM, van Berkel TJ, Quax PH, Kuiper J, Heeren RM, Biessen EA, Bot I. Lysophosphatidic acid triggers mast cell-driven atherosclerotic plaque destabilization by increasing vascular inflammation. *J Lipid Res.* 2013;54:1265-74.
 46. Laine P, Naukkarinen A, Heikkilä L, Penttilä A, Kovanen PT. Adventitial mast cells connect with sensory nerve fibers in atherosclerotic coronary arteries. *Circulation.* 2000;101:1665-9.
 47. Bot I, de Jager SC, Bot M, van Heiningen SH, de Groot P, Veldhuizen RW, van Berkel TJ, von der Thüsen JH, Biessen EA. The neuropeptide substance P mediates adventitial mast cell activation and induces intraplaque hemorrhage in advanced atherosclerosis. *Circ Res.* 2010;106:89-92.
 48. Lagraauw HM, Westra MM, Bot M, Wezel A, van Santbrink PJ, Pasterkamp G, Biessen EA, Kuiper J, Bot I. Vascular neuropeptide Y contributes to atherosclerotic plaque progression and perivascular mast cell activation. *Atherosclerosis.* 2014;235:196-203.
 49. Kounis NG. Coronary hypersensitivity disorder: the Kounis syndrome. *Clin Ther.* 2013;35:563-71.
 50. Undas A, Cieśla-Dul M, Drażkiewicz T, Potaczek DP, Sadowski J. Association between atopic diseases and venous thromboembolism: a case-control study in patients aged 45 years or less. *J Thromb*

- Haemost. 2011;9:870-3.
51. Knoflach M, Kiechl S, Mayr A, Willeit J, Poewe W, Wick G. Allergic rhinitis, asthma, and atherosclerosis in the Bruneck and ARMY studies. *Arch Intern Med.* 2005;165:2521-6.
 52. Skaaby T, Husemoen LL, Thuesen BH, Jeppesen J, Linneberg A. The association of atopy with incidence of ischemic heart disease, stroke, and diabetes. *Endocrine.* 2014; Epub ahead of print.
 53. Deliargyris EN, Upadhyya B, Sane DC, Dehmer GJ, Pye J, Smith SC Jr, Boucher WS, Theoharides TC. Mast cell tryptase: a new biomarker in patients with stable coronary artery disease. *Atherosclerosis.* 2005;178:381-6.
 54. van Haelst PL, Timmer JR, Crijns HJ, Kauffman HF, Gans RO, van Doormaal JJ. No long-lasting or intermittent mast cell activation in acute coronary syndromes. *Int J Cardiol.* 2001;78:75-80.
 55. Kovanen PT, Mänttari M, Palosuo T, Manninen V, Aho K. Prediction of myocardial infarction in dyslipidemic men by elevated levels of immunoglobulin classes A, E, and G, but not M. *Arch Intern Med.* 1998;158:1434-9. 56.
 56. Mayer FJ, Gruenberger D, Schillinger M, Mannhalter C, Minar E, Koppensteiner R, Arbesú I, Niessner A, Hoke M. Prognostic value of neutrophils in patients with asymptomatic carotid artery disease. *Atherosclerosis.* 2013;231:274-80.
 57. Matsumura T, Taketa K, Motoshima H, Senokuchi T, Ishii N, Kinoshita H, Fukuda K, Yamada S, Kukidome D, Kondo T, Hisada A, Katoh T, Shimoda S, Nishikawa T, Araki E. Association between circulating leukocyte subtype counts and carotid intima-media thickness in Japanese subjects with type 2 diabetes. *Cardiovasc Diabetol.* 2013;27;12:177.
 58. Gabbasov ZA, Kozlov SG, Lyakishev AA, Saburova OS, Smirnov VA, Smirnov VN. Polymorphonuclear blood leukocytes and restenosis after intracoronary implantation of drug-eluting stents. *Can J Physiol Pharmacol.* 2009;87:130-6.
 59. Holmes DR Jr, Savage M, LaBlanche JM, Grip L, Serruys PW, Fitzgerald P, Fischman D, Goldberg S, Brinker JA, Zeiher AM, Shapiro LM, Willerson J, Davis BR, Ferguson JJ, Popma J, King SB 3rd, Lincoff AM, Tchong JE, Chan R, Granett JR, Poland M. Results of Prevention of REStenosis with Tranilast and its Outcomes (PRESTO) trial. *Circulation.* 2002;106:1243-50.

Chapter 3

Complement factor C5a as mast cell activator mediates vascular remodelling in vein graft disease

Cardiovasc Res. 2013;97:311-20

Margreet R. de Vries^{1,2}

Anouk Wezel^{2,3}

Abbey Schepers²

Peter J. van Santbrink³

Trent M. Woodruff⁴

Hans W. M. Niessen⁵

Jaap F. Hamming²

Johan Kuiper³

Ilze Bot^{2,3}

Paul H. A. Quax^{1,2,6}

¹Eindhoven Laboratory for Experimental Vascular Medicine, Leiden, The Netherlands

²Department of Surgery, Leiden University Medical Center, Leiden, The Netherlands

³Division of Biopharmaceutics, Gorlaeus Laboratories, Leiden Academic Center for Drug Research, Leiden University, Leiden, The Netherlands

⁴School of Biomedical Sciences, University of Queensland, St Lucia, Australia

⁵Department of Pathology and Cardiac Surgery, ICaR-VU, VU University Medical Center, Amsterdam, The Netherlands

⁶Department of Vascular Surgery, Leiden University Medical Center, Leiden, The Netherlands

Abstract

Aims: Failure of vein graft conduits due to vein graft thickening, accelerated atherosclerosis, and subsequent plaque rupture is applicable to 50% of all vein grafts within 10 years. New potential therapeutic targets to treat vein graft disease may be found in components of the innate immune system, such as mast cells and complement factors, which are known to be involved in atherosclerosis and plaque destabilization. Interestingly, mast cells can be activated by complement factor C5a and, therefore, a direct role for C5a-mediated mast cell activation in vein graft disease is anticipated. We hypothesize that C5a-mediated mast cell activation is involved in the development and destabilization of vein graft lesions.

Methods and results: Mast cells accumulated in time in murine vein graft lesions, and C5a and C5a-receptor (CD88) expression was up-regulated during vein graft disease in apolipoprotein E-deficient mice. Mast cell activation with dinitrophenyl resulted in a profound increase in vein graft thickening and in the number of plaque disruptions. C5a application enhanced vein graft lesion formation, while treatment with a C5a-receptor antagonist resulted in decreased vein graft disease. C5a most likely exerts its function via mast cell activation since the mast cell inhibitor cromolyn totally blocked C5a-enhanced vein graft disease.

Conclusion: These data provide evidence that complement factor C5a-induced mast cell activation is highly involved in vein graft disease, which identifies new targets to prevent vein graft disease.

Introduction

Venous bypass grafting, frequently used in cardiac and peripheral vascular surgery, often fails acutely due to thrombosis and on the long term through vein graft thickening, accelerated atherosclerosis, and plaque rupture^{1,2}. Recently, our group and others have conclusively demonstrated that perivascular mast cells contribute to atherosclerotic plaque progression and destabilization in mice³⁻⁵. Although many similarities exist between atherosclerosis and vein graft disease (VGD), it is still unknown whether mast cells play a causal role in the development of VGD. Furthermore, the triggers that lead to mast cell activation in atherosclerosis or VGD are still unresolved. A potential mechanism for mast cell activation in patients is via the complement system⁶. Complement factors are expressed during the development of atherosclerosis⁷. In particular, C3a and C5a have been detected in advanced atherosclerotic plaques⁸ and we have previously demonstrated that complement factor C3 and C1q are involved in VGD in mice^{9,10}.

C5a is one of the major biologically active components of the complement cascade downstream of C3 and exerts its functions mainly via the canonical C5a receptor (C5aR, CD88). C5a induces chemotaxis of numerous cell types including mast cells and monocytes¹¹. It has been demonstrated that plasma C5a levels correlate with an adverse outcome in patients with severe atherosclerosis¹². Moreover, in a phase III trial with patients undergoing coronary artery bypass surgery or aortic valve replacement, the administration of an antibody against C5, which is the precursor to C5a, showed decreased mortality¹³.

In the current study, we aimed to investigate the role of mast cells and complement factor C5a in a mouse model of VGD. We show that either omission or stimulation of mast cells or C5a results in modulation of vein graft thickening (VGT). Furthermore, we demonstrate that C5a mediated the activation of mast cells is strongly involved in the processes implicated in VGD. These data strongly suggest that mast cells and the C5a-C5aR axis play a central role in the development of VGD and show that C5a is a potent mast cell activator during cardiovascular disease processes.

Methods

A detailed description of the Methods is available in the Supplementary material online.

This study was performed in compliance with Dutch government guidelines and the Directive 2010/63/EU of the European Parliament. All animal experiments were approved by the animal welfare committee of the Leiden University Medical Center (approval reference numbers 09148 and 10091). Vein graft surgery was performed by donor caval vein interpositioning (caval vein of \pm 2mm length) in the carotid artery of recipient mice. These were either C57BL/6 control mice, apolipoprotein E-deficient (apoE^{-/-}) or mast cell-deficient Kit(W^{sh}/W^{sh}) male mice (10–20 weeks old). Before surgery, mice were anaesthetized with midazolam (5 mg/kg, Roche Diagnostics), medetomidine (0.5 mg/kg, Orion), and fentanyl (0.05

mg/kg, Janssen Pharmaceutical). The adequacy of the anaesthesia was monitored by keeping track of the breathing frequency and the response to toe pinching of the mice. After the procedure, the mice were antagonized with atipamezol (2.5 mg/kg, Orion) and fluminasenil (0.5 mg/kg Fresenius Kabi). Buprenorphine (0.1 mg/kg, MSD Animal Health) was given after surgery to relieve pain.

A detailed flow chart displaying the *in vivo* experimental set-up is shown in the Supplementary material online, Figure S1. In all experiments vein grafts were left *in situ* for 28 days (with exception of the time courses). Formalin fixed, paraffin embedded, and vein grafts were histological and morphometrically analysed as previously described^{14,15}. Cholesterol levels were determined before surgery and at sacrifice. Furthermore, sysmex analysis of blood cells was performed for all experiments and no significant differences were detected in the % of WBC populations between the treatment groups and their appropriate controls. In Supplementary material online, Table S1, white blood cell analysis of the C5a and cromolyn (Cro) experiment is shown.

First, we aimed to demonstrate the presence of mast cells, C5a and C5aR in vein grafts of hypercholesterolaemic apoE^{-/-} mice. For this, we used immunohistochemistry and RT-PCR analysis on time courses of paraffin and RNA material of three to four mice per time point. Analyses were performed as described in the Supplementary material online.

Secondly, the involvement of mast cells in VGD was determined by the analysis of vein graft lesions in either mast cell-deficient Kit(W^{sh}/W^{sh}) mice ($n = 8$ mice/group) or by investigating the effect of local mast cell activation with dinitrophenyl hapten (DNP) on vein graft remodelling in apoE^{-/-} mice. After skin-sensitizing, apoE^{-/-} mice ($n = 11$ /group) were subjected to vein graft surgery and subsequently the vein grafts were treated locally with DNP in pluronic gel¹⁶.

Thirdly, the effect of interfering in C5a signalling was investigated. ApoE^{-/-} mice ($n = 7$ /group) were challenged perivascularly with either 0.5 or 5 µg of recombinant mouse C5a (HyCult Biotechnology) or vehicle in pluronic gel. The effects of inhibiting C5a function were also studied. ApoE^{-/-} mice ($n = 7$ /group) were treated daily with subcutaneous injections of the C5a-receptor antagonist hydrocinnamate-[OP-(D-Cha)WR] (PMX205) (0.3 mg/kg)¹⁷ or vehicle solution, starting 1 day prior to surgery.

To determine whether C5a effects were mast cell dependent, a group of C5a stimulated apoE^{-/-} mice (5 µg/mouse in pluronic gel) or PBS gel controls were treated twice weekly with the mast cell stabilizer Cro (50 mg/kg, Sigma) and compared with mice treated with PBS ($n = 9$ /group).

Finally, to confirm whether C5a activation of mast cells could be a functional pathway in human atherosclerotic lesions, the presence of mast cells, C5a and C5aR in human specimens were analysed. Human vein graft ($n = 8$) and carotid endarterectomy ($n = 25$) tissues were obtained in accordance with guidelines set out by the 'Code for Proper Secondary Use of Human Tissue' of the Dutch Federation of Biomedical Scientific Societies (Federa) and conform with the principles outlined in the Declaration of Helsinki.

All data are presented as mean ± SD. For the time courses, statistical analysis was performed using a repeated measures ANOVA with a Bonferroni *post hoc* test. *In vivo* experiments were compared with a Krukall-Wallis test followed by a non-parametric Mann-Whitney test to compare individual groups. For *in vitro* studies, a two-tailed Student's *t*-test was used. *P*-values <0.05 were regarded significant.

Results

Mast cells, C5a and C5aR in murine vein grafts

The presence of mast cells and expression levels of C5a and C5aR were assessed by immunohistochemistry and RT-PCR (primer sequences; Supplementary material online, Table S2) in vein grafts interpositioned in carotid arteries of hypercholesterolemic apolipoprotein E-deficient mice. The vein grafts were harvested at several time points after surgery ($n = 3-4$ per time point). Mast cells were found in small quantities in the adventitia of the ungrafted caval veins. Directly after engraftment the number of perivascular mast cells decreased and from 3 days on the number of mast cells increased profoundly ($t = 6$ h: 0.4 ± 0.1 mast cells/mm² vein graft vs. 28 days: 4.2 ± 0.6 mast cells/mm² vein graft, $P = 0.045$, Figure 1A). Mast cells in the atherosclerotic lesion itself were very rare. Both resting and activated mast cells were found in the perivascular tissue (Figure 1B). No differences in the activation status of the mast cells were found between the different time points (data not shown). An increase in C5 mRNA expression was seen at 6 h ($P = 0.015$) after surgery (Figure 1C), which is in agreement with the finding of increased C5a protein expression at this time point (Figure 1D). C5a was detected in leukocytes adhering to the lumen and in the adventitia, where mast cells particularly reside. C5a was also detected in the regenerating endothelium from 7 days on. At later time points (14 and 28 days), the expression of C5a was also seen in macrophages and some smooth muscle cells (SMCs) associated with thickening of the graft. C5aR mRNA was maximally expressed (nine-fold increase vs. ungrafted vein $P = 0.043$) at 1 day after surgery and declined after 3 days to a three-fold increase in relative expression ($P = 0.073$) (Figure 1E). In the first day after surgery, C5aR protein expression was seen in invading inflammatory cells and at later time points also in SMCs and macrophages (Figure 1F).

Effect of mast cell deficiency and mast cell stimulation on vein graft morphology

To investigate whether there is a causal relation between mast cell accumulation and the development of VGD, mast cell-deficient Kit^(W-sh/W-sh) and control C57BL/6 mice underwent vein graft surgery. At 28 days after surgery, a decrease in VGT of 36% was seen in the Kit^(W-sh/W-sh) mice when compared with control mice (0.52 ± 0.18 vs. 0.33 ± 0.13 mm², respectively, $P = 0.036$, Figure 2). The total vessel area (lesion area + lumen area) (0.89 ± 0.22 vs. 0.71 ± 0.22 mm², $P = 0.141$) and the lumen area (0.38 ± 0.09 vs. 0.38 ± 0.10 mm², $P = 0.753$) were not significantly different. Consequently, no effect on outward remodelling could be detected.

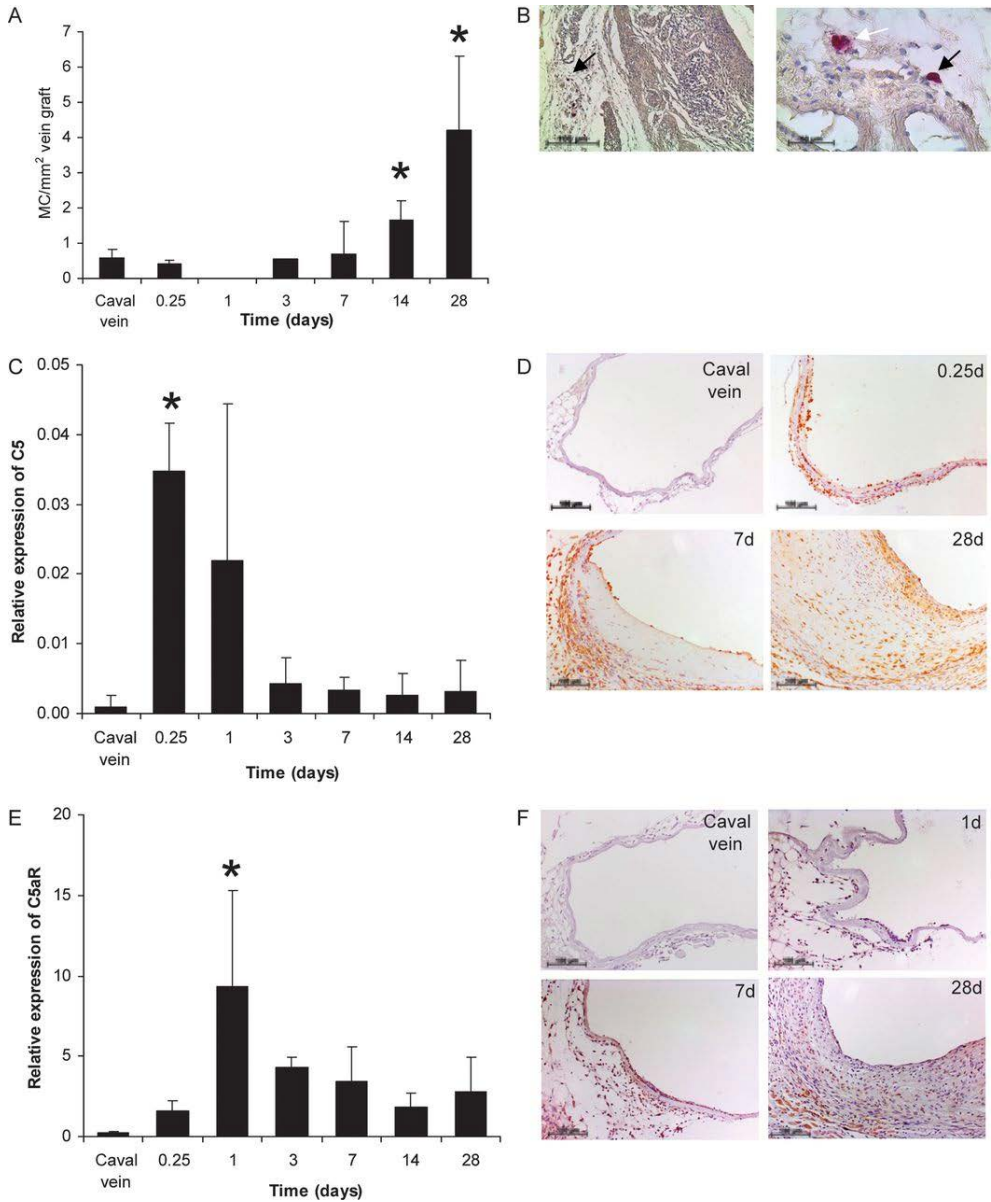


Figure 1. (A) Perivascular mast cells were scored in caval veins (0) and vein grafts at 6 h (0.25 day), 1, 3, 7, 14, and 28 days after surgery (three to four vein grafts/time point). Mast cell numbers increased from 3 days on to a significant increase (compared with vein graft at 0.25 day) at day 14 and 28 (B). Both resting (black arrow) and activated (white arrow) mast cells were found in the adventitia of the vein grafts. C5a and C5a-receptor expression on mRNA (C and E) and protein level (D and F) were assessed in time in vein grafts. Relative expression of both C5a and C5aR increased rapidly immediately after surgery due to the influx of positive inflammatory cells. At later time points expression decreased due to the influx in the vein graft of C5a- and C5aR-negative cells and extracellular matrix. * $P < 0.05$, representative scale bars are added to the photographs.

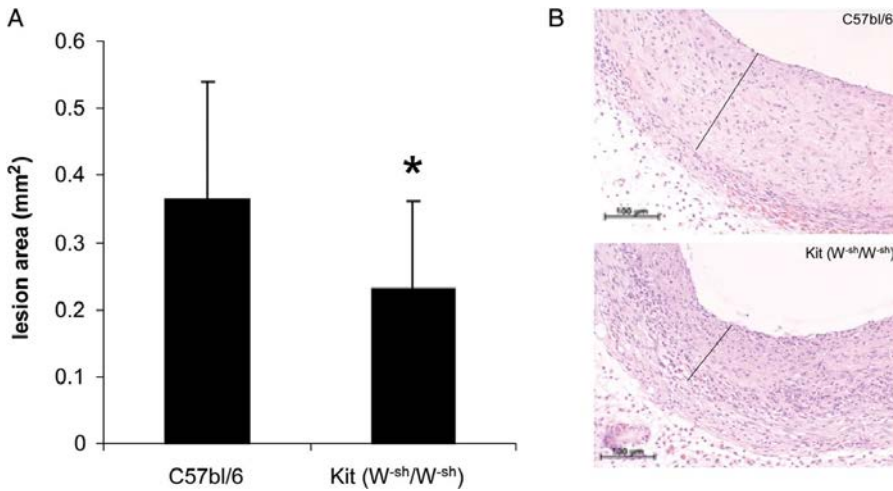


Figure 2. (A) A decrease in the *Kit*^(W-sh/W-sh) lesion area was seen when compared with control C57BL/6 lesions 28 days after surgery (**P* < 0.05). (B) Representative cross-sections of vein grafts in C57BL/6 and *Kit*^(W-sh/W-sh) mice (HPS staining, magnification ×20). Black line indicates the thickness of the lesion.

Next, skin-sensitized apoE^{-/-} mice were challenged locally at the vein graft with DNP, which results in acute mast cell activation, or vehicle control to study the effects of mast cell activation on VGD. Mast cell activation resulted in a 46% increase in the lesion area compared with the vehicle control group (0.36 ± 0.08 vs. 0.52 ± 0.20 mm² *P* = 0.011, Figure 3A and B). No significant differences were found in the total vessel area and the lumen area (data not shown). Plaque phenotype analysis revealed that the DNP-challenged group showed a 50% reduction in lesional SMCs (DNP: $12 \pm 6\%$, vehicle: $25 \pm 5\%$, *P* = 0.001, Figure 3C), especially in the cap region. The relative collagen content (DNP: $27 \pm 6\%$, vehicle: $25 \pm 10\%$, *P* = 0.457, Figure 3D) and the macrophage content (DNP: $18 \pm 3\%$, vehicle: $17 \pm 7\%$, *P* = 0.341, Figure 3E) did not differ significantly between the groups. At 28 days after DNP challenge, no differences in the number of mast cells were seen, nor did we detect a difference in the activation status (data not shown). Strikingly, vein grafts in the DNP group did show severe signs of plaque rupture complications¹⁵. Half of the vein grafts treated with DNP (*n* = 12) showed lesions with de-endothelialized areas and intramural thrombus (erosions) and two vein grafts showed a dissection, in which a tear starting at the lumen and up to the outer vein graft wall, filled with erythrocytes was seen. In contrast, only three vein grafts of the vehicle-treated group (*n* = 12) showed lesions with erosion (*P* = 0.05, Figure 3B). Plaque erosion is characterized by a loss of endothelial cells and therefore we scored the coverage of the lumen with CD31 positive cells. DNP treatment resulted in a 40% reduction in coverage compared with controls (*P* = 0.001, Figure 3G and H). Not only sections with intramural thrombi were devoid of endothelial cells, but also apparently asymptomatic lesions in the DNP group

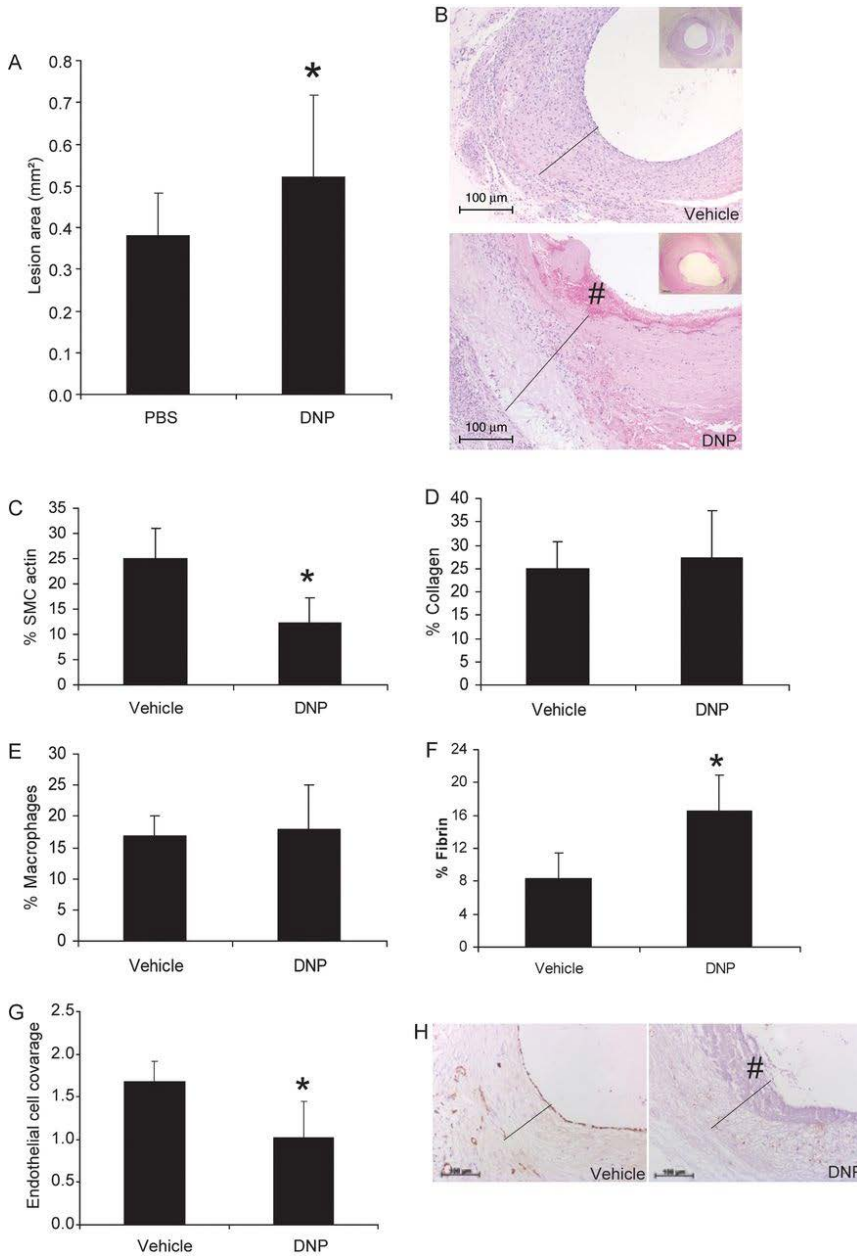


Figure 3. (A) Local treatment of apoE^{-/-} mice with dinitrofluorobenzene (DNP) in pluronic gel resulted in increased vein graft lesion areas at 28 days after surgery compared with the vehicle-treated group. (B) Typical cross-sections of vein grafts after treatment with vehicle or DNP (HPS staining, magnification $\times 20$, insets magnification $\times 5$). Note the erosion in the DNP-treated group (#). DNP treatment resulted in more disruptions of the vein grafts [8/12 (DNP) vs. 3/12 (PBS)] (C) Percentage of positive smooth muscle cells (SMC) was significantly decreased after DNP challenge. (D) The relative collagen content did not differ between the groups. (E) Percentage of the macrophage content was not affected by DNP challenge, whereas DNP treatment affected endothelium coverage significantly (F), which resulted in a significantly increased fibrin content in the DNP group (G and H). * $P < 0.05$; black lines in the photographs indicate the thickness of the lesions.

showed less endothelial coverage. De-endothelialization can result in enhanced fibrin deposition and indeed, the DNP group demonstrated a two-fold increase in the fibrin content (DNP; $17 \pm 3\%$, vehicle; $8 \pm 4\%$ $P = 0.001$, Figure 3F).

Effect of C5a application and C5aR antagonist PMX205 on vein graft morphology

C5a-induced mast cell activation was demonstrated by the release of tryptase and a concentration-dependent release of CCL2 from cultured bone marrow-derived mast cells (Supplementary material online, Table S3). To study the involvement of C5a in the development of VGT, recombinant C5a was applied in increasing concentrations (0, 0.5, and 5 μg) directly to the vein graft at the time of surgery. Topical application of C5a resulted in a dose-dependent increase in the lesion area (control: $0.24 \pm 0.05 \text{ mm}^2$, 0.5 μg C5a: $0.29 \pm 0.1 \text{ mm}^2$, 5 μg C5a: $0.41 \pm 0.1 \text{ mm}^2$, Figure 4A and B). The total vessel area and the luminal area were, however, comparable between the three groups (data not shown). Remarkably, at 28 days after surgery perivascular mast cell numbers show a trend towards an increase after C5a application (control: $2.77 \pm 1.7 \text{ cells/mm}^2$ vein graft, 0.5 μg C5a: $4.36 \pm 1.6 \text{ cells/mm}^2$ vein graft, $P = 0.100$, 5 μg C5a: $5.47 \pm 3.2 \text{ cells/mm}^2$ vein graft, $P = 0.086$ compared with control, Figure 4C). Since C5a is a potent chemotactic factor for monocytes/macrophages, the macrophage content was studied. A dose-dependent increase in macrophage contribution to the VGT was seen in C5a-treated vein grafts (Figure 4D). The amount of macrophages increased from $20 \pm 5\%$ in the controls to $22\% \pm 9\%$ ($P = 0.110$ compared with control) in mice treated with 0.5 μg C5a, and even up to $33 \pm 7\%$ in mice which received 5 μg C5a ($P < 0.05$ compared with both groups, Figure 4D). Next, the effect of the C5aR blockade by systemic treatment with the C5aR antagonist, PMX205 was delineated. Analysis of the thickened vein graft after 28 days revealed that treatment with PMX205 resulted in a 41% decrease in the lesion area, when compared with control mice (control: $0.39 \pm 0.16 \text{ mm}^2$, PMX205 $0.23 \pm 0.07 \text{ mm}^2$, $P = 0.035$, Figure 4E and F). The VGT consisted for $24 \pm 8\%$ of macrophages. In PMX205-treated vein grafts, the macrophage contribution was $16 \pm 8\%$ ($P = 0.012$, Figure 4G). Strikingly, adventitial mast cells were found to be reduced after PMX205 treatment (PMX205: $2.32 \pm 0.6 \text{ cells/mm}^2$ vein graft, control: $4.14 \pm 2.0 \text{ cells/mm}^2$ vein graft, $P = 0.042$, Figure 4H). No differences in rupture complications were seen between the groups.

C5a-induced vein graft thickening is abolished by mast cell stabilization

To elucidate the mast cell-dependent effects of C5a in VGD, mice were locally treated with either a PBS or C5a (5 μg) loaded pluronic gel ($n = 20/\text{group}$). Of each group, 10 mice were treated twice weekly with the mast cell inhibitor Cro or PBS control (ip). Cro treatment resulted in a decrease in the lesion area of 22% (PBS/PBS $0.38 \pm 0.1 \text{ mm}^2$, PBS/Cro $0.29 \pm 0.06 \text{ mm}^2$; $P = 0.044$, Figure 5A and B) and

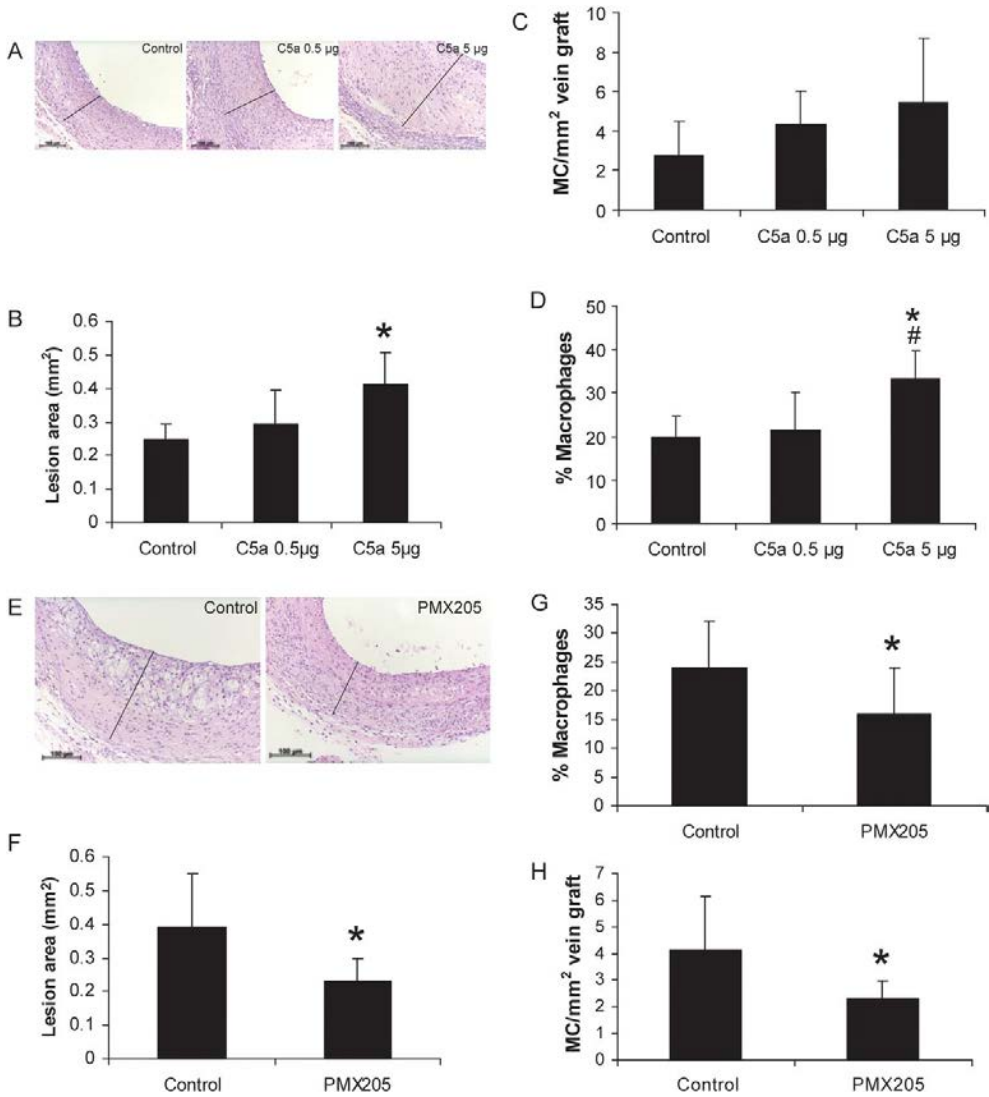


Figure 4. (A) Representative cross-sections of vein grafts, 28 days after surgery, treated with PBS or 0.5 or 5 μ g C5a (HPS staining, magnification 20 \times). (B) The quantification of vein graft lesion areas reveals a dose-dependent increase in the lesion size. (C) Perivascular mast cell numbers tend to increase after C5a application, although this did not reach significance. (D) The relative macrophage content of the vein graft wall tend to increase after 0.5 μ g C5a application. Application of 5 μ g C5a to the grafts significantly increased macrophage content (* P = 0.001 compared with control grafts; # P = 0.008 compared with grafts treated with 0.5 μ g C5a). (E) Direct effects of the C5aR blockade on vein graft disease was assessed by systemic treatment with a C5aR antagonist, hydrocinnamate-[OP-(D-Cha)WR] (PMX205). Representative cross-sections of vein grafts, 28 days after surgery (HPS staining, magnification 20 \times). (F) PMX205 treatment resulted in a significant decrease in the lesion area compared with control mice. (G) A significant reduction in relative macrophage contribution can be seen in the PMX205-treated vein grafts. (H) The number of adventitial mast cells was significantly reduced after PMX205 treatment. * P < 0.05; black lines in the photographs indicate the thickness of the lesions.

a decrease in the total vessel area of 19% ($P = 0.037$), whereas the lumen area was not affected. As shown previously, local C5a treatment resulted in an increase in the lesion area of 79% (C5a/PBS $0.68 \pm 0.11 \text{ mm}^2$ $P = 0.001$) compared with the control group (Figure 5A and B). Strikingly, treatment with both C5a and Cro (C5a/Cro $0.32 \pm 0.12 \text{ mm}^2$) resulted in a major decrease in the lesion area (compared with the C5a/PBS group, $P = 0.001$) to the level of the group treated with Cro only. A decrease in the total vessel area of 30% ($P = 0.003$) was seen, whereas no differences were observed in the lumen area when comparing C5a/Cro vs. C5a/PBS treatment. The relative SMC content was demonstrated to be reduced in the C5a/PBS group by 41% when compared with the PBS/PBS group ($P = 0.002$) and a decrease of 31% compared with the PBS/Cro group was found ($P = 0.021$, Figure 5C). The collagen content did not differ between the groups (PBS/PBS $26 \pm 6\%$, PBS/Cro $24 \pm 12\%$, C5a/PBS $26 \pm 14\%$, C5a/Cro 27 ± 11 , $P = 0.499$, Figure 5D). In contrast, Cro treatment alone resulted in a 25% reduction in the macrophage content when compared with controls ($P = 0.038$), which could be caused by inhibition of endogenous mast cell activation during the development of VGD (Figure 5E). The C5a/PBS group showed a 44% increase in the macrophage content when compared with the PBS/PBS group ($P = 0.001$). When compared with the C5a/PBS-treated mice, the C5a/Cro group displayed a decrease of 61% in the macrophage content ($P = 0.001$) as a result of the Cro treatment. Although local C5a treatment resulted in a more unstable morphology, no differences were found in the occurrence of plaque rupture complications (PBS/PBS 3/10, PBS/Cro 3/10, C5a/PBS 1/10, and C5a/Cro 2/10).

Expression of mast cells and C5a(R) in human vein graft and carotid endarterectomy specimens

To confirm whether C5a activation of mast cells is an endogenous and functional pathway in human atherosclerotic lesions, we analysed the presence of mast cells, C5a and C5aR in human saphenous vein grafts and carotid endarterectomy specimens. Mast cells were detected throughout the entire lesion in both types of tissue and were especially found in regions of neovascularization, either in the adventitia or in the intima (Figure 6). C5aR staining was abundantly present in all layers in both types of specimen. In SMCs, endothelial cells and regions of inflammatory cells, including mast cells, C5aR expression was detectable. C5a staining was less pronounced and mostly limited to regions of intimal SMCs, inflammatory cells, near necrotic cores, and neovascularization.

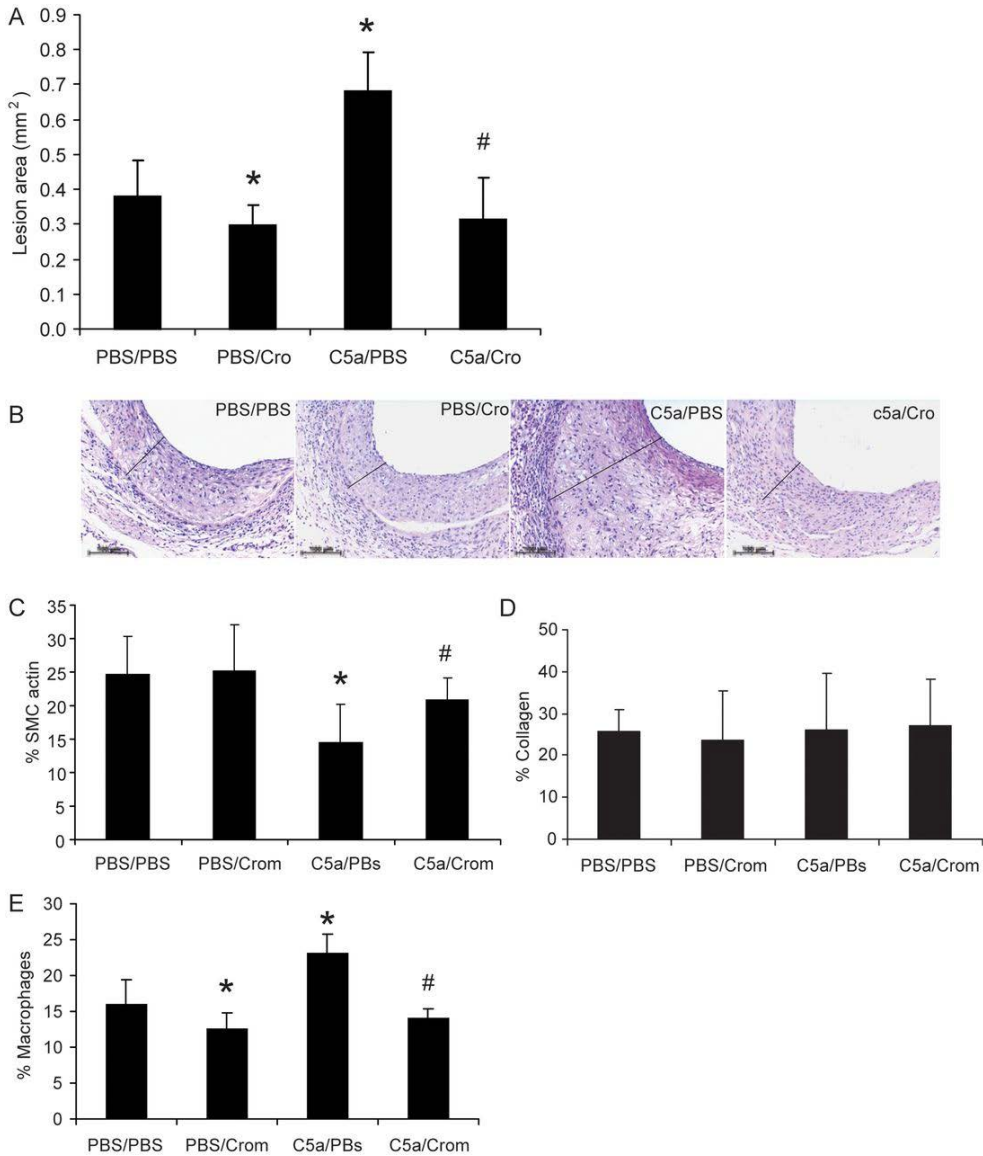


Figure 5. (A) Quantification of the vein graft wall area, 28 days after vein graft surgery, in *apoE*^{-/-} mice treated with combination of PBS or with 5 μ g C5a locally in pluronic gel and twice weekly injections with either PBS or cromolyn (Cro). Cro treatment resulted in a decrease in the lesion area (* $P < 0.05$ compared with the control group) C5a treatment results in increased lesion areas (* $P < 0.05$ compared with the control group). Treatment with both C5a and cromolyn resulted in lesion areas comparable with that of the cromolyn-alone-treated group (# $P < 0.05$ compared with the c5a-treated group) (B) Representative cross-sections of vein grafts (HPS staining, magnification $\times 20$, black lines indicate the thickness of the lesions). (C) Percentage of SMCs was significantly decreased after C5a application. (D) The quantification of the relative collagen content did not show significant differences between all groups. (E) The relative macrophage content was significantly decreased after Cro treatment and C5a application resulted in a significant increase in the macrophage content which could be abolished by Cro, * $P < 0.05$.

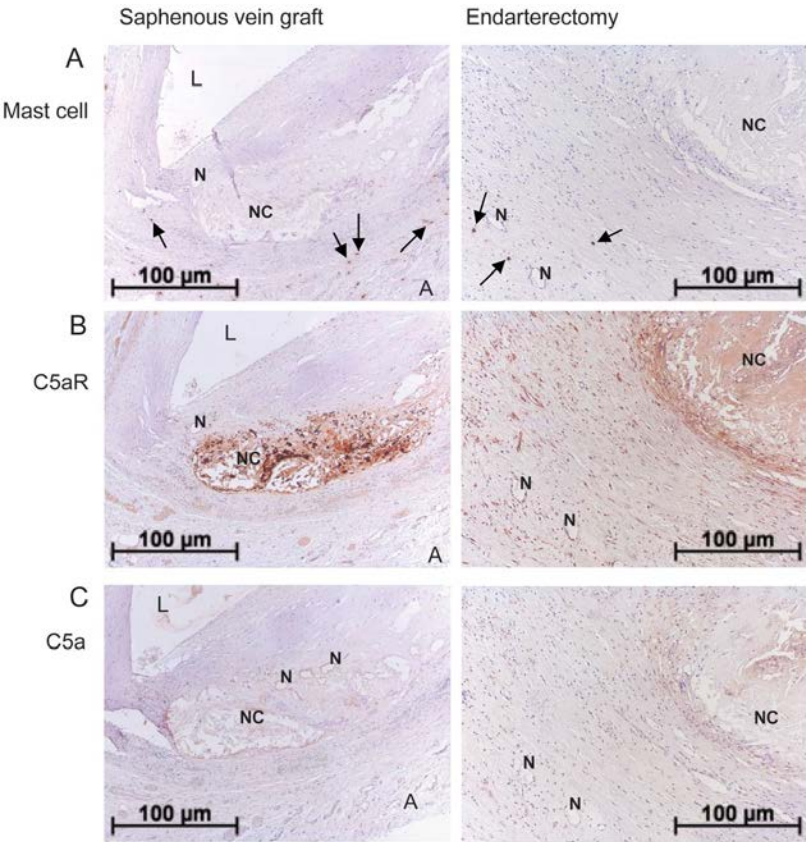


Figure 6. The presence and localization of mast cells, C5a and C5a-receptor in human saphenous vein grafts, and carotid endarterectomy material was assessed by immunohistochemistry. (A) Mast cells (black arrows) were found throughout all layers of the lesion but primarily in the adventitial and intimal regions near neovessels. (B) Abundant staining of C5aR was seen in all major cell types present in the lesions; inflammatory cells, smooth muscle cells, and endothelial cells. (C) C5a presence was seen near necrotic cores and neovessels. Furthermore colocalization of C5a with smooth muscle cells and inflammatory cells was seen frequently (NC, necrotic core; N, Neovessels; L, Lumen; and A, Adventitia).

Discussion

We have demonstrated that mast cells and complement factor C5a, both innate immunity members, are inextricably linked in the contribution to VGD. Mast cells, C5a and C5aR were demonstrated to be present in diseased human vein grafts as well as in carotid endarterectomy specimen. This is in accordance with colocalization of C5a and the C5aR with mast cells in other types of atherosclerotic lesions as shown previously^{8,18}. The expression of C5aR was shown in neointimal lesions and brachiocephalic artery plaques^{19,20}, and we now demonstrate co-expression and colocalization of mast cells, C5a and C5a receptor in murine vein grafts. This identifies the C5a-C5aR axis as a potential endogenous mast cell activation route.

Local mast cell challenge with C5a resulted in an increase in the number of perivascular mast cells together with a dose-dependent increase in VGD. Interestingly, treatment of vein grafts with a specific C5aR antagonist (PMX205) resulted in decreased VGT, which coincides with recent findings of decreased neointimal lesion development after C5aR targeting using C5aR-specific antibodies or the related C5aR antagonist PMX53^{19,20}. Morphologic analysis also revealed a strong reduction in the macrophage content. The recruitment of monocytes/macrophages into atherosclerotic plaques requires up-regulation of adhesion molecules and CCL2²¹. Shagdarsuren *et al*¹⁹ found that treatment with PMX53 resulted in decreased macrophage content and reduced VCAM-1 expression. In addition, C5aR antagonism in a renal allograft model resulted in attenuated macrophage infiltration due to reduced levels of CCL2 and ICAM-1²². Interestingly, adhesion molecules and the CCR2/CCL2 pathway have previously been shown to be involved in the recruitment of mast cells²³, which suggests that a reduction in CCL2 may have accounted for the reduced number of mast cells we found after C5aR treatment. *In vitro* studies demonstrated that C5a-mediated mast cell activation not only led to the release of the mast cell protease tryptase, but also to a dose-dependent release of chemokine CCL2, which may have, at least in part, caused the increased levels of lesional macrophages and mast cells that were seen in the C5a-treated mice.

To demonstrate a causal role for C5a activation of mast cells in VGD, vein grafts were treated locally with C5a while simultaneously mast cell activation was blocked by the use of Cro. Cro was shown to completely reverse the C5a-induced adverse effects on vein graft atherosclerosis, by decreasing the vein graft lesion size comparable with that of mice treated with Cro only. We have previously shown that Cro is a specific inhibitor of mast cells with no effects on macrophages or other cell types present in atherosclerotic plaques⁴. This demonstrates that C5a mainly acts on vein graft atherosclerosis through mast cell activation.

Mast cells do not only play a role in atherosclerotic lesion growth, but are also involved in plaque destabilization and plaque complications as rupture and erosions²⁴. We investigated the effect on plaque stability after modulation of mast cell activation or C5a intervention. Interestingly, challenge with DNP resulted in a major increase in plaque complications and in particular plaque erosions. Plaque erosion, a frequent cause of acute coronary death, is characterized by a loss of endothelial cells²⁵. Moreover, subendothelial mast cells have been demonstrated to colocalize with sites of atheromatous erosions²⁶. In this study, mast cell activation by DNP challenge resulted in diminished endothelial cell coverage, which may be a consequence of endothelial cell apoptosis due to mast cell activation⁴. Mast cell mediators, such as chymase, TNF- α , histamine, and tryptase, have separately been reported to induce increased endothelial cell permeability and apoptosis²⁷⁻²⁹,

suggesting that mast cells can actively induce plaque erosion. Furthermore, mast cells can also induce SMC^{30,31} and macrophage apoptosis⁴ and secrete and activate matrix metalloproteinases^{32,33}, all important promoters of plaque destabilization and rupture. Interestingly, factors involved in intramural thrombus formation (plasmin, thrombin) can cleave C5 into C5a³⁴. This C5a could in turn attract and activate mast cells in the vicinity of the plaque which can result in an on-going loop of atherothrombosis. We have previously shown that mast cell activation by means of a DNP challenge induced acute intraplaque haemorrhage in collar-induced atherosclerosis⁴ and we now show that a single DNP challenge directly after surgery resulted in vein graft destabilization and plaque disruptions. Together, these data provide clear evidence that mast cell degranulation can result in atherothrombotic events.

The increase in vein graft atherosclerosis after C5a application was accompanied by a decrease in plaque stability due to a reduction in relative SMC content and an increase in the macrophage content compared with the control group. In contrast, the C5a/Cro-treated group revealed a more stable composition (more SMC, less macrophages) than the C5a-treated group. Although there is evidence that C5a can induce rupture^{8,18,35}, we did not observe more rupture-associated complications in the lesions after C5a application when compared with control or Cro treatment. This may be caused by the difference in the activation route of C5a vs. DNP, which results in different mast cell releasate compositions¹⁴. This may thus affect endothelial survival differently. It is also described that C5a can inhibit angiogenesis³⁶, an important factor affecting plaque instability.

In this study, we conclusively demonstrate that mast cells actively contribute to the progression and destabilization of VGD. Furthermore, the complement factor C5a promotes mast cell-dependent VGT, suggesting that complement activation is an important endogenous route of mast cell activation in VGD. Previously, C5 inhibition was demonstrated to be effective in a phase III cardiovascular disease trial¹³. Our finding that mast cells and C5a colocalize in human endarterectomy and vein graft specimens is of importance for the working mechanism of C5 in cardiovascular disease. Although the mouse vein graft model used in the study shows strong homology with human VGD, it should be realized that differences exist between murine and human vein grafts. Despite these differences, we here conclude that C5a-mediated mast cell activation can be a promising therapeutic route of intervention to the prevention of VGD that definitely deserves further investigation.

Funding

This work was supported by the Netherlands Organization for Scientific Research (916.86.046 to I.B.) and the Netherlands Heart Foundation (2010B029 to A.W.).

Acknowledgments

The kind gift of PMX205 and useful suggestions for the experimental set-up by Professor Steve Taylor is greatly appreciated.

References

- Shukla N, Jeremy JY. Pathophysiology of saphenous vein graft failure: a brief overview of interventions. *Curr Opin Pharmacol.* 2012;12:114-1120.
- Waltz AE, Fishbein MC, Matloff JM. Thrombosed, ruptured atheromatous plaques in saphenous vein coronary artery bypass grafts: ten years' experience. *Am Heart J.* 1987;114:718-723.
- Kaartinen M, Penttilä A, Kovanen PT. Accumulation of activated mast cells in the shoulder region of human coronary atheroma, the predilection site of atheromatous rupture. *Circulation.* 1994;90:1669-1678
- Bot I, de Jager SC, Zernecke A, Lindstedt KA, van Berkel TJ, Weber C, et al. Perivascular mast cells promote atherogenesis and induce plaque destabilization in apolipoprotein E-deficient mice. *Circulation.* 2007;115:2516-2525.
- Sun J, Sukhova GK, Wolters PJ, Yang M, Kitamoto S, Libby P, et al. Mast cells promote atherosclerosis by releasing proinflammatory cytokines. *Nat Med.* 2007;13:719-724.
- Krishnaswamy G, Ajitawi O, Chi DS. The human mast cell: an overview. *Methods Mol Biol.* 2006;315:13-34.
- Niculescu F, Rus H. Complement activation and atherosclerosis. *Mol Immunol.* 1999;36:949-955.
- Oksjoki R, Laine P, Helske S, Vehmaan-Kreula P, Mayranpää MI, Gasque P, et al. Receptors for the anaphylatoxins C3a and C5a are expressed in human atherosclerotic coronary plaques. *Atherosclerosis.* 2007;195:90-99.
- Schepers A, de Vries MR, van Leuven CJ, Grimbergen JM, Holers VM, Daha MR, et al. Inhibition of complement component C3 reduces vein graft atherosclerosis in apolipoprotein E3-Leiden transgenic mice. *Circulation.* 2006;114:2831-2838.
- Krijnen PA, Kupreishvili K, de Vries MR, Schepers A, Stooker W, Vonk AB, et al. C1-esterase inhibitor protects against early vein graft remodeling under arterial blood pressure. *Atherosclerosis.* 2011;220:86-92.
- Guo RF, Ward PA. Role of C5a in inflammatory responses. *Annu Rev Immunol.* 2005;23:821-852.
- Speidl WS, Exner M, Amighi J, Kastl SP, Zorn G, Maurer G, et al. Complement component C5a predicts future cardiovascular events in patients with advanced atherosclerosis. *Eur Heart J.* 2005;26:2294-2299.
- Carrier M, Menasche P, Levy JH, Newman MF, Taylor KM, Haverich A, et al. Inhibition of complement activation by pexelizumab reduces death in patients undergoing combined aortic valve replacement and coronary artery bypass surgery. *J Thorac Cardiovasc Surg.* 2006;131:352-356.
- Bot I, de Jager SC, Bot M, van Heiningen SH, de Groot P, Veldhuizen RW, et al. The neuropeptide substance P mediates adventitial mast cell activation and induces intraplaque hemorrhage in advanced atherosclerosis. *Circ Res.* 2010;106:89-92.
- Ewing MM, de Vries MR, Nordzell M, Pettersson K, de Boer HC, van Zonneveld AJ, et al. Annexin A5 therapy attenuates vascular inflammation and remodeling and improves endothelial function in mice. *Arterioscler Thromb Vasc Biol.* 2011;31:95-101.
- Kraneveld AD, Buckley TL, van Heuven-Nolsen D, van Schaik Y, Koster AS, Nijkamp FP. Delayed-type hypersensitivity-induced increase in vascular permeability in the mouse small intestine: inhibition by depletion of sensory neuropeptides and NK1 receptor blockade. *Br J Pharmacol.* 1995;114:1483-1489.
- Woodruff TM, Pollitt S, Proctor LM, Stocks SZ, Mantey HD, Williams HM, et al. Increased potency of a novel complement factor 5a receptor antagonist in a rat model of inflammatory bowel disease. *J Pharmacol Exp Ther.* 2005;314:811-817.
- Speidl WS, Kastl SP, Hutter R, Katsaros KM, Kaun C, Bauriedel G, et al. The complement component C5a is present in human coronary lesions *in vivo* and induces the expression of MMP-1 and MMP-9 in human macrophages *in vitro*. *FASEB J.* 2011;25:35-44.
- Shagdarsuren E, Bidzhekov K, Mause SF, Simsekylmaz S, Polakowski T, Hawlisch H, et al. C5a receptor targeting in neointima formation after arterial injury in atherosclerosis-prone mice.

- Circulation. 2010;122:1026-1036.
20. Manthey HD, Thomas AC, Shiels IA, Zerneck A, Woodruff TM, Rolfe B, et al. Complement C5a inhibition reduces atherosclerosis in ApoE^{-/-} mice. *FASEB J*. 2011;25:2447-2455.
 21. Libby P, Sukhova G, Lee RT, Galis ZS. Cytokines regulate vascular functions related to stability of the atherosclerotic plaque. *J Cardiovasc Pharmacol*. 1995;25:S9-12.
 22. Gueller F, Rong S, Gwinner W, Mengel M, Brocker V, Schon S, et al. Complement 5a receptor inhibition improves renal allograft survival. *J Am Soc Nephrol*. 2008;19:2302-2312.
 23. Hallgren J, Gurish MF. Mast cell progenitor trafficking and maturation. *Adv Exp Med Biol*. 2011;716:14-28.
 24. Lindstedt KA, Kovanen PT. Mast cells in vulnerable coronary plaques: potential mechanisms linking mast cell activation to plaque erosion and rupture. *Curr Opin Lipidol*. 2004;15:567-573.
 25. Farb A, Burke AP, Tang AL, Liang TY, Mannan P, Smialek J, et al. Coronary plaque erosion without rupture into a lipid core. A frequent cause of coronary thrombosis in sudden coronary death. *Circulation*. 1996;96:1354-1363.
 26. Mayranpaa MI, Heikkila HM, Lindstedt KA, Walls AF, Kovanen PT. Desquamation of human coronary artery endothelium by human mast cell proteases: implications for plaque erosion. *Coron Artery Dis*. 2006;17:611-621.
 27. Heikkila HM, Latti S, Leskinen MJ, Hakala JK, Kovanen PT, Lindstedt KA. Activated mast cells induce endothelial cell apoptosis by a combined action of chymase and tumor necrosis factor- α . *Arterioscler Thromb Vasc Biol*. 2008;28:309-314.
 28. Winter MC, Shasby SS, Ries DR, Shasby DM. Histamine selectively interrupts VE-cadherin adhesion independently of capacitive calcium entry. *Am J Physiol Lung Cell Mol Physiol*. 2004;287:L816-L823.
 29. Wong RK, Baldwin AL, Heimark RL. Cadherin-5 redistribution at sites of TNF- α and IFN- γ -induced permeability in mesenteric venules. *Am J Physiol*. 1999;276:H736-H748.
 30. Leskinen MJ, Lindstedt KA, Wang Y, Kovanen PT. Mast cell chymase induces smooth muscle cell apoptosis by a mechanism involving fibronectin degradation and disruption of focal adhesions. *Arterioscler Thromb Vasc Biol*. 2003;23:238-243.
 31. Leskinen MJ, Heikkila HM, Speer MY, Hakala JK, Laine M, Kovanen PT, et al. Mast cell chymase induces smooth muscle cell apoptosis by disrupting NF- κ B-mediated survival signaling. *Exp Cell Res*. 2006;312:1289-1298.
 32. Johnson JL, Jackson CL, Angelini GD, George SJ. Activation of matrix-degrading metalloproteinases by mast cell proteases in atherosclerotic plaques. *Arterioscler Thromb Vasc Biol*. 1998;18:1707-1715.
 33. Fang KC, Wolters PJ, Steinhoff M, Bidgol A, Blount JL, Caughey GH. Mast cell expression of gelatinases A and B is regulated by kit ligand and TGF- β . *J Immunol*. 1999;162:5528-5535.
 34. Amara U, Flierl MA, Rittirsch D, Klos A, Chen H, Acker B, et al. Molecular intercommunication between the complement and coagulation systems. *J Immunol*. 2010;185:5628-5636.
 35. Laine P, Pentikainen MO, Wurzner R, Penttila A, Paavonen T, Meri S, et al. Evidence for complement activation in ruptured coronary plaques in acute myocardial infarction. *Am J Cardiol*. 2002;90:404-408.
 36. Langer HF, Chung KJ, Orlova VV, Choi EY, Kaul S, Kruhlak MJ, et al. Complement-mediated inhibition of neovascularization reveals a point of convergence between innate immunity and angiogenesis. *Blood*. 2010;116:4395-4403.

Online data supplement

Detailed Methods

Animals

All animal work was performed in compliance with Dutch government guidelines. Male mast cell deficient Kit(W^{sh}/W^{sh}) mice and apolipoprotein E-deficient (apoE^{-/-}) mice (cross bred for more than eighteen generations on a C57BL/6 background) and bred in the local animal facility and male C57BL/6 mice (Charles River Laboratories), were used for all experiments. All mice were between 10-20 weeks old at time of surgery. Before surgery apoE^{-/-} mice were randomized to the different groups on basis of plasma cholesterol levels (Roche Diagnostics) and body weight. At sacrifice (28 days after surgery, with exception of the time courses) cholesterol levels and body weight were not significantly different between the treatment groups and their controls. Furthermore, sysmex analyses of blood cells was performed for all experiments and no significant differences were detected in the % of WBC populations between the treatment groups and their appropriate controls. In Supplemental table I white blood cell analysis of the C5a and cromolyn experiment is shown.

In vivo experimental setup

A detailed flow-chart displaying the *in vivo* experimental setup is shown in Supplemental Figure 1. The presence of mast cells, C5a and C5aR was determined in vein grafts of hypercholesterolemic apoE^{-/-} mice. For this, immunohistochemistry and RT-PCR analysis were performed on time courses of paraffin and RNA material of 3-4 mice per time point. To demonstrate the contribution of mast cells to vein graft disease, autologous vein grafts were placed in mast cell deficient Kit(W^{sh}/W^{sh}) mice and control C57BL/6 mice (n=8/group). To determine the effect of local mast cell activation apoE^{-/-} mice were skin-sensitized for 2 consecutive days with dinitrofluorobenzene (DNFB, 0.5% v/v, Janssen Chimica) or vehicle control solution (acetone: olive oil 4:1, n=12 per group) as previous described¹. One week after skin-sensitization and directly after surgery 50 µg dinitrophenyl hapten (DNP) in pluronic gel (25% wt/vol, Sigma)² or pluronic gel alone was applied around the vein grafts.

The effect of modulation of C5a signalling was investigated by challenging apoE^{-/-} mice perivascularly with either 0.5 µg or 5 µg of recombinant mouse C5a (HyCult Biotechnology) or vehicle control, which was applied around the vein grafts in pluronic gel (25% wt/vol) directly after surgery (n=7/group). In order to inhibit C5a function, mice were treated daily, starting 1 day prior to surgery, with subcutaneous injections of 0.3mg/kg hydrocinnamate-[OP-(D-Cha)WR] (PMX205)³ or vehicle solution (propylene glycol: sterile water 3:7, n=7/group). PMX205 displays potent antagonizing activity for the C5a receptor and was synthesized as described previously⁴. To determine the mast cell dependent C5a effects, a group of C5a (5 µg) stimulated mice were treated twice weekly with intraperitoneal injection of the specific mast cell stabilizer, cromolyn (50 mg/kg, Sigma) versus C5a (5µg), cromolyn and PBS treated mice (n=9/group).

Vein graft surgery

Before surgery and at sacrifice, mice were anesthetized by an intra-peritoneal injection with midazolam (5 mg/kg, Roche), medetomidine (0.5 mg/kg, Orion) and fentanyl (0.05 mg/kg, Janssen). After the surgery mice were antagonized with subcutaneous injection of atipamezol (2.5 mg/kg, Orion), fluminasemid (0.5 mg/kg, Braun) and buprenorphine (0.05 mg/kg, Schering-Plough). The adequacy of the anaesthesia was monitored by keeping track of the breathing frequency and the response to toe pinching of the mice. Vein graft surgery was performed as described previously⁵. In brief, thoracic caval veins from donor littermates were harvested. In recipients, the right carotid artery was dissected and cut in the middle. The artery was everted around the cuffs that were placed at both ends of the artery and ligated with 8.0 sutures. The

caval vein was sleeved over the two cuffs, and ligated. At sacrifice, after 3 minutes of *in vivo* perfusion-fixation, vein grafts were harvested and fixed in 4% formaldehyde, dehydrated and paraffin-embedded for histology or snap frozen for RNA analysis.

RNA isolation, cDNA synthesis and RT-PCR

Total RNA was isolated from vein grafts harvested on several time points (3-4 vein grafts/time point, 6h, 24h, 3d; 7d; 14d and 28d after surgery). Also, caval veins of donor mice were included. RNA was isolated and cDNA was synthesized as described previously⁶. Intron-spanning polymerase chain reaction (PCR) primer sets were designed using Primer Express 1.5 software (Supplemental table II). Relative mRNA expression levels (ΔC_t) were calculated by subtracting the average cycle threshold (C_t) per time point from C_t value of the housekeeping gene hypoxanthine phosphoribosyl transferase (HPRT) ($\Delta C_t = C_{t \text{ target gene}} - C_{t \text{ average housekeeping genes}}$). The ΔC_t levels at each time point were compared with the mRNA expression levels of C5a and C5aR in the non-transplanted caval veins ($\Delta \Delta C_t$) and a mean fold induction was calculated as $2^{-\Delta \Delta C_t}$.

Histological and immunohistochemical assessment of vein grafts

Six consecutive sections, with 150 μm interspace (30 sections of 5 μm thick), per vessel segment were routinely stained with hematoxylin-phloxine-saffron (HPS). Picrosirius red staining was used to visualize collagen content. Mast cells were visualized with aqueous toluidine blue (Sigma), whilst mast cell activation status was detected with an enzymatic kit (Naphtol-CAE, Sigma). Mast cells were marked as activated when granules could be detected near the mast cells. The following antibodies were used for immunohistochemical stainings; C5a (HyCult Biotechnology) C5aR (CD188, SantaCruz), MAC3 (macrophages, BD-Pharmingen), smooth muscle cell actin (Sigma), fibrin (Quickzyme), CD31 (Endothelial cells, Abcam) and neutrophil (Serotec) as described previously^{2,7}. For each antibody, isotype-matched antibodies were used as negative controls and staining was absent in sections incubated with these antibodies (data not shown).

Morphometric analysis of vein grafts

Vein grafting in normocholesterolemic mice results in vessel wall thickening primarily caused by smooth muscle cell accumulation. Whereas under hypercholesterolemic conditions foam cell accumulation and accelerated atherosclerosis are observed. Since elastic laminae do not exist in these grafts of venous origin, we analyzed the putative vessel wall area (or lesion area) by measuring total vessel area (the area of the vessel within the adventitia) and the lumen area. Next the lesion area was calculated (total vessel area – lumen area). Plaque rupture complications were categorized in three categories⁷. Plaque hemorrhage; when extravasated erythrocytes were found adjacent to neovessels. A dissection was defined as a connection between the lumen and the part of the vessel wall underneath the adventitia filled with fibrin and erythrocytes. In case fibrin was found at the luminal side underneath a denudated endothelial layer, coinciding with erythrocytes and neutrophils, this was defined as erosion with intramural thrombosis. In this model occlusive thrombosis is rarely seen.

Quantitative morphometric analysis (Qwin, Leica) of vein grafts was performed on six HPS stained, equally spaced, sections. (Immuno) histochemical stainings were quantified by computer assisted analysis (Qwin, Leica)⁸. The immuno-positive area measured is expressed as a percentage of the lesion area. Mast cell presence was counted manually in four sections of each vein graft and expressed as number of mast cell per mm^2 vein graft. Endothelial coverage of the lumen was analyzed in 6 sections per vein graft. For this, sections were attributed to 3 grades; 0 for no endothelial cell coverage, 1 when partially coverage was detected and 2 for full coverage.

Cell culture

Bone marrow derived mast cells (BMMCs) were cultured as described before⁹. After 4 weeks in culture, BMMCs were degranulated in HEPES-tyrode supplemented with 0.1% fatty acid free BSA (Sigma) with either recombinant mouse C5a (Hycult) or 0.5 mg/mL compound 48/80 (Sigma-Aldrich) for 30 minutes at 37°C. Cells were centrifuged (1,500 rpm, 5 minutes) and the releasate was used for further experiments. Tryptase release was determined as shown previously (DAKO)². To determine release of CCL2, a mouse CCL2 ELISA kit (Biosource Diagnostics) was used according to manufacturer's protocol. Results were plotted as percentage of total release, which was measured in mast cells lysed with 10% Triton-X100 (Sigma), while supernatant of non-degranulated mast cell was used as control (0%).

Human Vascular Material Analysis

Vein graft (n=8) and endarterectomy (n=25) tissues were obtained in accordance with guidelines set out by the 'Code for Proper Secondary Use of Human Tissue' of the Dutch Federation of Biomedical Scientific Societies (Federa). Samples were collected, paraffin embedded and 5 µm sections were prepared. Antibodies against Tryptase (Dako) C5aR (SantaCruz) and C5a (Abcam) were used to detect mast cells, C5a and C5a Receptor in consecutive sections.

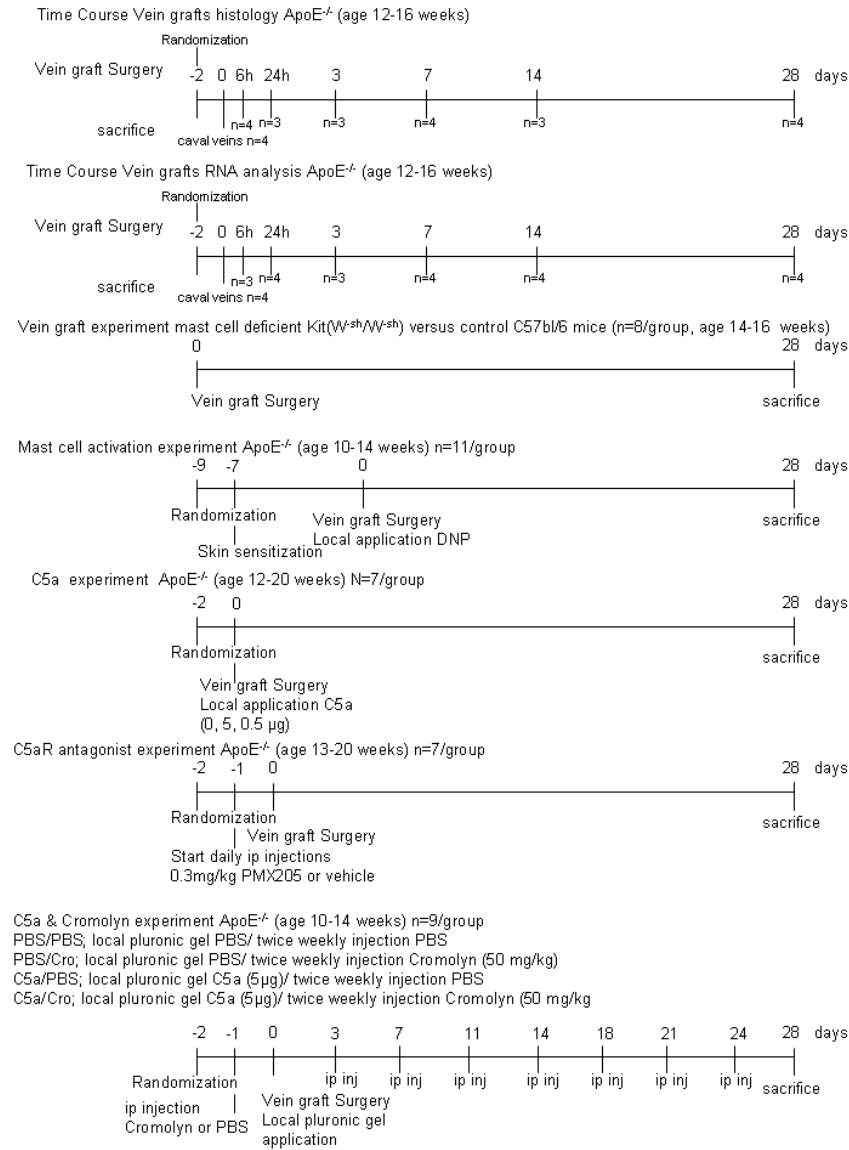
Statistical Analysis

All data are presented as mean ± SD. Statistical analysis was performed using SPSS 17.0 for Windows. For the time courses, statistical analysis was performed using a repeated measures ANOVA with a Bonferroni Post Hoc test. To determine statistical significance for the *in vivo* experiments, comparisons were made using the non-parametric Kruskal-Wallis test. In case of significance, each group was separately compared to the control group using the Mann-Whitney test. For *in vitro* studies a 2-tailed Student's t-test was used to compare individual groups. Probability-values <0.05 were regarded significant.

Supplemental Table I. White Blood Cell analysis (sysmex) of the C5a and cromolyn experiment

Group	Neutrophils (%)	Monocytes (%)	Lymphocytes (%)	Eosinophils (%)
PBS/PBS	22.0 ± 2.3	6.0 ± 0.5	69.7 ± 1.8	2.3 ± 0.2
C5a/PBS	18.6 ± 0.9	5.5 ± 0.3	73.2 ± 0.9	2.7 ± 0.5
PBS/Cro	27.6 ± 2.7	5.7 ± 0.3	64.0 ± 2.6	2.6 ± 0.5
C5a/Cro	24.4 ± 2.4	5.9 ± 0.7	66.9 ± 2.9	2.9 ± 0.8

Supplemental Figure I. Detailed flow-chart of the *in vivo* experimental setup



Supplemental Table II. Primer sequences of housekeeping gene HPRT, Complement factor C5a, and its receptor, C5aR.

Gene	Forward primer	Reverse primer
HPRT	TTGCTCGAGATGTCATGAAGGA	AGCAGGTCAGCAAAGAACTTATAG
C5a	GGATTCAAGCGCATAATAGCA	ACCCGGATGTTGACTCCTC
C5aR	GCATCCGTCGCTGGTTAC	TGCTGTTATCTATGGGGTCCA

Supplemental Table III. Tryptase and CCL2 content of bone marrow derived mast cells (BMMC) releasate after C5a and compound 48/80 stimulation indicated as % of total release. Stimulation of C5a resulted in a release of tryptase comparable to that of the positive control, compound 48/80. Furthermore, C5a stimulation of BMMC led to a dose-dependent release of CCL2.

Compound	Tryptase	CCL2
10 nM C5a	16.4 ± 0.5	1.5 ± 0.9
100 nM C5a	14.4 ± 2.8	9.4 ± 3.2
0.5 µg/mL compound 48/80	16.4 ± 1.5	10.3 ± 3.9

References

1. Kraneveld AD, Buckley TL, van Heuven-Nolsen D, van SY, Koster AS, Nijkamp FP. Delayed type hypersensitivity-induced increase in vascular permeability in the mouse small intestine: inhibition by depletion of sensory neuropeptides and NK1 receptor blockade. *Br J Pharmacol* 1995;114:1483-1489.
2. Bot I, de Jager SC, Zernecke A, Lindstedt KA, van Berkel TJ, Weber C *et al.* Perivascular mast cells promote atherogenesis and induce plaque destabilization in apolipoprotein E-deficient mice. *Circulation* 2007;115:2516-2525.
3. Woodruff TM, Pollitt S, Proctor LM, Stocks SZ, Manthey HD, Williams HM *et al.* Increased potency of a novel complement factor 5a receptor antagonist in a rat model of inflammatory bowel disease. *J Pharmacol Exp Ther* 2005;314:811-817.
4. March DR, Proctor LM, Stoermer MJ, Sbaglia R, Abbenante G, Reid RC *et al.* Potent cyclic antagonists of the complement C5a receptor on human polymorphonuclear leukocytes. Relationships between structures and activity. *Mol Pharmacol* 2004;65:868-879.
5. Lardenoye JH, de Vries MR, Lowik CW, Xu Q, Dhore CR, Cleutjens JP *et al.* Accelerated atherosclerosis and calcification in vein grafts: a study in APOE*3 Leiden transgenic mice. *Circ Res* 2002;91:577-584.
6. Eefting D, Bot I, de Vries MR, Schepers A, van Bockel JH, van Berkel TJ *et al.* Local lentiviral short hairpin RNA silencing of CCR2 inhibits vein graft thickening in hypercholesterolemic apolipoprotein E3-Leiden mice. *J Vasc Surg* 2009;50:152-160.
7. Ewing MM, de Vries MR, Nordzell M, Pettersson K, de Boer HC, van Zonneveld AJ *et al.* Annexin A5 therapy attenuates vascular inflammation and remodeling and improves endothelial function in mice. *Arterioscler Thromb Vasc Biol* 2011;31:95-101.
8. Karper JC, de Vries MR, van den Brand BT, Hoefer IE, Fischer JW, Jukema JW *et al.* Toll-like receptor 4 is involved in human and mouse vein graft remodeling, and local gene silencing reduces vein graft disease in hypercholesterolemic APOE*3Leiden mice. *Arterioscler Thromb Vasc Biol* 2011;31:1033-1040.
9. Razin E, Marx G. Thrombin-induced degranulation of cultured bone marrow-derived mast cells. *J Immunol* 1984;133:3282-3285.

Chapter 4

Complement factor C5a induces atherosclerotic plaque disruptions

J Cell Mol Med. 2014; 18:2020-30.

Anouk Wezel^{1,2}

Margreet R. de Vries^{2,3}

H. Maxime Lagraauw¹

Amanda C. Foks¹

Johan Kuiper¹

Paul H.A. Quax^{2,3}

Ilze Bot^{1,2}

¹ Division of Biopharmaceutics, Gorlaeus Laboratories, Leiden Academic Center for Drug Research, Leiden University, Leiden, The Netherlands

² Department of Surgery, Leiden University Medical Center, Leiden, The Netherlands

³ Einthoven Laboratory for Experimental Vascular Medicine, Leiden, The Netherlands

Abstract

Rationale: Complement factor C5a and its receptor C5aR are expressed in vulnerable atherosclerotic plaques; however, a causal relation between C5a and plaque rupture has not been established yet.

Methods and Results: Accelerated atherosclerosis was induced by placing vein grafts in male apoE^{-/-} mice. After 24 days, when advanced plaques had developed, C5a or PBS was applied locally at the lesion site in a pluronic gel. Three days later mice were sacrificed in order to examine the acute effect of C5a on late stage atherosclerosis. A significant increase of C5aR in the plaque was detectable in mice treated with C5a. Lesion size and plaque morphology did not differ between treatment groups, but interestingly, local treatment with C5a resulted in a striking increase in the amount of plaque disruptions with concomitant intraplaque hemorrhage. To identify the potential underlying mechanisms, smooth muscle cells and endothelial cells were treated *in vitro* with C5a. Both cell types revealed a marked increase in apoptosis after stimulation with C5a, which may contribute to lesion instability *in vivo*. Indeed, apoptosis within the plaque was seen to be significantly increased after C5a treatment.

Conclusions: We here demonstrate a causal role for C5a in atherosclerotic plaque disruptions, probably by inducing apoptosis. Therefore, intervention in complement factor C5a signalling may be a promising target in the prevention of acute atherosclerotic complications.

Introduction

Rupture of an atherosclerotic plaque is the main cause of myocardial infarction or stroke, which are still the leading causes of death worldwide^{1,2}. Features of an unstable plaque, prone to rupture, are a large lipid core covered by a thin fibrous cap depleted of smooth muscle cells. The exact mechanism of progression from an asymptomatic stable lesion to a vulnerable plaque with subsequent rupture is still incompletely understood, but apoptosis of smooth muscle cells and endothelial cells is thought to be crucial³⁻⁵. In search for new therapeutic strategies to reduce the incidence of plaque rupture, attention turned to the complement system, in particular to complement factor C5a.

The complement system, consisting of approximately 30 proteins, has been suggested to play an important role in cardiovascular diseases, amongst which atherosclerosis^{6,7}. The anaphylatoxin C5a, a split product of C5, is constantly produced during complement activation. C5a is one of the most potent inflammatory chemoattractants and promotes leukocyte recruitment to sites of inflammation⁸⁻¹¹. Furthermore, C5a has the ability to activate endothelium and induce the expression and release of numerous cytokines and chemokines such as CCL2^{12,13}. Various cell types, such as macrophages, endothelial cells, smooth muscle cells and mast cells, express receptors for C5a. Previously, we have shown that vein graft disease is aggravated by C5a as a result from attracting and activating mast cells¹⁴. Others have demonstrated that inhibition of C5aR signalling reduces atherosclerosis and neointima formation in apoE^{-/-} mice^{15,16}. Due to its pronounced effects on a number of cell types within the atherosclerotic plaque, C5a may also be one of the key components in plaque destabilization and acute plaque rupture. Previously, it has been demonstrated that elevated levels of C5a are associated with increased cardiovascular risk in patients with advanced atherosclerosis¹⁷. However, since that study was mere observational, a direct causal role for C5a could not be assigned.

A major drawback in preclinical research aiming at the identification of factors involved in acute cardiovascular syndromes is the lack of suitable atherosclerotic mouse models that resemble the complex human atherosclerotic plaque morphology with concomitant plaque rupture. Interestingly, we have recently established that lesions induced in a murine vein graft model are more complex and display both plaque disruptions and intraplaque hemorrhages¹⁸, which are important features of acute atherosclerotic plaque destabilization in humans. These findings render this an excellent model to study late stage atherosclerosis and acute complications.

In the present study we thus aimed to investigate the acute effect of complement factor C5a on late stage atherosclerosis and concomitant plaque complications in this mouse model.

Material and Methods

Mice

This study was performed in compliance with Dutch government guidelines and the Directive 2010/63/EU of the European Parliament. All animal experiments were approved by the animal welfare committee of the Leiden University Medical Center (approval reference number 10091). Male apoE^{-/-} mice (PBS/PBS treated mice: n=8; C5a/PBS treated mice: n=9; C5a/cromolyn treated mice: n=7), were obtained from the Gorlaeus Laboratory animal breeding facility (Leiden, The Netherlands) and were given water and chow *ad libitum*. Plasma total cholesterol levels were measured by enzymatic procedures using precipath standardized serum as an internal standard (Boehringer Mannheim, Germany).

Surgical intervention

Before surgery, gel placement and sacrifice, mice were anesthetized by an intra-peritoneal injection with midazolam (5 mg/kg, Roche, Woerden, The Netherlands), Domitor (0.5 mg/kg, AST Farma, Oudewater, The Netherlands) and fentanyl (0.05 mg/kg, Janssen, Beerse, Belgium). After surgery mice were antagonized with a subcutaneous injection of flumazenil (0.5 mg/kg, Fresenius Kabi, Schelle, Belgium), Antisedan (2.5 mg/kg, AST farma) and buprenorphine (0.1 mg/kg, MSD animal Health, Boxmeer, The Netherlands). Vein graft surgery was performed in order to induce advanced atherosclerotic lesions. In brief, the carotid artery of the recipient mice was cut in the middle; both ends of the artery were everted around cuffs and ligated with 8.0 sutures. The vena cava from donor littermates was harvested and sleeved over the cuffs. By placing the vein in the arterial circulation with high blood pressure, endothelial damage was induced with subsequent accelerated atherosclerosis. After 24 days when advanced lesions were present, age and weight matched mice were anesthetized. A F-127 pluronic gel (25% w/v) was placed in the surrounding tissue of the vein graft (the perivascular tissue) completely surrounding the vessel, enabling us to investigate the local effect rather than the systemic effect of our compound. The gel contained either C5a (5 µg, Hycult Biotech, Uden, The Netherlands) as has been previously described¹⁴, or PBS.

As we have previously established that C5a may exert its effects on atherosclerosis via activation of mast cells¹⁴, we have treated a subgroup of C5a challenged mice with the mast cell stabilizer cromolyn in order to identify mast cell dependent effects. Thus, from gel placement until sacrifice at day 28, mice received daily intra-peritoneal injections with a commonly used mast cell stabilizer cromolyn (50 mg/kg/day, Sigma-Aldrich, Zwijndrecht, The Netherlands)^{19,20} or PBS.

Histological and immunohistochemical analysis

Cross-sections of paraffin embedded vein grafts (5 µm thick) were stained with hematoxylin-phloxine saffron (HPS) for measurement of lesion size, fibrin content and plaque dissection analysis. Fibrin content was graded by two blinded independent investigators on a scale from 0 to 3, with 0 representing no fibrin and 3 representing severe transmural fibrin depositions. Collagen content was visualized with a picrosirius red staining. Mast cell and neutrophil staining was performed using an enzymatic chloroacetate esterase kit (Sigma-Aldrich); when granules were apparent in the vicinity of the mast cell they were scored as activated. Neutrophils were stained light pink, while the segmented nuclei were visualized by Gill's hematoxylin²¹. Composition of the atherosclerotic lesion was further evaluated by immunohistochemical stainings for macrophages (MAC3, 1:200, BD-Pharmingen, San Diego, CA, USA), smooth muscle cell actin (1:1000; Sigma-Aldrich); C5a (1:400; Hycult Biotechnology) and C5aR (1:400; SantaCruz, Dallas, Texas, USA). A TUNEL staining was performed according to manufacturer's protocol in order to detect apoptotic cells in the atherosclerotic plaque (*in situ* cell death detection kit, POD, Roche). The total amount of cells in the vessel wall area, as well as the amount of apoptotic cells, was counted manually, after which the percentage of apoptosis was calculated. All staining measurements were performed on six consecutive

cross-sections of the vein grafts, approximately 150 μm spaced, in a blinded manner by a single observer. Plaque dissection analysis was determined over a total vein graft length of 1800 mm. The disruptions were defined as a connection or fissure between the lumen and part of the vessel wall underneath the adventitia, filled with fibrin and erythrocytes. Quantification of the lesion area and immunostained positive area were performed using computer assisted software (Qwin, Leica, Cambridge, UK). In brief, the total intimal area was measured, as well as the stained area. The stained area was then calculated as a percentage of the total intimal area.

Cell culture

To generate bone marrow derived macrophages (BMDMs), cells were isolated from bone marrow of C57Bl/6 mice and cultured for 7 days in RPMI medium supplemented with 20% fetal calf serum (FCS), 2 mmol/L L-glutamine, 100 U/mL penicillin, 100 mg/mL streptomycin (all from PAA, Colbe, Germany) and 30% L929 cell-conditioned medium (as the source of macrophage colony-stimulating factor (M-CSF)) as has been described previously²²⁻²⁴. Primary cultured murine smooth muscle cells (vSMC)²⁵ and a murine cell line for endothelial cells H5V²⁶ were cultured in DMEM medium supplemented with 10% FCS, 2 mmol/L L-glutamine, 100 U/mL penicillin and 100 mg/mL streptomycin.

Collagen synthesis assay

To measure collagen production by vSMC, cells were seeded at a density of 0.2×10^6 cells per well. Control medium or medium containing 0.2 nM, 2 nM or 20 nM C5a was added after attachment of the cells. Also, 1 μCi [^3H]Proline (Perkin Elmer, Groningen, The Netherlands) together with 50 $\mu\text{g/mL}$ ascorbic acid was added and incubated overnight at 37°C. Cells were taken up in 20 mM Tris HCl/0.36 mM CaCl_2 (pH=7.6) and sonicated for 2 minutes. Collagen was degraded by incubation with 100 U/mL collagenase for 2 hours at 37°C, after which samples were centrifuged for 15 minutes at maximum speed. Proteins were precipitated for 30 minutes on ice using 50% trichloroacetic acid, after which [^3H]Proline content in the supernatant as a measure for collagen production was quantified in a liquid scintillation analyzer (Packard 1500 Tricarb, Downers Grove, IL, USA). Protein content was measured using a standard BCA protein assay.

Macrophage activation

BMDMs were plated in triplicate at a density of 0.5×10^6 cells/mL. C5a was added in a concentration range of 0.2 nM, 2 nM, 20 nM or 200 nM and incubated overnight at 37°C. In order to investigate the effect of C5a on cytokine release, IL-6 and MCP-1 were measured by means of ELISA (BD Bioscience, San Diego, CA, USA). Cells were lysed for RNA isolation.

RNA isolation, cDNA synthesis and qPCR

Guanidine thiocyanate (GTC) was used to extract total RNA from BMDMs²⁷. RNA was reverse transcribed by M-MuLV reverse transcriptase (RevertAid, MBI Fermentas, Leon-Roth) and used for quantitative analysis of mouse genes (Supplemental Table 1) with an ABI PRISM 7700 Taqman apparatus (Applied Biosystems, Foster City, CA, USA). Murine hypoxanthine phosphoribosyltransferase (HPRT) and murine ribosomal protein 27 (RPL27) were used as standard housekeeping genes.

Annexin V staining

Annexin V staining was performed to detect apoptosis. vSMC and H5V were plated in quadruplicate at 0.4×10^6 cells/mL in medium. After attachment of the cells, C5a was added overnight in a concentration range of 2 nM, 20 nM or 200 nM, which is based on previous literature²⁸ or H_2O_2 as a positive control. Cells were washed and stained with fluorochrome-conjugated Annexin V. To distinguish late stage apoptosis

from early apoptosis, cells were subsequently stained with Propidium Iodide Staining Solution. In late stage apoptosis the cell membrane loses its integrity, these cells then become double-positive for Annexin V and Propidium Iodide. Analysis was performed by flow cytometry (FACS CantoII, BD Bioscience, Breda, The Netherlands).

Statistical analysis

Data are expressed as mean \pm SEM. A Fisher's exact test was used to measure the statistical significance between the amounts of plaque dissections. A 2-tailed Student's t-test was used to compare individual groups. Multiple group comparisons were analysed by 2 way ANOVA. Non-parametric data were analyzed using a Mann-Whitney U test. A value of $P < 0.05$ was considered significant.

Results

Lesion size, C5a and C5aR expression

In order to investigate the effect of C5a on the composition of advanced plaques, age- and weight-matched apoE^{-/-} mice with advanced lesions were treated locally with C5a or PBS. No differences were found in plasma cholesterol levels; also, plasma IL-6 concentration did not differ between groups (Supplemental Figure 1). Analysis of atherosclerotic plaques revealed no difference between groups in lesion size, measured as vessel wall area (PBS: $3.9 \pm 0.4 \times 10^5 \mu\text{m}^2$; C5a: $3.9 \pm 0.3 \times 10^5 \mu\text{m}^2$; C5a/cromolyn: $4.4 \pm 0.4 \times 10^5 \mu\text{m}^2$; Figure 1A).

The presence of C5a and C5aR in the atherosclerotic lesions was determined by immunohistochemical stainings. No differences in C5a expression were found between the three groups (PBS: $2.1\% \pm 0.6\%$; C5a: $1.4\% \pm 0.4\%$ $P=0.4$ compared to PBS; C5a/cromolyn: $1.0\% \pm 0.4\%$ $P=0.2$ compared to PBS; Figure 1B). Interestingly, treatment with C5a resulted in a significant increase of C5aR expression in the lesions (PBS: $0.6\% \pm 0.1\%$; C5a: $1.6\% \pm 0.3\%$ $P < 0.01$ compared to PBS; C5a/cromolyn: $1.8\% \pm 0.4\%$ $P < 0.05$ compared to PBS; Figure 1C). Both C5a and C5a receptor staining was distributed heterogeneously within the lesions, suggesting expression by multiple cell types in the intimal layer. In line with literature^{7,8}, we found C5a and C5aR to be expressed by macrophages, endothelial cells and vascular smooth muscle cells (Supplemental Figure 2).

Plaque morphology

Macrophage, smooth muscle cell and collagen content were measured to establish plaque phenotype. C5a treatment did not affect macrophage content as measured by MAC3 staining (PBS: $13.2\% \pm 1.2\%$; C5a: $13.3\% \pm 3.9\%$; C5a/cromolyn: $9.2\% \pm 2.2\%$; Figure 2A). Also, the collagen content (PBS: $21.7\% \pm 3.1\%$; C5a: $19.9\% \pm 2.4\%$; C5a/cromolyn: $18.3\% \pm 2.1\%$; Figure 2B) and the amount of smooth muscle cells (PBS: $29.0\% \pm 3.9\%$; C5a: $36.9\% \pm 2.3\%$; C5a/cromolyn: $31.7\% \pm 4.6\%$; Figure 2C) did not differ between groups.

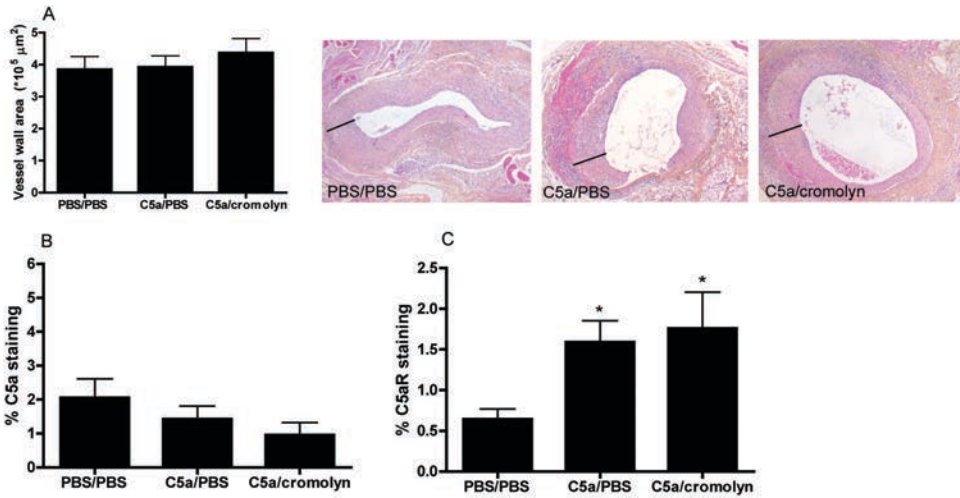


Figure 1. Local application of C5a in late stage atherosclerosis did not result in a change of lesion size (A). Three representative pictures (40x magnifications) show HPS (hematoxylin-phloxine saffron) stained vessel wall segments of all treatment groups, used for measurement of lesion size and plaque rupture analysis. Lines indicate vessel wall thickness. Immunohistochemical staining revealed no changes in C5a expression between treatment groups (B). However, C5a receptor (C5aR) expression was significantly upregulated in mice treated with C5a (C). (PBS/PBS treated mice: $n=8$; C5a/PBS treated mice: $n=9$; C5a/cromolyn treated mice: $n=7$; $*P<0.05$ compared to PBS/PBS)

Local application of C5a resulted in a trend towards an increased amount of activated mast cells ($P=0.07$; Figure 2E), which was decreased in mice treated with cromolyn. Moreover, the total amount of perivascular mast cells was significantly increased after C5a treatment, which could partly be inhibited by cromolyn (PBS: 0.3 ± 0.1 mast cells/ mm^2 ; C5a: 0.9 ± 0.2 mast cells/ mm^2 ; C5a/cromolyn: 0.6 ± 0.1 mast cells/ mm^2 ; Figure 2D). These findings are in line with our previous data, where we established that local treatment with a specific mast cell activator results in activation of perivascular mast cells and subsequent recruitment of newly infiltrating mast cells into the vessel wall¹⁹.

Neutrophil count in the intima did not differ between the three treatment groups (Figure 2F). Also, no signs of leaky vessels were detected, defined as the presence of erythrocytes outside vascular-like structures in the intima; excluding areas in which erythrocytes were present due to plaque disruptions¹⁸.

Plaque disruptions and fibrin depositions in C5a treated groups

HPS staining was used for further analysis of lesion morphology. Interestingly, local treatment with C5a showed an increase in the amount of plaque disruptions from 13% in the PBS treated group up to 56% in the C5a treated group. Plaque disruptions were defined as the presence of erythrocytes in the lesions with concomitant fibrin depositions. Moreover, additional analysis revealed a significant increase in the length of disruptions after C5a application ($P<0.05$). Cromolyn treatment did not reduce the number (71%) or length of the disruptions (Figure

3A and 3B). Analysis of fibrin content in the plaque revealed a significant increase after treatment with C5a (Figure 3C; $P<0.05$). Again, cromolyn application did not reduce this effect, indicating a mast cell independent role of C5a in plaque rupture. To explain these findings, we next performed *in vitro* studies to evaluate the direct effect of C5a on macrophages, smooth muscle cells and endothelial cells.

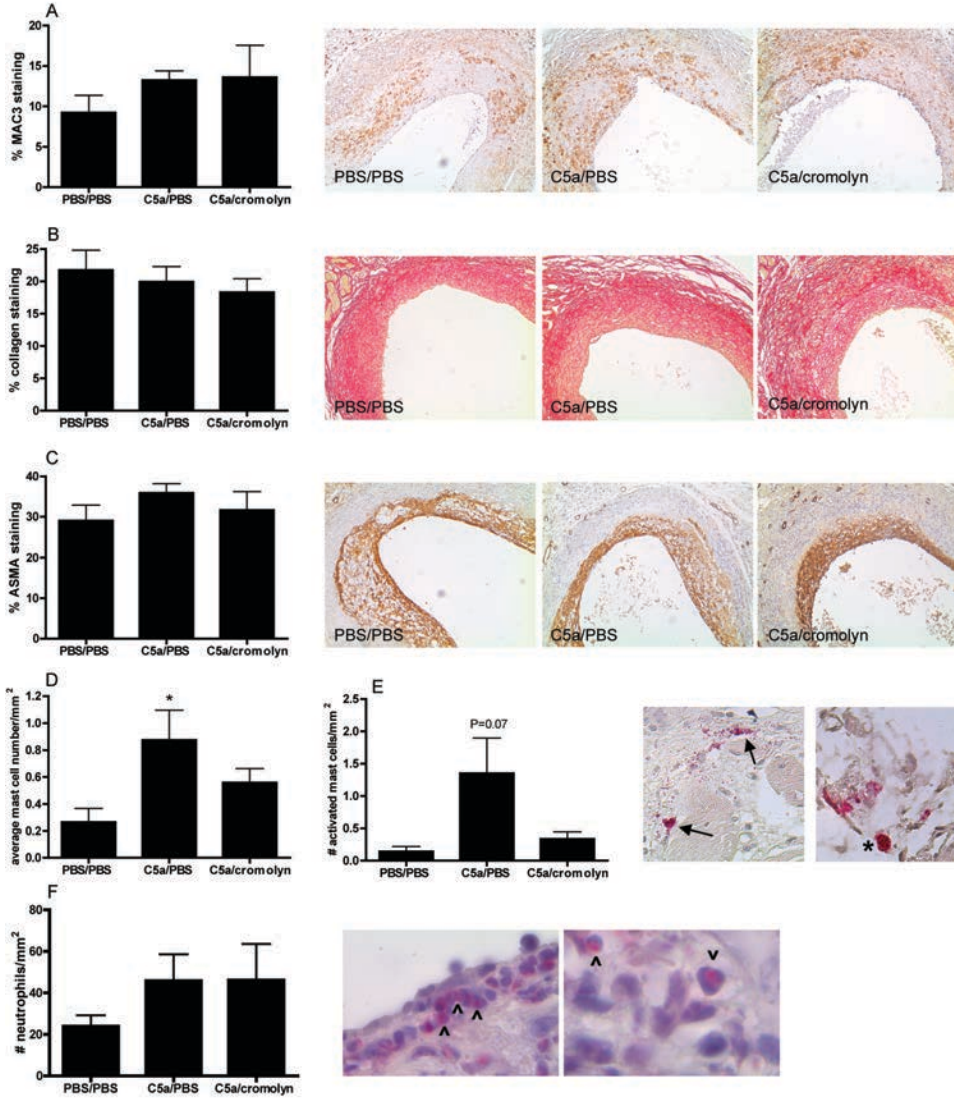


Figure 2. Plaque composition was investigated by staining for macrophages (MAC3, A), collagen (Sirius Red, B) and smooth muscle cells (ASMA, C). Representative pictures (100x magnifications) show immunohistochemical stainings of all treatment groups. Also, the total amount of mast cells in the perivascular tissue was determined (D) as well as the amount of activated mast cells (E). Pictures show activated mast cells (arrows) with granules present in the vicinity of the cell. Also, a resting mast cell (*) is shown with all granules contained inside the cell. Neutrophils in the intima were stained with a naphtol CAE staining (F). Pictures show neutrophils stained light pink with clearly visible segmented nuclei (^). (PBS/PBS treated mice: n=8; C5a/PBS treated mice: n=9; C5a/cromolyn treated mice: n=7; * $P<0.05$ compared to PBS/PBS).

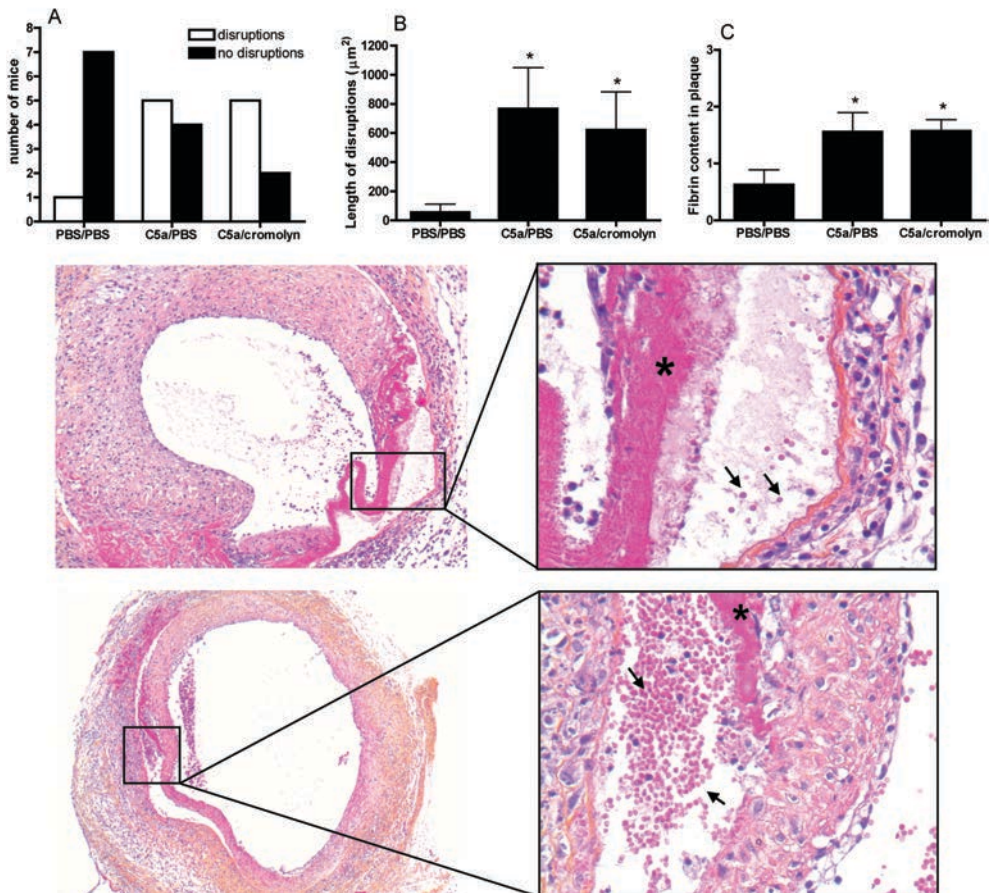


Figure 3. Three days after local application of C5a in late stage atherosclerosis, increased amount of plaque disruptions, as defined by the presence of erythrocytes in the lesions (arrows) with concomitant fibrin depositions, were present in the treated groups (A), while also the length of the disruptions was increased (B). Fibrin content (*) was significantly increased in mice treated with C5a (B). Cromolyn, a common mast cell stabilizer, did not reduce this effect. (PBS/PBS treated mice: $n=8$; C5a/PBS treated mice: $n=9$; C5a/cromolyn treated mice: $n=7$; * $P<0.05$ compared to PBS/PBS).

In vitro activation by C5a

Activation of BMDMs by C5a resulted in an increase of MCP-1 secretion of almost seven fold (200 nM C5a: 888.0 pg/ml; control: 128.8 pg/ml; $P<0.001$). No changes were detected in IL-6 secretion by C5a activated macrophages. Collagen synthesis rate of smooth muscle cells remained unchanged after treatment with C5a (data not shown). Furthermore, the TIMP1/MMP9 ratio, as a marker of the proteolytic status of C5a stimulated macrophages, did not significantly change after C5a stimulation (Figure 4).

Treatment of endothelial cells with a concentration range of C5a (2 nM -200 nM) did not induce changes in the expression of the adhesion molecules V-CAM, I-CAM or PECAM (Supplemental Figure 3).

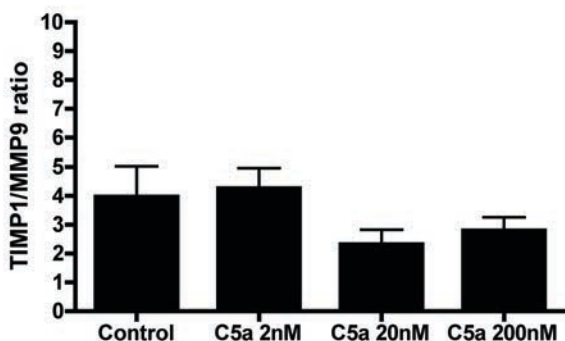


Figure 4. Expression levels of TIMP1/MMP9 ratio in BM derived macrophages showed no significant differences after activation with increasing concentrations of C5a.

In vitro apoptosis

One of the features of plaque instability is smooth muscle cell apoptosis^{3,4}. To investigate the effect of C5a on smooth muscle cells viability, we added C5a in concentrations ranging from 2 nM, 20 nM to 200 nM to cultured smooth muscle cells. Interestingly, we found a clear dose-dependent increase in smooth muscle cell apoptosis after exposure to C5a. Both the percentage of early apoptosis (200 nM C5a: 37.8% \pm 0.9%; control: 13.2% \pm 3.9%; $P < 0.001$; Figure 5B), as the percentage of late stage apoptosis (200 nM C5a: 34.6% \pm 2.3%; control: 3.8% \pm 0.8%; $P < 0.0001$; Figure 5D), were significantly increased compared to the negative control. Consequently, the amount of viable cells was drastically decreased after C5a treatment (200 nM C5a: 20.0% \pm 2.2%; control: 77.4% \pm 5.2%; $P < 0.0001$; Figure 5F).

Since disturbed endothelial lining along the luminal site of the vessel predisposes to plaque erosions and instability as well, we stimulated endothelial cells with the same C5a concentration range. Early apoptosis was significantly increased compared to the negative control (200 nM C5a: 24.3% \pm 2.4%; control: 10.3% \pm 0.9%; $P < 0.005$; Figure 5A) in a dose-dependent manner. Also, a concomitant trend towards increased late stage apoptosis was detected (200 nM C5a: 24.9% \pm 3.9%; control: 15.9% \pm 1.6%; $P = 0.07$; Figure 5C). The percentage of viable cells was significantly decreased after treatment with C5a (200 nM C5a: 35.3% \pm 4.1%; control: 57.2% \pm 3.1%; $P < 0.01$; Figure 5E). Cromolyn did not affect C5a-induced apoptosis of either endothelial cells or smooth muscle cells (data not shown).

To investigate whether apoptosis is induced via apoptotic caspases, we measured mRNA levels of caspase-1, caspase-3 and Bax in endothelial cells after stimulation with 2 nM, 20 nM or 200 nM C5a. We did not detect any changes between caspase-1 or Bax expression, however, we observed a significant dose-dependent increase of caspase-3 expression after C5a stimulation (Supplemental Figure 4), suggesting that C5a mediated apoptosis is mediated via the caspase cascade.

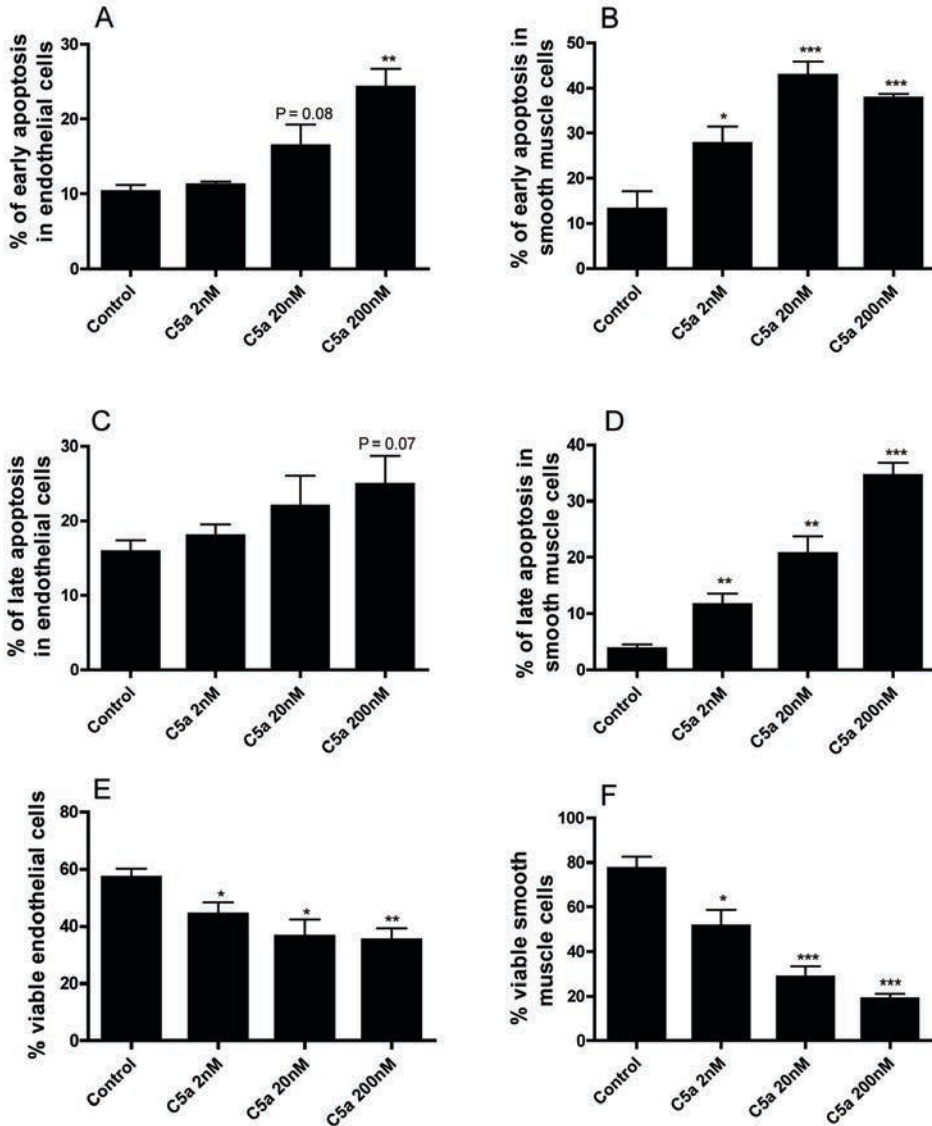


Figure 5. Treatment of smooth muscle cells *in vitro* by C5a 2 nM, C5a 20 nM and C5a 200 nM showed a marked dose-dependent increase of both early (B) and late apoptosis (D). Consequently, the amount of viable smooth muscle cells after C5a stimulation was significantly decreased (F). Also, early apoptosis (A) and late apoptosis (C) of endothelial cells were increased after C5a stimulation. The amount of viable endothelial cells showed a dose-dependent decrease (E). Both endothelial cell and smooth muscle cell apoptosis can contribute to plaque destabilization. (* $P < 0.05$; ** $P < 0.01$; *** $P < 0.001$).

In vivo apoptosis

In order to confirm our *in vitro* results, we performed a TUNEL staining to detect apoptosis within the atherosclerotic plaque. Local application of C5a resulted in a significant increase in the percentage of apoptotic cells in the vessel wall, thereby

validating our *in vitro* findings (PBS: $2.4\% \pm 0.6\%$ of the total cell population; C5a: $5.9\% \pm 1.4\%$; $P < 0.05$; Figure 6). Cromolyn treatment slightly reduced this effect, however there was still an increase in apoptotic cells apparent (PBS: $2.4\% \pm 0.6\%$; C5a/cromolyn: $4.1\% \pm 0.6\%$; $P = 0.075$ compared to PBS; Figure 6). Apoptotic cells were apparent along the endothelial lining of luminal site of the vessel, as well as in smooth muscle cell rich areas. These data identify the induction of apoptosis as a potential mechanism via which C5a can induce plaque disruptions.

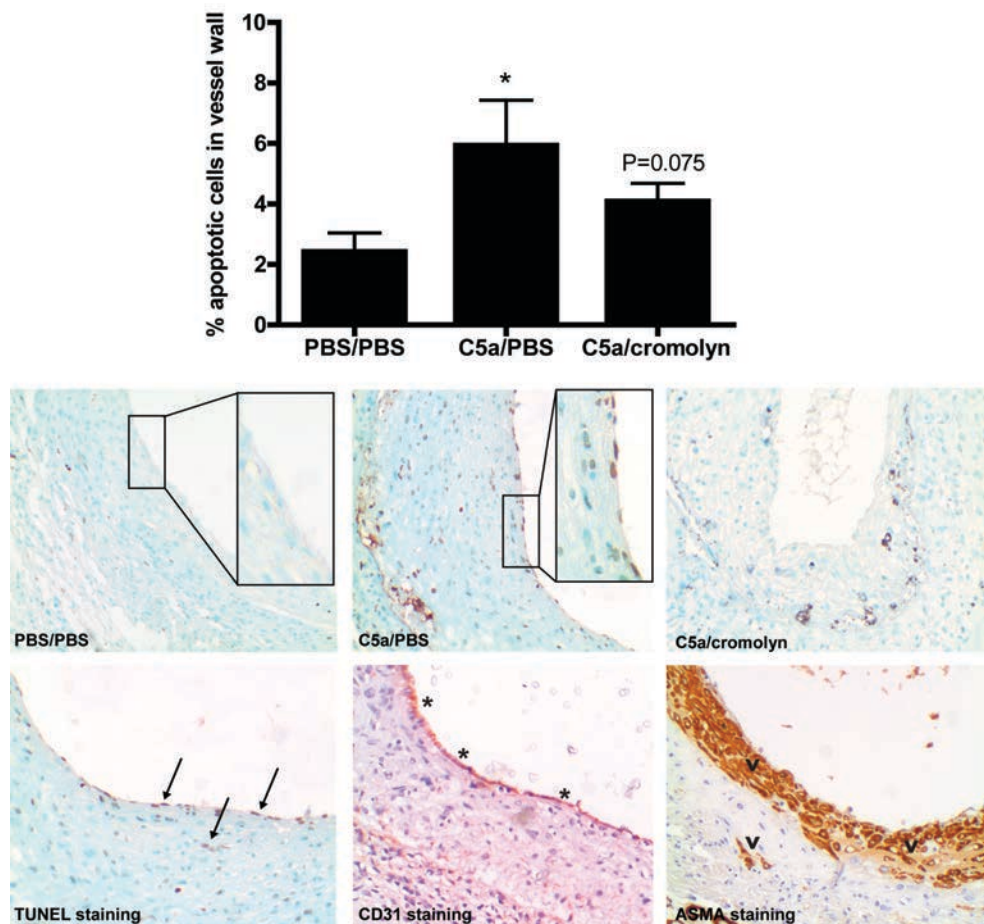


Figure 6. Apoptosis measurement is depicted as the percentage of apoptotic cells of the total number of cells within the vessel wall. Perivascular treatment with C5a resulted in an increase of apoptosis ($*P < 0.05$), which was not affected by cromolyn treatment. Top pictures show representative TUNEL stained sections of all three treatment groups (200x magnifications). Enlargements demonstrate endothelial cell apoptosis in C5a treated groups, which is mostly absent in control mice (400x magnifications). Pictures in the lower panel show representative micrographs of consecutive slides (200x magnifications). From left to right are shown: TUNEL positive staining for apoptotic cells (arrows); CD31 positive staining for endothelial cells (*) and alpha smooth muscle cell actin positive staining (^). (PBS/PBS treated mice: $n = 8$; C5a/PBS treated mice: $n = 9$; C5a/cromolyn treated mice: $n = 7$; $*P < 0.05$ compared to PBS/PBS).

Discussion

The current study describes a causal role for complement factor C5a in acute atherosclerotic plaque disruptions, which was studied by the perivascular application of C5a in advanced atherosclerotic lesions. Acute activation by C5a resulted in increased amount of plaque disruptions with concomitant intraplaque hemorrhage and fibrin depositions. *In vitro* stimulation with C5a led to a striking increase of smooth muscle cell and endothelial cell apoptosis. Moreover, increased apoptosis was confirmed in the vessel wall after C5a treatment, which may contribute to the plaque disruptions observed in this study.

Previously, we have demonstrated that local application of C5a at time of graft placement aggravates vein graft disease via activation of perivascular mast cells¹⁴. In that previous study, mice received C5a treatment only during the first days after surgery; therefore C5a had the most prominent effects on the initiation of the lesion. In this initial process both attraction and activation of mast cells have shown to be important. Interestingly, in the current study, where effects of C5a on advanced lesions were investigated, results are indicative of a mast cell independent mechanism as the mast cell stabilizer cromolyn did not prevent the C5a induced effects on plaque disruptions. These effects can be explained by differences in relative cellular content of early versus advanced lesions. In early lesions recruitment of inflammatory cells, possibly via mast cell derived chemokines such as MCP-1, plays a prominent role, while in advanced lesions a loss of matrix deposition and increased apoptosis are detrimental for plaque stability. The mechanism behind C5a activation may therefore differ between early as compared to advanced stages of atherosclerosis. Indeed, in our previous study, we have established that C5a attracts and activates mast cells, resulting in a more profound influx of inflammatory cells and accelerated vein graft disease. In mature lesions however, the amount of immune cells present in the vessel wall is already strongly increased. Although we again observe an increased number of mast cells in this study, and mast cell proteases have been implicated in plaque stability and apoptosis^{19,29,30}, C5a itself may have more direct and pronounced effects on other cell types involved in maintaining plaque stability, such as the smooth muscle cell. Features of an unstable atherosclerotic plaque, prone to rupture, have been described extensively³¹. A thin fibrous cap devoid of collagen and smooth muscle cells, a large acellular necrotic core and increased inflammation and neovascularization are detrimental for plaque stability. Disruptions described in the current experiment are not equal to plaque ruptures in the classical definition, in which a thin cap covering a lipid core ruptures, resulting in atherothrombosis³². This may be due to the fact that the vein grafts described in the current study do not contain large necrotic cores similar to human plaques, but smaller necrotic cores distributed heterogeneous throughout the intima. However, we would like to

emphasize that, as of yet, there have not been any mouse models described that completely resemble human plaque rupture, and its complex lesion morphology³³⁻³⁵. In contrast to many other mouse models, this vein graft model does exhibit a complex morphology including neovascularization, calcifications and disruptions consisting of fibrin depositions and intraplaque hemorrhage, which has extensively been described by De Vries *et al.*¹⁸. We therefore believe that this model can make a valuable contribution to research regarding the underlying mechanisms behind plaque disruptions.

To elucidate the mechanism by which C5a causes plaque disruptions, we investigated the effect of C5a *in vitro* on various cell types. Speidl *et al.* have previously demonstrated an increase of MMP expression after C5a administration to human macrophages³⁶. Because collagen turnover is important for the integrity of the fibrous cap, we determined the ratio of TIMP1/MMP9 expression after treating murine macrophages with C5a. In line with our *in vivo* data, where we did not observe any effects on lesional collagen content, we did not observe any changes in the TIMP1/MMP9 ratio, while we also did not observe any effects on smooth muscle cell dependent collagen production. Taken together, these data suggest that C5a does not acutely affect plaque stability via interference in matrix homeostasis.

Next, we investigated the effect of C5a on cellular apoptosis, a pathway which has also been suggested to contribute to plaque instability^{37,38}. Intriguingly, a marked dose-dependent increase of both early and late apoptosis was detected when administering C5a to smooth muscle cells as well as to endothelial cells. These results are in line with previous findings that C5a can induce apoptosis of adrenomedullary cells and neuronal cells^{39,40}. We here demonstrate that C5a causes a striking increase in apoptosis of smooth muscle cells. In late stage atherosclerosis, smooth muscle cell apoptosis is responsible for a potent inflammatory response, loss of collagen and thinning of the fibrous cap, whereas it causes no inflammation or thrombosis in normal arteries⁴¹. Specific apoptosis of smooth muscle cells in established atherosclerotic lesions resulted in plaques with unstable features⁴². Also, it has been shown that induction of smooth muscle cell apoptosis by specific SIRT1 deletion results in reduced cap/intima ratio⁴³. Together, these data highlight the importance of viable smooth muscle cells to the fibrous cap. Furthermore, we detected a remarkable increase of endothelial cell apoptosis after addition of C5a. Previously it has been described that C5a induces apoptosis of endothelial cells⁴⁴. Induction of endothelial cell apoptosis may result in erosions at the luminal site of atherosclerotic lesions, making the surface prone to thrombus formation and subsequent acute cardiovascular syndromes⁴⁵. Indeed, local C5a treatment resulted in an increased percentage of apoptotic cells within the atherosclerotic plaque. However, it should be noted that most of the cells in the lesion are C5aR positive; therefore we cannot completely exclude the

possibility of effects of C5a on other C5aR positive cells besides endothelial and smooth muscle cells.

Although the local concentration of C5a *in vivo* was artificially created in this study, it should be realized that previous reports described an increase in serum C5a in patients suffering from cardiovascular disease, furthermore, C5a levels did correlate with cardiovascular events and late lumen loss in drug eluting stents^{17,46}. C5a in the plaque and adventitia may thus derive via diffusion through perivessels; also, it may be locally derived from various cell types in the vessel wall, such as smooth muscle cells, macrophages and endothelial cells.

In conclusion, we here demonstrate a causal role for C5a in the induction of atherosclerotic plaque disruptions. C5a exposure resulted in a marked increase of endothelial cell and smooth muscle cell apoptosis *in vitro*. Moreover, increased apoptosis *in vivo* was observed, which may contribute to plaque destabilization. With respect to rheumatoid arthritis and psoriasis, phase Ib/IIa clinical trials for a C5a inhibitor have already been completed⁴⁷, and a similar therapeutic strategy using complement factor C5a as a target may be promising in the prevention of acute cardiovascular events.

References

1. Glass CK, Witztum JL. Atherosclerosis. the road ahead. Cell. 2001; 104; 503–16.
2. Roger VL, Go AS, Lloyd-Jones DM, et al. Heart disease and stroke statistics--2012 update: a report from the American Heart Association. Circulation. 2012; 125:e2-220.
3. Von der Thüsen JH, van Vlijmen BJM, Hoebe RC, et al. Induction of atherosclerotic plaque rupture in apolipoprotein E-/- mice after adenovirus-mediated transfer of p53. Circulation. 2002; 105; 2064–70.
4. Stoneman VEA, Bennett MR. Role of apoptosis in atherosclerosis and its therapeutic implications. Clin Sci Lond Engl 1979. 2004;107:343–54.
5. Libby P. The molecular mechanisms of the thrombotic complications of atherosclerosis. J Intern Med. 2008;263:517–27.
6. Oksjoki R, Kovanen PT, Meri S, et al. Function and regulation of the complement system in cardiovascular diseases. Front Biosci J Virtual Libr. 2007;12:4696–708.
7. Haskard DO, Boyle JJ, Mason JC. The role of complement in atherosclerosis. Curr Opin Lipidol. 2008;19:478–82.
8. Speidl WS, Kastl SP, Huber K, et al. Complement in atherosclerosis: friend or foe? J Thromb Haemost. 2011; 9: 428–40.
9. Distelmaier K, Adlbrecht C, Jakowitsch J, et al. Local complement activation triggers neutrophil recruitment to the site of thrombus formation in acute myocardial infarction. Thromb Haemost. 2009;102:564–72.
10. Haas P-J, van Strijp J. Anaphylatoxins: their role in bacterial infection and inflammation. Immunol Res. 2007; 37; 161–75.
11. Guo R-F, Ward PA. Role of C5a in inflammatory responses. Annu Rev Immunol. 2005 ;23:821–52.
12. Buono C, Come CE, Witztum JL, et al. Influence of C3 deficiency on atherosclerosis. Circulation. 2002;105:3025–31.
13. Conroy A, Serghides L, Finney C, et al. C5a enhances dysregulated inflammatory and angiogenic responses to malaria in vitro: potential implications for placental malaria. PloS One. 2009;4:e4953.
14. De Vries MR, Wezel A, Schepers A, et al. Complement factor C5a as mast cell activator mediates vascular remodelling in vein graft disease. Cardiovasc Res. 2013;97:311–20.

15. Manthey HD, Thomas AC, Shiels IA, et al. Complement C5a inhibition reduces atherosclerosis in ApoE^{-/-} mice. *FASEB J Off Publ Fed Am Soc Exp Biol.* 2011;25:2447–55.
16. Shagdarsuren E, Bidzhekov K, Mause SF, et al. C5a receptor targeting in neointima formation after arterial injury in atherosclerosis-prone mice. *Circulation.* 2010;122:1026–36.
17. Speidl WS, Exner M, Amighi J, et al. Complement component C5a predicts future cardiovascular events in patients with advanced atherosclerosis. *Eur Heart J.* 2005;26:2294–9.
18. De Vries MR, Niessen HWM, Löwik CWGM, et al. Plaque rupture complications in murine atherosclerotic vein grafts can be prevented by TIMP-1 overexpression. *PLoS One.* 2012;7:e47134.
19. Bot I, de Jager SCA, Zernecke A, et al. Perivascular mast cells promote atherogenesis and induce plaque destabilization in apolipoprotein E-deficient mice. *Circulation.* 2007;115:2516–25.
20. Bot M, de Jager SCA, MacAleese L, et al. Lysophosphatidic acid triggers mast cell-driven atherosclerotic plaque destabilization by increasing vascular inflammation. *J Lipid Res.* 2013;54:1265–74.
21. Zernecke A, Bot I, Djalali-Talab Y, et al. Protective role of CXC receptor 4/CXC ligand 12 unveils the importance of neutrophils in atherosclerosis. *Circ Res.* 2008;102:209–17.
22. Zhao Y, Pennings M, Hildebrand RB, et al. Enhanced foam cell formation, atherosclerotic lesion development, and inflammation by combined deletion of ABCA1 and SR-BI in Bone marrow-derived cells in LDL receptor knockout mice on western-type diet. *Circ Res.* 2010;107:e20–31.
23. Lammers B, Zhao Y, Hoekstra M, et al. Augmented atherogenesis in LDL receptor deficient mice lacking both macrophage ABCA1 and ApoE. *PLoS One.* 2011;6:e26095.
24. Meurs I, Lammers B, Zhao Y, et al. The effect of ABCG1 deficiency on atherosclerotic lesion development in LDL receptor knockout mice depends on the stage of atherogenesis. *Atherosclerosis.* 2012; 221:41–7.
25. Michon IN, Hauer AD, von der Thüsen JH, et al. Targeting of peptides to restenotic vascular smooth muscle cells using phage display in vitro and in vivo. *Biochim Biophys Acta.* 2002;1591:87–97.
26. Garlanda C, Parravicini C, Sironi M, et al. Progressive growth in immunodeficient mice and host cell recruitment by mouse endothelial cells transformed by polyoma middle-sized T antigen: implications for the pathogenesis of opportunistic vascular tumors. *Proc Natl Acad Sci U S A.* 1994;91:7291–5.
27. Chomczynski P, Sacchi N. Single-step method of RNA isolation by acid guanidinium thiocyanate-phenol-chloroform extraction. *Anal Biochem.* 1987;162:156–9.
28. Bosmann M, Haggadone MD, Hemmila MR, et al. Complement activation product C5a is a selective suppressor of TLR4-induced, but not TLR3-induced, production of IL-27(p28) from macrophages. *J Immunol Baltim Md 1950.* 2012;188:5086–93.
29. Albrecht EA, Sarma JV, Ward PA. Activation by C5a of endothelial cell caspase 8 and cFLIP. *Inflamm Res.* 2009;58:30–7.
30. Flierl MA, Rittirsch D, Chen AJ, et al. The complement anaphylatoxin C5a induces apoptosis in adrenomedullary cells during experimental sepsis. *PLoS ONE.* 2008;3:e2560.
31. Pavlovski D, Thundiyil J, Monk PN, et al. Generation of complement component C5a by ischemic neurons promotes neuronal apoptosis. *FASEB J.* 2012;26:3680–90.
32. Den Dekker WK, Tempel D, Bot I, et al. Mast cells induce vascular smooth muscle cell apoptosis via a toll-like receptor 4 activation pathway. *Arterioscler Thromb Vasc Biol.* 2012;32:1960–9.
33. Lindstedt KA, Kovanen PT. Mast cells in vulnerable coronary plaques: potential mechanisms linking mast cell activation to plaque erosion and rupture. *Curr Opin Lipidol.* 2004;15:567–73.
34. Finn AV, Nakano M, Narula J, et al. Concept of vulnerable/unstable plaque. *Arterioscler Thromb Vasc Biol.* 2010;30:1282–92.
35. Shah PK. Mechanisms of plaque vulnerability and rupture. *J Am Coll Cardiol.* 2003;41:15S–22S.
36. Silvestre-Roig C, de Winther MP, Weber C, et al. Atherosclerotic plaque destabilization: mechanisms, models, and therapeutic strategies. *Circ Res.* 2014;114:214–26.
37. Schwartz SM, Galis ZS, Rosenfeld ME, et al. Plaque rupture in humans and mice. *Arterioscler Thromb Vasc Biol.* 2007;27:705–13.
38. Cullen P, Baetta R, Bellosa S, et al. Rupture of the atherosclerotic plaque: does a good animal model exist? *Arterioscler Thromb Vasc Biol.* 2003;23:535–42.
39. Speidl WS, Kastl SP, Hutter R, et al. The complement component C5a is present in human coronary lesions in vivo and induces the expression of MMP-1 and MMP-9 in human macrophages in vitro. *FASEB J.* 2011;25:35–44.
40. Myoishi M, Hao H, Minamino T, et al. Increased endoplasmic reticulum stress in atherosclerotic plaques associated with acute coronary syndrome. *Circulation.* 2007;116:1226–33.
41. Kolodgie FD, Burke AP, Farb A, et al. The thin-cap fibroatheroma: a type of vulnerable plaque: the

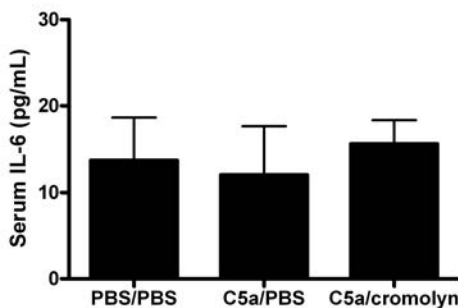
- major precursor lesion to acute coronary syndromes. *Curr Opin Cardiol.* 2001;16:285–92.
42. Clarke MCH, Figg N, Maguire JJ, et al. Apoptosis of vascular smooth muscle cells induces features of plaque vulnerability in atherosclerosis. *Nat Med.* 2006;12:1075–80.
 43. Clarke MCH, Littlewood TD, Figg N, et al. Chronic apoptosis of vascular smooth muscle cells accelerates atherosclerosis and promotes calcification and medial degeneration. *Circ Res.* 2008;102:1529–38.
 44. Gorenne I, Kumar S, Gray K, et al. Vascular smooth muscle cell sirtuin 1 protects against DNA damage and inhibits atherosclerosis. *Circulation.* 2013;127:386–96.
 45. Durand E, Scoazec A, Lafont A, et al. In vivo induction of endothelial apoptosis leads to vessel thrombosis and endothelial denudation: a clue to the understanding of the mechanisms of thrombotic plaque erosion. *Circulation.* 2004;109:2503–6.
 46. Speidl WS, Katsaros KM, Kastl SP, et al. Coronary late lumen loss of drug eluting stents is associated with increased serum levels of the complement components C3a and C5a. *Atherosclerosis.* 2010;208:285–9.
 47. Köhl J. Drug evaluation: the C5a receptor antagonist PMX-53. *Curr Opin Mol Ther.* 2006;8:529–38.

Supplemental Figures

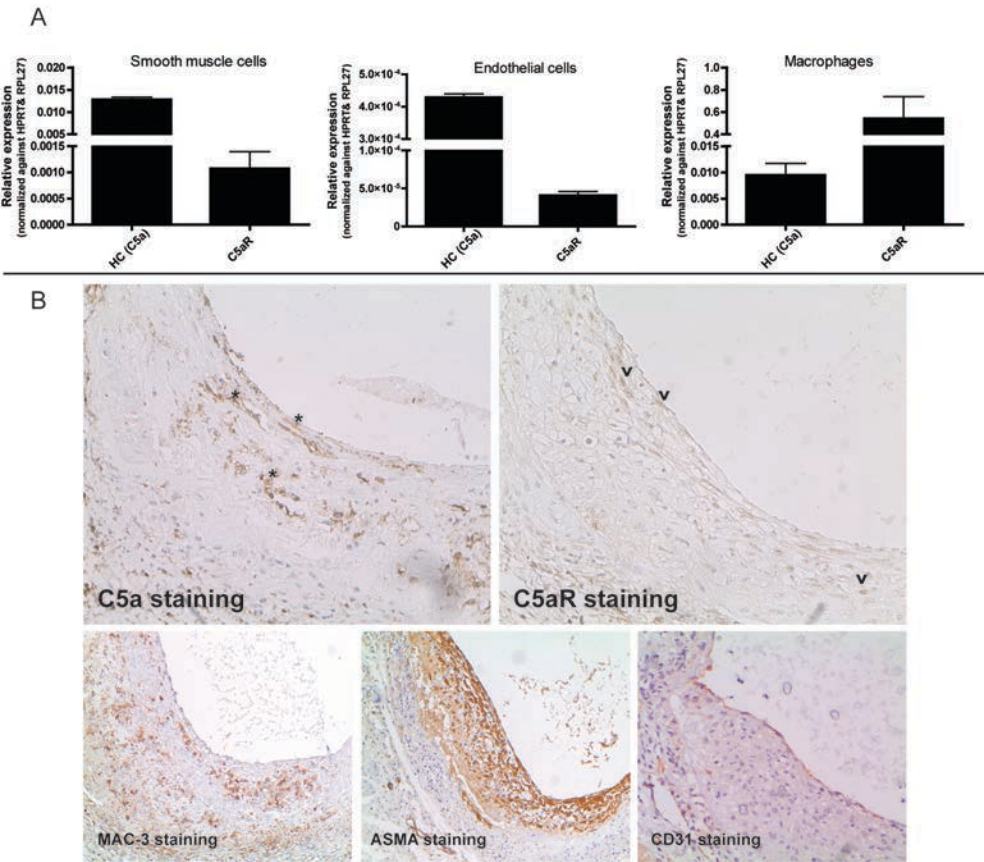
Supplemental Table 1. QPCR primers used for the *in vitro* experiments.

Gene	Forward primer	Reversed primer
TIMP1	ACACCCAGTCATGGAAAGC	CTTAGGCGGCCCGTGAT
MMP9	CCCTGGAAGTCACACGACATCTTC	CTCATTTTGAAACTCACACGCCAG
I-CAM-1	GTCCGCTTCCGCTACCATCAC	GGTCCTTGCCTACTTGCTGCC
V-CAM-1	AGACTGAAGTTGGCTCACAATTAAGAAG	AGTAGAGTGCAAGGAGTTCGGG
PECAM-1	GTCTTGTGCGAGTATCAGAATTCAG	TACCAGGCCGCTTCTCTTGA
HC (C5a)	ACACTGCGACTCTTCTGGTCACT	CCAGGTTGGCATTGGTACAGCTC
C5aR	GACCCCATAGATAACAGCA	CAGAGGCAACACAAAACCCA
Caspase-1	GGCATTAAAGAAGGCCCATATAGAGA	TGAGCCCTGACAGGATGTC
Caspase-3	AACCTCCATAAGAGCACTGGAATGTC	ACTTGGTATTTAGGCCCATGA
Bax	CGTGGTTGCCCTCTTCTACTTT	TGATCAGCTCGGGCACTTTA
TNFα	GCCTCTTCTCATTCTGCTTGTG	ATGATCTGAGTGTGAGGGTCTGG
HPRT	TTGCTCGAGATGTCATGAAGGA	AGCAGGTCAGCAAAGAACTTATAG
RPL27	TGAAAGGTTAGCGGAAGTGC	TTTCATGAACTTGCCCATCTC

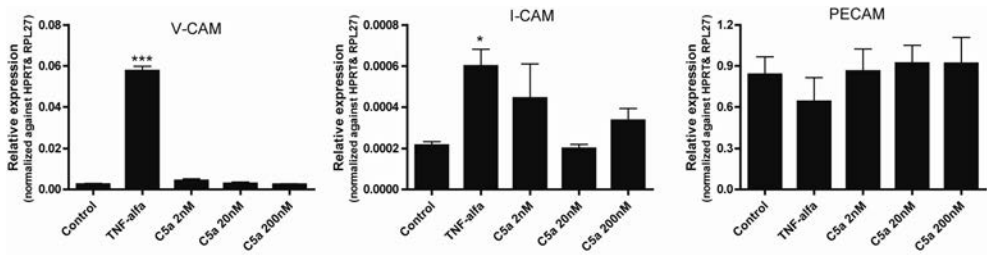
Supplemental Figure 1. Plasma IL-6 concentration did not differ between the three treatment groups. (PBS/PBS treated mice: n=8; C5a/PBS treated mice: n=9; C5a/cromolyn treated mice: n=7).



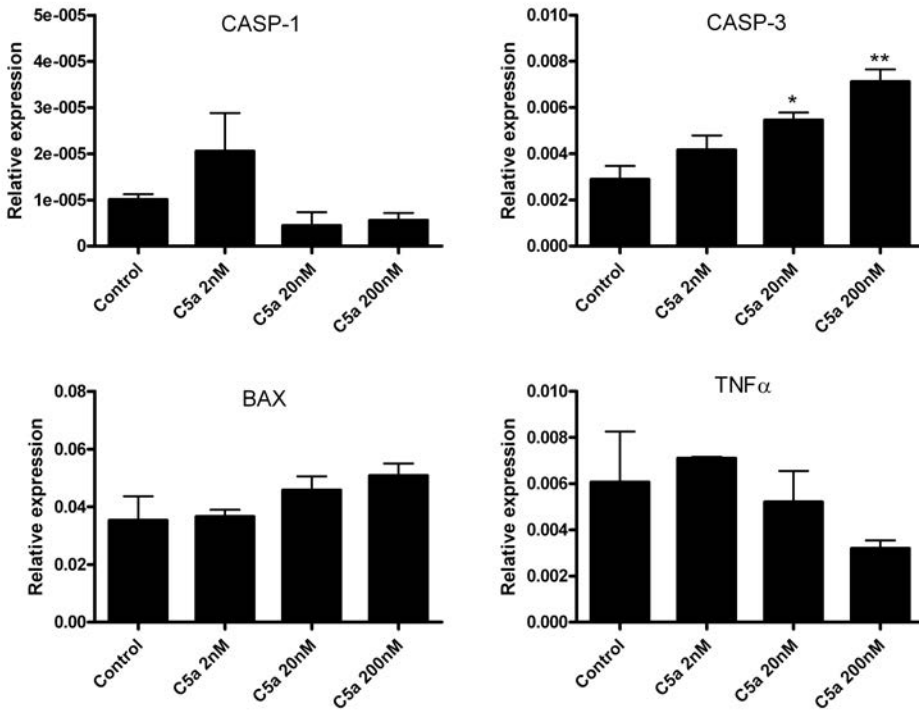
Supplemental Figure 2. Q-PCR analysis of mRNA, isolated from smooth muscle cells, macrophages and endothelial cells, show the expression of both HC (C5a) and C5aR (A). (B) Representative micrographs (C5a(*), C5aR(^); CD31: 200x magnification. MAC-3, ASMA: 100x magnification) indicate that cells expressing C5a and C5aR in the vessel wall are mostly smooth muscle cells, endothelial cells and macrophages.



Supplemental Figure 3. Mouse endothelial cells (H5V) were stimulated with increasing concentrations of C5a *in vitro*. TNF α stimulation was used as a positive control and resulted in a significant upregulation of both V-CAM and I-CAM. Stimulation with C5a however did not result in a changed expression of V-CAM, I-CAM or PECAM. (* $P < 0.05$; *** $P < 0.001$).



Supplemental Figure 4. Mouse endothelial cells (H5V) were stimulated with 2 nM, 20 nM, or 200 nM C5a *in vitro*. No changes were observed in the gene expression levels of caspase-1 or Bax, however the expression of caspase-3 was significantly and dose-dependently increased after C5a treatment. The expression level of the pro-apoptotic cytokine TNF α did not show any differences after C5a stimulation. (* $P < 0.05$; ** $P < 0.01$).



Chapter 5

Mast cells mediate neutrophil recruitment during atherosclerotic plaque progression

Submitted for publication

*Anouk Wezel^{1,2}

*H. Maxime Lagraauw¹

Daniël van der Velden^{1,3}

Saskia C.A. de Jager⁴

Paul H. A. Quax^{2,5}

Johan Kuiper¹

Ilze Bot¹

*These authors contributed equally

¹Division of Biopharmaceutics, Gorlaeus Laboratories, Leiden Academic Center for Drug Research, Leiden University, Leiden, The Netherlands

²Department of Surgery, Leiden University Medical Center, Leiden, The Netherlands

³Department of Rheumatology, Leiden University Medical Center, Leiden, The Netherlands

⁴Laboratory of Experimental Cardiology, University Medical Center Utrecht, Utrecht

⁵Eindhoven Laboratory for Experimental Vascular Medicine, Leiden, The Netherlands
Netherlands

Abstract

Aims: Activated mast cells have been identified in the intima and perivascular tissue of human atherosclerotic plaques. As mast cells have been described to release a whole array of chemokines that mediate leukocyte fluxes, we propose that activated mast cells play a pivotal role in leukocyte recruitment during atherosclerotic plaque progression.

Methods and Results: Systemic IgE-mediated mast cell activation in apoE^{-/-}μMT mice resulted in an increase in atherosclerotic lesion size as compared to control mice, and interestingly, the number of neutrophils was highly increased in these lesions. In addition, peritoneal mast cell activation led to a massive neutrophil influx into the peritoneal cavity in C57Bl6 mice, while neutrophil numbers in mast cell deficient Kit(W^{sh}/W^{sh}) mice were not affected. Moreover, increased levels of CXCR2⁺ and CXCR4⁺ neutrophils were observed after mast cell activation. Indeed, mast cells were seen to contain and release CXCL1 and CXCL12, the ligands for CXCR2 and CXCR4. Intriguingly, peritoneal mast cell activation in combination with anti-CXCR2 receptor antagonist resulted in decreased neutrophil recruitment, thus establishing a direct role of the CXCL1/CXCR2 axis in mast cell-mediated neutrophil recruitment.

Conclusions: Our data suggest that chemokines, and in particular CXCL1, released from activated perivascular mast cells induce neutrophil recruitment to the site of inflammation, thereby aggravating the ongoing inflammatory response and thus possibly affecting plaque progression and destabilization.

Introduction

Acute cardiovascular syndromes such as myocardial infarction and stroke remain the principal cause of death in western society despite increasing insight in the mechanisms of atherosclerosis, which is the underlying cause of disease¹. Atherosclerosis has been identified as a lipid-driven inflammatory disorder, in which various immune cells such as monocytes, macrophages but also mast cells and neutrophils have been implicated^{2,3}. Although statin treatment has reduced the risk of acute cardiovascular events by its lipid-lowering and anti-inflammatory effects⁴, this treatment is still insufficient for 70% of the patients, thus establishing the need for further research to obtain new therapeutic leads.

The mast cell, a potent inflammatory cell of the innate immune system, is currently mainly known for its role in allergy and asthma. However, evidence suggesting a detrimental role for the mast cell in atherosclerosis and acute cardiovascular syndromes is accumulating. For example, we and others have previously established that mast cells induce atherosclerotic plaque growth and destabilization in a number of different mouse models of atherosclerosis^{5,6}. In human atherosclerotic plaques, mast cell presence has also been previously established^{7,8}. More importantly, mast cell numbers were recently shown to correlate with plaque progression and were even demonstrated to associate with future cardiovascular events⁹, thereby further emphasizing the crucial contribution of mast cells to plaque destabilization. Currently, most research is aimed at identifying the endogenous mast cell activators in atherosclerosis. Immunoglobulin E (IgE) is commonly known for its acute effects on mast cell activation in allergy. In men with hyperlipidemia and in patients with acute cardiovascular disorders¹⁰, plasma IgE levels were shown to be increased as well. Further *in vitro* and *in vivo* evidence has also established a role for complement factors^{11,12}, neuropeptides^{13,14}, immune complexes¹⁵ and lipid mediators¹⁶ in mast cell activation during the development and progression of atherosclerosis.

Mast cells exert their detrimental effects on plaque stability by the release of a number of mediators, such as the mast cell specific proteases chymase and tryptase, histamine, and a vast amount of cytokines and chemokines¹⁷. We have previously established that chymase released from mast cells can induce plaque progression¹⁸. Additionally, it has been shown that mast cells can promote apoptosis of various cell types present in the plaque, such as vascular smooth muscle cells¹⁹, endothelial cells²⁰ and macrophages⁵, thereby contributing to plaque necrosis and destabilization. However, as mast cells secrete a whole panel of cytokines and chemokines, in this study we aimed to establish to which extent mast cells are capable of inducing leukocyte recruitment towards the plaque, thereby fuelling the ongoing inflammatory response and possibly aggravating plaque progression.

Materials and Methods

Systemic mast cell activation

This study was performed in compliance with Dutch government guidelines and the Directive 2010/63/EU of the European Parliament. All animal experiments were approved by the animal welfare committee of the Leiden University Medical Center (approval reference number 08014). Mice were obtained from the local animal breeding facility (Gorlaeus Laboratories, Leiden, The Netherlands). We used 10-12 weeks old male B cell deficient $\text{apoE}^{-/-}$ μMT mice, kindly provided by Prof. B.H. Toh (Monash University, Melbourne, Australia) for our observational study. These mice lack endogenous IgE, which results in a more pronounced effect of IgE mediated mast cell activation. Mice were fed a western-type diet containing 0.25% cholesterol and 15% cocoa butter (SDS, Sussex, UK) for eight weeks. During these eight weeks, the mice were challenged with IgE ($n=13$) or PBS ($n=10$) control for 6 times (~every 1.5 weeks). In order to do so, mice were given 1 μg of antiDNP-IgE by intraperitoneal injection, and 24 hours later the mice received an intravenous injection containing 0.5 mg DNP. At sacrifice, mice were anaesthetized by subcutaneous injection of ketamine (60 mg/kg, Eurovet Animal Health, Bladel, The Netherlands), fentanyl citrate and fluanisone (1.26 and 2 mg/kg, respectively, Janssen Animal Health, Sauterton, UK). Adequacy of anaesthesia was monitored by regular visual inspection and toe pinch reflex. Mice were exsanguinated via orbital bleeding and *in situ* fixation through the left cardiac chamber was performed, after which the hearts were excised for further analysis. The hearts were dissected just below the atria and sectioned perpendicular to the axis of the aorta, starting within the heart and working in the direction of the aortic arch. Once the aortic root was identified by the appearance of aortic valve leaflets, 10 μm sections were taken and mounted on gelatin-coated slides. Mean lesion area (in μm^2) was calculated from six Oil-Red-O stained sections in distal direction starting at the point where all three aortic valve leaflets first appeared. Collagen content in the lesion was determined with a Sirius Red staining, while macrophages were visualized with a Moma-2 antibody (1:1000, Serotec, Puchheim, Germany). The necrotic core size was defined as the acellular, debris-rich plaque area as percentage of the total plaque area. The aortic roots were quantified by the Leica image analysis system (Leica Ltd, Cambridge, UK). T cell numbers in the intima and adventitia were determined by staining for CD3 (1:50, Neomarkers, Fremont, CA, USA) and were counted manually. Mast cells and neutrophils were visualized by staining of 10 μm cryosections with a naphthol AS-D chloroacetate esterase staining kit (Sigma, Zwijndrecht, The Netherlands) and counted manually. A mast cell was considered resting when all granula were maintained inside the cell, while mast cells were assessed as activated when granula were deposited in the tissue surrounding the mast cell. Neutrophils were identified as round cells with a characteristic lobular nucleus and pink granular cytoplasm. All morphometric analyses were performed by blinded independent operators.

Leukocyte influx

Mice were obtained from the local animal breeding facility (Gorlaeus Laboratories, Leiden, The Netherlands). Peritoneal mast cells of either male C57BL/6 or mast cell deficient male $\text{Kit}^{W^{\text{sh}}/W^{\text{sh}}}$ mice were activated by intraperitoneal injection of compound 48/80 (1.2 mg/kg). After 30 minutes and 3 hours ($n=4$ per group), mice were anaesthetized as described above, after which peritoneal cells were collected by flushing the peritoneal cavity with 10 ml PBS. After collection of the peritoneal fluid, mice were sacrificed via cervical dislocation. Total cell count and neutrophil, lymphocyte, monocyte and eosinophil counts in blood were analyzed using an automated XT-2000iV veterinary hematology analyzer (Sysmex Europe GmbH, Norderstedt, Germany). After centrifugation of the cells (1500 rpm for 5 minutes), supernatant was collected for protease activity as described below and for chemokine quantification by ELISA according to manufacturer's protocol. Subsequently, leukocyte suspensions were incubated with 1% mouse serum in PBS and stained for surface markers (0.25 $\mu\text{g}/0.2 \times 10^6$ cells, eBioscience, San Diego, CA, USA),

after which surface marker expression was determined by FACS analysis (FACS Canto, BD Biosciences, Breda, The Netherlands).

An additional influx study was performed in order to investigate CXCR2 mediated neutrophil influx after mast cell activation. Male apoE^{-/-} mice (n=8) were injected intraperitoneally with anti-CXCR2 (5 µg/mouse, R&D systems, Minneapolis, MN, USA) or PBS. One day later the mice received a second injection with anti-CXCR2 an hour prior to intraperitoneal mast cell activation with compound 48/80 (1.2 mg/kg) or PBS. 3 Hours later mice were anaesthetized and peritoneal fluid was collected as described above, after which mice were sacrificed via cervical dislocation. Subsequently, cells were stained for CD11b, NK1.1, Ly6C, Ly6G and CXCR2, after which they were analyzed by FACS.

β-Hexosaminidase activity was determined by adding 50 µL of peritoneal fluid to 50 µL 2 mM 4-nitrophenyl N-acetyl-b-D-glucosaminide (Sigma) in 0.2 M citrate (pH 4.5) and incubated at 37 °C for 2 hours. After addition of 150 µL 1 M Tris (pH 9.0), absorbance (optical density, OD) was measured at 405 nm. To measure chymase release after degranulation, 50 µL peritoneal fluid was added to 2 mM S-2586 (chymase substrate, Chromogenix, Llanelli, UK) in PBS supplemented with 100 U/mL heparin. After 24 hours at 37 °C, OD405 was measured. Values are expressed as percentage of total content. The CXCL1 ELISA was performed according to manufacturer's protocol (Life Technologies, Bleiswijk, The Netherlands).

Neutrophil isolation

Neutrophils were isolated by negative selection from bone marrow as described earlier²¹. In short, C57BL/6 mice were anaesthetized as described above and sacrificed via cervical dislocation after which bone marrow was isolated by flushing the femurs and tibias. Cell suspensions were incubated with an antibody cocktail containing α-CD5, α-CD45R, α-CD49b, α-CD117, α-F4/80 and α-TER119 (4°C, 10 minutes under constant shaking). After washing, cells were incubated with α-biotin microbeads (Miltenyi, Leiden, the Netherlands, 4°C, 10 minutes under constant shaking). Subsequently neutrophils were isolated by magnetic bead isolation (magnetic-activated cell sorting LS column, Miltenyi). We obtained neutrophils at ≈90% purity, as validated by flow cytometry and histology²², which were used for further experiments.

Cell culture

C57BL/6 mice were anaesthetized as described above and sacrificed via cervical dislocation after which bone marrow was isolated by flushing the femurs and tibias. Bone marrow derived mast cells (BMMCs) were grown by culturing bone marrow cells at a density of 0.25*10⁶ cells in RPMI containing 10% fetal bovine serum (FBS), 2 mmol/L l-glutamine, 100 U/mL penicillin, 100 µg/mL streptomycin (all from PAA, Cölbe, Germany) and mIL3 supernatant (supernatant from WEHI cells overexpressing murine Interleukin (IL)-3) for 4 weeks in T175 tissue culture flasks (Greiner Bio-one, Alphen aan den Rijn, Netherlands). Total RNA was extracted from these cells with GTC, reverse transcribed using M-MuLV reverse transcriptase (RevertAid, MBI Fermentas, Leon-Roth, Germany) and expression of target genes (Supplemental table 1) was measured by qPCR on an ABI PRISM 7500 Taqman apparatus (Applied Biosystems, Foster City, CA, USA).

BMMCs (5*10⁵) were activated by incubation with compound 48/80 (0.5 µg/mL, Sigma, Zwijndrecht, the Netherlands (n=4 per condition) for 15-30 minutes at 37°C in HEPES-tyrode supplemented with 0.1% fatty acid free bovine serum albumin (BSA, Sigma). For total (100%) content measurements, mast cells were lysed with 10% Triton X-100 and untreated control cell supernatant served as 0% release controls.

Migration assay

BMMCs were degranulated as described above and the supernatant was collected. Neutrophils (10⁵ per well) were applied to the upper chamber of a transwell system (24 wells, 8 µm pore size, PAA) in RPMI containing 10% fetal bovine serum (FBS), 2 mmol/L l-glutamine, 100 U/mL penicillin, 100 µg/mL strep-

tomycin. Mast cell releasate was added to the basolateral chamber. To establish the role of neutrophil derived CXCR2 and CXCR4, anti-CXCR2 or AMD3100 (500 ng/mL) were added to the system. After 4 hours incubation, the number of migrated neutrophils was counted manually.

RNA isolation, cDNA synthesis and qPCR

Total RNA was isolated using a standard TRIzol-chloroform extraction protocol. RNA concentration, purity and integrity were examined by nanodrop (Nanodrop® Technologies). RNA was reverse transcribed by M-MuLV reverse transcriptase (RevertAid, MBI Fermentas, Landsmeer, The Netherlands) and used for quantitative analysis of mouse genes (Table 1) with an ABI PRISM 7700 Taqman apparatus (Applied Biosystems, Bleiswijk, The Netherlands). Murine HPRT and RPL27 were used as standard housekeeping genes.

Statistical analysis

Data are expressed as mean \pm SEM. A 2-tailed Student's t-test was used to compare individual groups. Non-Gaussian distributed data were analyzed using a Mann-Whitney U test. Frequency data analysis was performed by means of the Fisher's exact test. A level of $P < 0.05$ was considered significant.

Results

Mast cell activation correlates with increased neutrophil influx to the plaque

Repeated IgE treatment of apoE^{-/-}μMT mice did not significantly affect total mast cell numbers in the aortic root (controls: 15.8 ± 2.2 mast cells/section versus IgE: 20.5 ± 3.1 mast cells/section), but did result in a significant increase in mast cell activation (controls: $35.2 \pm 3.9\%$ versus IgE: $48.2 \pm 3.4\%$, $P < 0.05$, Figure 1A). Concomitantly, plaque size in the aortic root was increased by 40% from $2.0 \pm 0.2 \times 10^5 \mu\text{m}^2$ in control mice to $2.8 \pm 0.3 \times 10^5 \mu\text{m}^2$ in IgE treated mice ($P = 0.05$, Figure 1B). Collagen content did not differ between the groups (controls: $12.0 \pm 1.7\%$ versus IgE: $9.6 \pm 1.0\%$, $P = \text{NS}$, Figure 1C), while macrophage staining revealed a significant decrease in relative MOMA-2⁺ area (controls: $27.4 \pm 2.7\%$ versus IgE: $9.9 \pm 1.7\%$, $P < 0.001$, Figure 1D). Necrotic core area was increased from $51.7 \pm 14.2 \times 10^3 \mu\text{m}^2$ in the control mice to $82.6 \pm 18.6 \times 10^3 \mu\text{m}^2$ in the IgE treated group (Figure 1E), which is suggested to be caused by increased macrophage apoptosis upon mast cell activation as established previously⁵. Furthermore, intimal and adventitial T cell numbers did not differ between the groups (Figure 1F). Interestingly, IgE mediated mast cell activation resulted in a striking increase in the number of neutrophils in the intima (controls: 12 ± 3 versus IgE: 39 ± 12 neutrophils/mm² tissue, $P = 0.06$) and particularly in the perivascular tissue (controls: 58 ± 11 versus IgE: 183 ± 39 neutrophils/mm² tissue, $P < 0.05$, Figure 1G,H). The number of neutrophils in the control mice remained below 25 neutrophils/mm² tissue (10 out of 10 plaques), while in IgE treated mice 6 out of 13 plaques had more than 25 neutrophils/mm² tissue ($P < 0.05$). Similarly, within the perivascular tissue only 1 out of 10 control mice contained over 100 neutrophils/mm² tissue, while IgE treatment resulted in >100 neutrophils/mm² tissue in

9 out of 13 sections ($P < 0.01$). Furthermore, mast cell activation status was seen to correlate with the number of perivascular neutrophils ($R^2 = 0.28$, $P < 0.05$).

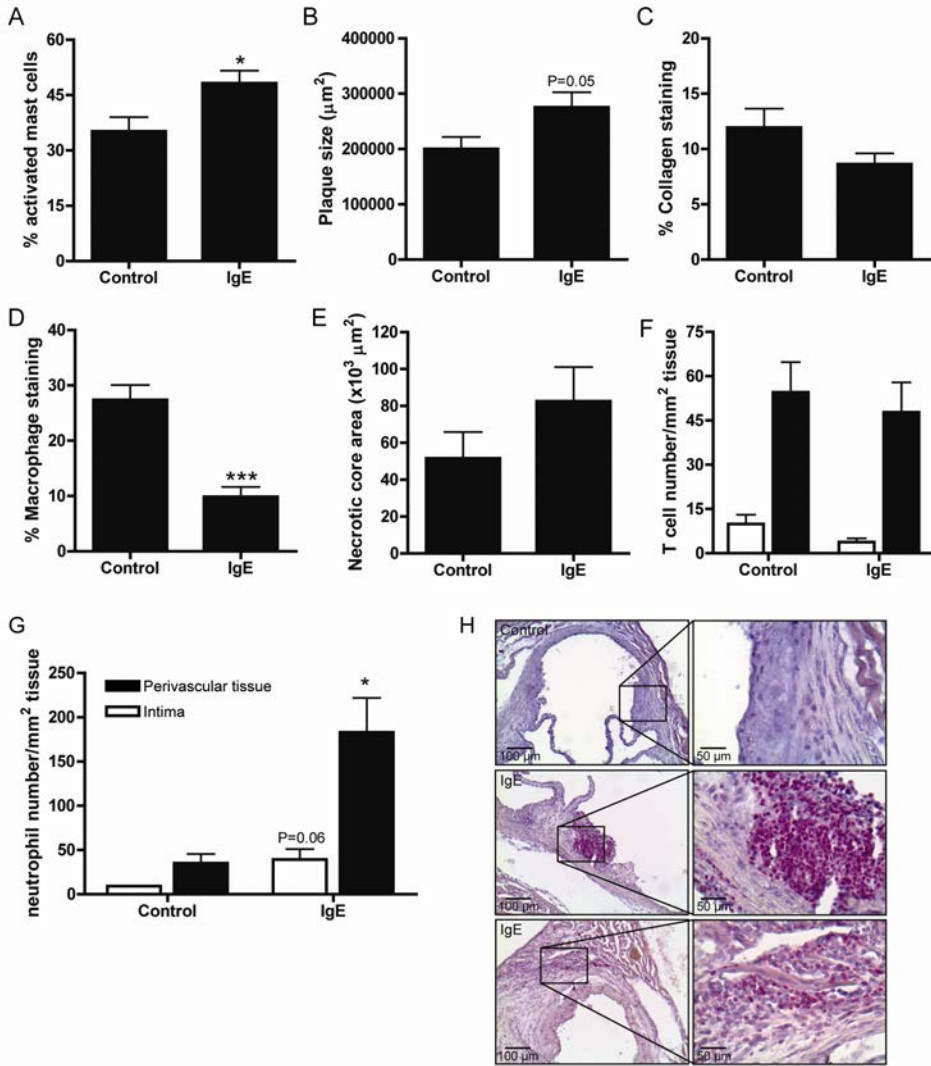


Figure 1. IgE induced mast cell activation in $\text{apoE}^{-/-}\mu\text{MT}$ mice. During eight weeks, male $\text{apoE}^{-/-}\mu\text{MT}$ mice were challenged with IgE ($n = 13$) or PBS ($n = 10$) control for 6 times (~every 1.5 weeks). IgE treatment resulted in enhanced mast cell activation within the aortic root (A) and concomitant lesion progression (B). (C) Collagen content was not affected by the IgE induced mast cell activation, while macrophage content was significantly reduced (D). (E) Necrotic core area was somewhat, but not significantly increased in the IgE treated group. (F) T cell numbers in the intima (white bars) and the perivascular tissue (black bars) did not differ between the groups (G). Neutrophil numbers were increased in the intima (white bars) and even more pronounced in the perivascular tissue (black bars) after IgE mediated mast cell activation. (F) Representative images of aortic root sections stained with a naphthol chloroacetate esterase staining, illustrating large neutrophil accumulations within the lesion (middle panel) and the perivascular tissue (lower panel) after IgE treatment, but not in control mice (upper panel). Magnifications: left panels 100x, right panels 400x. * $P < 0.05$, *** $P < 0.001$.

In vivo mast cell activation results in neutrophil recruitment

To further investigate whether neutrophil recruitment is indeed mast cell mediated, we activated peritoneal mast cells in mast cell competent C57BL/6 mice and mast cell deficient Kit(W^{sh}/W^{sh}) mice, by intraperitoneal injection of the commonly used mast cell activator compound 48/80. This resulted in acute mast cell activation as indicated by β -hexosaminidase (Figure 2A) and chymase (Figure 2B) activity in the peritoneal cavity of C57BL/6 mice, but not in that of Kit(W^{sh}/W^{sh}) mice, at 30 minutes and up to 3 hours after injection. Leukocyte differentiation analysis using Sysmex revealed a striking influx of predominantly neutrophils in response to mast cell activation. This effect on recruitment was not observed for monocytes and lymphocytes. Total populations were even slightly decreased after mast cell activation with compound 48/80 and these numbers remained identical between C57BL/6 and Kit(W^{sh}/W^{sh}) mice (Figure 2C-E).

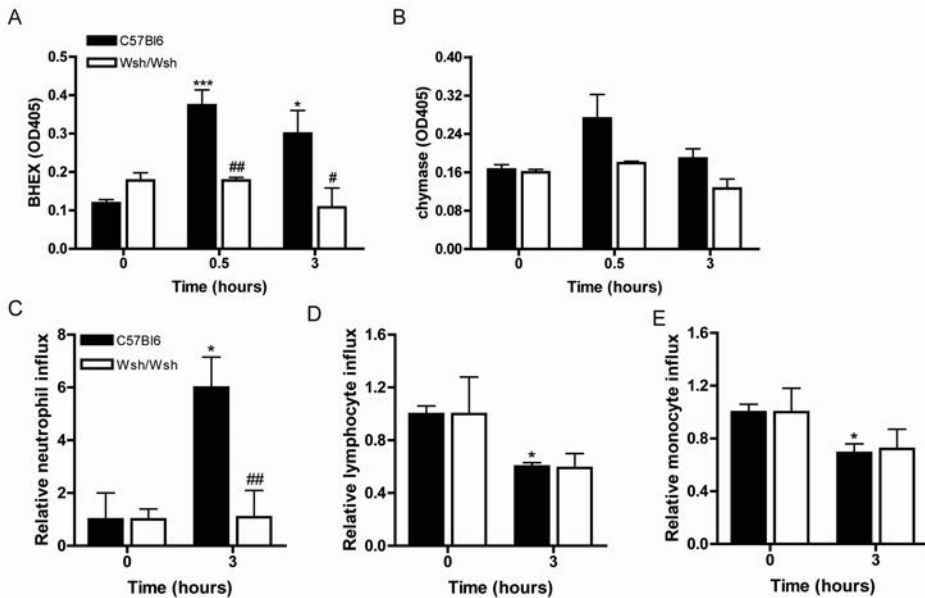


Figure 2. Mast cell induced neutrophil recruitment in vivo. C57BL/6 or mast cell deficient Kit(W^{sh}/W^{sh}) mice (n=4) were intraperitoneal injected with compound 48/80, which resulted in acute mast cell activation as indicated by increased β -hexosaminidase (A) and chymase (B) activity in the peritoneal cavity of C57BL/6 mice (black bars) at 30 minutes and still at 3 hours after injection, which did not occur in mast cell deficient Kit(W^{sh}/W^{sh}) mice (white bars). Acute peritoneal mast cell activation by compound 48/80 induced recruitment of neutrophils (C), but not of lymphocytes (D) or monocytes (E) in C57BL/6 mice as measured by Sysmex cell differentiation analysis. *P<0.05 compared to T=0, ***P<0.001 compared to T=0, #P<0.05 compared to C57BL/6, ##P<0.01 compared to C57BL/6.

By means of FACS analysis we confirmed the influx of CD11b⁺Ly6G^{high}CD71⁺ neutrophils in C57BL/6 mice as displayed in Figure 3A. Interestingly, the recruited neutrophils were CXCR2 and/or CXCR4 positive (Figure 3B,C), suggesting that the

ligands of these specific receptors, i.e. CXCL1 (or KC, the murine analogue of IL-8) and CXCL12, are involved in mast cell mediated neutrophil recruitment.

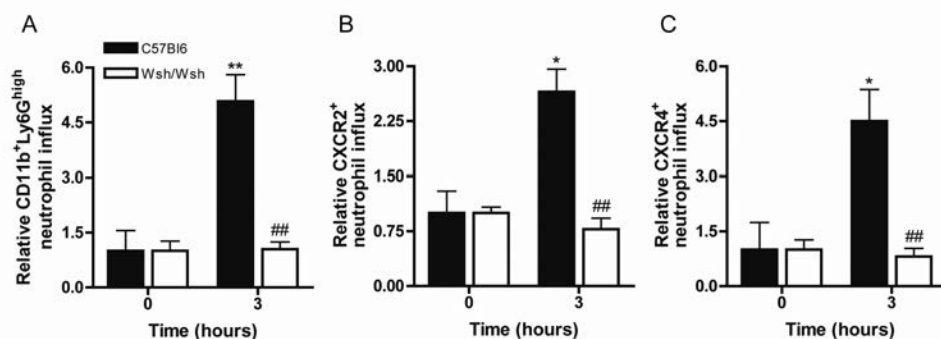


Figure 3. Mast cells recruit CXCR2⁺ and CXCR4⁺ neutrophils. C57BL/6 or mast cell deficient Kit(W^{sh}/W^{sh}) mice (n=4) were intraperitoneally injected with compound 48/80 (A). FACS analysis confirmed the recruitment of CD11b⁺Ly6G^{high}CD71⁺ neutrophils in response to compound 48/80 induced mast cell activation in C57BL/6 mice but not in Kit(W^{sh}/W^{sh}) mice. The mast cell dependent neutrophil influx appeared to be CXCR2 (B) and CXCR4 (C) dependent. *P<0.05 compared to T=0, **P<0.01 compared to T=0, #P<0.05 compared to C57BL/6, ##P<0.01 compared to C57BL/6.

Mast cells express and secrete CXCL1 and CXCL12

Next, we aimed to establish whether mast cell induced neutrophil recruitment was mediated via CXCL1 or CXCL12, the ligands for CXCR2 and CXCR4. First, mRNA expression of these chemokines was measured in cultured bone marrow derived mast cells (BMMCs). Indeed, we observed that both CXCL1 (relative expression: 0.005 ± 0.004) and CXCL12 (0.002 ± 0.001) were expressed by BMMCs. 5×10^5 BMMCs were seen to contain 1.5 ± 0.3 ng of CXCL1 as measured by ELISA. After activation with compound 48/80, release of CXCL1 into the supernatant of BMMCs could be detected (102 ± 15 pg/mL compared to 6 ± 12 pg/mL in the releasate of unstimulated control cells, $P < 0.05$). Similarly, we observed an increase in CXCL12 release after stimulation with compound 48/80 (OD 450 nm: 0.26 ± 0.008 versus 0.19 ± 0.004 in the releasate of unstimulated control BMMCs, $P < 0.05$). These data indicate that mast cells, in accordance to previous literature, express and secrete chemokines such as CXCL1 and CXCL12 that can recruit neutrophils to the site of mast cell activation.

Neutrophil recruitment *in vitro*

To confirm our *in vivo* findings, we isolated neutrophils from bone marrow by negative selection as described previously²¹ and allowed these cells to migrate towards supernatant of BMMCs stimulated with IgE. As expected, neutrophil migration towards the basolateral side of the migration chamber was significantly increased as compared to supernatant of unstimulated BMMCs ($32.3 \pm 4.7 \times 10^3$ cells versus $11.6 \pm 2.5 \times 10^3$ neutrophils, $P < 0.01$, Figure 4). Blocking neutrophil CXCR2

with a specific mouse α -CXCR2 blocking antibody inhibited the mast cell induced neutrophil migration ($18.8 \pm 2.2 \times 10^3$ neutrophils, $P < 0.05$ compared to IgE stimulated mast cells), while addition of the CXCR4 receptor antagonist AMD3100 was not as effective ($24.8 \pm 6.9 \times 10^3$ neutrophils, $P = \text{NS}$). These data illustrate that mast cells, when activated, can indeed directly induce neutrophil recruitment.

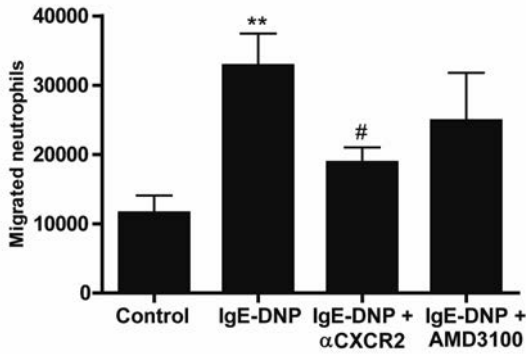


Figure 4. Mast cell induced neutrophil recruitment *in vitro*. Supernatant from IgE stimulated BMMCs resulted in enhanced migration of freshly isolated neutrophils, which could be inhibited by a CXCR2 blocking antibody. ** $P < 0.01$ compared to supernatant of unstimulated control BMMCs. # $P < 0.05$ compared to IgE stimulated BMMCs.

α CXCR2 inhibits mast cell-mediated neutrophil recruitment in vivo

We aimed to validate our *in vitro* findings in an *in vivo* setting by activating peritoneal mast cells while blocking CXCR2 with α CXCR2 (Figure 5A). Similar to the previous results in C57BL/6 mice, compound 48/80-mediated mast cell activation in apoE^{-/-} mice induced a striking 36-fold increase in CD11b⁺Ly6G^{high} neutrophil influx to the peritoneum compared to control mice as measured by FACS analysis (Figure 5B; $P < 0.05$). In line with these results, the peritoneal CXCL1 concentration was indeed increased after mast cell activation (Figure 5D). As observed in the previous influx study, total monocytes in the peritoneum were reduced after mast cell activation.

Mast cell activation in combination with α CXCR2 resulted in a strong reduction in neutrophil chemotaxis (Figure 5B; $P = 0.056$), underlining the importance of mast cell derived CXCL1 in neutrophil recruitment. Previously, mast cell derived mediators have been described to influence neutrophil effector functions^{22,23}. Interestingly, in our study we observed a similar increase in activation of recruited neutrophils after peritoneal mast cell stimulation, which was not affected by α CXCR2 treatment (Figure 5E).

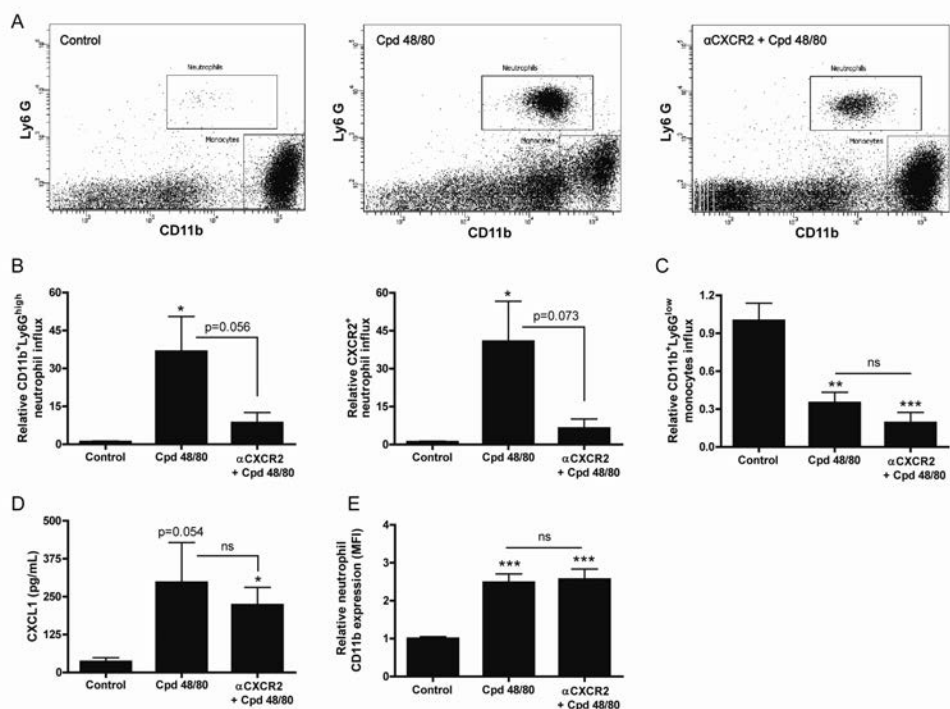


Figure 5. *In vivo* mast cell mediated neutrophil influx is mediated by CXCR2. Intraperitoneal mast cell activation of apoE^{-/-} mice (n=8) with compound 48/80 resulted in a significant influx of especially CXCR2⁺ neutrophils and this effect was strongly diminished by blocking CXCR2 (A, B). Monocyte influx was significantly decreased after mast cell activation in a CXCR2-independent manner (C). Mast cell activation caused a local increase in CXCL1 (D). Peritoneal neutrophil activation was significantly increased after mast cell activation, which was unaffected by αCXCR2 treatment (E). *P<0.05, **P<0.01, ***P<0.001 compared to control group.

Discussion

The current study is the first to demonstrate a correlation between chronic IgE mediated mast cell activation and neutrophil influx into the atherosclerotic plaque. Moreover, mast cell activation was seen to directly cause neutrophil recruitment both *in vitro* and *in vivo*, in particular via the secretion of the chemokine CXCL1. The mast cell is currently accepted as a potent contributing cell in the process of atherosclerosis. Mast cells can induce plaque destabilization by the release of a number of mediators such as chymase and tryptase, which can degrade matrix molecules that give rise to plaque stability and by the induction of plaque cell apoptosis^{5,19,20}. Mast cells are also known for their capacity to store and produce a large number of cytokines and chemokines. Previously, we have provided evidence showing that MCP-1 release after either C5a¹² or lysophosphatidic acid-mediated¹⁶ mast cell activation may result in the recruitment of monocytes towards

the plaque. Acute mast cell activation can also induce upregulation of adhesion molecules on endothelial cells, thereby enabling the influx of inflammatory cells into the subendothelial space²⁴. Furthermore, it was previously shown that mast cell-derived IL-6 and IFN γ are crucial for the induction of mast cell dependent atherosclerotic lesion development⁶, suggesting that the contribution of mast cell derived cytokines and chemokines to atherosclerotic lesion development as such is more important than previously thought. Chemokines are known for their function in the recruitment of leukocytes towards the site of inflammation, which may in turn aggravate the process of atherosclerosis. In this study, we therefore aimed to determine to what extent mast cell activation affects leukocyte recruitment, in specific to the atherosclerotic lesion.

To establish a pronounced effect of mast cell activation, we used apoE^{-/-} mice that lack B cells and thus not produce endogenous IgE, and chronically injected these mice with IgE. Besides increased mast cell activation and lesion size, we observed a striking increase in neutrophil numbers in the intima, and even more pronounced in the perivascular tissue. We then aimed to determine whether these effects are mast cell specific by investigating leukocyte influx to the peritoneum in mast cell deficient and control mice. Indeed, mast cell activation resulted in exaggerated neutrophil influx to the peritoneum, which was absent in mast cell deficient mice. Neutrophils were seen to be primarily CXCR2 and CXCR4 positive, suggestive of involvement of the CXCR2 ligand CXCL1 and the CXCR4 ligand CXCL12. We then confirmed that mast cells produce and secrete both CXCL1, as previously established^{15,25}, and CXCL12, and investigated the contribution of these chemokines to neutrophil migration *in vitro*. Blockage of CXCR2, but not that of CXCR4, in an *in vitro* setup was seen to significantly reduce mast cell induced neutrophil migration, indicating that mast cell derived CXCL1 may be more important in neutrophil recruitment than mast cell derived CXCL12. Previously, it has been described that systemic disruption of the CXCL12/CXCR4 axis aggravates atherosclerosis by expansion of neutrophils in the blood and in the plaque²⁶. Also, functional blockade of CXCR4 in later stages of atherosclerosis was seen to exacerbate plaque progression, accompanied by hyperactivation of circulating neutrophils²⁷. Taking into account these previous findings, and the lack effects we observed on neutrophil migration *in vitro* after blocking CXCR4, we consider it unlikely that mast cell derived CXCL12 is a major contributor in neutrophil influx to the atherosclerotic plaque. However, blockage of CXCR2 did significantly reduce mast cell mediated neutrophil migration *in vitro*, which we then aimed to confirm *in vivo*. Again, after peritoneal mast cell activation, a massive neutrophil influx was observed, which could be partially inhibited by α CXCR2 pretreatment. Based on these data we postulate that mast cell derived CXCL1 is a major contributor to neutrophil migration to the site of inflammation, which is in line with a previous report demonstrating that mast cell and macrophage derived CXCL1 and CXCL2

induce neutrophil recruitment in an LPS-induced peritonitis model²⁸. Furthermore, in the current study, we made use of compound 48/80 and IgE mediated mast cell activation, which are well-known to cause mast cell degranulation. We showed that both these general mast cell activators are capable of inducing neutrophil recruitment to the site of inflammation. Also, these mast cell mediated effects are not strain specific, as we demonstrate neutrophil recruitment after mast cell activation in both apoE^{-/-} and C57BL/6 mice.

In advanced atherosclerosis, we have previously established that mast cells can activate endothelial cells, thereby inducing the adhesion of leukocytes to the endothelial layer in a CXCR2 and VCAM-1 dependent fashion⁵. Direct mast cell dependent neutrophil recruitment has been previously associated with diseases such as EAE²⁹, skin diseases³⁰ and rheumatoid arthritis³¹, either via CXCL1 or other mechanisms such as the tryptase/heparin complex. We now postulate that also in atherosclerosis mast cells may directly induce neutrophil recruitment via the CXCL1/CXCR2 axis, thus providing another mechanism by which mast cells can fuel the ongoing inflammatory response. This mechanism may also explain the massive increase in perivascular neutrophils, which can be caused by activation of perivascular mast cells and subsequent neutrophil recruitment via perivascular microvessels instead of influx through the endothelium.

In the observational *in vivo* study, both increased mast cell activation as well as increased neutrophil numbers were observed. It is therefore difficult to distinguish between effects on plaque formation caused by either the mast cell itself or indirectly by the neutrophil. However, a detrimental role for neutrophils in both early and late stage atherosclerosis has been previously described. Hypercholesterolemia in apoE^{-/-} mice was shown to increase the amount of circulating neutrophils, which correlated with early atherosclerotic lesion size³². The direct presence of neutrophils has been readily detected in early fatty streaks and in advanced atherosclerosis they accumulate especially in shoulder regions of the plaque³³. In human atherosclerotic plaques neutrophils are detected as well, and moreover, increased numbers of neutrophils correlated with rupture-prone lesions³⁴. Markers of so-called neutrophil extra-cellular traps are even associated with adverse cardiac events³⁵. Furthermore, neutrophils release granules containing large amounts of matrix-degrading proteases, they produce vast amounts of reactive oxygen species and go rapidly into apoptosis³⁶. Thus, there are a number of mechanisms via which neutrophils can contribute to atherosclerotic plaque growth and destabilization. In our study, we have provided evidence that stimulation of mast cells resulted in increased activation of recruited neutrophils, which may cause additional detrimental effects on local inflammation.

In conclusion, systemic mast cell activation results in neutrophil accumulation within the vessel wall, and enhanced atherosclerotic lesion development. Recruitment studies revealed a direct role for mast cell derived CXCL1, which attracts

CXCR2⁺ neutrophils. These data may thus provide a novel mechanism by which mast cells can aggravate the ongoing inflammatory response in atherosclerotic lesion development and progression.

Funding

This work was supported by the Netherlands Heart Foundation (grant numbers 2010B029 (A.W.), 2010B224 (H.M.L.), 2012T083 (I.B.)). D.v.d.V. was financed by the Leiden Center for Translational Drug Discovery & Development (LCTD3) program. We acknowledge the support from the Netherlands CardioVascular Research Initiative[†]: the Dutch Heart Foundation, Dutch Federation of University Medical Centres, the Netherlands Organisation for Health Research and Development and the Royal Netherlands Academy of Sciences[‡] for the GENIUS project “Generating the best evidence-based pharmaceutical targets for atherosclerosis” (CVON2011-19).

References

1. Murray CJ, Vos T, Lozano R, Naghavi M, Flaxman AD, Michaud C, Ezzati M, Shibuya K, Salomon JA, Abdalla S, Aboyans V, Abraham J, Ackerman I, Aggarwal R, Ahn SY, Ali MK, Alvarado M, Anderson HR, Anderson LM, Andrews KG, Atkinson C, Baddour LM, Bahalim AN, Barker-Collo S, Barrero LH, Bartels DH, Basáñez MG, Baxter A, Bell ML, Benjamin EJ, Bennett D, Bernabé E, Bhalla K, Bhandari B, Bikbov B, Bin Abdulhak A, Birbeck G, Black JA, Blencowe H, Blore JD, Blyth F, Bolliger I, Bonaventure A, Boufous S, Bourne R, Boussinesq M, Braithwaite T, Brayne C, Bridgett L, Brooker S, Brooks P, Brugha TS, Bryan-Hancock C, Bucello C, Buchbinder R, Buckle G, Budke CM, Burch M, Burney P, Burstein R, Calabria B, Campbell B, Canter CE, Carabin H, Carapetis J, Carmona L, Cella C, Charlson F, Chen H, Cheng AT, Chou D, Chugh SS, Coffeng LE, Colan SD, Colquhoun S, Colson KE, Condon J, Connor MD, Cooper LT, Corriere M, Cortinovis M, de Vaccaro KC, Couser W, Cowie BC, Criqui MH, Cross M, Dabhadkar KC, Dahiya M, Dahodwala N, Damsere-Derry J, Danaei G, Davis A, De Leo D, Degenhardt L, Dellavalle R, Delossantos A, Denenberg J, Derrett S, Des Jarlais DC, Dharmaratne SD, Dherani M, Diaz-Torne C, Dolk H, Dorsey ER, Driscoll T, Duber H, Ebel B, Edmond K, Elbaz A, Ali SE, Erskine H, Erwin PJ, Espindola P, Ewoigbokhan SE, Farzadfar F, Feigin V, Felson DT, Ferrari A, Ferri CP, Fèvre EM, Finucane MM, Flaxman S, Flood L, Foreman K, Forouzanfar MH, Fowkes FG, Fransen M, Freeman MK, Gabbe BJ, Gabriel SE, Gakidou E, Ganatra HA, Garcia B, Gaspari F, Gillum RF, Gmel G, Gonzalez-Medina D, Gosselin R, Grainger R, Grant B, Groeger J, Guillemin F, Gunnell D, Gupta R, Haagsma J, Hagan H, Halasa YA, Hall W, Haring D, Haro JM, Harrison JE, Havmoeller R, Hay RJ, Higashi H, Hill C, Hoen B, Hoffman H, Hotez PJ, Hoy D, Huang JJ, Ibeanusi SE, Jacobsen KH, James SL, Jarvis D, Jasrasaria R, Jayaraman S, Johns N, Jonas JB, Karthikeyan G, Kashebaum N, Kawakami N, Keren A, Khoo JP, King CH, Knowlton LM, Kobusingye O, Koranteng A, Krishnamurthi R, Laden F, Laloo R, Laslett LL, Lathlean T, Leasher JL, Lee YY, Leigh J, Levinson D, Lim SS, Limb E, Lin JK, Lipnick M, Lipshultz SE, Liu W, Loane M, Ohno SL, Lyons R, Mabweijano J, MacIntyre MF, Malekzadeh R, Mallinger L, Manivannan S, Marceses W, March L, Margolis DJ, Marks GB, Marks R, Matsumori A, Matzopoulos R, Mayosi BM, McAnulty JH, McDermott MM, McGill N, McGrath J, Medina-Mora ME, Meltzer M, Mensah GA, Merriman TR, Meyer AC, Miglioli V, Miller M, Miller TR, Mitchell PB, Mock C, Mocumbi AO, Moffitt TE, Mokdad AA, Monasta L, Montico M, Moradi-Lakeh M, Moran A, Morawska L, Mori R, Murdoch ME, Mwaniki MK, Naidoo K, Nair MN, Naldi L, Narayan KM, Nelson PK, Nelson RG, Nevitt MC, Newton CR, Nolte S, Norman P, Norman R, O'Donnell M, O'Hanlon S, Olives C, Omer SB, Ortblad K, Osborne R, Ozgediz D, Page A, Pahari B, Pandian JD, Rivero AP, Patten SB, Pearce N, Padilla RP, Perez-Ruiz F, Perico N, Pesudovs K, Phillips D, Phillips MR, Pierce K, Pion S, Polanczyk GV, Polinder S, Pope CA 3rd, Popova S, Porrini E, Pourmalek F, Prince M, Pullan RL, Ramaiah KD,

- Ranganathan D, Razavi H, Regan M, Rehm JT, Rein DB, Remuzzi G, Richardson K, Rivara FP, Roberts T, Robinson C, De Leòn FR, Ronfani L, Room R, Rosenfeld LC, Rushton L, Sacco RL, Saha S, Sampson U, Sanchez-Riera L, Sanman E, Schwebel DC, Scott JG, Segui-Gomez M, Shahrz S, Shepard DS, Shin H, Shivakoti R, Singh D, Singh GM, Singh JA, Singleton J, Sleet DA, Sliwa K, Smith E, Smith JL, Stapelberg NJ, Steer A, Steiner T, Stolk WA, Stovner LJ, Sudfeld C, Syed S, Tamburlini G, Tavakkoli M, Taylor HR, Taylor JA, Taylor WJ, Thomas B, Thomson WM, Thurston GD, Tleyjeh IM, Tonelli M, Towbin JA, Truelsen T, Tsilimbaris MK, Ubeda C, Undurraga EA, van der Werf MJ, van Os J, Vavilala MS, Venketasubramanian N, Wang M, Wang W, Watt K, Weatherall DJ, Weinstock MA, Weintraub R, Weisskopf MG, Weissman MM, White RA, Whiteford H, Wiebe N, Wiersma ST, Wilkinson JD, Williams HC, Williams SR, Witt E, Wolfe F, Woolf AD, Wulf S, Yeh PH, Zaidi AK, Zheng ZJ, Zonies D, Lopez AD, AlMazroa MA, Memish ZA. Disability-adjusted life years (DALYs) for 291 diseases and injuries in 21 regions, 1990-2010: a systematic analysis for the Global Burden of Disease Study 2010. *Lancet* 2012;380:2197-2223.
- Kulik A, Voisine P, Le May M, Ruel M. Correlates of saphenous vein graft hyperplasia and occlusion 1 year after coronary artery bypass grafting: analysis from the CASCADE randomized trial. *Circulation*. 2013;128:S213-8.
2. Weber C, Zernecke A, Libby P. The multifaceted contributions of leukocyte subsets to atherosclerosis: lessons from mouse models. *Nat. Rev. Immunol.* 2008;8:802-815.
 3. Libby P, Lichtman AH, Hansson GK. Immune effector mechanisms implicated in atherosclerosis: from mice to humans. *Immunity* 2013;38:1092-1104.
 4. Cholesterol Treatment Trialists' (CTT) Collaborators, Mihaylova B, Emberson J, Blackwell L, Keech A, Simes J, Barnes EH, Voysey M, Gray A, Collins R, Baigent C. The effects of lowering LDL cholesterol with statin therapy in people at low risk of vascular disease: meta-analysis of individual data from 27 randomised trials. *Lancet* 2012;380:581-590.
 5. Bot I, de Jager SC, Zernecke A, Lindstedt KA, van Berkel TJC, Weber C, Biessen EA. Perivascular mast cells promote atherogenesis and induce plaque destabilization in apolipoprotein E-deficient mice. *Circulation* 2007;115:2516-2525.
 6. Sun J, Sukhova GK, Wolters PJ, MacFarlane LA, Libby P, Sun C, Zhang Y, Liu J, Ennis TL, Knispel R, Xiong W, Thompson RW, Baxter BT, Shi GP. Mast cells promote atherosclerosis by releasing proinflammatory cytokines. *Nat. Med.* 2007;13:719-724.
 7. Kaartinen M, Penttilä A, Kovanen PT. Accumulation of activated mast cells in the shoulder region of human coronary atheroma, the predilection site of atheromatous rupture. *Circulation* 1994;90:1669-1678.
 8. Kovanen P, Kaartinen M, Paavonen T. Infiltrates of activated mast cells at the site of coronary atheromatous erosion or rupture in myocardial infarction. *Circulation* 1995;92:1084-1088.
 9. Willems S, Vink A, Bot I, Quax PH, de Borst GJ, de Vries JP, van de Weg SM, Moll FL, Kuiper J, Kovanen PT, de Kleijn DP, Hoefer IE, Pasterkamp G. Mast cells in human carotid atherosclerotic plaques are associated with intraplaque microvessel density and the occurrence of future cardiovascular events. *Eur. Heart J.* 2013;34:3699-3706.
 10. Kovanen PT, Mänttari M, Palosuo T, Manninen V, Aho K. Prediction of myocardial infarction in dyslipidemic men by elevated levels of immunoglobulin classes A, E, and G, but not M. *Arch. Intern. Med.* 1998;158:1434-1439.
 11. Oksjoki R, Laine P, Helske S, Vehmaan-Kreula P, Mäyränpää MI, Gasque P, Kovanen PT, Pentikäinen MO. Receptors for the anaphylatoxins C3a and C5a are expressed in human atherosclerotic coronary plaques. *Atherosclerosis* 2007;195:90-99.
 12. De Vries MR, Wezel A, Schepers A, van Santbrink PJ, Woodruff TM, Niessen HW, Hamming JF, Kuiper J, Bot I, Quax PH. Complement factor C5a as mast cell activator mediates vascular remodelling in vein graft disease. *Cardiovasc. Res.* 2013;97:311-320.
 13. Laine P, Naukkarinen A, Heikkilä L, Penttilä A, Kovanen PT. Adventitial mast cells connect with sensory nerve fibers in atherosclerotic coronary arteries. *Circulation* 2000;101:1665-1669.
 14. Bot I, de Jager SC, Bot M, van Heiningen SH, de Groot P, Veldhuizen RW, van Berkel TJ, von der Thüsen JH, Biessen EA. The neuropeptide substance P mediates adventitial mast cell activation and induces intraplaque hemorrhage in advanced atherosclerosis. *Circ. Res.* 2010;106:89-92.
 15. Lappalainen J, Lindstedt KA, Oksjoki R, Kovanen PT. OxLDL-IgG immune complexes induce expression and secretion of proatherogenic cytokines by cultured human mast cells. *Atherosclerosis* 2011;214:357-363.
 16. Bot M, de Jager SC, MacAleese L, Lagrauw HM, van Berkel TJ, Quax PH, Kuiper J, Heeren RM, Biessen EA. Lysophosphatidic acid triggers mast cell-driven atherosclerotic plaque destabilization by

- increasing vascular inflammation. *J. Lipid Res.* 2013;54:1265–1274.
17. Kalesnikoff J, Galli SJ. New developments in mast cell biology. *Nat. Immunol.* 2008;9:1215–1223.
 18. Bot I, Bot M, van Heiningen SH, van Santbrink PJ, Lankhuizen IM, Hartman P, Gruener S, Hilpert H, van Berkel TJ, Fingerle J, Biessen EA. Mast cell chymase inhibition reduces atherosclerotic plaque progression and improves plaque stability in ApoE^{-/-} mice. *Cardiovasc. Res.* 2011;89:244–252.
 19. Leskinen M, Wang Y, Leszczynski D, Lindstedt KA, Kovanen PT. Mast cell chymase induces apoptosis of vascular smooth muscle cells. *Arterioscler. Thromb. Vasc. Biol.* 2001;21:516–522.
 20. Lätti S, Leskinen M, Shiota N, Wang Y, Kovanen PT, Lindstedt KA. Mast cell-mediated apoptosis of endothelial cells in vitro: a paracrine mechanism involving TNF-alpha-mediated down-regulation of bcl-2 expression. *J. Cell. Physiol.* 2003;195:130–138.
 21. Hasenberg M, Köhler A, Bonifatius S, Borucki K, Riek-Burchardt M, Achilles J, Männ L, Baumgart K, Schraven B, Gunzer M. Rapid immunomagnetic negative enrichment of neutrophil granulocytes from murine bone marrow for functional studies in vitro and in vivo. *PLoS One.* 2001;6:e17314.
 22. Kishimoto TK, Jutila MA, Berg EL, Butcher EC. Neutrophil Mac-1 and MEL-14 adhesion proteins inversely regulated by chemotactic factors. *Science.* 1989;245:1238–41.
 23. Doener F, Michel A, Reuter S, Friedrich P, Böhm L, Rille M, et al. Mast cell-derived mediators promote murine neutrophil effector functions. *Int Immunol.* 2013;25:553–61.
 24. Zhang J, Alcaide P, Liu L, Sun J, He A, Lusinskas FW, Shi GP. Regulation of endothelial cell adhesion molecule expression by mast cells, macrophages, and neutrophils. *PLoS One* 2011;6:e14525.
 25. Grützkau A, Krüger-Krasagakes S, Kögel H, Möller A, Lippert U, Henz BM. Detection of intracellular interleukin-8 in human mast cells: flow cytometry as a guide for immunoelectron microscopy. *J. Histochem. Cytochem. Off. J. Histochem. Soc.* 1997;45:935–945.
 26. Zernecke A, Bot I, Djalali-Talab Y, Shagdarsuren E, Bidzhekov K, Meiler S, Krohn R, Schober A, Sperandio M, Soehnlein O, Bornemann J, Tacke F, Biessen EA, Weber C. Protective role of CXCR4/CXCL12 ligand 12 unveils the importance of neutrophils in atherosclerosis. *Circ. Res.* 2008;102:209–217.
 27. Bot I, Daissormont IT, Zernecke A, van Puijvelde GH, Kramp B, de Jager SC, Sluimer JC, Manca M, Hélias V, Westra MM, Bot M, van Santbrink PJ, van Berkel TJ, Su L, Skjelland M, Gullestad L, Kuiper J, Halvorsen B, Aukrust P, Koenen RR, Weber C, Biessen EA. CXCR4 blockade induces atherosclerosis by affecting neutrophil function. *J Mol Cell Cardiol.* 2014;74:44–52.
 28. De Filippo K, Dudeck A, Hasenberg M, Nye E, van Rooijen N, Hartmann K, Gunzer M, Roers A, Hogg N. Mast cell and macrophage chemokines CXCL1/CXCL2 control the early stage of neutrophil recruitment during tissue inflammation. *Blood.* 2013;121:4930–4937.
 29. Christy AL, Walker ME, Hessner MJ, Brown MA. Mast cell activation and neutrophil recruitment promotes early and robust inflammation in the meninges in EAE. *J. Autoimmun.* 2013;42:50–61.
 30. Schramm R, Schaefer T, Menger MD, Thorlacius H. Acute mast cell-dependent neutrophil recruitment in the skin is mediated by KC and LFA-1: inhibitory mechanisms of dexamethasone. *J. Leukoc. Biol.* 2002;72:1122–1132.
 31. Shin K, Nigrovic PA, Crish J, Boilard E, McNeil HP, Larabee KS, Adachi R, Gurish MF, Gobeze R, Stevens RL, Lee DM. Mast cells contribute to autoimmune inflammatory arthritis via their tryptase/heparin complexes. *J. Immunol. Baltim. Md 1950* 2009;182:647–656.
 32. Drechsler M, Megens RT, van Zandvoort M, Weber C, Soehnlein O. Hyperlipidemia-triggered neutrophilia promotes early atherosclerosis. *Circulation.* 2010;122:1837–1845.
 33. Rotzius P, Thams S, Soehnlein O, Kenne E, Tseng CN, Björkström NK, Malmberg KJ, Lindbom L, Eriksson EE. Distinct infiltration of neutrophils in lesion shoulders in ApoE^{-/-} mice. *Am. J. Pathol.* 2010;177:493–500.
 34. Ionita MG, van den Borne P, Catanzariti LM, Moll FL, de Vries JP, Pasterkamp G, Vink A, de Kleijn DP. High neutrophil numbers in human carotid atherosclerotic plaques are associated with characteristics of rupture-prone lesions. *Arterioscler. Thromb. Vasc. Biol.* 2010;30:1842–1848.
 35. Borissoff JI, Joosen IA, Versteijlen MO, Brill A, Fuchs TA, Savchenko AS, Gallant M, Martinod K, Ten Cate H, Hofstra L, Crijns HJ, Wagner DD, Kietselaer BL. Elevated levels of circulating DNA and chromatin are independently associated with severe coronary atherosclerosis and a prothrombotic state. *Arterioscler. Thromb. Vasc. Biol.* 2013;33:2032–2040.
 36. Soehnlein O. Multiple roles for neutrophils in atherosclerosis. *Circ. Res.* 2012;110:875–888.

Chapter 6

RP105 deficiency aggravates vein graft disease and lesion instability via increased inflammation and mast cell activation

Submitted for publication

*Anouk Wezel^{1,2}

*Margreet R. de Vries^{2,3}

Johanna M. Maassen¹

Peter Kip²

Erna A. Peters^{2,3}

Jacco C. Karper^{2,3}

Johan Kuiper¹

Ilze Bot¹

Paul H. A. Quax^{2,3}

*These authors contributed equally

¹Division of Biopharmaceutics, Gorlaeus Laboratories, Leiden Academic Center for Drug Research, Leiden University, Leiden, The Netherlands

²Department of Surgery, Leiden University Medical Center, Leiden, The Netherlands

³Eindhoven Laboratory for Experimental Vascular Medicine, Leiden, The Netherlands Netherlands

Abstract

Aims: Venous bypass grafts are often used to bypass atherosclerotic lesions; however, the patency of these grafts is usually poor due to the development of vein graft disease. Previously, we have demonstrated that deficiency of TLR4, a key initiator of inflammatory signalling, results in a reduction of vein graft disease. As TLR4 signalling is regulated by the accessory molecule RadioProtective 105 (RP105), we aimed to investigate the effects of RP105 on vein graft disease.

Methods and results: RP105^{-/-} mice and C57BL/6 mice as controls underwent vein graft surgery; interestingly, a 90% increase in vein graft lesion area was observed in RP105^{-/-} mice. As lesions in vein grafts are often accompanied by superimposed atherosclerosis, we also determined the effect of RP105 on vein graft disease in a hypercholesterolemic setting. Lesion area did not differ between LDLr^{-/-}/RP105^{-/-} mice and LDLr^{-/-} mice fed a western type diet, but interestingly, we did observe a significant increase in the number of unstable lesions and intraplaque hemorrhage upon RP105 deficiency. In both experimental setups, an increase in lesional macrophages was seen. *In vitro*, RP105^{-/-} smooth muscle cells and mast cells secreted increased levels of the monocyte chemoattractant CCL2. *In vivo*, the number of activated perivascular mast cells was increased in RP105^{-/-} mice, as well as the amount of lesional CCL2.

Conclusions: Together, these data indicate that aggravated vein graft disease caused by RP105 deficiency may be the result of an increased inflammatory response and exacerbated CCL2 production by both mast cells and smooth muscle cells.

Introduction

Rupture of an atherosclerotic lesion with subsequent thrombus formation may lead to distal embolization of the blood vessel, resulting in main adverse cardiovascular events¹. Restoring blood flow to the ischemic tissue is therefore crucial, which can be accomplished by interventions such as placement of a (drug eluting) stent or a venous graft. Vein grafts are often used because of their long length, making it possible to bypass multiple atherosclerotic lesions, and their easy availability²⁻⁴. However, after ten years only an approximate 40% of the grafts is still patent, caused by late graft failure due to intimal hyperplasia and atherosclerosis⁵⁻⁸. It is thus of high importance to elucidate the underlying mechanisms of vein graft disease and identify new therapeutic targets to prevent vein graft failure. Harvesting of the venous graft with subsequent placement in the arterial circulation leads to damage of the endothelium, which causes platelets to adhere^{9,10}. Smooth muscle cells (SMC) then become activated and undergo a phenotypic switch. They start to migrate into the intima where they produce extracellular matrix necessary for the strength of the vein graft. However, excessive uncontrolled smooth muscle cell proliferation results in the formation of intimal hyperplasia. This process is accompanied by leukocyte influx into the vessel wall, which aggravates the inflammatory process and leads to superimposed atherosclerosis. Late vein graft failure may eventually be the result of complete occlusion caused by intimal hyperplasia or rupture of the vein graft lesion¹¹.

To study the complex mechanisms behind vein graft disease, as well as to explore possible treatment options, a previously described murine vein graft model has been used¹². In this model, lesions display typical concentric hyperplasia as well as lesional disruptions with intraplaque hemorrhage, with high resemblance to the complex lesions present in human vein grafts. When vein grafts are placed in mice on a high cholesterol diet, superimposed atherosclerosis will add to the lesional burden, as illustrated by lipid depositions and foam cell accumulation¹³. Taken together, excessive SMC proliferation, lipid accumulation and an enhanced inflammatory response seem to be causing vein graft disease. Highlighting the importance of vascular inflammation in vein graft disease, we have previously shown that local silencing of Toll-like receptor 4 (TLR4) significantly reduces vessel wall thickening in these murine venous grafts¹⁴, rendering this pathway of interest for future therapeutic interventions.

TLR4 belongs to the TLR family, a type of pattern recognition receptors, capable of inducing potent inflammatory signalling. A unique feature of TLR4, compared to other TLRs, is that it does not directly bind to its ligands. Instead, TLR4 forms a complex with the adaptor molecule MD2, which is the primary recognition site for lipopolysaccharide (LPS). The co-receptor CD14 may augment TLR4 signalling through binding of LPS and mediating its transfer to the TLR4/MD2 complex¹⁵. An

additional accessory molecule known to regulate TLR4 signalling is RadioProtective 105 (RP105). Similar to TLR4, RP105 forms a complex with the adaptor molecule MD1, but in contrast, the RP105/MD1 complex does not have an intracellular Toll interleukin 1 receptor (TIR) signalling domain¹⁶. Originally, RP105 was described as a B cell specific surface molecule, capable of enhancing cellular proliferation and activation¹⁶. However, RP105 was later on demonstrated to be expressed on the cell membrane of dendritic cells (DCs) and macrophages as well. In contrast to its role on the B cell, RP105 inhibits TLR4 mediated responses in DCs and macrophages, leading for instance to an aggravated inflammatory response after LPS injection in RP105 deficient mice¹⁷.

Taking into account the profound regulatory effects of RP105 on TLR4, and the previous finding that TLR4 signalling aggravates vein graft disease, it is compelling to investigate the role of RP105 in vein graft disease. Therefore, in the current study we used the murine vein graft model to establish whether RP105 deficiency affects lesion formation. We hypothesized that lack of RP105, via increased TLR4 signalling, will result in aggravated vein graft disease. Also, we aimed to determine how RP105 affects vein graft disease in a hypercholesterolemic setting with superimposed atherosclerosis.

Material and methods

Mice

All animal experiments were approved by the animal welfare committee of the Leiden University Medical Center (approval reference number 09098 and 12153). This study was performed in compliance with Dutch government guidelines and the Directive 2010/63/EU of the European Parliament. RP105^{-/-} mice were kindly provided by K. Miyake (Tokyo University, Japan) and were described previously¹⁶. Male wild type (WT, C57BL/6, 10-12 weeks old) (n=11) and RP105^{-/-} animals (C57BL/6 background, backcrossed for more than 10 generations, 10-12 weeks old) (n=13) were bred in our facility at the Leiden University Medical Center (Leiden, The Netherlands) and during the experiment, mice were given water and chow ad libitum.

To study the effects of RP105 deficiency on vein graft disease in a hyperlipidemic setting, male LDLR^{-/-} mice (n=12, 12-16 weeks old) and male LDLR^{-/-}/RP105^{-/-} mice (n=12, 12-16 weeks old) were used. Mice were fed a western-type diet containing 0.25% cholesterol and 15% cacaobutter (SDS, Sussex, UK) for 4 weeks. Plasma total cholesterol levels were measured by enzymatic procedures using precipath standardized serum as an internal standard (Boehringer Mannheim, Germany).

Surgical intervention

Before surgery and sacrifice, mice were anesthetized by an intraperitoneal injection with Midazolam (5 mg/kg, Roche, Woerden, The Netherlands), Domitor (0.5 mg/kg, AST Farma, Oudewater, The Netherlands) and fentanyl (0.05 mg/kg, Janssen, Beerse, Belgium). Adequacy of anaesthesia was monitored by regular visual inspection and toe pinch reflex. After surgery mice were antagonized with a subcutaneous injection of flumazenil (0.5 mg/kg, Fresenius Kabi, Schelle, Belgium) and Antisedan (2.5 mg/kg, AST farma). Buprenorphine (0.1 mg/kg, MSD animal Health, Boxmeer, The Netherlands) was given after sur-

gery to relieve pain. Vein graft surgery was performed in order to induce intimal hyperplasia in the venous grafts¹². In brief, the carotid artery of the recipient mice was cut in the middle; both ends of the artery were everted around cuffs and ligated with 8.0 sutures. Donor littermates were anesthetized as described above, after which the vena cava was harvested and donor mice were exsanguinated. The vena cava was then sleeved over the cuffs in the recipient mice. The high blood pressure in the arterial circulation leads to endothelial damage of the vein graft, which is followed by accelerated neointimal hyperplasia. At sacrifice after 28 days, mice were exsanguinated via orbital bleeding. Vein grafts were harvested and fixed in 4% formaldehyde, dehydrated and paraffin-embedded for histology.

Histological and immunohistochemical analysis

All (immuno)-histochemical stainings and measurements were performed on six consecutive cross-sections, approximately 150 μm interspaced, of paraffin embedded vein grafts segments (5 μm thick). Hematoxylin-phloxine saffron (HPS) staining and Masson trichrome stainings were used for the measurement of vein graft lesion area and plaque dissection analysis, while collagen content was visualized with a picrosirius red staining. Composition of the vein graft lesions was further evaluated by staining for macrophages (MAC3, BD-Pharmingen, San Diego, CA, USA), smooth muscle cell actin (Sigma, Zwijndrecht, The Netherlands), CCL2 (Santa Cruz Biotechnology, Dallas, TX, USA) and CCR2 (Abcam, Cambridge, UK). Mast cell staining was performed using an enzymatic chloroacetate esterase kit (Sigma); when granules were apparent in the vicinity of the mast cell they were scored as activated.

Plaque dissection analysis was performed over a total vein graft length of 1800 μm . The disruptions were defined as a connection or fissure between the lumen and part of the vessel wall underneath the adventitia, filled with fibrin and erythrocytes¹². Quantification of the lesion area and immunostained positive area were performed using computer assisted software (Qwin, Leica, Cambridge, UK). In brief, the total intimal area was measured, as well as the stained area. The stained area was then calculated as a percentage of the total intimal area. All measurements were performed in a blinded manner by a single observer.

Cell culture

LDLr^{-/-} and LDLr^{-/-}/RP105^{-/-} mice were anaesthetized as described above and sacrificed via cervical dislocation, after which bone marrow (BM) suspensions were isolated by flushing the femurs and tibias with PBS. BM derived mast cells (BMMCs) were grown by culturing BM cells from LDLr^{-/-} mice and LDLr^{-/-}/RP105^{-/-} mice at a density of 0.25×10^6 cells in RPMI containing 10% fetal bovine serum (FBS), 2 mmol/L l-glutamine, 100 U/mL penicillin, 100 $\mu\text{g}/\text{mL}$ streptomycin (all from PAA, Cölbe, Germany) and mIL3 supernatant (supernatant from WEHI cells overexpressing murine Interleukin (IL)-3) for 4 weeks in T175 tissue culture flasks (Greiner Bio-one, Alphen aan den Rijn, Netherlands). RAW 264.7 cells (a murine macrophage cell line) were cultured in Dulbecco's modified Eagle's medium (DMEM) supplemented with 10% Fetal Calf's Serum (FCS), 2 mmol/L l-glutamine, 100 U/mL penicillin and 100 $\mu\text{g}/\text{mL}$ streptomycin in T75 tissue culture flasks (Greiner Bio-one).

To generate bone marrow derived macrophages (BMDM), BM cells from BM of LDLr^{-/-} mice and LDLr^{-/-}/RP105^{-/-} mice were cultured for 7 days in RPMI medium supplemented with 20% fetal calf serum (FCS), 2 mmol/L l-glutamine, 100 U/mL penicillin, 100 $\mu\text{g}/\text{mL}$ streptomycin (all from PAA) and 30% L929 cell-conditioned medium (as the source of macrophage colony-stimulating factor (M-CSF)) in petridishes (Greiner Bio-one)¹⁸.

Murine vSMCs explanted from aortas of RP105^{-/-} mice and control mice were cultured and incubated overnight with either LPS (1 ng/mL or 3 ng/mL) or control medium (n=4). These mice were anesthetized as described above and sacrificed via cervical dislocation. IL-6, TNF α and CCL2 ELISAs were performed according to manufacturer's protocol (BD Biosciences, Breda, The Netherlands).

Macrophage activation

Bone marrow derived LDLr^{-/-} and LDLr^{-/-}/RP105^{-/-} macrophages cultured as described above, were activated with 1 ng/mL, 10 ng/mL or 50 ng/mL LPS (from E. Coli, Sigma-Aldrich) for 4 hours (n=3) at a density of 10⁶ cells per well. Cells were then spun down (1500 rpm, 5 minutes) and used for RNA isolation.

Proliferation assay

To measure the effect of RP105 on macrophage proliferation, LDLr^{-/-}/RP105^{-/-} BMDM and control LDLr^{-/-} BMDM were seeded at a density of 4*10⁴ cells per well (n=4). Cells were incubated overnight with 0.5 µCi [³H]thymidine (PerkinElmer, Groningen, The Netherlands) per well at 37°C. [³H]Thymidine incorporation was quantified in a liquid scintillation analyzer (Packard 1500 Tricarb, Downers Grove, IL, USA).

To investigate the effect of RP105 deficiency on mast cell proliferation, LDLr^{-/-} and LDLr^{-/-}/RP105^{-/-} BMMCs were seeded at a density of 10⁴ cells per well. Cells were incubated overnight with 0.5 µCi [³H]thymidine (PerkinElmer) per well. [³H]Thymidine incorporation was measured as described above. The effect of RP105^{-/-} mast cell supernatant on macrophage proliferation was investigated by seeding RAW cells at a density of 4*10⁴ cells per well. The next day, cells were exposed to supernatant of non-activated LDLr^{-/-} or LDLr^{-/-}/RP105^{-/-} mast cells (n=4). After overnight incubation 0.5 µCi [³H]thymidine (PerkinElmer), proliferation was measured as described above.

Mast cell activation

LDLr^{-/-} and LDLr^{-/-}/RP105^{-/-} BMMCs were seeded at a density of 10⁶ cells per well (n=3), after which they were stimulated with 1 ng/mL, 10 ng/mL or 100 ng/mL LPS (from E. Coli, Sigma-Aldrich, St. Louis, MO, USA). After 4 hours and 24 hours activation, cells were spun down (1500 rpm, 5 minutes) and the supernatant was collected for further analysis. ELISAs were performed according to manufacturer's protocol. Expression of the surface markers RP105 and TLR4 on control LDLr^{-/-} mast cells was determined by means of FACS analysis (FACS Canto, BD Biosciences).

RNA isolation, cDNA synthesis and qPCR

Guanidine thiocyanate (GTC) was used to extract total RNA from BMMCs and BMDMs¹⁹. RNA was reverse transcribed by M-MuLV reverse transcriptase (RevertAid, MBI Fermentas, Leon-Rot, Germany) and used for quantitative analysis of mouse genes (Supplemental Table 1) with an ABI PRISM 7700 Taqman apparatus (Applied Biosystems, Foster City, CA, USA). Murine hypoxanthine phosphoribosyltransferase (HPRT) and murine ribosomal protein 27 (RPL27) were used as standard housekeeping genes.

Statistical analysis

Data are expressed as mean±SEM. A 2-tailed Student's t-test was used to compare individual groups. Non-Gaussian distributed data were analyzed using a Mann-Whitney U test. Frequency data analysis was performed by means of the Fisher's exact test. A level of P<0.05 was considered significant.

Results*RP105^{-/-} mice show aggravated vein graft lesion development*

Vein grafts were placed in RP105^{-/-} mice and control C57BL/6 mice to investigate the effect of RP105 deficiency on vein graft disease. Interestingly, lack of RP105 resulted in a 90% increased vein graft lesion area (C57BL/6: 0.36 ± 0.02 mm²; RP105^{-/-}: 0.69 ± 0.12 mm²; Figure 1A; P<0.05).

Plaque morphology was further analyzed by staining for macrophages, smooth muscle cells and collagen. The percentage of lesional macrophages was significantly increased in mice deficient for RP105 (C57BL/6: $2.2 \pm 1.8\%$; RP105^{-/-}: $7.5 \pm 0.9\%$; Figure 1B; $P < 0.05$), while no changes were observed in the percentage of smooth muscle cells between the two groups (Figure 1C). Picrosirius red staining revealed a significant reduction of collagen content in the lesions of RP105^{-/-} mice compared to control mice (C57BL/6: $63.0 \pm 3.0\%$; RP105^{-/-}: $54.6 \pm 1.6\%$; Figure 1D; $P < 0.05$), which indicates that the lesional phenotype may be more unstable.

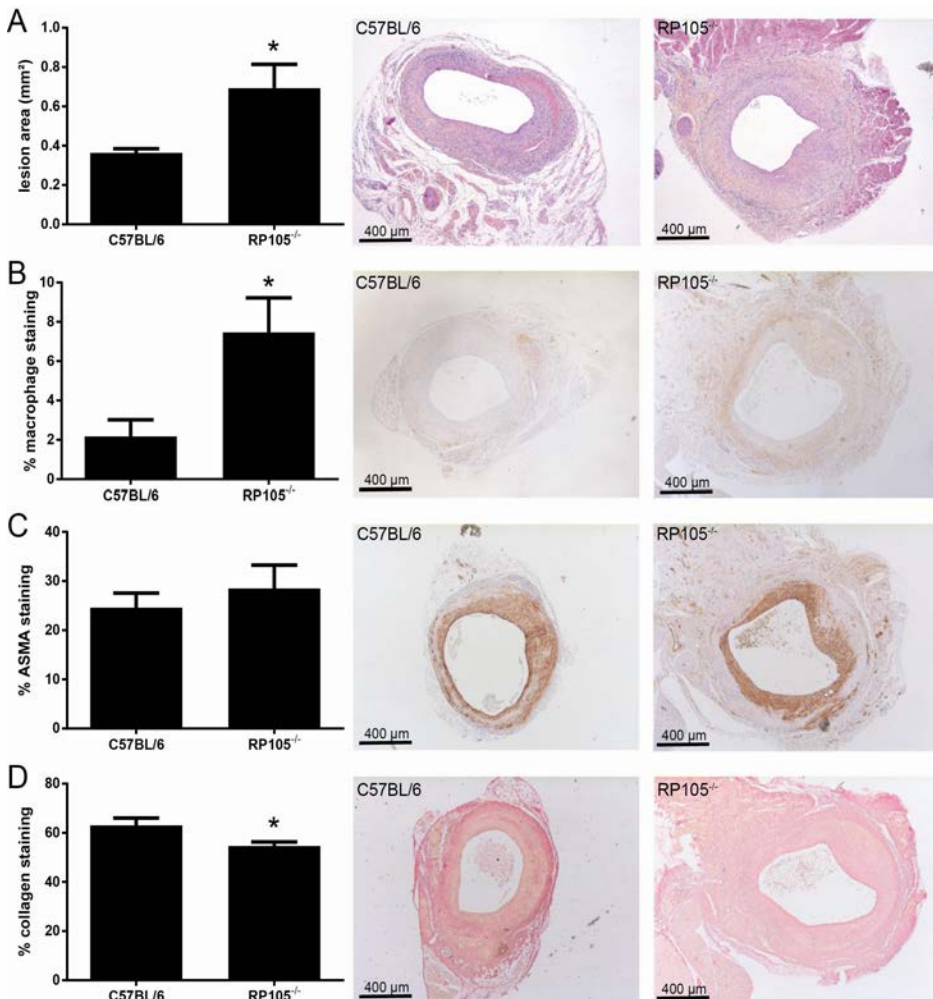


Figure 1. Vein graft lesion area was significantly increased in RP105^{-/-} mice compared to control C57BL/6 mice (A). The macrophage content, expressed as the percentage of stained area in the intimal hyperplasia, was higher in RP105^{-/-} mice compared to control (B), while no changes were found in the percentage of smooth muscle cells (ASMA, alpha-smooth muscle cell actin, C). Collagen content was decreased in RP105^{-/-} mice, indicative of less stable lesions (D). The micrographs show representative images of each group (50x). N=11 C57BL/6 mice/group, N=13 RP105^{-/-} mice/group. * $P < 0.05$.

To further determine lesion stability, we analyzed sections for the presence of erythrocytes in the lesions accompanied by fibrin layers. In RP105^{-/-} mice, 3 out of 13 mice displayed plaque dissections, while 0 out of 11 disruptions were observed in C57BL/6 mice.

LDLr^{-/-}/RP105^{-/-} mice display lesions with an unstable phenotype

Next, we investigated whether high-fat diet feeding would alter the effects of RP105 deficiency on vein graft disease. LDLr^{-/-}/RP105^{-/-} mice and LDLr^{-/-} mice as controls received autologous vein grafts while fed a western-type diet for 4 weeks. No changes were detected in total bodyweight or plasma total cholesterol levels between the two groups (data not shown). In contrast to mice on chow diet, no changes in vein graft lesion area were observed in LDLr^{-/-}/RP105^{-/-} mice compared to control LDLr^{-/-} mice (LDLr^{-/-}: 0.59 ± 0.05 mm²; LDLr^{-/-}/RP105^{-/-}: 0.54 ± 0.05 mm²; Figure 2A; P=NS).

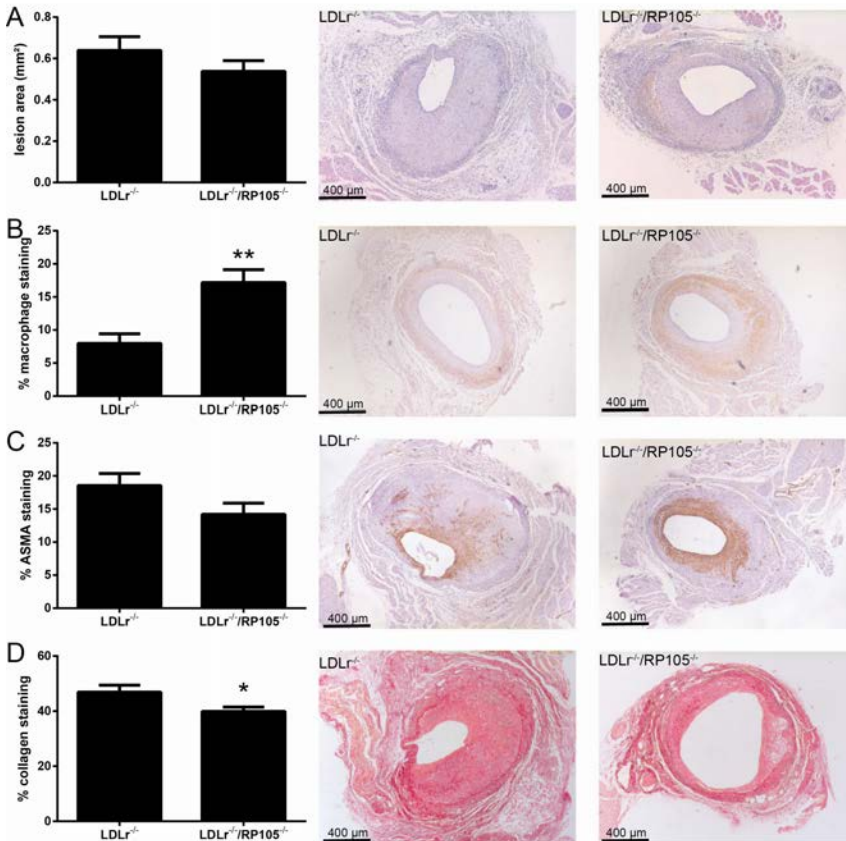


Figure 2. No changes were observed in the vessel wall area of LDLr^{-/-}/RP105^{-/-} mice compared to control LDLr^{-/-} mice (A). Similar to mice fed a chow diet, a higher percentage of macrophages was observed in LDLr^{-/-}/RP105^{-/-} (B). Smooth muscle cell content was unaltered between the two groups (ASMA, C) and again a decrease in lesional collagen was observed (D). The micrographs show representative images of each group (50x). N=12 LDLr^{-/-} mice/group. N=12 LDLr^{-/-}/RP105^{-/-} mice/group. *P<0.05. **P<0.01.

Analysis of plaque morphology showed an increase in macrophage staining in lesions of LDLr^{-/-}/RP105^{-/-} mice compared to control (LDLr^{-/-}: 8.0 ± 1.5%; LDLr^{-/-}/RP105^{-/-}: 15.9 ± 2.2%; Figure 2B; P<0.05). A trend towards a reduction in smooth muscle cell staining was observed in mice deficient for RP105 (P=0.069; Figure 2C), and furthermore, lesional collagen content was significantly reduced in these mice (LDLr^{-/-}: 46.9 ± 2.5%; LDLr^{-/-}/RP105^{-/-}: 39.9 ± 1.6%; Figure 2D; P<0.05). Interestingly, the total number of plaque dissections and intraplaque hemorrhages was profoundly increased in LDLr^{-/-}/RP105^{-/-} mice compared to LDLr^{-/-} control mice (LDLr^{-/-} mice: 3 out of 12 mice; LDLr^{-/-}/RP105^{-/-}: 10 out of 12 mice; Figure 3A; P<0.05). Also, the average length of the dissections was significantly increased in the LDLr^{-/-}/RP105^{-/-} mice (Figure 3B; P<0.05).

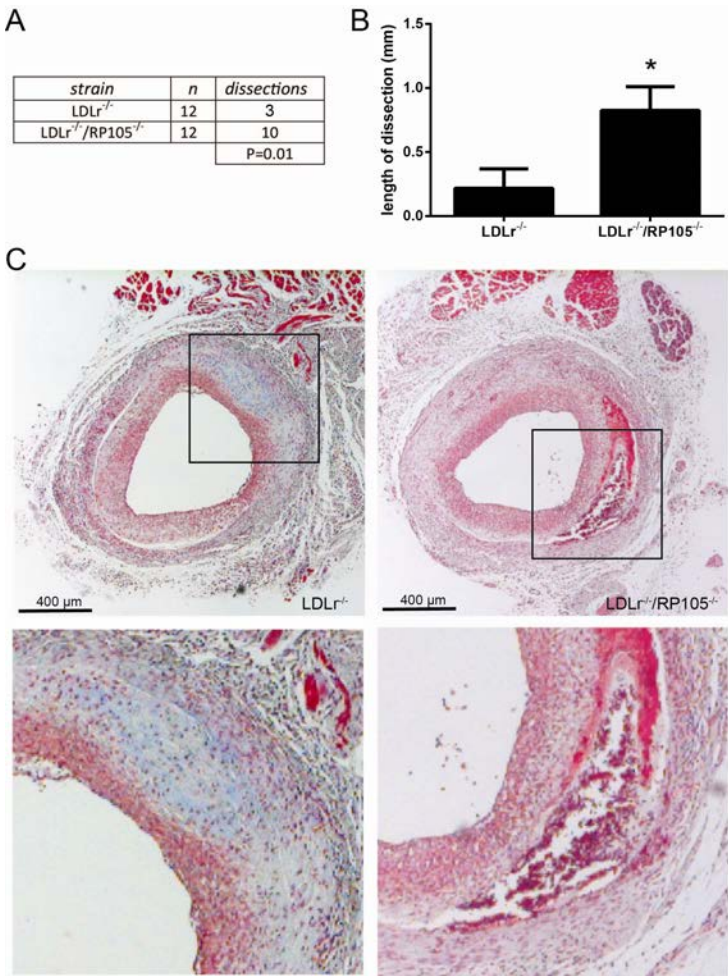


Figure 3. The number of plaque dissections in LDLr^{-/-}/RP105^{-/-} mice was significantly higher compared to control LDLr^{-/-} mice (A). Also, the total length of plaque dissections was increased in LDLr^{-/-}/RP105^{-/-} mice compared to control (B). The micrographs show representative images of each group (50x). N=12 LDLr^{-/-} mice/group. N=12 LDLr^{-/-}/RP105^{-/-} mice/group. *P<0.05.

Unaltered MMP expression in RP105 deficient macrophages

As we observed a reduced collagen content in the lesions of RP105 deficient mice, and matrix metalloproteinases (MMPs) are known for its involvement in collagen homeostasis, we measured MMP expression in macrophages. However, no major changes were found in the expression of MMP2, MMP8 and MMP9 as well as in the expression of TIMP1, TIMP2 and TIMP3 at baseline or after stimulation with a concentration range of LPS in RP105^{-/-} macrophages compared to control (Supplemental Figure 1).

Macrophage proliferation rate is not altered by RP105 deficiency

To elucidate the mechanisms behind the increased percentage of lesional macrophages observed in both *in vivo* studies, we aimed to determine macrophage proliferation, since it has recently been described that local macrophage proliferation may add to the lesional burden²⁰. We cultured RP105 deficient macrophages and control macrophages and determined the cellular proliferation rate, which was unaltered under basal conditions (Supplemental Figure 2).

RP105^{-/-} smooth muscle cells produce increased levels of CCL2

To further examine why we observe the increased percentage of lesional macrophages in RP105 deficient mice, we determined CCL2 secretion *in vitro*, which is known to be one of the key chemokines involved in monocyte recruitment to the lesion²¹. Since the smooth muscle cell is one of the major determinants of vein graft disease, we investigated whether smooth muscle cells deficient in RP105 produce altered levels of CCL2. Indeed, primary cultured smooth muscle cells lacking RP105 were seen to secrete significantly increased CCL2 amounts after stimulation with LPS, compared to control smooth muscle cells (Figure 4; $P < 0.05$).

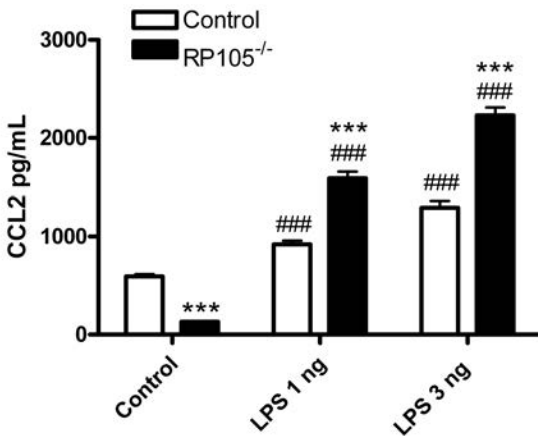


Figure 4. After 24 hours stimulation with 1 and 3 ng/mL LPS, RP105^{-/-} vascular smooth muscle cells (vSMCs) secrete dose-dependent increased levels of CCL2, which was significantly higher compared to control vSMCs (N=4). *** $P < 0.001$ compared to control vSMCs. ### $P < 0.001$ compared to unstimulated vSMCs.

RP105 deficiency aggravates mast cell activation

In addition to the smooth muscle cell, we have previously shown that mast cells also play a key role in vein graft disease²². Moreover, mast cells can contribute to plaque destabilization, for instance via the degradation of collagen by mast cell derived tryptase and chymase^{23,24}. Therefore, we aimed to determine the relevance of RP105 in mast cell function. First, we analyzed whether mast cells express RP105, which is indeed the case at both mRNA and protein level (Supplemental Figure 3A,B). Next, we examined whether RP105 plays a functional role in mast cell activation by culturing bone marrow derived mast cells from RP105 deficient mice and control mice. Mast cells were stimulated with 10 ng/mL and 100 ng/mL LPS for 4 and 24 hours. Interestingly, RP105 deficient mast cells were seen to secrete increased levels of IL-6 and TNF α compared to control mast cells, which was dose-dependent increased after 4 hours of LPS activation (Figure 5A,B). Also, CCL2 secretion of RP105^{-/-} mast cells was highly increased compared to control mast cells, which may also have contributed to the increased lesional macrophages *in vivo* (Figure 5C). Furthermore, 24 hours of activation still showed a significant increase in IL-6 and CCL2 production of RP105^{-/-} mast cells compared to control. These data indicate that RP105 deficiency on the mast cell results in increased activation and cytokine release.

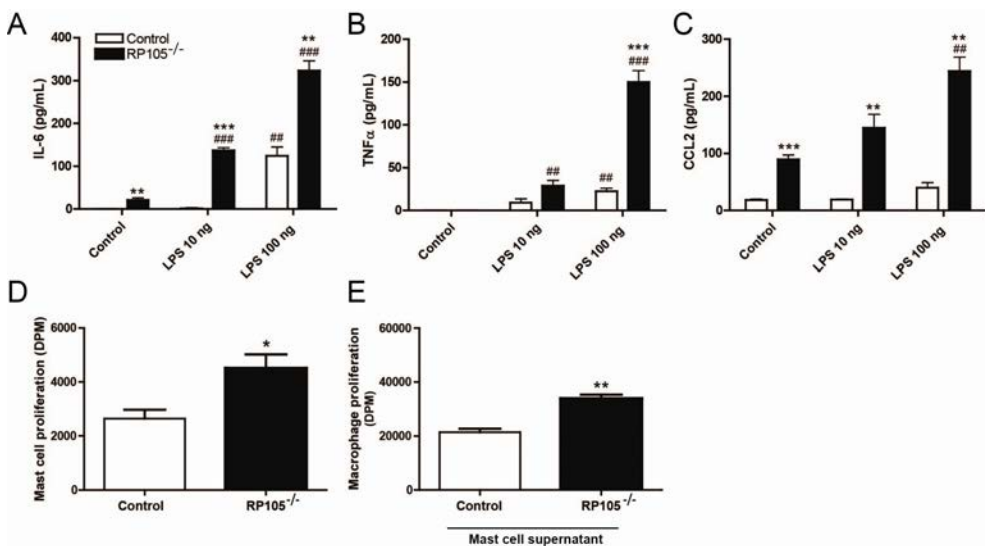


Figure 5. After 4 hours stimulation with 10 ng/mL and 100 ng/mL LPS, bone marrow derived RP105^{-/-} mast cells secreted dose-dependently increased levels of IL-6 (A), TNF α (B) and CCL2 (C), which was significantly higher compared to control mast cells (N=3). The basal proliferation rate of RP105^{-/-} mast cells was seen to be significantly higher compared to control mast cells (D) (N=4). Addition of the supernatant from RP105^{-/-} mast cells to macrophages resulted in increased proliferation compared to the addition of supernatant from control mast cells (E) (N=4). * $P < 0.05$. ** $P < 0.01$. *** $P < 0.001$ compared to control mast cells. ## $P < 0.01$. ### $P < 0.001$ compared to unstimulated mast cells.

We then investigated whether cellular proliferation is altered in RP105 deficient mast cells. Interestingly, RP105 deficient mast cells show an increased proliferation rate compared to control mast cells under basal conditions (Figure 5D).

Since we observed an increased activation status of RP105^{-/-} mast cells, and mast cells are known to secrete a variety of growth factors, we assessed whether the releasate of activated RP105^{-/-} mast cells has differential effects on macrophages compared to control mast cells. Indeed, after adding supernatant of RP105^{-/-} mast cells to macrophages, we observed an increased proliferation of macrophages compared to the addition of supernatant from control mast cells (Figure 5E).

Increased perivascular mast cell numbers and activation status in vivo

Considering the profound effects of RP105 deficiency on the mast cell found *in vitro*, we aimed to determine whether mast cell numbers and activation status *in vivo* are altered as well. Indeed, the average number of peri-adventitial mast cells was increased in RP105^{-/-} mice compared to control mice (C57BL/6: 0.67 ± 0.28 mast cells/mm²; RP105^{-/-}: 3.24 ± 0.98 mast cells/mm²; Figure 6A; $P < 0.05$). Moreover, in RP105^{-/-} mice the average number of activated mast cells was significantly higher (C57BL/6: 0.29 ± 0.12 activated mast cells/mm²; RP105^{-/-}: 1.80 ± 0.60 activated mast cells/mm²; Figure 6B; $P < 0.05$).

In LDLr^{-/-} mice, basal mast cells levels were increased already upon western type diet feeding compared to C57BL/6 controls (5.2 ± 0.5 mast cells/mm²), which was further increased in mice lacking RP105, however this did not reach significance (7.4 ± 1.0 mast cells/mm²; Figure 6C; $P = 0.062$). Also, the number of activated mast cells showed a trend towards an increase in LDLr^{-/-}/RP105^{-/-} mice compared to control (LDLr^{-/-}: 3.0 ± 0.3 mast cells/mm²; LDLr^{-/-}/RP105^{-/-}: 4.1 ± 0.5 mast cells/mm²; Figure 6D; $P = 0.057$).

Increased CCL2 expression in vivo

Taking into consideration the increased amount of CCL2 secreted *in vitro* by both RP105 deficient smooth muscle cells and mast cells, we aimed to determine whether lesional CCL2 expression was increased in RP105^{-/-} mice as well. Intriguingly, the CCL2 positive area in the lesions was significantly increased in RP105^{-/-} mice compared to control mice (C57BL/6: 0.03 ± 0.007 mm²; RP105^{-/-}: 0.7 ± 0.008 mm²; Figure 7A; $P < 0.01$). Also, the lesional CCL2 positive area in hypercholesterolemic LDLr^{-/-}/RP105^{-/-} mice was profoundly increased compared to control mice (LDLr^{-/-}: 0.08 ± 0.01 mm²; LDLr^{-/-}/RP105^{-/-}: 0.3 ± 0.05 mm²; Figure 7B; $P < 0.001$). The higher expression of CCL2 in vein graft lesions of RP105 deficient mice may thus explain the increased macrophage content observed in these lesions. The expression of lesional CCR2, the receptor for CCL2 remained unaltered in both experimental groups (Figure 7C,D).

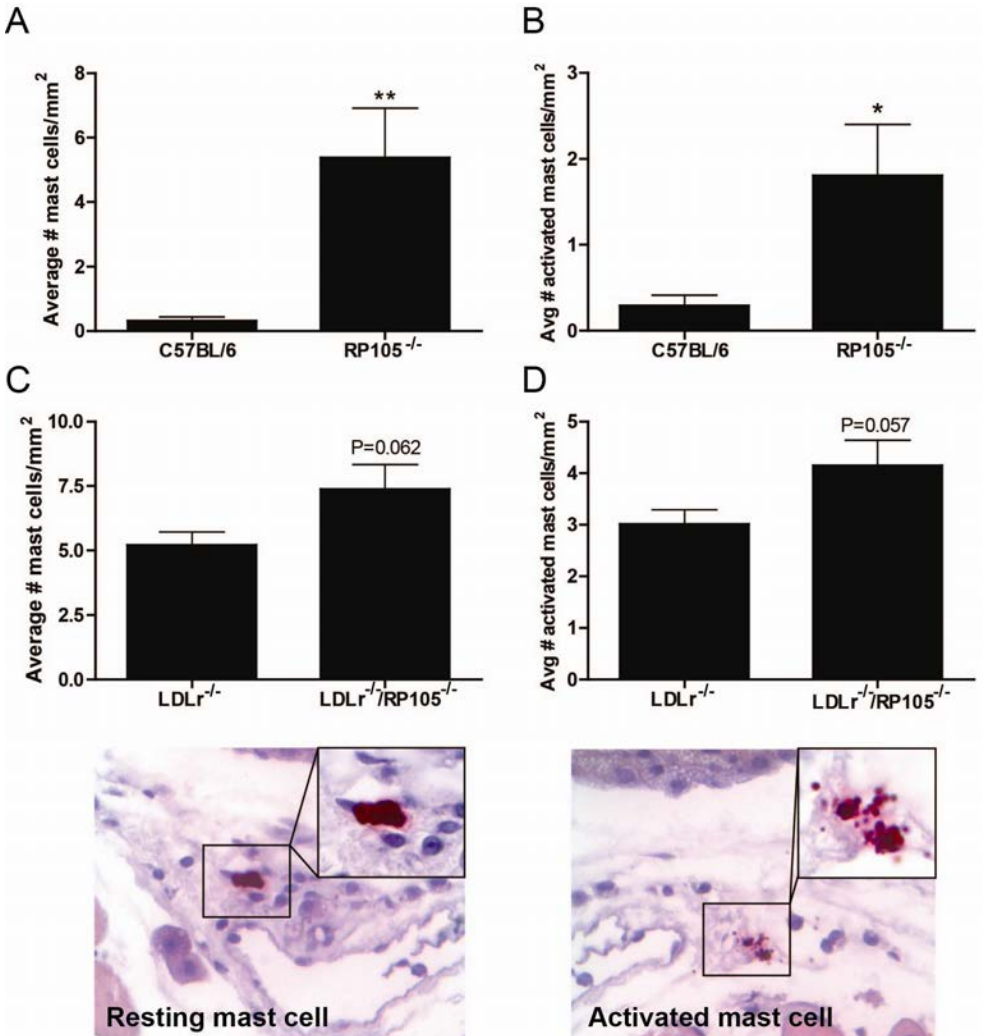


Figure 6. The amount of perivascular mast cells was markedly increased in the perivascular tissue from vein grafts of RP105 deficient mice compared to control C57BL/6 mice (A). Also, the number of activated mast cells was significantly higher in RP105^{-/-} mice (B). Mast cell numbers, as well as the amount of activated mast cells, showed a trend towards an increase in LDLr^{-/-}/RP105^{-/-} mice fed a western type diet compared to LDLr^{-/-} mice (C,D). Micrographs show representative pictures of perivascular mast cells in a resting state (left panel) and in an activated state (right panel), with granules clearly surrounding the mast cell N=11 C57BL/6 mice/group, N=13 RP105^{-/-} mice/group, N=12 LDLr^{-/-} mice/group. N=12 LDLr^{-/-}/RP105^{-/-} mice/group. (1000x). *P<0.05. **P<0.01.

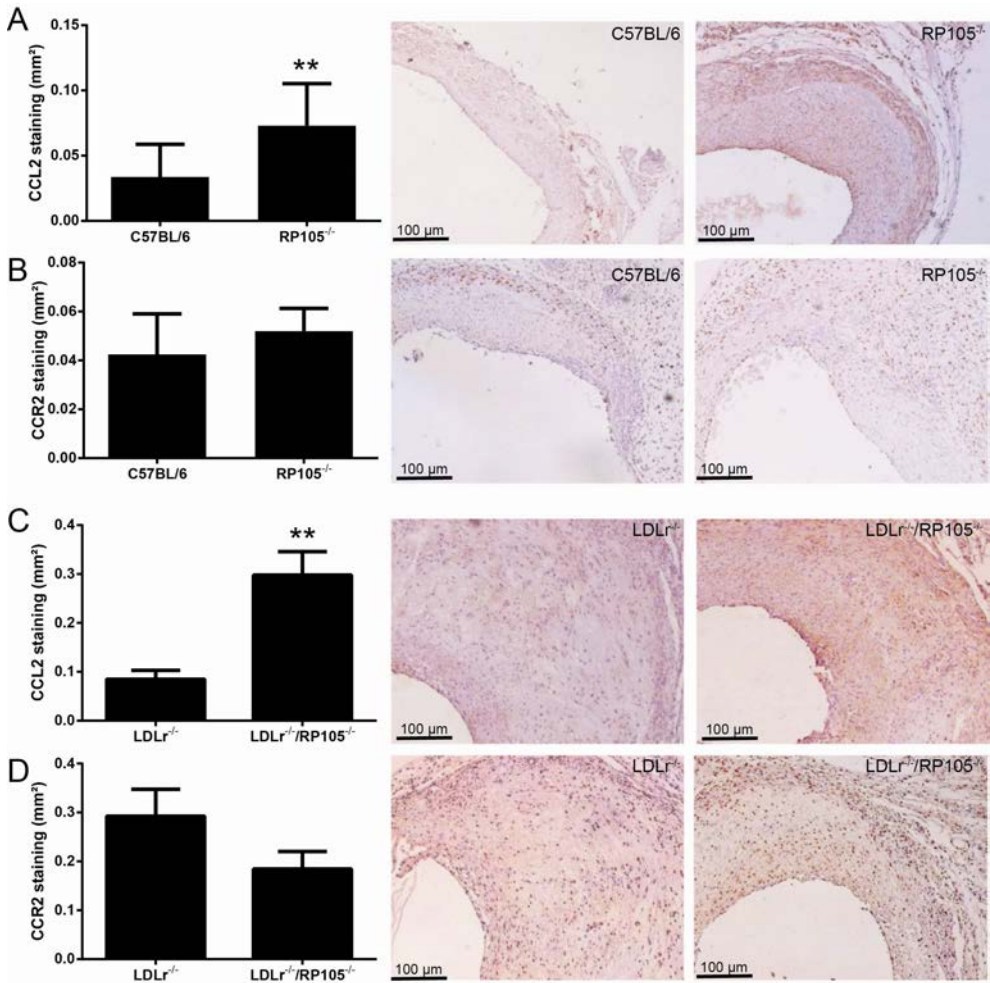


Figure 7. *In vivo* CCL2 and CCR2 staining. Immunohistochemical stainings revealed a significant increase in the CCL2 positive area in the lesions of RP105^{-/-} mice compared to control C57BL/6 mice (A). Also, the lesional CCL2 area was profoundly increased in hypercholesterolemic LDLr^{-/-}/RP105^{-/-} mice compared to control LDLr^{-/-} mice (C). No differences were observed in lesional CCR2 expression in both experimental groups (B,D). N=11 C57BL/6 mice/group, N=13 RP105^{-/-} mice/group, N=12 LDLr^{-/-} mice/group. N=12 LDLr^{-/-}/RP105^{-/-} mice/group. **P<0.01.

Discussion

In the current study we demonstrate that lack of the regulatory molecule RP105 results in a marked increase in vein graft lesion area. Furthermore, we show that in a hypercholesterolemic setting lesions display an increase in plaque dissections and plaque destabilization. In both studies decreased lesional collagen content was observed while the macrophage content was enhanced. Our *in vitro* data

demonstrate that RP105 deficient smooth muscle cells as well as RP105^{-/-} mast cells secrete excessive levels of CCL2 compared to control cells, which may contribute to the increase of macrophages in the plaque. Moreover, we are the first to demonstrate that RP105 plays a functional role in mast cell activation and proliferation, possibly aggravating lesion destabilization.

Mast cells are potent inflammatory cells which have previously been implicated in vein graft disease and plaque destabilization^{23,24,25}. They exert their detrimental effects through the secretion of specific proteases, tryptase and chymase, histamine, VEGF and a variety of cytokines and chemokines, which all contribute to increased inflammation²⁶. Activation of mast cells may be induced by a range of mediators, such as IgE; neuropeptides²⁷; complement components C5a and C3a²²; or via Toll-like receptors, in particular TLR4²⁸. Whether TLR4 signalling may actually lead to mast cell degranulation is still under debate, however, it is well established that TLR4 activation results in increased proinflammatory cytokine secretion²⁹. RP105 is known to inhibit TLR4 signalling in macrophages and dendritic cells; however up to date evidence describing a role for RP105 in mast cells is lacking. As expected, we found a dose-dependent increase of CCL2, IL-6 and TNF α after stimulation of mast cells with LPS. Interestingly, this increase was significantly higher in RP105 deficient mast cells, indicating that these cells, upon activation, secrete excessive amounts of cytokines in its surroundings. We now thus show that also on the mast cell, RP105 has an inhibitory effect and consequently, lack of RP105 leads to increased activation. Therefore, we postulate that the increase in vessel wall thickening observed in RP105^{-/-} mice on a chow diet may at least partly be caused by aggravated mast cell activation. This is in line with previous findings, in which we also show that perivascular mast cell activation by a dinitrophenyl hapten results in exacerbated vein graft thickening²². Also, mast cell derived tryptase and chymase have previously been shown to increase collagen degradation²⁴, which thus may have contributed to the decreased lesional collagen content observed in the current study.

In LDLr^{-/-}/RP105^{-/-} mice fed a western type diet, we observed an increase in plaque dissections, however, we did not observe any effects on vessel wall thickening, which was accompanied by less pronounced effects on mast cell activation. Previously, we have seen that upon western type diet feeding, vascular mast cell activation is enhanced (unpublished data). Indeed, control LDLr^{-/-} mice fed a western type diet already displayed higher numbers of activated mast cells, compared to control C57BL/6 mice on a chow diet. Therefore, the additive inflammatory effect of RP105 deficiency on mast cells in mice receiving a high cholesterol diet may be less pronounced.

Previously, we have investigated the effects of RP105 in other mouse models of vascular remodelling as well. Besides vein graft surgery, balloon angioplasty with

stent placement is used for the treatment of atherosclerosis; however in-stent restenosis impairs the success rate of this operation³⁰. In a murine mouse model for restenosis we have shown that RP105 deficiency results in increased neo-intima formation³¹, which is in line with the observed effects on vein graft disease in the current study. Conversely, in a setting of atherosclerosis, mice on a western type diet lacking RP105 on their myeloid cells develop reduced atherosclerotic lesions due to changes in B cells³². Also, total body RP105 deficiency was seen to reduce atherosclerosis and decrease lesional macrophage content, induced by a reduced monocyte influx (unpublished data). These disturbances in monocyte migration were also observed in RP105^{-/-} mice with hind limb ischemia³³. The fact that we observe an increase in lesional macrophages may be explained by the profound increase in CCL2 secretion by both RP105^{-/-} smooth muscle cells and mast cells, thus resulting in increased monocyte recruitment to the lesion. Indeed, CCL2 expression in the vein graft lesions of mice deficient for RP105 was significantly increased compared to controls. As vein graft lesions are highly enriched in smooth muscle cells compared to atherosclerotic plaques, the effect of smooth muscle cell derived products, such as CCL2, is more prominent in vein graft disease as compared to atherosclerosis. These contrasting effects highlight the difference in underlying mechanisms of diet-induced atherosclerotic lesion development versus restenosis and vein graft disease, the latter two in which smooth muscle cells play a dominant role.

In summary, the current study is the first to demonstrate that lack of RP105 results in increased lesion area in murine vein grafts. In a hypercholesterolemic setting, RP105 deficiency resulted in an increase of unstable lesions and a higher number of plaque dissections accompanied by intraplaque hemorrhage. *In vitro* investigations suggest that this may be caused by excessive CCL2 secretion by RP105^{-/-} smooth muscle cells, as well as by an increased inflammatory and proliferative phenotype of RP105^{-/-} mast cells.

Funding

This work was supported by grants from the Dutch Heart Foundation (A.W.: 2010B029 and I.B.: 2012T083). We acknowledge the support from the Netherlands CardioVascular Research Initiative: "the Dutch Heart Foundation, Dutch Federation of University Medical Centres, the Netherlands Organisation for Health Research and Development and the Royal Netherlands Academy of Sciences" for the GENIUS project "Generating the best evidence-based pharmaceutical targets for atherosclerosis" (CVON2011-19).

References

1. Frostegård J. Immunity, atherosclerosis and cardiovascular disease. *BMC Med* 2013;11:117.
2. Une D, Kulik A, Voisine P, Le May M, Ruel M. Correlates of saphenous vein graft hyperplasia and occlusion 1 year after coronary artery bypass grafting: analysis from the CASCADE randomized trial. *Circulation*. 2013;128:S213-8.
3. Donker JMW, Ho GH, Te Slaa A, de Groot HG, van der Waal JC, Veen EJ, van der Laan L. Midterm results of autologous saphenous vein and ePTFE pre-cuffed bypass surgery in peripheral arterial occlusive disease. *Vasc Endovascular Surg* 2011;45:598-603.
4. Al-Sabti HA, Al Kindi A, Al-Rasadi K, Banerjee Y, Al-Hashmi K, Al-Hinai A. Saphenous vein graft vs. radial artery graft searching for the best second coronary artery bypass graft. *J Saudi Heart Assoc* 2013;25:247-54.
5. Fitzgibbon GM, Kafka HP, Leach AJ, Keon WJ, Hooper GD, Burton JR. Coronary bypass graft fate and patient outcome: angiographic follow-up of 5,065 grafts related to survival and reoperation in 1,388 patients during 25 years. *J Am Coll Cardiol* 1996;28:616-26.
6. Motwani JG, Topol EJ. Aortocoronary saphenous vein graft disease: pathogenesis, predisposition, and prevention. *Circulation* 1998;97:916-31.
7. Campeau L, Enjalbert M, Lespérance J, Bourassa MG, Kwiterovich P Jr, Wacholder S, Sniderman A. The relation of risk factors to the development of atherosclerosis in saphenous-vein bypass grafts and the progression of disease in the native circulation. A study 10 years after aortocoronary bypass surgery. *N Engl J Med* 1984;311:1329-32.
8. Desai M, Mirzay-Razzaz J, von Delft D, Sarkar S, Hamilton G, Seifalian AM.. Inhibition of neointimal formation and hyperplasia in vein grafts by external stent/sheath. *Vasc Med Lond Engl* 2010;15:287-97.
9. Roubos N, Rosenfeldt FL, Richards SM, Conyers RA, Davis BB.. Improved preservation of saphenous vein grafts by the use of glyceryl trinitrate-verapamil solution during harvesting. *Circulation* 1995;92:II31-36.
10. Mitra AK, Gangahar DM, Agrawal DK. Cellular, molecular and immunological mechanisms in the pathophysiology of vein graft intimal hyperplasia. *Immunol Cell Biol* 2006;84:115-24.
11. Shukla N, Jeremy JY. Pathophysiology of saphenous vein graft failure: a brief overview of interventions. *Curr Opin Pharmacol* 2012;12:114-20.
12. De Vries MR, Niessen HWM, Löwik CWGM, Hamming JF, Jukema JW, Quax PH. Plaque rupture complications in murine atherosclerotic vein grafts can be prevented by TIMP-1 overexpression. *PLoS One* 2012;7:e47134.
13. Lardenoye JHP, de Vries MR, Löwik CWGM, Xu Q, Dhore CR, Cleutjens JP, van Hinsbergh VW, van Bockel JH, Quax PH. Accelerated atherosclerosis and calcification in vein grafts: a study in APOE*3 Leiden transgenic mice. *Circ Res* 2002;91:577-84.
14. Karper JC, de Vries MR, van den Brand BT, Hoefer IE, Fischer JW, Jukema JW, Niessen HW, Quax PH. Toll-like receptor 4 is involved in human and mouse vein graft remodeling, and local gene silencing reduces vein graft disease in hypercholesterolemic APOE*3Leiden mice. *Arterioscler Thromb Vasc Biol* 2011;31:1033-40.
15. Akashi-Takamura S, Miyake K. TLR accessory molecules. *Curr Opin Immunol* 2008;20:420-5.
16. Miyake K, Yamashita Y, Ogata M, Sudo T, Kimoto M. RP105, a novel B cell surface molecule implicated in B cell activation, is a member of the leucine-rich repeat protein family. *J Immunol* 1995;154:3333-40.
17. Divanovic S, Trompette A, Atabani SF, Madan R, Golenbock DT, Visintin A, Finberg RW, Tarakhovsky A, Vogel SN, Belkaid Y, Kurt-Jones EA, Karp CL. Negative regulation of Toll-like receptor 4 signaling by the Toll-like receptor homolog RP105. *Nat Immunol* 2005;6:571-8.
18. Zhao Y, Pennings M, Hildebrand RB, Ye D, Calpe-Berdiel L, Out R, Kjerrulf M, Hurt-Camejo E, Groen AK, Hoekstra M, Jessup W, Chimini G, Van Berkel TJ, Van Eck M. Enhanced foam cell formation, atherosclerotic lesion development, and inflammation by combined deletion of ABCA1 and SR-BI in Bone marrow-derived cells in LDL receptor knockout mice on western-type diet. *Circ Res* 2010;107:e20-31.
19. Chomczynski P, Sacchi N. Single-step method of RNA isolation by acid guanidinium thiocyanate-phenol-chloroform extraction. *Anal Biochem* 1987;162:156-9.
20. Robbins CS, Hilgendorf I, Weber GF, Theurl I, Iwamoto Y, Figueiredo JL, Gorbатов R, Sukhova GK,

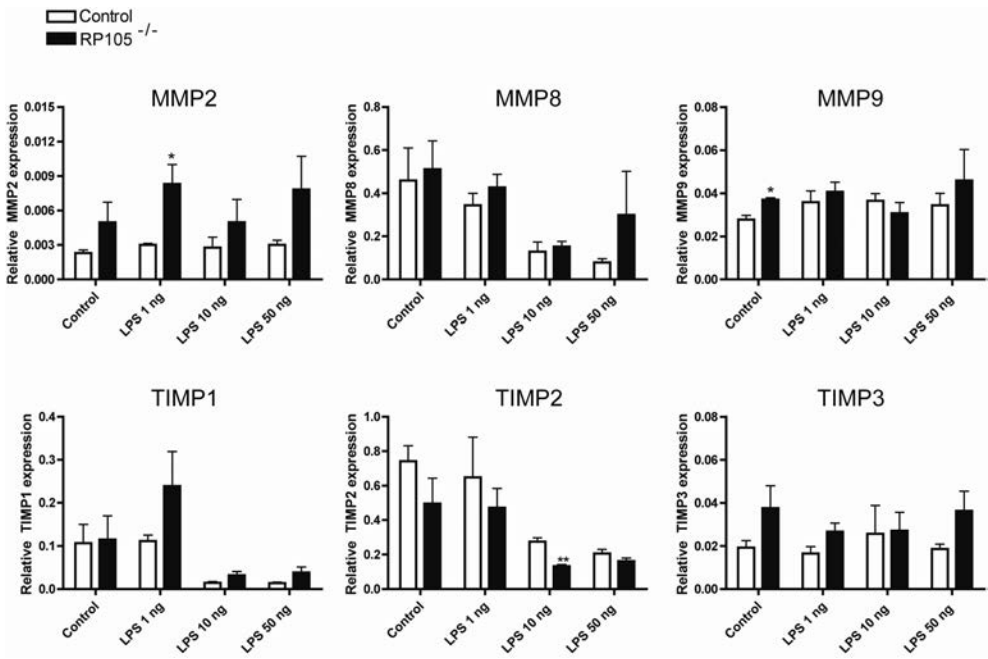
- Gerhardt LM, Smyth D, Zavitz CC, Shikatani EA, Parsons M, van Rooijen N, Lin HY, Husain M, Libby P, Nahrendorf M, Weissleder R, Swirski FK. Local proliferation dominates lesional macrophage accumulation in atherosclerosis. *Nat Med* 2013;19:1166-72.
21. Boring L, Gosling J, Cleary M, Charo IF. Decreased lesion formation in CCR2^{-/-} mice reveals a role for chemokines in the initiation of atherosclerosis. *Nature* 1998;394:894-7.
 22. De Vries MR, Wezel A, Schepers A, van Santbrink PJ, Woodruff TM, Niessen HW, Hamming JF, Kuiper J, Bot I, Quax PH. Complement factor C5a as mast cell activator mediates vascular remodelling in vein graft disease. *Cardiovasc Res* 2013;97:311-20.
 23. Bot I, de Jager SCA, Zernecke A, Lindstedt KA, van Berkel TJ, Weber C, Biessen EA. Perivascular mast cells promote atherogenesis and induce plaque destabilization in apolipoprotein E-deficient mice. *Circulation* 2007;115:2516-25.
 24. Bot I, Bot M, van Heiningen SH, van Santbrink PJ, Lankhuizen IM, Hartman P, Gruener S, Hilpert H, van Berkel TJ, Fingerle J, Biessen EA. Mast cell chymase inhibition reduces atherosclerotic plaque progression and improves plaque stability in ApoE^{-/-} mice. *Cardiovasc Res* 2011;89:244-52.
 25. Bot I, de Jager SCA, Bot M, van Heiningen SH, de Groot P, Veldhuizen RW, van Berkel TJ, von der Thüsen JH, Biessen EA. The neuropeptide substance P mediates adventitial mast cell activation and induces intraplaque hemorrhage in advanced atherosclerosis. *Circ Res* 2010;106:89-92.
 26. Rao KN, Brown MA. Mast cells: multifaceted immune cells with diverse roles in health and disease. *Ann N Y Acad Sci* 2008;1143:83-104.
 27. Lagraauw HM, Westra MM, Bot M, Wezel A, van Santbrink PJ, Pasterkamp G, Biessen EA, Kuiper J, Bot I. Vascular neuropeptide Y contributes to atherosclerotic plaque progression and perivascular mast cell activation. *Atherosclerosis* 2014;235:196-203.
 28. Den Dekker WK, Tempel D, Bot I, Biessen EA, Joosten LA, Netea MG, van der Meer JW, Cheng C, Duckers HJ. Mast cells induce vascular smooth muscle cell apoptosis via a toll-like receptor 4 activation pathway. *Arterioscler Thromb Vasc Biol* 2012;32:1960-9.
 29. Sandig H, Bulfone-Paus S. TLR signaling in mast cells: common and unique features. *Front Immunol* 2012;3:185.
 30. Rastan A, Krankenberg H, Baumgartner I, Blessing E, Müller-Hülsbeck S, Pilger E, Scheinert D, Lammer J, Gießler M, Noory E, Neumann FJ, Zeller T. Stent placement versus balloon angioplasty for the treatment of obstructive lesions of the popliteal artery: a prospective, multicenter, randomized trial. *Circulation* 2013;127:2535-41.
 31. Karper JC, Ewing MM, de Vries MR, de Jager SC, Peters EA, de Boer HC, van Zonneveld AJ, Kuiper J, Huizinga EG, Brondijk TH, Jukema JW, Quax PH. TLR accessory molecule RP105 (CD180) is involved in post-interventional vascular remodeling and soluble RP105 modulates neointima formation. *PLoS One* 2013;8:e67923.
 32. Karper JC, de Jager SC, Ewing MM, de Vries MR, Bot I, van Santbrink PJ, Redeker A, Mallat Z, Binder CJ, Arens R, Jukema JW, Kuiper J, Quax PH. An unexpected intriguing effect of Toll-like receptor regulator RP105 (CD180) on atherosclerosis formation with alterations on B-cell activation. *Arterioscler Thromb Vasc Biol* 2013;33:2810-7.
 33. Bastiaansen AJ, Karper JC, Wezel A, de Boer HC, Welten SM, de Jong RC, Peters EA, de Vries MR, van Oeveren-Rietdijk AM, van Zonneveld AJ, Hamming JF, Nossent AY, Quax PH. TLR4 Accessory Molecule RP105 (CD180) Regulates Monocyte-Driven Arteriogenesis in a Murine Hind Limb Ischemia Model. *PLoS One* 2014;9:e99882.

Supplemental data

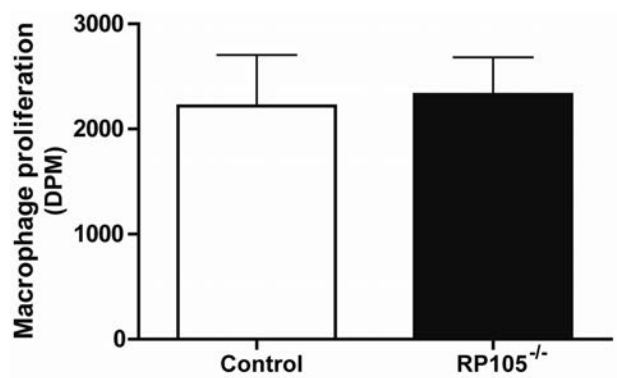
Supplemental table 1. List of primers used for the *in vitro* experiments.

Gene	Forward primer	Reversed primer
RP105	ACCATTCAAACACGACCTTCAGCAGA	GGGGATTTGCGGTTAGTACAAGTGTGT
TLR4	CCAATTTTTCAGAACTTCAGTGGCTGG	TTGAGAGGTGGTGTAAGCCATGC
MMP2	CCGAGGACTATGACCGGGATA	GGGCACCTTCTGAATTTCCA
MMP8	TGACCTCAATTCATATCTCTGTTCTG	TCATAGCCACTTAGAGCCCAGTACT
MMP9	CCCTGGAACCTCACACGACATCTTC	CTCATTTTGAAACTCACACGCCAG
TIMP1	ACACCCCAGTCATGGAAAGC	CTTAGGCGGCCCGTGAT
TIMP2	GTTTATCTACACGGCCCCCTCTT	ATCTTGCCATCTCCTTCTGCCTT
TIMP3	ACTGTGCAACTTTGTGGAGAGGT	GAGACACTCATTCTTGGAGGTCA
HPRT	TTGCTCGAGATGTCATGAAGGA	AGCAGGTCAGCAAAGAACTTATAG
β -actin	CGCCAAGCGATCCAAGATCAAGTCC	AGCTGGGTCCTGAACACATCCTTG

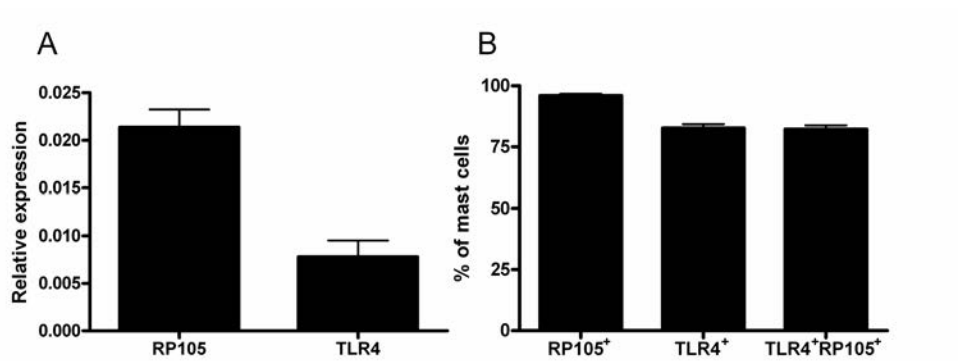
Supplemental Figure 1. Relative expression of MMPs and TIMPs in RP105 deficient and control BM derived macrophages after stimulation with 1 ng, 10 ng or 50 ng LPS, or with control medium.



Supplemental Figure 2. The cellular proliferation rate of control and RP105 deficient BM derived macrophages is unaltered under basal conditions.



Supplemental Figure 3. Bone marrow derived mast cells express RP105 and TLR4 on mRNA (A) and protein level (B).



Chapter 7

RP105 deficiency attenuates early atherosclerosis via decreased monocyte influx in a CCR2 dependent manner

Conditionally accepted by Atherosclerosis

Anouk Wezel^{1,2}
Daniël van der Velden^{1,3}
Johanna M. Maassen¹
H. Maxime Lagraauw¹
Margreet R. de Vries^{2,4}
Jacco C. Karper^{2,4}
Johan Kuiper¹
Ilze Bot¹
Paul H. A. Quax^{2,4}

¹Division of Biopharmaceutics, Gorlaeus Laboratories, Leiden Academic Center for Drug Research, Leiden University, Leiden, The Netherlands

²Department of Surgery, Leiden University Medical Center, Leiden, The Netherlands

³Department of Rheumatology, Leiden University Medical Center, Leiden, The Netherlands

⁴Eindhoven Laboratory for Experimental Vascular Medicine, Leiden, The Netherlands

Abstract

Objective: Toll-like receptor 4 (TLR4) plays a key role in inflammation and previously it was established that TLR4 deficiency attenuates atherosclerosis. Radio-Protective 105 (RP105) is a structural homolog of TLR4 and an important regulator of TLR4 signalling, suggesting that RP105 may also be an important effector in atherosclerosis. We thus aimed to determine the role of RP105 in atherosclerotic lesion development using RP105 deficient mice on an atherosclerotic background.

Methods and Results: Atherosclerosis was induced in Western-type diet fed low density lipoprotein receptor deficient ($LDLr^{-/-}$) and $LDLr/RP105$ double knockout ($LDLr^{-/-}/RP105^{-/-}$) mice by means of perivascular carotid artery collar placement. Lesion size was significantly reduced by 58% in $LDLr^{-/-}/RP105^{-/-}$ mice, and moreover, plaque macrophage content was markedly reduced by 40%. In a model of acute peritonitis, monocyte influx was almost 3-fold reduced in $LDLr^{-/-}/RP105^{-/-}$ mice, while neutrophil influx remained unaltered, suggestive of an altered migratory capacity of monocytes upon deletion of RP105. Interestingly, *in vitro* stimulation of monocytes with LPS induced a downregulation of CCR2, a chemokine receptor crucially involved in monocyte influx to atherosclerotic lesions, which was more pronounced in $LDLr^{-/-}/RP105^{-/-}$ monocytes as compared to $LDLr^{-/-}$ monocytes.

Conclusion: We here show that RP105 deficiency results in reduced early atherosclerotic plaque development with a marked decrease in lesional macrophage content, which may be due to disturbed migration of RP105 deficient monocytes resulting from CCR2 downregulation.

Introduction

Atherosclerotic lesions in the large and medium sized arteries are the major cause of cardiovascular events and complications worldwide¹. It has been well established that inflammation plays a key role in the initiation, growth and rupture of an atherosclerotic plaque²⁻⁵. Early steps in this process involve the adhesion of monocytes to dysfunctional endothelium, where they subsequently migrate into the vessel wall and take up oxidized LDL⁶. Influx of additional inflammatory cells from both the innate and adaptive immune system, such as dendritic cells, T cells and mast cells, further aggravates lesion formation^{7,8}.

Toll-like receptors (TLRs) are the primary receptors of the innate immune system: they recognize highly conserved molecular motifs called pathogen associated molecular patterns (PAMPs) as well as endogenous damage-associated molecular patterns (DAMPs)^{9,10}. TLR4, one of the most characterized receptors of the TLR family, has been subjected to extensive research regarding its role in atherosclerosis. Atherosclerosis-prone mice deficient for TLR4 develop smaller atherosclerotic lesions¹¹, while also antagonism of TLR4 results in reduced early lesion formation¹². RadioProtective 105 (RP105) is a TLR homologue capable of regulating TLR4 signalling. RP105 is structurally similar to TLR4, but lacks the intracellular Toll Interleukin Receptor (TIR) signalling domain. Originally, RP105 was described as a B cell specific molecule, able to drive cellular proliferation and to enhance B cell dependent inflammatory processes^{13,14}. However, additional research revealed that the expression of RP105 on antigen presenting cells directly mirrors that of TLR4, in which it acts as a negative regulator. Consequently, LPS injection in RP105 deficient mice results in an exaggerated inflammatory response¹⁵, and the inhibitory effect of RP105 on TLR4 responses is thought to be exerted via a direct extracellular interaction with TLR4^{16,17}.

Because of the opposite regulatory role that RP105 seems to play in different cell types, it is compelling to study the effect of RP105 deficiency in inflammatory diseases including atherosclerotic vascular remodelling. Previously, we have demonstrated that in a hyperlipidemic setting, lethally irradiated mice receiving RP105^{-/-} bone marrow display an unexpected decrease in plaque size. This reduction in atherosclerosis was mainly explained by decreased B cell activation, proliferation and immunoglobulin production¹⁸. These data would suggest that deficiency of RP105 is a novel route via which atherosclerosis can be inhibited. However, we have also shown that lack of RP105 results in increased neointima formation in a mouse model for damage induced post-interventional vascular remodelling¹⁹. Smooth muscle cells deficient for RP105 display increased proliferation following LPS stimulation, which may explain the increase in neointima formation. These opposing roles of RP105 on smooth muscle cells and B cells make it difficult to conclude on the effect of total body RP105 deficiency on atherosclerosis, since

both cell types are known to contribute to lesion formation. Therefore, it remains to be studied whether the contribution of RP105 mediated smooth muscle cell proliferation or RP105 dependent changes in leukocyte function play a more pre-dominant role in atherosclerosis.

In the current study we thus aim to investigate what the effect of total body RP105 deficiency is on atherosclerosis. Also, we determined how RP105 expression is regulated during the process of atherosclerotic lesion formation.

Material and Methods

Mouse atherosclerosis time course

All animal work was approved by the animal welfare committee of the Leiden University Medical Center and mice were bred in our facility at the Gorlaeus Laboratories (Leiden, the Netherlands). For the generation of a mouse atherosclerosis time course, male $LDLr^{-/-}$ were fed a Western type diet (0.25% cholesterol and 15% cacao butter, SDS, Sussex, UK) starting two weeks before surgery and throughout the experiment. Mice were anaesthetized by subcutaneous injection of ketamine (60 mg/kg, Eurovet Animal Health, Bladel, The Netherlands), fentanyl citrate and fluanisone (1.26 mg/kg and 2 mg/kg respectively, Janssen Animal Health, Sauterton, UK). All mice received perivascular collars around the carotid artery to induce plaque formation as previously described²⁰. In brief, a semi-constrictive collar was placed around both carotid arteries of the mice two weeks after start of the Western type diet. Disturbed flow at the proximal site of the collar results in endothelial activation with subsequent atherosclerotic lesion formation.

Gene expression profiles of carotid artery plaques in $LDLr^{-/-}$ mice were determined at 0 to 8 weeks after perivascular collar placement. Hereto, a subset of mice was sacrificed at the time points indicated below. Fixation through the left cardiac chamber was performed with phosphate-buffered saline (PBS). Subsequently, both common carotid arteries were excised and snap-frozen in liquid nitrogen for optimal RNA preservation. A schematic overview of the mouse atherosclerosis time course is depicted in Suppl. Figure 1A. For RNA isolation, two to three carotid artery segments carrying the plaque from 0,2,4,6, or 8 weeks after collar placement were pooled for each sample and homogenized by grounding in liquid nitrogen with a pestle. Of each time point, three samples of pooled carotids were obtained for RNA extraction. Total RNA was extracted from the tissue homogenates using Trizol reagent according to manufacturer's instructions (Invitrogen, Breda, The Netherlands). Gene expression levels were determined using an Illumina Bead-Chip Whole Genome Microarray (ServiceXS, Leiden, The Netherlands).

Atherosclerosis in $LDLr^{-/-}/RP105^{-/-}$ versus $LDLr^{-/-}$ mice

$RP105^{-/-}$ mice were kindly provided by K. Miyake (Tokyo University, Japan) and were described previously²¹. Male $LDLr^{-/-}$ (n=12) and male $LDLr^{-/-}/RP105^{-/-}$ mice ($LDLr^{-/-}$ background, backcrossed for more than 10 generations) (n=12) bred in our laboratory (Gorlaeus Laboratories), were fed a Western type diet throughout the experiment. After two weeks of diet feeding, body weight was measured and plasma total cholesterol levels were determined by incubation with 0.025 U/ml cholesterol oxidase (Sigma, Zwijndrecht, The Netherlands) and 0.065 U/ml peroxidase and 15 µg/mL cholesterol esterase (Roche Diagnostics, Mannheim, Germany) in polyoxyethylene-9-laurylether, and 7.5% methanol). Precipath was used as an internal standard (standardized serum; Boehringer, Mannheim, Germany) and absorbance was read at 490 nm. At that time-point, mice were anaesthetized and collars were placed as described in the previous section, after which lesions were allowed to develop for another four weeks (schematic overview in Suppl. Figure 1B). At sacrifice, four weeks after collar placement, *in situ* fixation through the left cardiac

chamber was performed, after which carotid artery lesion size and morphology were analyzed.

Histology and morphometry

Paraffin embedded carotid plaques were cut in sections of 5 μm thick and stained with hematoxylin-phloxine-saffron (HPS) to determine lesion size. (Immuno)histochemical staining were performed for macrophages (MAC3;1:200;BD-Pharmingen, San Diego, USA), alpha smooth muscle cell actin (1:1000;Sigma), collagen (picosirius red staining) and CCR2 (1:400;Abcam, Cambridge, UK). An enzymatic staining (CAE, Sigma) was used for visualizing mast cells.

Morphometric analysis (Leica Qwin image-analysis software) was performed at site of maximal stenosis. (Immuno)histochemical stainings were quantified by computer assisted analysis (Leica, Qwin, Cambridge, UK) and expressed as the percentage of positive stained area of the total intimal area. Perivascular mast cells were counted manually and scored as either resting when all granula were inside the cell, or activated when granula were deposited in the tissue surrounding the mast cell.

Flow cytometry

At sacrifice, blood was collected and peritoneal cells were isolated ($n=5/\text{group}$) by flushing the peritoneal cavity with 10 mL PBS. Erythrocytes were removed using an erythrocyte lysis buffer (pH 7.3). Blood cells were stained with CD11b;Ly6C;Ly6G to determine the amount of neutrophils and monocytes. CD4;CD8;CD25;CD19 antibodies were used to detect T and B cells. Peritoneal cells were stained to analyze B cells (CD19⁺), B cell subsets (B1 cells: CD5⁺;CD4⁺;IgM⁺, and B2 cells: IgM⁺;IgD⁺, both calculated as a percentage of CD19⁺ cells), and mast cells (CD117;IgE;FcγR;FcεRI). FACS analysis was performed on a FACSCantoII (BD-Biosciences, San Jose, USA) and data were analyzed using FACSDiva software.

Serum immunoglobulin detection and MCP-1 levels

IgM, IgG1 and IgG2a levels in serum were detected with the use of a mouse immunoglobulin isotyping ELISA kit according to manufacturer's protocol (BD Biosciences). Total IgE in serum was determined by a mouse IgE quantitative ELISA (Bethyl Laboratories, Montgomery, USA). To detect MCP-1 in serum an ELISA was performed according to manufacturer's protocol (BD-Biosciences).

In vivo influx to peritoneum

LDLr^{-/-}/RP105^{-/-} and LDLr^{-/-} mice ($n=5/\text{group}$) were injected intra-peritoneal with 1 mL 3% Brewer's thioglycollate (Difco) or 1 mL PBS as a control. Five days after injection the peritoneal cavity was flushed with 10 mL PBS, cells were centrifuged for 5 minutes at 1500 rpm and resuspended in 1 mL PBS. Flow cytometry was used to analyze monocyte numbers (CD11b;Ly6G;Ly6C), monocyte chemokine receptor expression (CD11b;CCR2;CX3CR1) and macrophages numbers (F4/80;CD40;CD80). FACS analysis was performed on a FACSCantoII (BD-Biosciences) and data were analyzed using FACSDiva software.

Cell culture

Bone marrow (BM) derived monocytes were isolated and differentiated as described previously²². In brief, BM was isolated by flushing femurs and tibias with PBS. Cells were cultured for 5 days in RPMI 1640 medium supplemented with 10% FCS, 2 mmol/L l-glutamine, 100 U/mL penicillin and 100 $\mu\text{g}/\text{mL}$ streptomycin and 20 ng/mL recombinant murine M-CSF (eBioscience, San Diego, USA) to generate BM-derived monocytes. After 5 days, non-adherent cells were harvested and analyzed by FACS for CD11b and Ly6C expression to determine monocyte purity, which reached approximately 84%.

BM derived monocytes (10^6 cells) were stimulated with LPS (1 or 10 ng/mL, from E. Coli, Sigma) or control medium overnight at 37°C, after which cells were harvested for RNA isolation.

For FACS analysis of CCR2 and CCR5 expression on monocytes, cells were stimulated for 2 hours with LPS

(1 or 10 ng /mL) and stained with antibodies for CD11b;Ly6C;CCR2;CCR5.

RNA isolation and cDNA synthesis

RNA was isolated using a standard TRIzol-chloroform extraction protocol after which RNA was examined by nanodrop (Nanodrop® Technologies). Relative quantitative mRNA PCR was performed on reverse transcribed cDNA using Taqman gene expression assays and qPCRs were run on a 7900HT Fast Real-Time PCR System (Applied Biosystems, Foster City, USA). The relative expression of CCR2, CCR5, CCR1 and CX3CR1 was determined using the murine housekeeping genes HPRT, RPL27, B-actin (Suppl. table 1).

Statistical analysis

Data are expressed as mean \pm SEM. A 2-tailed Student's t-test was used to compare individual groups. The *in vivo* influx study was analyzed by performing a one-way ANOVA, followed by a Tukey's multiple comparison test. Non-parametric data were analyzed using a Mann-Whitney U test. $P < 0.05$ was considered significant.

Results

RP105 deficiency results in reduced plaque size

During atherosclerosis, RP105 was seen to be significantly upregulated during early lesion development, which directly mirrors the upregulation of TLR4 expression (Suppl. Figure 2A). In order to investigate the effect of RP105 deficiency on early atherosclerosis, $LDLr^{-/-}$ /RP105 $^{-/-}$ mice and $LDLr^{-/-}$ mice on a high fat diet received perivascular collars around the carotid arteries. Weight and cholesterol levels did not differ between the groups (Figure 1A). FACS analysis of the blood at sacrifice revealed no changes in the percentage of monocytes (CD11b $^{+}$ Ly6G low cells), neutrophils (CD11b $^{+}$ Ly6G high cells) or in the percentage of B cells (CD19 $^{+}$ cells) (Figure 1B).

Analysis of plaque size, using hematoxylin-phloxine-saffron (HPS) stained sections, revealed a marked decrease in atherosclerotic lesion formation in the RP105 deficient mice ($LDLr^{-/-}$: $20.66 \pm 4.7 \times 10^3 \mu m^2$; $LDLr^{-/-}$ /RP105 $^{-/-}$: $8.7 \pm 2.3 \times 10^3 \mu m^2$; $P < 0.05$; Figure 1C). Medial thickness remained unaltered between the two groups ($LDLr^{-/-}$: $55.0 \pm 2.8 \times 10^3 \mu m^2$; $LDLr^{-/-}$ /RP105 $^{-/-}$: $49.6 \pm 3.6 \times 10^3 \mu m^2$; $P = 0.25$).

Lesional macrophages are decreased in $LDLr^{-/-}$ /RP105 $^{-/-}$ mice

Plaque composition was further analyzed by staining for smooth muscle cells, collagen content, mast cells, and macrophages. The percentage of intimal smooth muscle cells of total plaque area was not affected by RP105 deficiency ($LDLr^{-/-}$: $11.1\% \pm 2.6\%$; $LDLr^{-/-}$ /RP105 $^{-/-}$: $18.9\% \pm 3.8\%$; Figure 2A) and also, Sirius red staining revealed no differences in relative collagen content ($LDLr^{-/-}$: $16.2\% \pm 1.9\%$; $LDLr^{-/-}$ /RP105 $^{-/-}$: $17.8\% \pm 1.6\%$; Figure 2B). The number of mast cells in the perivascular tissue and their activation status, as measured by the amount

of granules present in the vicinity of the cell, did not differ between the groups (Figure 2C,D). However, we observed a profound 40% decrease in lesional macrophage content (as percentage of total plaque area, $LDLr^{-/-}$: $26.0\% \pm 3.7\%$; $LDLr^{-/-}/RP105^{-/-}$: $15.6\% \pm 2.3\%$; $P < 0.05$; Figure 2E). Interestingly, RP105 expression in the atherosclerosis time course was seen to increase mostly during the first two weeks after collar placement, which was highly comparable to the expression patterns of monocyte/macrophage markers during lesion development (Suppl. Figure 2B), suggesting that intra-lesional RP105 is predominantly monocyte/macrophage derived.

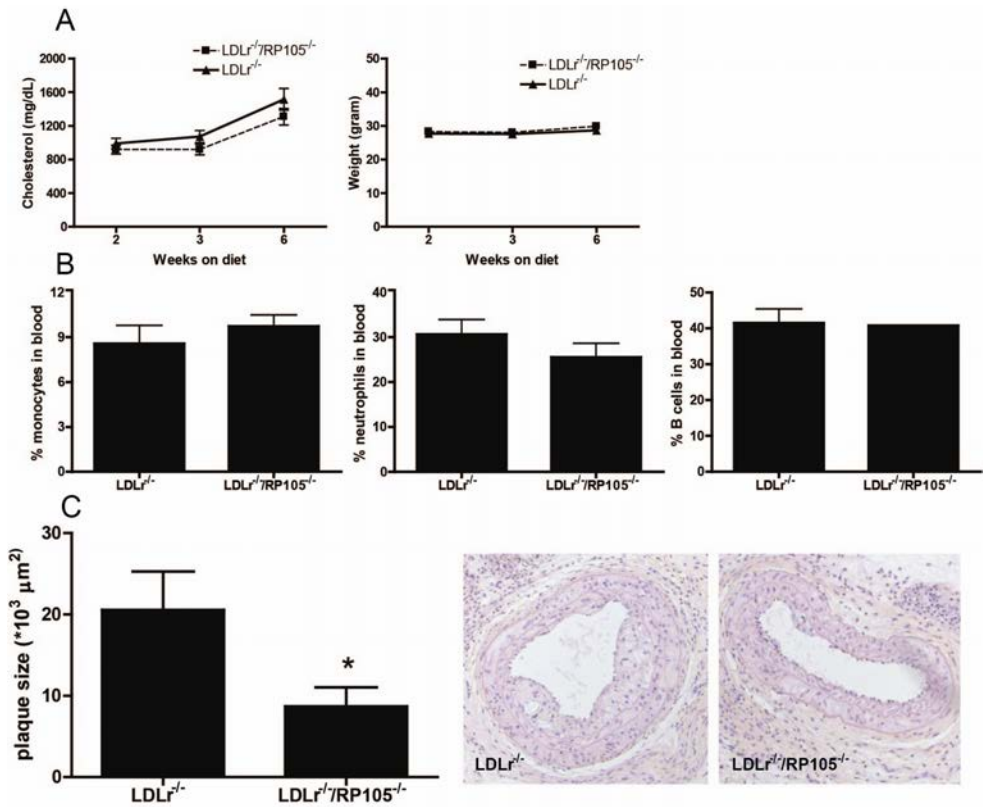


Figure 1. RP105 deficiency results in reduced plaque size. After 2, 3 and 6 weeks of diet, no changes were seen in cholesterol levels and weight between $LDLr^{-/-}/RP105^{-/-}$ mice and $LDLr^{-/-}$ control mice (A). FACS analysis of the blood at time of sacrifice revealed no changes in monocytes ($CD11b^{+};Ly6G^{low}$), neutrophils ($CD11b^{+};Ly6G^{high}$) or B cells ($CD19^{+}$) between $LDLr^{-/-}/RP105^{-/-}$ mice and control $LDLr^{-/-}$ mice (B). Plaque size was significantly reduced in $LDLr^{-/-}/RP105^{-/-}$ mice compared to $LDLr^{-/-}$ mice (C). Micrographs show representative images of each group (100x). $N = 12$ mice/group. $*P < 0.05$. A 2-tailed Student's *t*-test was used to compare individual groups.

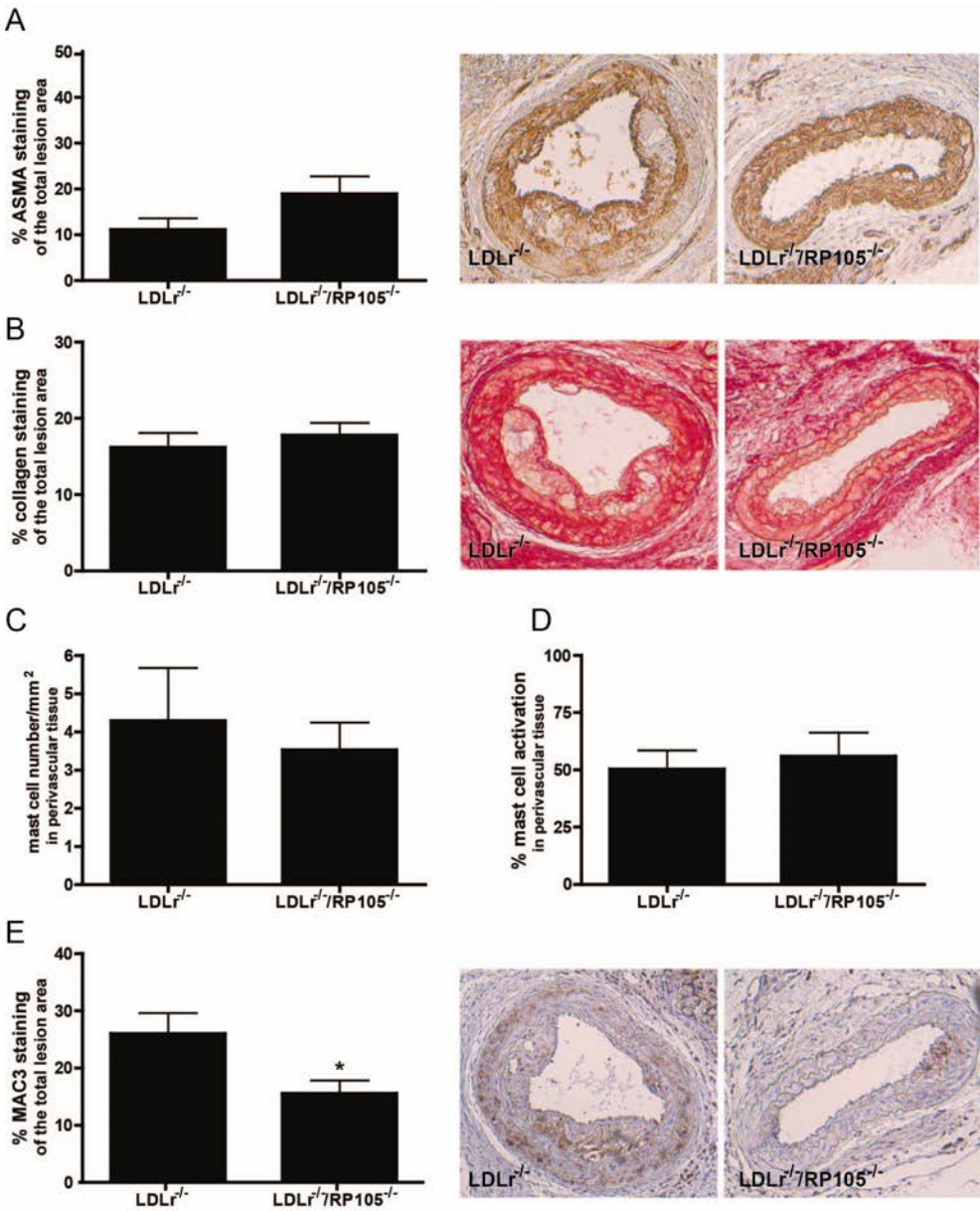


Figure 2. Lesional macrophages are decreased in LDLr^{-/-}/RP105^{-/-} mice. Plaque morphology was analyzed by staining for macrophages, collagen, smooth muscle cells and mast cells. No differences were found between the percentage of smooth muscle cells (ASMA, A), collagen content (Sirius Red, B), or perivascular mast cell numbers and activation status (C,D). Macrophage content in LDLr^{-/-}/RP105^{-/-} mice was significantly reduced compared to LDLr^{-/-} mice (MAC3, E). Micrographs show representative images of both groups (100x). N=12 mice/group. *P<0.05. A 2-tailed Student's t-test was used to compare individual groups.

Decrease in peritoneal B cells and reduction in plasma IgE and IgM levels

Since RP105 deficiency has been described to affect B cell activation and proliferation²³, we further analyzed the percentage and subpopulations of B cells in the peritoneum by FACS analysis. The percentage of B cells (CD19⁺ cells) was significantly decreased in mice deficient for RP105 (LDLr^{-/-}: 68.1%±3.6%; LDLr^{-/-}/RP105^{-/-}: 51.4%±4.1%; P<0.05; Figure 3A). B cell subsets, determined as a percentage of the total B cell population, did not differ between the groups (Figure 3B,C). Also, mast cell content did not differ (Figure 3D). RP105 deficiency markedly reduced plasma IgE and IgM levels, while not affecting plasma IgG1 or IgG2a concentrations (Figure 3E-H).

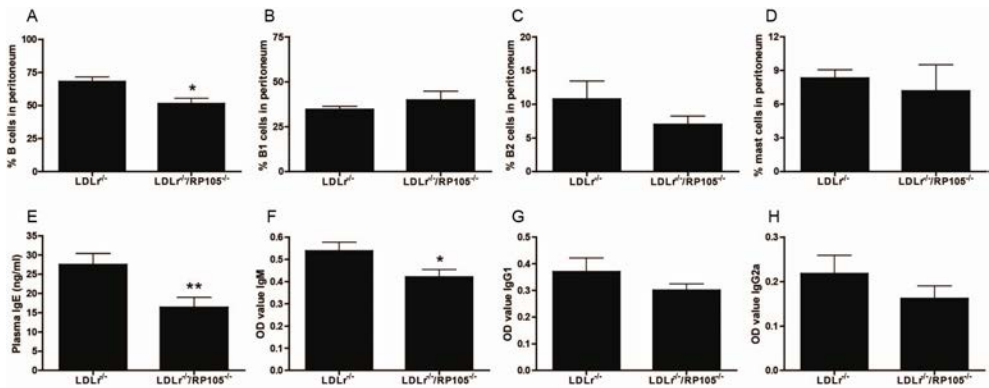


Figure 3. Decrease in peritoneal B cells and reduction in plasma IgE and IgM levels. B cells in the peritoneum (CD19⁺) were significantly decreased in LDLr^{-/-}/RP105^{-/-} mice compared to LDLr^{-/-} mice (A). No changes were observed between the percentage of peritoneal B1 cells (percentage of CD5⁺CD4⁺IgM⁺ cells within CD19⁺ cells) (B) and B2 cells (percentage of IgM⁺IgD⁺ cells within CD19⁺ cells) (C). The percentage of mast cells in the peritoneum did not differ between the two groups (D). A significant reduction of plasma IgE (E) and IgM (F) was detected in LDLr^{-/-}/RP105^{-/-} mice at time of sacrifice, while no changes were seen in IgG1 (G) or IgG2a (H) levels. N=12 mice/group. *P<0.05, **P<0.01. A 2-tailed Student's t-test was used to compare individual groups.

In vivo migration is impaired in RP105 deficient monocytes

In order to elucidate the mechanism behind the decreased amount of lesional macrophages found *in vivo*, we aimed to investigate whether monocyte migration was disturbed in mice lacking RP105. Monocyte influx to the peritoneum was measured after thioglycollate injection in LDLr^{-/-} and LDLr^{-/-}/RP105^{-/-} mice by staining for CD11b⁺Ly6G⁻ cells. Interestingly, monocyte migration in RP105 deficient mice is markedly disturbed compared to LDLr^{-/-} mice as revealed by FACS analysis (LDLr^{-/-}: 31.3±1.3 fold increased influx; LDLr^{-/-}/RP105^{-/-}: 11.9±3.7 fold increased influx; P<0.001; Figure 4A). Concomitantly, a decrease in the percentage of CCR2 positive monocytes was observed in LDLr^{-/-}/RP105^{-/-} mice P<0.05; Figure 4B). No changes were detected in neutrophil influx (Figure 4C).

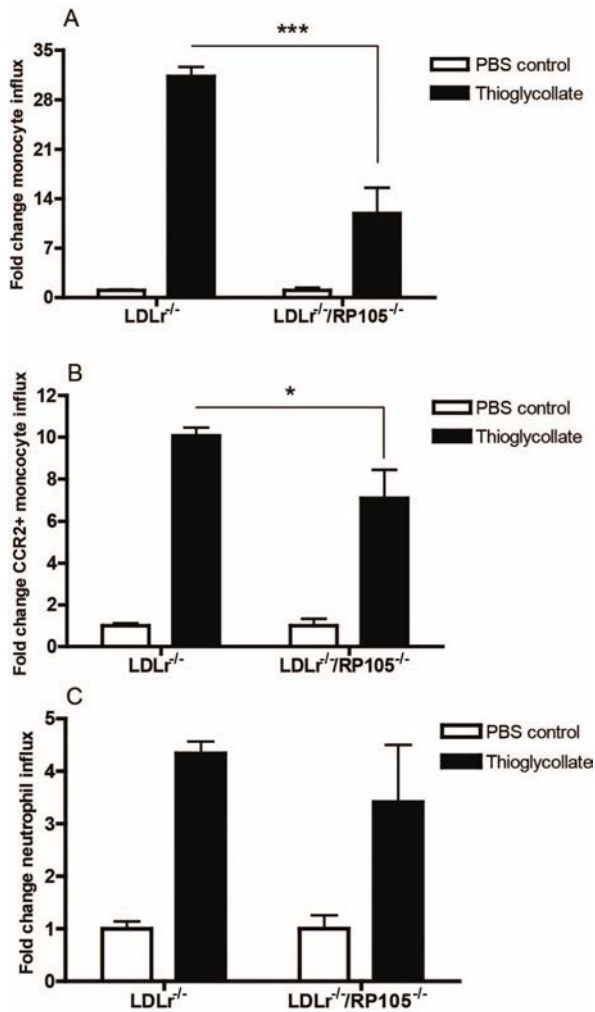


Figure 4. In vivo migration is impaired in *LDLr*^{-/-}/*RP105*^{-/-} monocytes. FACS analysis showed a significant reduction of monocyte influx to the peritoneum in *LDLr*^{-/-}/*RP105*^{-/-} mice compared to *LDLr*^{-/-} mice after intra-peritoneal injection of thioglycollate, depicted as a fold change compared to PBS injection (A). Also, decreased influx of CCR2⁺ monocytes was observed in *LDLr*^{-/-}/*RP105*^{-/-} mice (B). No changes were found in the relative influx of neutrophils (C). N=5 mice/group. *P<0.05 compared to thioglycollate treated *LDLr*^{-/-} mice. ***P<0.001 compared to thioglycollate treated *LDLr*^{-/-} mice. A one-way ANOVA was performed, followed by a Tukey's multiple comparison test.

Decrease of CCR2⁺ *LDLr*^{-/-}/*RP105*^{-/-} monocytes after LPS activation in vitro

To further investigate the effects of *RP105* deficiency on monocyte migration we observed *in vivo*, we determined the expression of chemokine receptors CCR2 and CCR5 on bone marrow derived monocytes *in vitro*. FACS analysis showed an increased percentage of CCR2⁺ positive *LDLr*^{-/-}/*RP105*^{-/-} monocytes compared to *LDLr*^{-/-} monocytes when unstimulated. However, after stimulation with 1 or 10 ng LPS, a significant dose-dependent decrease in the percentage of CCR2⁺ cells was observed in the *LDLr*^{-/-}/*RP105*^{-/-} monocyte population, which did not occur in *LDLr*^{-/-} monocytes (Figure 5A). Moreover, after stimulation with 10 ng LPS, the percentage of CCR2⁺ *LDLr*^{-/-}/*RP105*^{-/-} monocytes was significantly reduced compared to *LDLr*^{-/-} monocytes. The percentage of CCR5 positive *LDLr*^{-/-}/*RP105*^{-/-} monocytes was increased compared to monocytes from *LDLr*^{-/-} mice, also after stimulation

with 1 ng LPS. However 10 ng LPS stimulation did not result in changes between the two groups (Figure 5B).

Expression of CCR2 at mRNA level after LPS stimulation showed a decrease in both $LDLr^{-/-}$ and $LDLr^{-/-}/RP105^{-/-}$ monocytes, however this decrease was more pronounced in $LDLr^{-/-}/RP105^{-/-}$ monocytes (Figure 5C). After stimulation with 1 ng LPS, CCR2 expression was significantly decreased in $LDLr^{-/-}/RP105^{-/-}$ monocytes compared to $LDLr^{-/-}$ monocytes. Stimulation with 10 ng LPS resulted in such a strong reduction of CCR2 expression that no significant differences were detectable any more between the two groups. We have measured the expression of CCR1, CCR5 and CX3CR1 in *in vitro* cultured $LDLr^{-/-}$ and $LDLr^{-/-}/RP105^{-/-}$ monocytes as well, which did not show a similar downregulation after LPS stimulation as CCR2 (Suppl. Figure 3). CX3CR1 gene expression is somewhat reduced in $LDLr^{-/-}/RP105^{-/-}$ monocytes, suggesting that RP105 deficiency may affect this chemokine receptor as well, however not to the extent of CCR2.

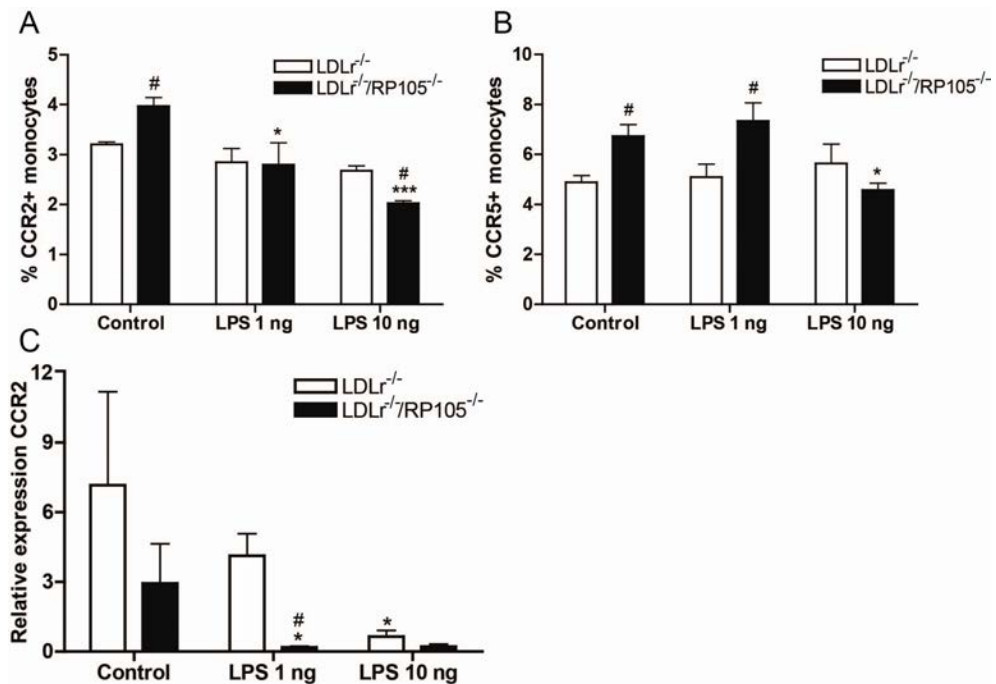


Figure 5. Decrease in CCR2⁺ $LDLr^{-/-}/RP105^{-/-}$ monocytes after LPS activation *in vitro*. FACS analysis of *in vitro* cultured $LDLr^{-/-}/RP105^{-/-}$ monocytes stimulated with 1 or 10 ng LPS revealed a significant dose-dependent decrease in the percentage of CCR2⁺ RP105 deficient monocytes. After stimulation with 10 ng LPS, the percentage of CCR2⁺ monocytes was significantly reduced in $LDLr^{-/-}/RP105^{-/-}$ monocytes compared to control $LDLr^{-/-}$ monocytes (A). The percentage of CCR5⁺ $LDLr^{-/-}/RP105^{-/-}$ monocytes was increased compared to $LDLr^{-/-}$ monocytes in the unstimulated control and after stimulation with 1 ng LPS stimulation, 10 ng LPS stimulation did not result in changes between the two groups (B). LPS stimulation decreased the relative CCR2 expression in both $LDLr^{-/-}$ and $LDLr^{-/-}/RP105^{-/-}$ monocytes; however, after stimulation with 1 ng LPS, CCR2 expression was significantly decreased in $LDLr^{-/-}/RP105^{-/-}$ monocytes compared to $LDLr^{-/-}$ monocytes (C). N=4. [#]P<0.05 compared to $LDLr^{-/-}$ monocytes; ^{*}P<0.05 compared to unstimulated monocytes; ^{***}P<0.001 compared to unstimulated monocytes. A 2-tailed Student's t-test was used to compare individual groups.

CCR2 expression in atherosclerotic plaques

Atherosclerotic plaques of LDLr^{-/-} and LDLr^{-/-}/RP105^{-/-} mice were stained for CCR2 to determine whether expression of this chemokine receptor within the lesion is altered by RP105 deficiency. No significant differences were observed in CCR2 staining (as percentage of intimal area) between the LDLr^{-/-}/RP105^{-/-} and LDLr^{-/-} mice (LDLr^{-/-}: 29.9%±4.2%; LDLr^{-/-}/RP105^{-/-}: 21.6%±2.5%; P=0.1; Suppl. Figure 4). To determine whether RP105 deficiency affected circulating levels of MCP-1, one of the most important ligands for CCR2, we analyzed plasma MCP-1 levels in LDLr^{-/-} and LDLr^{-/-}/RP105^{-/-} mice at time of sacrifice. We did not observe any changes between the two groups (Suppl. Figure 5).

Discussion

The current study is the first to demonstrate that expression of RP105 is upregulated early in atherogenesis, as shown in the time course experiment, and that total body RP105 deficiency attenuates early atherosclerotic lesion formation via decreased monocyte influx. Also, we show that LPS stimulation of RP105 deficient monocytes results in a downregulation of the chemokine receptor CCR2, which may be the cause of the observed reduction in migratory capacity of RP105 deficient monocytes.

In the current study, the most prominent finding is a 40% reduction in lesional macrophage content in LDLr^{-/-}/RP105^{-/-} mice resulting in reduced lesion development as compared to LDLr^{-/-} controls, fuelling the hypothesis that a disturbed monocyte influx into the vessel wall underlies the reduction in atherosclerosis in LDLr^{-/-}/RP105^{-/-} mice. Indeed, influx of LDLr^{-/-}/RP105^{-/-} monocytes into the peritoneum was significantly decreased compared to LDLr^{-/-} monocytes. *In vitro*, the percentage of CCR2⁺ LDLr^{-/-}/RP105^{-/-} monocytes was significantly reduced after LPS stimulation, while the relative expression of CCR2 on LDLr^{-/-}/RP105^{-/-}, as compared to LDLr^{-/-} monocytes, was also significantly reduced. These results indicate that CCR2 may be one of the chemokine receptors involved in decreased monocyte migration in LDLr^{-/-}/RP105^{-/-} mice, which leads to the decrease in early lesion formation with reduced macrophage content observed *in vivo*^{24,25}. In addition, future research may point to regulation of other chemokine receptors in RP105 deficient monocytes as well.

Previously, we have shown that lethally irradiated atherosclerosis prone LDLr^{-/-} mice receiving RP105^{-/-} bone marrow display reduced lesion development, in which the atheroprotective effects were attributed to a reduction in B cell numbers, and in particular of B2 cells¹⁸. However, in that study, leukocyte specific RP105 deficiency was investigated, thereby excluding effects that RP105 deficiency may have on non-myeloid cells, such as on vascular smooth muscle cells. In fact, it

has also been previously established that RP105 deficiency results in increased neointima formation via enhanced smooth muscle cell proliferation¹⁹. Therefore, in the current study, we aimed to investigate total body RP105 deficiency, in order to take into account the effects of both myeloid and non-myeloid deletion of RP105. Our results indicate that smooth muscle cell derived RP105 does not significantly impact atherosclerotic lesion development, as smooth muscle cell and collagen staining failed to show any significant changes between plaques of LDLr^{-/-} and LDLr^{-/-}/RP105^{-/-} mice. Similar to the previous study we observed a decrease in B cells; however, this was not as prominent and the ratio between B cell subsets remained unaltered. This reduction of B cells observed in the current study is reflected by decreased levels of total plasma IgE and IgM. Previous studies have shown that B cells are hardly present within the atherosclerotic plaque or perivascular tissue²⁶, suggesting that effects B cells can have on the plaque may be predominantly systemically or indirect. For example, it has been described that IgM specific for oxLDL may be atheroprotective by limiting accumulation of apoptotic cells and inhibiting inflammatory gene expression²⁷. In the present study we measured only total IgM, instead of oxLDL specific IgM and therefore, in this experimental setup, it remains unclear whether the observed reduction of total plasma IgM contributed to lesion formation.

Influx of monocytes at predisposed areas into the vessel wall is considered an important initial step in atherosclerosis³⁻⁵. Suppression of monocyte recruitment in atherogenesis has been shown to result in reduced plaque size and altered plaque composition, however, these effects were not seen when monocytes were reduced in late stage atherosclerosis, stressing the importance of monocyte influx in early atherogenesis²⁸. Intriguingly, we have recently found that RP105 deficient monocytes display signs of increased activation and disturbed migration towards the adductor muscle in hind limb ischemia²⁹. This led to the hypothesis that disturbed monocyte migration into the vessel wall in LDLr^{-/-}/RP105^{-/-} mice may be the cause of decreased atherosclerotic lesion formation observed in the current study. Monocyte migration occurs via the well-known chemokine receptors CCR1, CCR2, CCR5 and CX3CR1^{16,30}. Already 15 years ago it has been shown that lesion development in apoE^{-/-} mice deficient for the C-C chemokine receptor CCR2 is markedly decreased, demonstrating an important role of CCR2 in atherosclerosis^{25,26,31,32}. Interestingly, activation of monocytes via the TLR4 route has been shown to downregulate chemokine receptors, in particular CCR2³³⁻³⁶. In the current study, we have also demonstrated that stimulation of monocytes with LPS, the most important activator of TLR4, decreases both the percentage of CCR2 positive monocytes as well as the relative expression of CCR2. Intriguingly, this effect was more pronounced in monocytes deficient for RP105. RP105 is thought to act as a negative regulator in dendritic cells and macrophages via direct interaction with TLR4 on the cell membrane¹⁶. RP105 expression has shown to inhibit

TLR4-driven NF- κ B transactivation and IL-8 production by HEK293, while lack of RP105 results in increased activation and cytokine release³⁷. Therefore, we speculate that the more pronounced decrease of CCR2 in RP105 deficient monocytes may be due to increased signalling via the TLR4 route.

CCR2 staining in the atherosclerotic plaques was not significantly reduced in LDLr^{-/-}/RP105^{-/-} mice as compared to LDLr^{-/-} mice, despite changes in CCR2 expression in LDLr^{-/-}/RP105^{-/-} monocytes. Apart from the difficulty to detect subtle differences in protein expression levels by immunohistochemistry, this may also be due to the fact that monocytes, once arrived in the plaque, differentiate into macrophages and thereby alter expression of receptors, and in particular of chemokine receptors³⁸. CCR2 expression may thus be altered on LDLr^{-/-}/RP105^{-/-} monocytes, but upon arrival in the vessel wall and subsequent differentiation, these changes in chemokine receptor expression become less pronounced. Further research is aimed at the elucidation of mechanisms causing disturbed CCR2 expression upon RP105 deficiency in atherosclerosis and other inflammatory disorders.

In conclusion, we here show that LDLr^{-/-}/RP105^{-/-} mice develop reduced early atherosclerotic plaques with a marked decrease in lesional macrophages. Our data suggest that this is due to disturbed migration of RP105 deficient monocytes, caused by a downregulation of CCR2.

Conclusions

In this study, we found a significant upregulation of RP105 expression in early atherogenesis. Total body RP105 deficiency in LDLr^{-/-}/RP105^{-/-} mice resulted in a marked reduction of atherosclerotic lesion size, compared to control LDLr^{-/-} mice. No changes were observed in the smooth muscle cell percentage in the plaque; however, macrophage content was significantly reduced in LDLr^{-/-}/RP105^{-/-} mice. We deliver *in vivo* experimental proof that monocyte migration is reduced in RP105 deficient mice, which may explain the reduction in lesional macrophages. Furthermore, *in vitro* investigations show that this decreased migratory capacity may be due to a more pronounced downregulation of CCR2 in LDLr^{-/-}/RP105^{-/-} monocytes compared to LDLr^{-/-} monocytes, after LPS stimulation. These data may thus provide a novel mechanism via which RP105 deficiency may attenuate atherosclerosis.

Funding

This work was supported by grants from the Dutch Heart Foundation (A.W.:2010B029 and H.M.L.:2010B244). D.v.d.V. was financed by the LCTD3 program. We acknowledge the support from the Netherlands CardioVascular Research Initiative: "the Dutch Heart Foundation, Dutch Federation of University Medical Centres, the Netherlands Organisation for Health Research and Development and the Royal Netherlands Academy of Sciences" for the GENIUS project

“Generating the best evidence-based pharmaceutical targets for atherosclerosis” (CVON2011-19).

References

1. Roger VL, Go AS, Lloyd-Jones DM, Benjamin EJ, Berry JD, Borden WB, Bravata DM, Dai S, Ford ES, Fox CS, Fullerton HJ, Gillespie C, Hailpern SM, Heit JA, Howard VJ, Kissela BM, Kittner SJ, Lackland DT, Lichtman JH, Lisabeth LD, Makuc DM, Marcus GM, Marelli A, Matchar DB, Moy CS, Mozaffarian D, Mussolino ME, Nichol G, Paynter NP, Soliman EZ, Sorlie PD, Sotoodehnia N, Turan TN, Virani SS, Wong ND, Woo D, Turner MB; American Heart Association Statistics Committee and Stroke Statistics Subcommittee. Heart disease and stroke statistics--2012 update: a report from the American Heart Association. *Circulation* 2012;125:e2-e220.
2. Hansson GK. Inflammation, atherosclerosis, and coronary artery disease. *N Engl J Med* 2005;352:1685-95.
3. Galkina E, Ley K. Immune and inflammatory mechanisms of atherosclerosis (*). *Annu Rev Immunol* 2009;27:165-97.
4. Weber C, Noels H. Atherosclerosis: current pathogenesis and therapeutic options. *Nat Med* 2011;17:1410-22.
5. Woollard KJ. Immunological aspects of atherosclerosis. *Clin Sci (Lond)* 2013;125:221-35.
6. Drechsler M, Soehnlein O. The complexity of arterial classical monocyte recruitment. *J Innate Immun* 2013;5:358-66.
7. Hansson GK, Libby P, Schönbeck U, Yan ZQ. Innate and adaptive immunity in the pathogenesis of atherosclerosis. *Circ Res* 2002;91:281-91.
8. Bot I, Biessen EA. Mast cells in atherosclerosis. *Thromb Haemost* 2011;106:820-6.
9. Cole JE, Georgiou E, Monaco C. The expression and functions of toll-like receptors in atherosclerosis. *Mediators Inflamm* 2010;2010:393946.
10. Mann DL. The emerging role of innate immunity in the heart and vascular system: for whom the cell tolls. *Circ Res* 2011;108:1133-45.
11. Ding Y, Subramanian S, Montes VN, Goodspeed L, Wang S, Han C, Teresa AS 3rd, Kim J, O'Brien KD, Chait A. Toll-like receptor 4 deficiency decreases atherosclerosis but does not protect against inflammation in obese low-density lipoprotein receptor-deficient mice. *Arterioscler Thromb Vasc Biol* 2012;32:1596-604.
12. Lu Z, Zhang X, Li Y, Jin J, Huang Y. TLR4 antagonist reduces early-stage atherosclerosis in diabetic apolipoprotein E-deficient mice. *J Endocrinol* 2013;216:61-71.
13. Divanovic S, Trompette A, Petiniot LK, Allen JL, Flick LM, Belkaid Y, Madan R, Haky JJ, Karp CL. Regulation of TLR4 signaling and the host interface with pathogens and danger: the role of RP105. *J Leukoc Biol* 2007;82:265-71.
14. Akashi-Takamura S, Miyake K. TLR accessory molecules. *Curr Opin Immunol* 2008;20:420-5.
15. Divanovic S, Trompette A, Atabani SF, Madan R, Golenbock DT, Visintin A, Finberg RW, Tarakhovsky A, Vogel SN, Belkaid Y, Kurt-Jones EA, Karp CL. Negative regulation of Toll-like receptor 4 signaling by the Toll-like receptor homolog RP105. *Nat Immunol* 2005;6:571-8.
16. Yoon SI, Hong M, Wilson IA. An unusual dimeric structure and assembly for TLR4 regulator RP105-MD-1. *Nat Struct Mol Biol* 2011;18:1028-35.
17. Ohto U, Miyake K, Shimizu T. Crystal structures of mouse and human RP105/MD-1 complexes reveal unique dimer organization of the toll-like receptor family. *J Mol Biol* 2011;413:815-25.
18. Karper JC, de Jager SC, Ewing MM, de Vries MR, Bot I, van Santbrink PJ, Redeker A, Mallat Z, Binder CJ, Arens R, Jukema JW, Kuiper J, Quax PH. An unexpected intriguing effect of Toll-like receptor regulator RP105 (CD180) on atherosclerosis formation with alterations on B-cell activation. *Arterioscler Thromb Vasc Biol* 2013;33:2810-7.
19. Karper JC, Ewing MM, de Vries MR, de Jager SC, Peters EA, de Boer HC, van Zonneveld AJ, Kuiper J, Huizinga EG, Brondijk TH, Jukema JW, Quax PH. TLR accessory molecule RP105 (CD180) is involved in post-interventional vascular remodeling and soluble RP105 modulates neointima formation. *PLoS One* 2013;8:e67923.
20. von der Thüsen JH, van Berkel TJ, Biessen EA. Induction of rapid atherogenesis by perivascular carotid collar placement in apolipoprotein E-deficient and low-density lipoprotein receptor-deficient

- mice. *Circulation* 2001;103:1164-70.
21. Miyake K, Yamashita Y, Ogata M, Sudo T, Kimoto M. RP105, a novel B cell surface molecule implicated in B cell activation, is a member of the leucine-rich repeat protein family. *J Immunol* 1995;154:3333-40.
 22. Francke A, Herold J, Weinert S, Strasser RH, Braun-Dullaeus RC. Generation of mature murine monocytes from heterogeneous bone marrow and description of their properties. *J Histochem Cytochem* 2011;59:813-25.
 23. Ogata H, Su I, Miyake K, Nagai Y, Akashi S, Mecklenbräuker I, Rajewsky K, Kimoto M, Tarakhovsky A. The toll-like receptor protein RP105 regulates lipopolysaccharide signaling in B cells. *J Exp Med* 2000;192:23-9.
 24. Tsiantoulas D, Diehl CJ, Witztum JL, Binder CJ. B Cells and Humoral Immunity in Atherosclerosis. *Circ Res* 2014;114:1743-1756.
 25. Eefting D, Bot I, de Vries MR, Schepers A, van Bockel JH, Van Berkel TJ, Biessen EA, Quax PH. Local lentiviral short hairpin RNA silencing of CCR2 inhibits vein graft thickening in hypercholesterolemic apolipoprotein E3-Leiden mice. *J Vasc Surg* 2009;50:152-60.
 26. Campbell KA, Lipinski MJ, Doran AC, Skaflen MD, Fuster V, McNamara CA. Lymphocytes and the adventitial immune response in atherosclerosis. *Circ Res*. 2012;110:889-900.
 27. Bot I, Guo J, Van Eck M, Van Santbrink PJ, Groot PH, Hildebrand RB, Seppen J, Van Berkel TJ, Biessen EA. Lentiviral shRNA silencing of murine bone marrow cell CCR2 leads to persistent knockdown of CCR2 function in vivo. *Blood* 2005;106:1147-53.
 28. Stoneman V, Braganza D, Figg N, Mercer J, Lang R, Goddard M, Bennett M. Monocyte/macrophage suppression in CD11b diphtheria toxin receptor transgenic mice differentially affects atherogenesis and established plaques. *Circ Res* 2007;100:884-93.
 29. Bastiaansen AJ, Karper JC, Wezel A, de Boer HC, Welten SM, de Jong RC, Peters EA, de Vries MR, van Oeveren-Rietdijk AM, van Zonneveld AJ, Hamming JF, Nossent AY, Quax PH. TLR4 Accessory Molecule RP105 (CD180) Regulates Monocyte-Driven Arteriogenesis in a Murine Hind Limb Ischemia Model. *PLoS One* 2014;9:e99882.
 30. Strauss-Ayali D, Conrad SM, Mosser DM. Monocyte subpopulations and their differentiation patterns during infection. *J Leukoc Biol* 2007;82:244-52.
 31. Boring L, Gosling J, Cleary M, Charo IF. Decreased lesion formation in CCR2^{-/-} mice reveals a role for chemokines in the initiation of atherosclerosis. *Nature* 1998;394:894-7.
 32. Dawson TC, Kuziel WA, Osahar TA, Maeda N. Absence of CC chemokine receptor-2 reduces atherosclerosis in apolipoprotein E-deficient mice. *Atherosclerosis* 1999;143:205-11.
 33. Yi L, Chandrasekaran P, Venkatesan S. TLR signaling paralyzes monocyte chemotaxis through synergized effects of p38 MAPK and global Rap-1 activation. *PLoS One* 2012;7:e30404.
 34. Xu L, Khandaker MH, Barlic J, Ran L, Borja ML, Madrenas J, Rahimpour R, Chen K, Mitchell G, Tan CM, DeVries M, Feldman RD, Kelvin DJ. Identification of a novel mechanism for endotoxin-mediated down-modulation of CC chemokine receptor expression. *Eur J Immunol* 2000;30:227-35.
 35. Heesen M, Renckens R, de Vos AF, Kunz D, van der Poll T. Human endotoxemia induces down-regulation of monocyte CC chemokine receptor 2. *Clin Vaccine Immunol* 2006;13:156-9.
 36. Parker LC, Whyte MK, Vogel SN, Dower SK, Sabroe I. Toll-like receptor (TLR)2 and TLR4 agonists regulate CCR expression in human monocytic cells. *J Immunol* 2004;172:4977-86.
 37. Divanovic S, Trompette A, Atabani SF, Madan R, Golenbock DT, Visintin A, Finberg RW, Tarakhovsky A, Vogel SN, Belkaid Y, Kurt-Jones EA, Karp CL. Inhibition of TLR4/MD-2 signaling by RP105/MD-1. *J Endotoxin Res* 2005;11:363-8.
 38. Moore KJ, Sheedy FJ, Fisher EA. Macrophages in atherosclerosis: a dynamic balance. *Nat Rev Immunol* 2013;13:709-21.

Supplemental Material

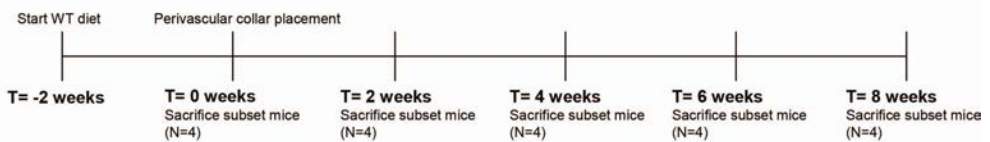
Supplemental table 1.

Gene	Forward primer	Reversed primer
CCR2	CCTTGGGAATGAGTAAGTGTGA	TGGAGAGATACCTTCGGAAGTCT
CCR5	AATTCTTTGGACTGAATAAGTCA	TGGATCGGGTATAGACTGAGCTT
CCR1	CAATCAGTGTGAGCAGAGTAAGCA	CACAACAGTGGGTGTAGGCAA
CX3CR1	AAGTTCCCTTCCCATCTGCT	CAAAATTCTCTAGATCCAGTTCAGG
RPL27	CGCCAAGCGATCCAAGATCAAGTCC	AGCTGGGTCCCCTGAACACATCCTTG
HPRT	TTGCTCGAGATGTCATGAAGGA	AGCAGGTCAGCAAAGAACTTATAG
β -actin	CGCCAAGCGATCCAAGATCAAGTCC	AGCTGGGTCCCCTGAACACATCCTTG

Supplemental figure 1. (A) Schematic overview of the atherosclerosis time course used for RNA analysis (N=4 mice/group). **(B)** Schematic overview of the atherosclerosis study induced in $LDLr^{-/-}/RP105^{-/-}$ versus $LDLr^{-/-}$ mice (N=12 mice/group).

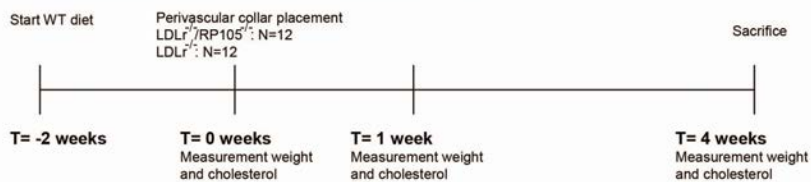
A

Atherosclerosis time course RNA analysis $LDLr^{-/-}$ mice

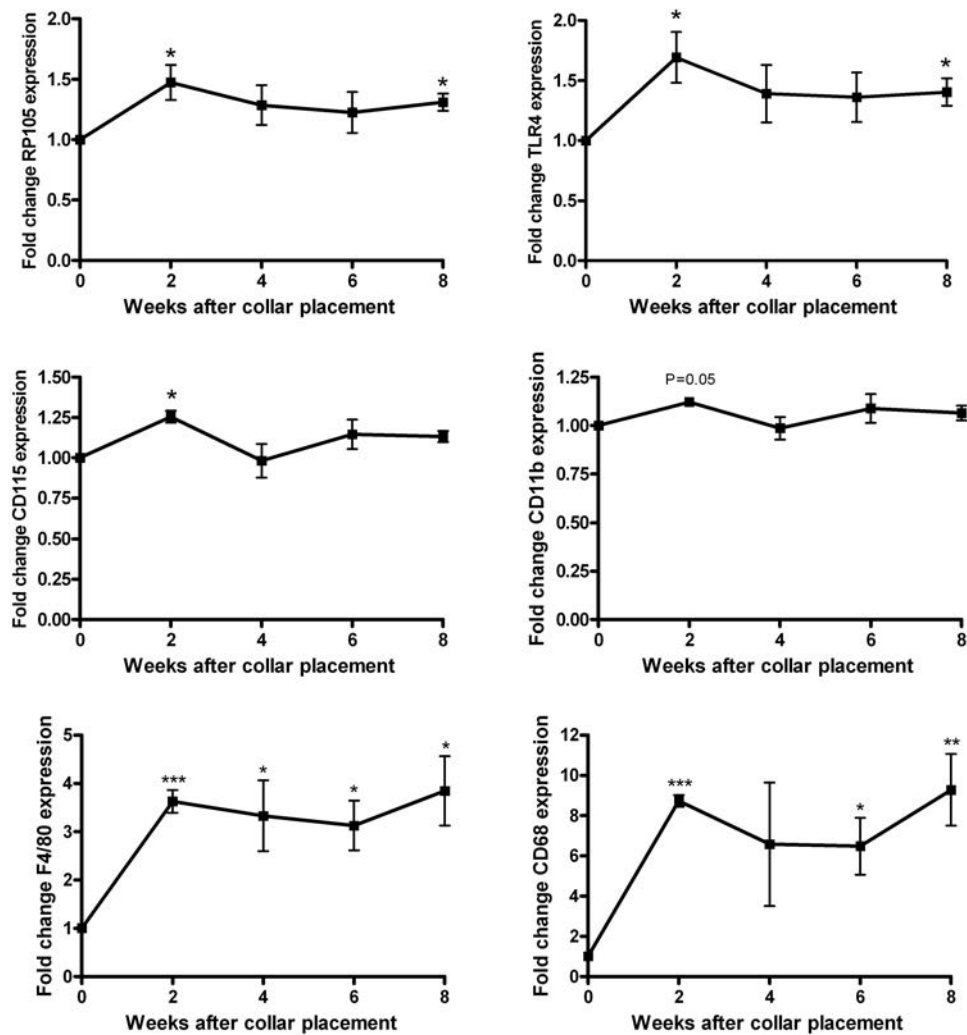


B

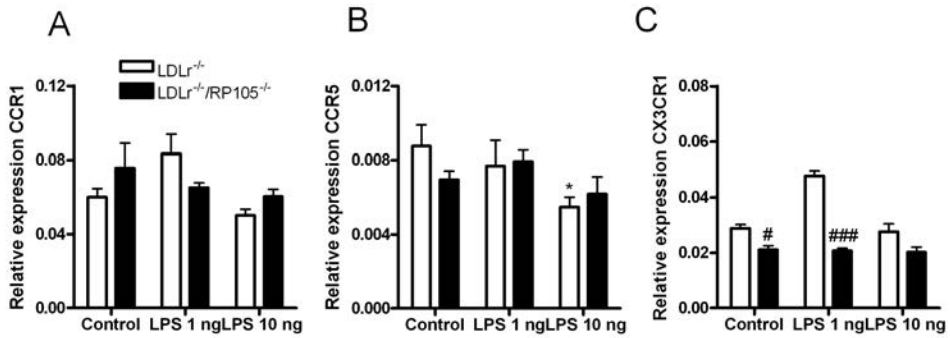
Atherosclerosis in $LDLr^{-/-}/RP105^{-/-}$ versus $LDLr^{-/-}$ mice



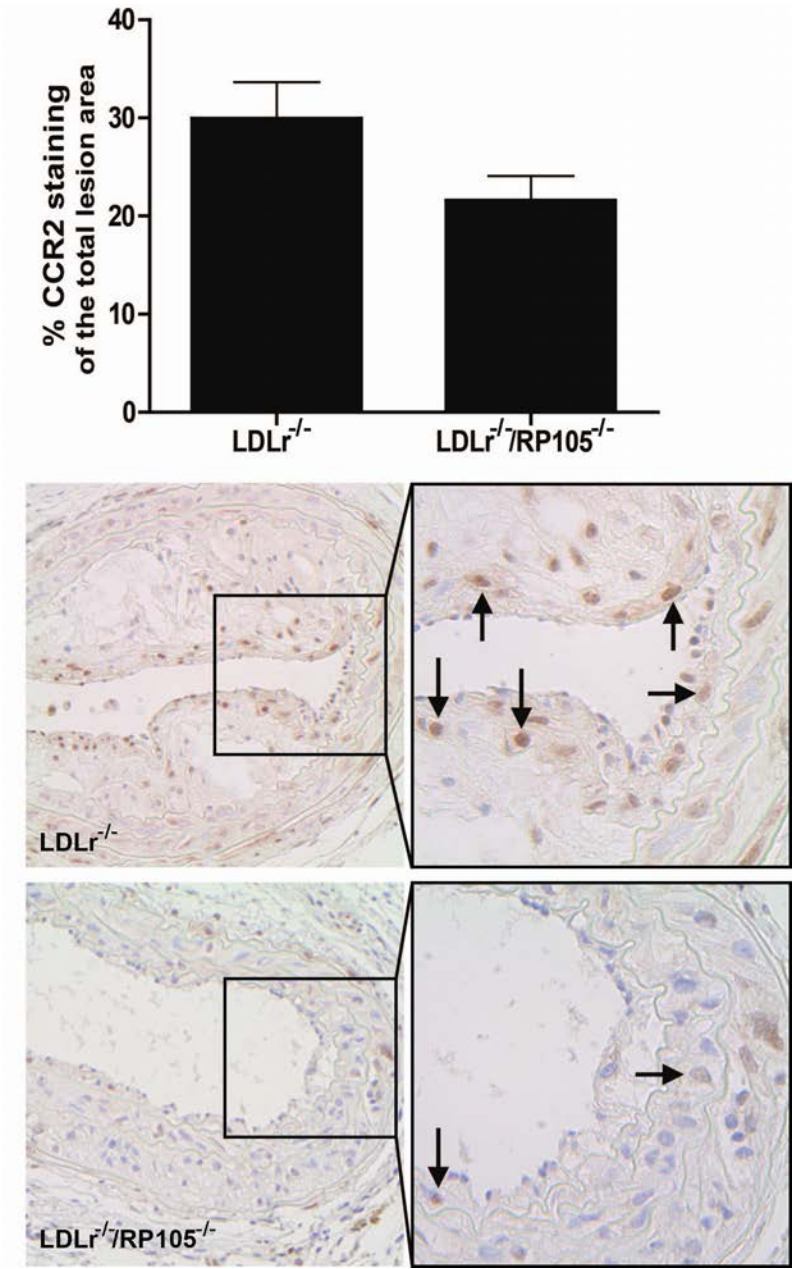
Supplemental Figure 2. (A) Fold change in expression of RP105 en TLR4 compared to 0 weeks of diet. (B) Fold change in expression of monocyte/macrophage markers CD115, CD11b, F4/80 and CD68 compared to 0 weeks of diet. *P<0.05, **P<0.01, ***P<0.0001.



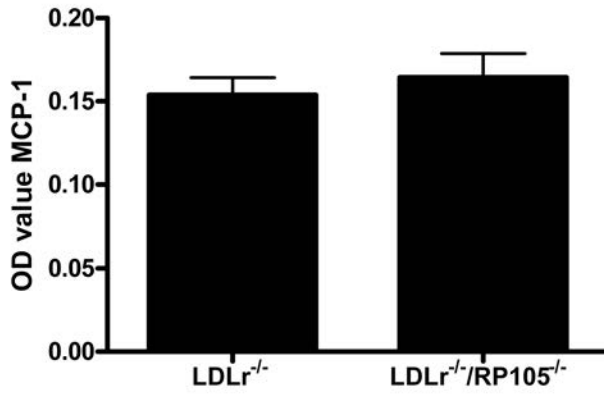
Supplemental figure 3. (A) CCR1 expression remained unaltered after stimulation with 1 ng and 10 ng LPS in both $LDLr^{-/-}$ and $LDLr^{-/-}/RP105^{-/-}$ monocytes. (B) The relative expression of CCR5 was slightly reduced in $LDLr^{-/-}$ monocytes after stimulation with 10 ng LPS, however, no significant changes were found between $LDLr^{-/-}$ and $LDLr^{-/-}/RP105^{-/-}$ monocytes. (C) The CX3CR1 expression in $LDLr^{-/-}$ monocytes was increased after stimulation with 1 ng LPS, while no changes were observed in CX3CR1 expression when comparing unstimulated $LDLr^{-/-}/RP105^{-/-}$ monocytes with LPS stimulated $LDLr^{-/-}/RP105^{-/-}$ monocytes. N=4. # $P<0.05$ compared to $LDLr^{-/-}$ monocytes; ### $P<0.001$ compared to $LDLr^{-/-}$ monocytes; *** $P<0.001$ compared to unstimulated monocytes. A 2-tailed Student's t-test was used to compare individual groups.



Supplemental figure 4. CCR2 protein expression was measured as the percentage of staining in the intimal area. The micrographs below show representative images of CCR2 staining in both groups (200x). Cells positive for CCR2 are indicated with arrows in the enlarged micrographs (400x). N=12 mice/group. A 2-tailed Student's t-test was used to compare individual groups.



Supplemental figure 5. Plasma MCP-1 levels, as measured by means of ELISA, did not differ between $LDLr^{-/-}/RP105^{-/-}$ mice and control $LDLr^{-/-}$ mice. N=12 mice/group. A 2-tailed Student's t-test was used to compare individual groups.



Chapter 8

Inhibition of microRNA-494 reduces atherosclerotic lesion development and increases plaque stability

Submitted for publication

Anouk Wezel^{1,2}

Sabine M.J. Welten^{2,3}

Wida Razawy¹

H. Maxime Lagraauw¹

Margreet R. de Vries^{2,3}

Eveline A.C. Goossens²

Martin C. Boonstra²

Ekambar R. Kandimalla⁴

Johan Kuiper¹

Paul H.A. Quax^{2,3}

*A. Yaël Nossent^{2,3}

*Ilze Bot^{1,2}

*These authors contributed equally

¹ Division of Biopharmaceutics, Gorlaeus Laboratories, Leiden Academic Center for Drug Research, Leiden University, Leiden, The Netherlands

² Department of Surgery, Leiden University Medical Center, Leiden, The Netherlands

³ Einthoven Laboratory for Experimental Vascular Medicine, Leiden, The Netherlands

⁴ Idera Pharmaceuticals, Cambridge, MA, United States of America

Abstract

Objective: Atherosclerosis is a multifactorial disease involving inflammatory, metabolic and lipid-related processes. Targeting the combination of these processes would be a useful strategy to prevent the development of atherosclerosis. MicroRNAs can regulate multiple targets and therefore, they have great potential as novel multifactorial drug targets. We aimed to identify a microRNA that exerts a broad effect on atherosclerosis and establish its role in atherosclerotic plaque formation and stability *in vivo*.

Approach and Results: A Reversed Target Prediction strategy was developed, using 164 genes involved in atherosclerosis, to identify microRNAs that may affect lesion formation. Interestingly, enrichment of binding sites was found for multiple microRNAs from the 14q32 microRNA-gene cluster. In human atherosclerotic lesions, we found that one of these 14q32 microRNAs, miR-494, was abundantly expressed, particularly in the most unstable lesions. Also, in a number of murine organs involved in the development of atherosclerosis, including the liver, spleen and arteries, expression of miR-494 was detected. We inhibited miR-494 *in vivo* by injecting apoE^{-/-} mice with a Gene Silencing Oligonucleotide specifically targeting miR-494. Effective uptake of GSOs in the affected areas of the arteries was confirmed using fluorescently labeled GSOs. After treatment with GSO-494 we observed a significant downregulation of miR-494 expression in the carotid artery while multiple miR-494 target genes were upregulated. Atherosclerotic lesion size was reduced with 65% while plaque stability was increased, as illustrated by a decreased necrotic core size and a concomitant increase in collagen content. Finally, inhibition of miR-494 resulted in a decrease in plasma total cholesterol levels and increased cholesterol efflux *in vitro*.

Conclusions: This study is the first to report that miR-494 from the 14q32 microRNA-gene cluster affects atherosclerotic lesion development. Inhibition of miR-494 results in a decreased lesion size, while increasing plaque stability, rendering this microRNA a promising novel therapeutic target in the prevention of atherosclerotic disease.

Introduction

Atherosclerosis is a complex, multifactorial disease in which various processes in immune modulation and cholesterol homeostasis are involved. Damage to the endothelial layer in large and medium-sized arteries results in local upregulation of adhesion molecules and chemokine production, together facilitating the influx of monocytes into the vessel wall^{1,2}. Subsequent uptake of modified lipoproteins through scavenger receptors leads to the formation of early fatty streaks. Continued inflammation attracts multiple immune cells to the lesion, eventually resulting in an advanced atherosclerotic plaque^{3,4}, which is defined as a plaque with a large lipid core covered by a thin fibrous cap containing little collagen and few smooth muscle cells^{5,6}. Rupture of an advanced plaque can cause severe acute cardiovascular events such as myocardial infarction and stroke. Despite current lipid lowering therapies, cardiovascular diseases are still the main cause of death in western society. Taking into account the multifactorial nature of atherosclerosis, improvement of treatment strategies may be accomplished by targeting the process as a whole rather than focusing on single factors.

MicroRNAs (miRs) are a class of short, non-coding RNAs, approximately 20 nucleotides long, capable of downregulating target gene expression at post-transcriptional level⁷. A single miR has, on average, 200 predicted target genes⁸. Their ability to fine-tune expression of multiple genes makes miRs excellent drug targets for complex diseases such as atherosclerosis⁹. Inhibition of miRs in atherosclerosis has been investigated in several studies. For example, Rayner *et al.* showed that inhibiting miR-33 results in a lowering of plasma VLDL while increasing plasma HDL¹⁰. Besides regulation of cholesterol homeostasis, miRs have also been implicated in other cellular mechanisms affecting atherosclerosis. MiR-126 for instance regulates post-transcriptional VCAM-1 expression in response to triglyceride-rich lipoproteins¹¹. Also, inhibition of miR-92a has been demonstrated to upregulate the expression of endothelial KLF-2 and KLF-4¹², which are Kruppel-like Factors with atheroprotective properties¹³. Furthermore, smooth muscle cell proliferation and migration can be repressed by miR-195; consequently, neo-intima formation can be reduced by miR-195 gene therapy¹⁴. MiR-155 has been shown to repress the transcription factor Bcl6, thereby increasing NF- κ B activation and CCL2 expression in macrophages¹⁵. It seems therefore that results in this area of research are very promising. However, it is apparent that most of these studies focus on the effect of miRs on a single cell type or process, thereby failing to do justice to the ability of miRs to exert a broad range of effects.

A commonly used tool to identify miRs involved in atherosclerosis is microarray profiling^{16,17}. However, in order to utilize the specific characteristic of miRs to regulate many genes, we used a Reverse Target Prediction (RTP) strategy. Instead of investigating the miR with the highest upregulation in atherosclerosis, we made

use of a 'reversed' approach by taking multiple target genes as a starting point and subsequently selecting miRs that are predicted to regulate these genes. An *in silico* analysis was performed based on a selection of 164 genes that play an important role in atherosclerosis, known both from literature and previous studies within our group. For these genes we determined predicted binding sites for known miRs in the 3'UTR region, and ranked the miRs based on the prevalence of target genes with binding sites in this gene set. MiRs obtained by this method have the potential to target a large subset of atherosclerosis-related genes and may thus function as a so-called 'master switch' in the development of atherosclerosis.

Using our unique RTP strategy, we identified miRs that are predicted to exert a broad effect on atherosclerosis. Moreover, we singled out one miR from the 14q32 miR-gene cluster, miR-494, which has thus far not been linked to atherosclerosis. Subsequently, we inhibited this miR in order to investigate its *in vivo* effect on atherosclerotic plaque formation and stability.

Material and Methods

Reverse Target Prediction

Based on existing knowledge from both literature¹⁸⁻²² and previous studies within our group, we compiled a list of 164 genes involved in atherosclerosis (both pro- and anti-atherogenic), including chemokines, cytokines, adhesion molecules, scavenger receptors, lipid related targets, complement factors, matrix metalloproteinases (MMPs) and growth factors. Using the online algorithm Targetscan (www.targetscan.org), a list was generated of all miRs predicted to target our selected genes. This list was then transferred to a spreadsheet and the number of times an individual miR was listed, was counted manually. We ranked the miRs according to the number of putative target genes with a predicted 3'UTR binding site. The RTP was performed by analyzing binding sites in human target genes to ensure clinical relevance (Table 1A). We then performed the RTP by analyzing binding sites in murine target genes, to confirm the validity of the use of our mouse model for atherosclerosis (Table 1B).

Human carotid artery plaques

Human atherosclerotic plaques were collected anonymously during endarterectomy surgery at the Leiden University Medical Center. Plaques were fixed in 4% formaldehyde and embedded in paraffin. From a biobank of approximately 50 human carotid artery plaques, 6 highly unstable and 6 relatively stable plaques were selected based on three parameters for plaque instability (i.e. necrotic core size, macrophage content and intra-plaque hemorrhage). Total RNA was isolated using the RNeasy FFPE Kit according to manufacturer's protocol (Qiagen). Sufficient RNA was isolated from 3 stable and 5 unstable plaques for miR quantification as described below.

Mice

All animal work was performed in compliance with the Dutch government guidelines and the Directive 2010/63/EU of the European Parliament. Male apoE^{-/-} mice, obtained from the local animal breeding facility (Gorlaeus Laboratories, Leiden University, Leiden, the Netherlands), were fed a Western type diet, containing 0.25% cholesterol and 15% cacao butter (SDS, Sussex, UK) for six weeks. Before surgical

intervention mice were age-, cholesterol-, and weight-matched. Details of cholesterol measurement are described below. White blood cell (WBC) numbers and cellular differentiation were determined on a Sysmex cell differentiation apparatus (Goffin Meyvis, Etten-Leur, The Netherlands).

Carotid collar placement

Two weeks after start of the Western type diet, carotid artery plaque formation was induced by perivascular collar placement as described previously²³. Before surgery and sacrifice, mice were anaesthetized by an intra-peritoneal injection with midazolam (5 mg/kg; Roche, Woerden, The Netherlands), domitor (0.5 mg/kg; AST Farma, Oudewater, The Netherlands) and fentanyl (0.05 mg/kg; Janssen, Beerse, Belgium). After surgery, mice were antagonized with a subcutaneous injection of flumazenil (0.5 mg/kg; Fresenius Kabi, Schelle, Belgium), antisedan (2.5 mg/kg; AST Farma) and buprenorphine (0.1 mg/kg; MSD Animal Health, Boxmeer, The Netherlands). In brief, a semi-constrictive collar was placed around both left and right carotid arteries of the mice. Low shear stress and disturbed flow at the proximal site of the collar result in increased expression of endothelial adhesion molecules and atherosclerotic lesion formation. At either one week or four weeks after collar placement, mice were anaesthetized and *in situ* perfused, after which carotid artery lesions were harvested for further analysis.

Treatment with IRDye labelled GSOs

Four male adult apoE^{-/-} mice received one perivascular collar around the right carotid artery, while the contra-lateral carotid artery was left unaffected. At day 4 and day 28 after surgery, mice were injected intravenously with IRDye-800CW-labelled GSO-494 (0.4 mg/mouse; Idera Pharmaceuticals, Cambridge MA) or control unlabelled IRDye. Mice were sacrificed by orbital exsanguination one day after injection. Near-InfraRed (NIR) fluorescence measurements were performed using the FLARETM NIR imaging system²⁴.

Treatment with GSOs

At day 4 after surgery, mice received an intravenous injection of either 1 mg Gene Silencing Oligonucleotide dissolved in 200 μ l PBS (GSO, kindly provided by Idera Pharmaceuticals, Cambridge, MA, USA) or 200 μ l PBS control at day 4 after surgery. A subset of mice ($n=6$ per group) was sacrificed 3 days later (1 week after surgery) in order to establish downregulation of miR-494 *in vivo*. For effects on atherosclerosis, the remaining mice received a second injection of 0.5 mg GSO dissolved in 200 μ l PBS per mouse at day 18 ($n=15$ per group). GSO-494 was designed with perfect reverse complementarity to the mature target miR sequence and synthesized by Idera Pharmaceuticals. As a negative control, a scrambled sequence was used, designed not to target any known murine miR. GSOs consist of two single-stranded O-methyl-modified DNA strands, linked together at their 5'ends by a phosphorothioate-linker to avoid TLR-activation^{25,26}. Sequences of GSOs used are given in Table S1 (Supplemental Data).

Plasma analysis

Blood was collected from the mice by tail bleeding. The concentration of cholesterol in plasma was determined by incubation with 0.025 U/mL cholesterol oxidase (Sigma, Zwijndrecht, The Netherlands) and 0.065 U/ml peroxidase and 15 μ g/mL cholesterol esterase (Roche Diagnostics, Mannheim, Germany) in polyoxyethylene-9-laurylether, and 7.5% methanol). Precipath (standardized serum; Boehringer Mannheim, Germany) was used as an internal standard. Absorbance was measured at 490 nm.

For lipid profiling, plasma was pooled ($n=3$ mice per sample) and diluted 6 times, after which fractionation of plasma lipoproteins was performed using an AKTA-FPLC. Triglyceride levels and total cholesterol levels were determined in each fraction and in the original pooled sample by incubation with cholesterol CHOD-PAP Reagent (Roche, Woerden, The Netherlands). Absorbance was measured at 492 nm.

Plasma cytokines and chemokines were measured using ProcartaPlex™ Multiplex Immunoassays Mouse Cytokine and Chemokine Panel 1 (26 plex), according to manufacturers protocol (eBioscience, San Diego, CA, USA) and read on a Luminex Magpix (Luminex Corporation, Austin, Tx, USA).

Histology and morphometry

Paraffin sections (5 µm thick) were routinely stained with HPS (hematoxylin-phloxine-saffron), which were used to determine plaque size. Picrosirius red staining was used to visualize collagen and for measurement of necrotic core size. Plaque composition was further examined by staining for smooth muscle cells (alpha smooth muscle actin, Sigma) and macrophages (MAC 3, BD-Pharmingen, San Diego, CA, USA). The amount of mast cells and their activation status was visualized using an enzymatic staining kit (Naphtol-CAE, Sigma).

Morphometric analysis (Leica Qwin image analysis software) was performed on HPS-stained atherosclerotic lesions at site of maximal stenosis. (Immuno) histochemical stainings were quantified by computer assisted analysis (Leica, Qwin, Cambridge, UK) and expressed as the percentage of positive stained area of the total lesion area. Mast cells were counted manually. A mast cell was considered resting when all granula were maintained inside the cell, while mast cells were assessed as activated when granula were deposited in the tissue surrounding the mast cell. The necrotic core was defined as the a-cellular, debris-rich plaque area as percentage of total plaque area.

Cell culture

Bone marrow (BM) cells isolated from C57Bl/6 mice were cultured in petridishes (Greiner Bio-one, Alphen aan den Rijn, Netherlands) for 7 days in RPMI medium supplemented with 20% fetal calf serum (FCS), 2 mmol/L L-glutamine, 100 U/mL penicillin and 100 µg/mL streptomycin and 30% L929 cell-conditioned medium, as the source of macrophage colony-stimulating factor (M-CSF), to generate BM-derived macrophages (BMDMs)²⁷. For generation of primary mast cells, BM cells were cultured in RPMI medium supplemented with 10% IL-3 supernatant (supernatant of WEHI-cells overexpressing and secreting murine Interleukin 3 (mIL3)), 1 mM sodium pyruvate, MEM non-essential amino acids, 10% FCS, 2 mmol/L L-glutamine, 100 U/mL penicillin and 100 µg/mL streptomycin for 4 weeks²⁸. Mast cell purity and maturation was determined microscopically by staining of cytopins with 0.5% aqueous toluidin blue. Primary cultured murine smooth muscle cells (vSMC) and cell lines for fibroblasts (3T3) and endothelial cells (H5V) were cultured in complete DMEM medium supplemented with 10% FCS, 2 mmol/L L-glutamine, 100 U/mL penicillin and 100 µg/mL streptomycin in T75 tissue culture flasks (Greiner Bio-one).

Mast cells, fibroblasts, smooth muscle cells and endothelial cells were plated in triplicate at a density of 10⁶ cells/mL. GSOs were added overnight at a concentration of 5 µg/mL, after which the cells were lysed for RNA isolation.

For BMDMs, GSOs were added immediately after isolation from BM in a concentration of 5 µg/mL. After three days medium was refreshed with a similar addition of GSOs in a concentration of 5 µg/mL. Four days later, medium was removed and cells were lysed for RNA isolation.

RNA isolation, cDNA synthesis and qPCR

Three carotid artery segments from 7 days after collar placement were pooled and homogenized by grounding using a Pellet Pestle Cordless Motor (Kimble Chase Life Science, USA). Spleen, liver and intestines from these mice were isolated and homogenized by grounding with the use of liquid nitrogen. Also, BM was isolated, after which total RNA was extracted using a standard TRIzol-chloroform protocol. RNA concentration, purity and integrity were examined by nanodrop (Nanodrop® Technologies). MiR quantification was performed according to manufacturer's protocol using TaqMan® miR assays (Applied Biosystems, Foster City, CA, USA). qPCRs were run on a 7900HT Fast Real-Time PCR System (Applied

Biosystems). Normalization of data was performed using a stably expressed endogenous control (*mmu-let-7c*; for the liver *miR-122* was used).

For the *in vitro* experiments, total RNA was extracted from the cells using the guanidine thiocyanate (GTC) method²⁹. RNA was reverse transcribed by M-MuLV reverse transcriptase (RevertAid, MBI Fermentas, Leon-Roth, Germany) and used for quantitative analysis of mouse genes (Supplemental Table 2) with an ABI PRISM 7700 Taqman apparatus (Applied Biosystems). Murine HPRT and RPL27 were used as standard housekeeping genes.

Cholesterol efflux assay

BMDMs, cultured and treated with GSOs as described above, were seeded at a density of 0.5×10^6 per well. The next day, medium was aspirated and cells were loaded with 20 mg/mL cholesterol for 24 hours with 1 μ Ci/mL 3 H-cholesterol in DMEM with 10% BSA, with the addition of either GSO-control or GSO-494 (5 μ g/mL) ($n=6$). The following day, loading medium was removed and the cells were washed with PBS, after which DMEM/10%BSA was added to the cells for one hour. Subsequently, the medium was removed and cells were incubated overnight with control DMEM/10%BSA medium or DMEM/10%BSA medium supplemented with HDL (50 μ g/mL). After a 24-hour efflux period, radioactivity in the cells and medium was determined by liquid scintillation counting (Packard 1500 Tricarb, Downers Grove, IL, USA). Cholesterol efflux is defined as $(\text{dpm}_{\text{medium}} / (\text{dpm}_{\text{cells}} + \text{dpm}_{\text{medium}})) \times 100\%$, and is depicted as the percentage HDL specific efflux, which was corrected for non-specific efflux to control medium.

Collagen synthesis assay

To measure collagen production by vSMC, cells were seeded at a density of 0.2×10^6 cells per well. After attachment of the cells, control medium or medium containing GSO-control or GSO-494 (5 μ g/mL), was added. Subsequently, 1 μ Ci [3 H]proline (Perkin Elmer, Groningen, The Netherlands) in the presence of 50 μ g/mL ascorbic acid was added and incubated overnight at 37°C. Cells were detached from the wells in 20 mM Tris*HCl/0.36 mM CaCl₂ (pH=7.6) and sonicated for 2 minutes. Collagen was degraded by incubation with 100 U/mL collagenase for 2 hours at 37°C, after which samples were centrifuged for 15 minutes at 13.2 g. Proteins were precipitated for 30 minutes on ice using 50% trichloroacetic acid, after which [3 H]proline content in the supernatant as a measure for collagen production was quantified in a liquid scintillation analyzer as described above. Protein content was measured using a standard BCA protein assay.

Statistical analysis

Data are expressed as mean \pm SEM. Two-tailed Student's t-tests were used to compare individual groups in the *in vivo* studies. Non-parametric data were analyzed using a Mann-Whitney U test. A level of $P < 0.05$ was considered significant.

Results

Identification of miRs from the 14q32 miR gene cluster by Reversed Target Prediction

We performed a Reversed Target Prediction based on a list we compiled of atherosclerosis-related genes known from literature and previous studies. As expected, we identified multiple miRs that have previously been described in atherosclerosis, including *miR-155*¹⁵, *miR-23/24*³⁰ and *miR-33*¹⁰. Less established

miRs were identified as well, such as miR-590-3p. MiR-590-3p, which has recently been described to be regulated in minimally-oxidized LDL induced vSMC phenotype transformation³¹, was predicted to target the most genes (65 putative targets). Interestingly, we found enrichment of binding sites for multiple miRs from one single miR-gene cluster, located in an imprinted region on the long arm of human chromosome 14 (14q32; chromosome 12F1 in mice) (Table 1A). We identified 11 miRs of this gene cluster, including miR-495 (45 putative targets), miR-494 (38 putative targets) and miR-329 (30 putative targets). To ensure relevance for our murine atherosclerosis model we also performed our RTP by analyzing for murine target genes (Table 1B), in which we again identified multiple targets for miR-495 (37 putative targets), miR-494 (34 putative targets), and miR-329 (26 putative targets). Recently, our group has shown an important role for miR-494, miR-495 and miR-329 in vascular remodelling³²; therefore we selected these miRs for further investigations.

Expression of miR-494, miR-495 and miR-329 in human atherosclerotic plaques

To investigate whether miR-494, miR-495 and miR-329 are expressed in human atherosclerotic plaques, we isolated RNA from both stable and unstable lesions obtained from patients undergoing endarterectomy. We detected abundant expression of miR-494 in all 5 unstable lesions and in one of three stable lesions. MiR-495 was expressed in all lesions, but at lower levels than miR-494, while the expression of miR-329 was not detectable in any of the lesions (Figure 1A).

Expression of miR-494, miR-495 and miR-329 in murine organs

Next, we measured the expression of miR-494, miR-495 and miR-329 in various murine organs involved in mechanisms of atherosclerotic lesion development, including arteries (the carotid artery and the aorta), the liver, the spleen and the bone marrow. To ensure relevance to atherosclerosis, the expression levels of these miRs were measured in mice fed a western type diet for 3 weeks. In the carotid artery, miR-494 and miR-495 are expressed approximately twice as high as miR-329 (Figure 1B). Analysis of the aorta revealed that the expression of miR-495 and miR-329 is higher compared to that of miR-494. However, measurement of miR expression in the liver, spleen and bone marrow all demonstrate that the expression of miR-494 is higher compared to that of miR-495 and miR-329 (Figure 1B). Also, we determined whether these miRs are expressed in white blood cells, which is only the case for miR-494. Taken into account these expression levels of miR-494 in murine organs, as well as the higher expression of miR-494 in human atherosclerotic plaques, we selected miR-494 for further investigation regarding its effect on atherosclerotic lesion development.

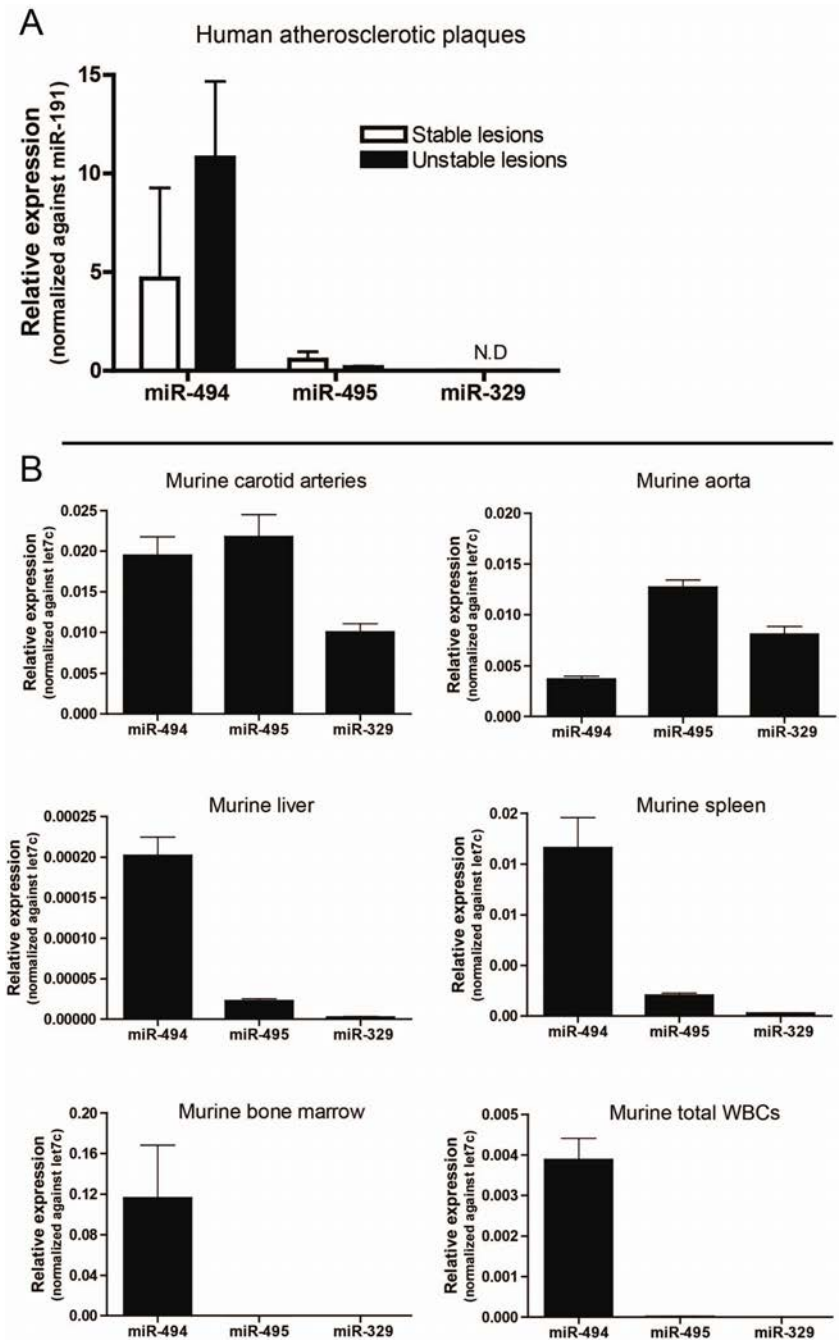


Figure 1. (A) Relative expression of miR-494, miR-495 and miR-329 in stable and unstable human atherosclerotic plaques. (B) In mice fed a western type diet for three weeks, expression of miR-494 and miR-495 is approximately twice as high as that of miR-329 in the vessel wall. MiR-495 and miR-329 expression in the aorta is higher than that of miR-494. However, measurement of the liver, spleen, bone marrow and blood cells all demonstrate that the expression of miR-494 is higher compared to that of miR-495 and miR-329.

In vitro target gene upregulation after inhibition of miR-494

In order to verify upregulation of target gene expression after inhibition of miR-494, cultured cells were treated with GSOs. To reflect the involvement of various cell types in atherosclerosis, smooth muscle cells, endothelial cells, macrophages, fibroblasts and mast cells were used for these assays. Multiple putative target genes, including cytokines, lipid-related targets and tissue inhibitor of metalloproteinases (TIMP), were investigated in order to examine the broad effects that miR-494 may exert.

Inhibition of miR-494 led to a significant upregulation of the chemokine receptor CXCR4 in both endothelial cells and smooth muscle cells. Also, its ligand CXCL12 (SDF-1) was significantly increased in macrophages and mast cells. It has previously been shown that CXCR4/CXCL12 plays a protective role in atherosclerosis^{32,33}. Inhibition of miR-494 also led to an upregulation of TIMP3, of ACVR1 (a member of the TGF-beta superfamily) and of ADIPOR2 (involved in fatty acid oxidation) (Supplemental Figure 1).

Uptake of GSO-494 at site of collar placement

4 or 28 days after collar placement, mice were injected with either IRDye 800CW-labeled GSO-494, or control unlabeled IRDye 800CW. At both time-points, uptake of labeled GSO-494 was clearly visible in the carotid artery in which the collar was placed, while no uptake was detected in the control carotid artery. Uptake of labeled GSO-494 was not observed in the aortic arch of mice fed a western type diet for 2 weeks (Figure 2E,F). However, a clear uptake of labeled GSO-494 was detected in the aortic arch of mice fed a western type diet for 6 weeks (Figure 2H,I), which are known to contain early lesions. The descending aorta did not show any uptake of GSO-494 (Figure 2B,C,H,I). Also, no uptake was detected in the carotid arteries and aorta of control IRDye 800CW treated mouse (Figure 2E,F,K,L).

In vivo repression of miR-494 and target gene upregulation after GSO-494 treatment

Atherosclerotic lesions were induced in apoE^{-/-} mice by placement of perivascular collars around both carotid arteries. Three days after GSO injection a subgroup of mice (n=6) was sacrificed to investigate miR and target gene expression. After GSO-494 treatment, miR-494 was significantly downregulated by 46% in the carotid arteries compared to GSO-control (Figure 3A). Moreover, we observed upregulation of the selected target genes TIMP3, IL33 and TGFB2 in the carotid arteries of mice treated with GSO-494 (Figure 3B; P<0.05).

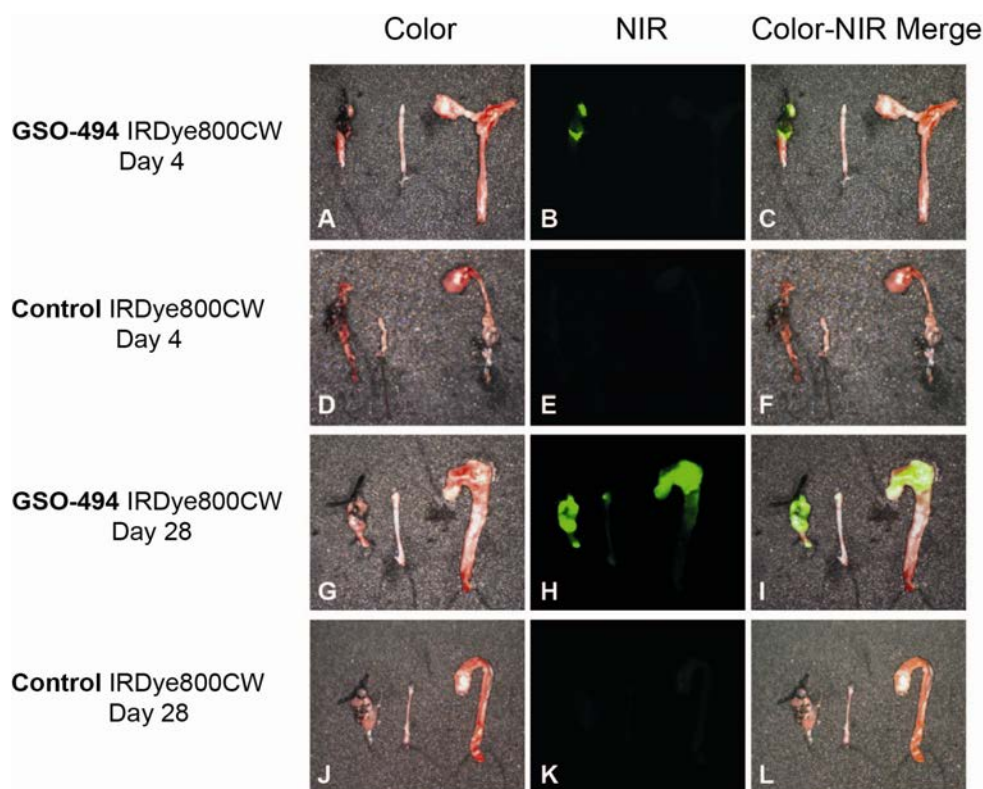


Figure 2. Uptake of IRDye 800CW-labeled GSO-494 or control IRDye 800CW in the vessel wall. In each micrograph is displayed: a carotid artery with collar induced atherosclerosis (left), contra-lateral control carotid artery from the same mouse without collar (middle) and aortic arch with descending aorta from the same mouse (right). Of note: all collars are removed before visualization.

A-F: Arteries from mice receiving a high cholesterol diet, 4 days after collar placement. (A) Arteries from mice 24 hours after intravenous injection of IRDye 800CW-labeled GSO-494. (B) near-infrared (NR) image showing uptake of GSO-494 by the carotid artery in which a collar has been placed, which is absent in the control carotid artery. (C) Merged picture showing uptake of labeled GSO-494. (D,E,F): Uptake of control unlabeled IRDye 800CW 24 hours after intravenous injection, 4 days after collar placement.

G-L: Arteries from mice receiving a high cholesterol diet, 28 days after collar placement. (G,H,I) 24 hours after intravenous injection, uptake of labeled GSO-494 is observed in the carotid artery in which the collar has been placed; also, GSO-494 has been taken up in the aortic arch, which is not detectable in the descending aorta. (J,K,L) Uptake of control unlabeled IRDye 800CW 24 hours after intravenous injection, 4 weeks after collar placement.

Inhibition of miR-494 affects plasma cholesterol levels

To assess the effect of miR-494 inhibition on the development of atherosclerotic lesions, mice treated with either GSO-494 or GSO-control (n=15 per group) were sacrificed four weeks after collar placement. Body weight did not differ between mice treated with GSO-494 and GSO-control (Supplemental Figure 2). Plasma cholesterol levels showed a reduction of 13% after treatment with GSO-494 (GSO-control: 30.4 ± 1.1 mM; GSO-494: 26.4 ± 0.7 mM; $P < 0.01$; Figure 4A). No changes in body weight or plasma cholesterol levels were observed between the PBS and GSO-control treated groups (Supplemental Figure 3A,B). Lipid profiling

by AKTA-FPLC revealed that the reduced cholesterol level after inhibition of miR-494 was mainly due to decreased VLDL fractions (Figure 4B).

We aimed to elucidate the mechanism behind these changes in cholesterol levels by measurement of different target genes in the liver, which did not show any upregulation in gene expression after GSO-494 treatment (Supplemental Figure 4A). Also, we did not detect alterations in the expression of target genes related to cholesterol metabolism in the small intestines (Supplemental Figure 4B). However, treatment of macrophages with GSO-494 *in vitro* resulted in a significant increase of cholesterol efflux towards HDL, compared to GSO-control treated cells (GSO-control: $8.1 \pm 0.6\%$ efflux; GSO-494: $10.4 \pm 0.8\%$; $P < 0.05$; Figure 4C).

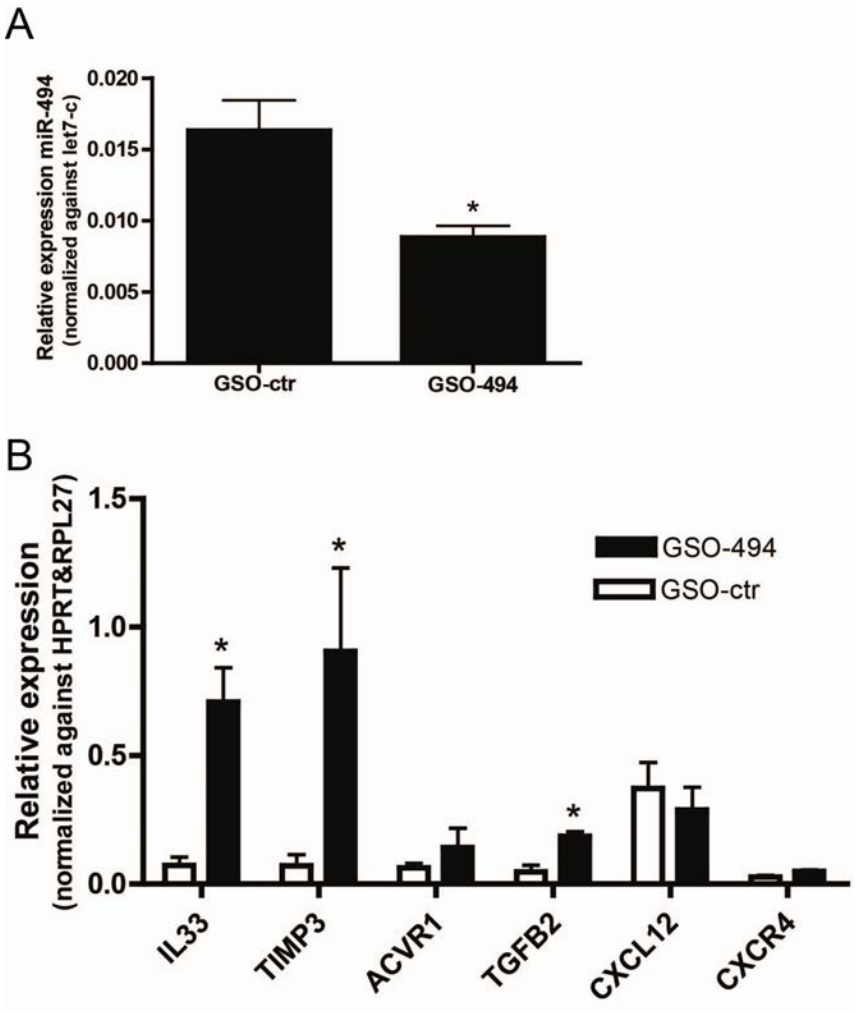


Figure 3. (A) A significant downregulation of miR-494 was observed in the carotid arteries, while the selected target genes *TIMP3*, *IL33* and *TGFB2* in the carotids were upregulated 4 days after GSO-494 treatment (B). * $P < 0.05$ compared to GSO-control (GSO-ctr).

Inhibition of miR-494 reduces atherosclerotic lesion formation

Atherosclerotic plaques were analyzed for size and composition and interestingly, HPS (hematoxylin-phloxine-saffron) stained sections revealed a marked reduction of 65% in atherosclerotic plaque size in the group treated with GSO-494 (GSO-control: $47 \pm 11 \times 10^3 \mu\text{m}^2$; GSO-494: $16 \pm 3 \times 10^3 \mu\text{m}^2$; $P < 0.05$; Figure 4D). We did not observe differences in lesion size between PBS and GSO-control treated groups (Supplemental Figure 3C), illustrating that the GSO-control did not exert aspecific effects.

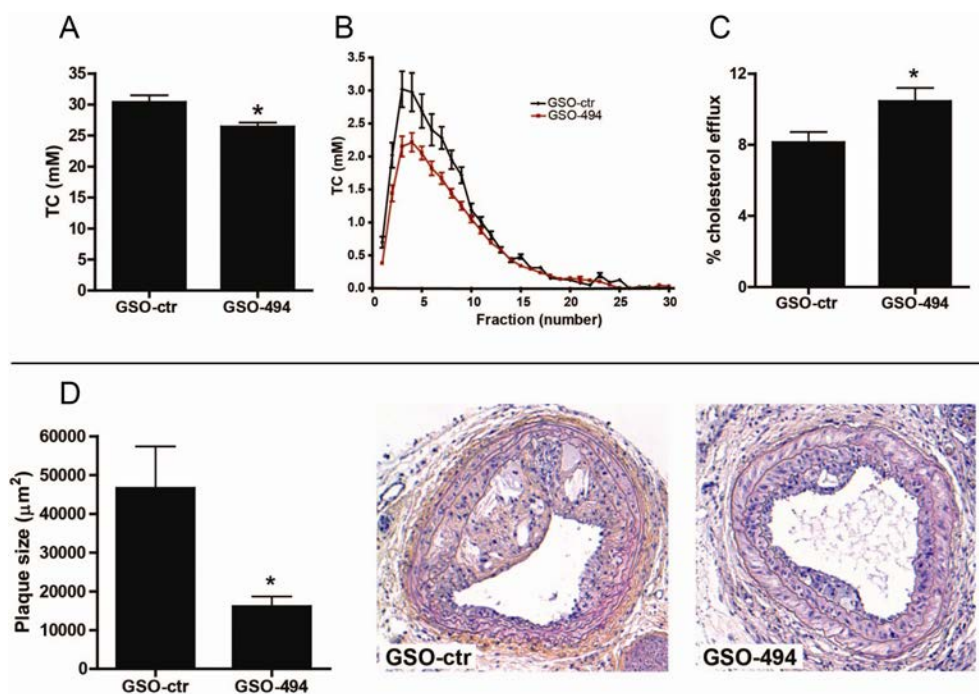


Figure 4. (A) Cholesterol levels were reduced in mice treated with GSO-494 compared to GSO-control, 6 weeks after start of the western type diet. (B) AKTA-FPLC analysis revealed a decrease in VLDL/LDL levels. (C) Cholesterol efflux towards HDL was significantly increased in macrophages treated with GSO-494 in vitro. (D) Inhibition of miR-494 by GSOs led to a significant reduction of atherosclerotic plaque formation in carotid arteries of apoE^{-/-} mice. The micrographs show representative images of both treatment groups (100x). * $P < 0.05$, compared to GSO-control (GSO-ctr).

Treatment with GSO-494 leads to an enhanced stable phenotype of atherosclerotic lesions

Atherosclerotic plaques were not only reduced in size after treatment with GSO-494; the plaques also showed an increase in plaque stability. So-called 'stable lesions' are characterized by a small necrotic core and a thick fibrous cap rich in collagen and smooth muscle cells. Indeed, necrotic core size was significantly reduced by 80% in mice treated with GSO-494 (GSO-control: $33 \pm 6\%$; GSO-494: $6 \pm 3\%$; $P < 0.001$; Figure 5A). Furthermore, collagen content was significantly

increased after inhibition of miR-494 (GSO-control: $6.6 \pm 1.6\%$; GSO-494: $12.7 \pm 2.1\%$; $P < 0.05$; Figure 5B). Taken together, the decrease in necrotic core size with concomitant increase in collagen content illustrates enhanced plaque stability. Plaque morphometry was further examined by visualizing smooth muscle cells using an alpha smooth muscle actin staining. The percentage of positively stained lesion area was similar in both treatment groups (GSO-control: $4.6 \pm 1.0\%$; GSO-494: $6.4 \pm 1.8\%$; Figure 5C); also, lesional macrophage content remained unaltered after GSO-494 treatment (GSO-control: $20.0 \pm 2.2\%$; GSO-494: $23.6 \pm 2.7\%$; Figure 5D). We stained for mast cells as well, since these have previously been described as important players in atherosclerotic plaque development and destabilization^{34,35}. However no differences were found in either mast cell numbers (GSO-control: 2.9 ± 0.6 mast cells/mm²; GSO-494: 2.2 ± 0.5 mast cells/mm²; Figure 5E) or in their activation status (data not shown).

Systemic effect of GSO treatment on white blood cell and cytokine levels

Analysis of white blood cells by Sysmex cell differentiation analysis showed a trend towards a decrease in absolute amount of lymphocytes 4 days after treatment with GSO-494 (Figure 6A). No changes were detected in the absolute numbers of neutrophils, monocyte or eosinophils (Figure 6A). We also measured the levels of various cytokines and chemokines in the blood to detect whether these would be affected, such as IL-33, RANTES, IL-5, IL-6, Gro- α , MIP2, IL27 and Eotaxin (Figure 6B). However, we did not detect any major changes after GSO treatment, suggesting that the observed reduction in atherosclerotic plaque development is not reflected by a systemic effect of the GSO-494 on plasma cytokine levels.

Inhibition of miR-494 results in altered collagen homeostasis

In order to elucidate the mechanism behind the increased amount of collagen present in the plaque, we studied both collagen synthesis and collagen degradation in an *in vitro* setup. Inhibition of miR-494 in smooth muscle cells did not result in increased collagen synthesis rate (Figure 7A).

Regarding collagen degradation, we determined TIMP expression after treatment of cultured cells with GSO-494, as TIMPs inhibit matrix degradation by MMPs. TIMP3 is a predicted target of miR-494 and indeed, the expression levels of TIMP3 were increased in mast cells (1.5 fold; $P < 0.05$) and macrophages (21 fold; $P < 0.05$) after inhibition of miR-494. We then measured the expression of MMP9, which is known to be important in plaque stability, as MMPs can degrade collagen leading to thinning of the fibrous cap. The expression levels of MMP9 remained unchanged after treatment with GSO-494, resulting in a net increase in TIMP/MMP ratio (Figure 7B). Therefore, we postulate that the increased collagen content observed in the plaque is most likely caused by a decrease in degradation rather than by increased collagen synthesis.

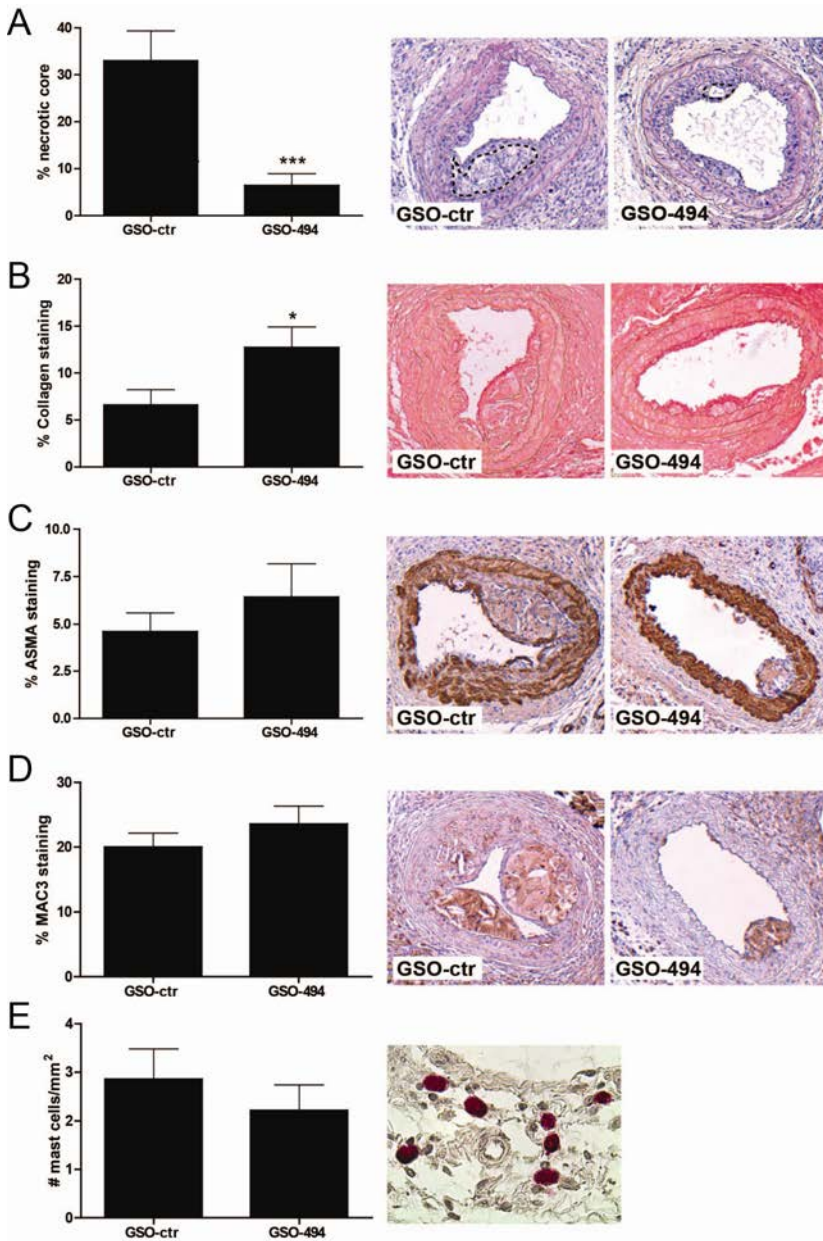


Figure 5. Effect of miR-494 inhibition on plaque morphology and lesion stability. (A) Necrotic core size was defined as an a-cellular area rich of debris and was measured as a percentage of total plaque area. Interestingly, inhibition of miR-494 led to a decrease of necrotic core size. (B) Collagen content in the lesions of mice treated with GSO-494 was increased, which is, together with the decrease in necrotic core size, suggestive of an increased stable phenotype. (C) Smooth muscle cells in the plaque were stained with aSMA while macrophages were visualized with a MAC-3 antibody (D), and no differences were found between both treatment groups. Also, the number of mast cells per mm² was not affected by GSO-494 treatment. The micrographs show representative images of both groups (100x). Bottom picture shows resting mast cells in the perivascular tissue (400X). * $P < 0.05$, *** $P < 0.001$, compared to GSO-control (GSO-ctr).

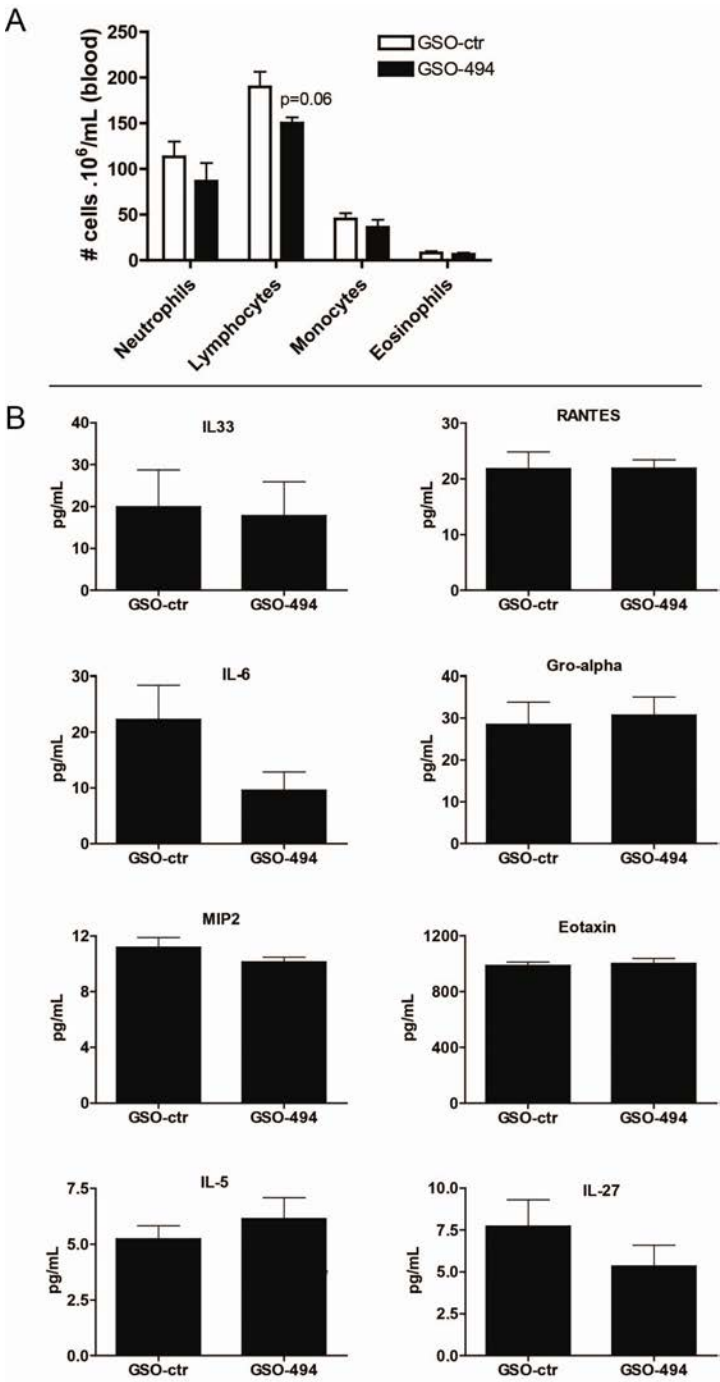


Figure 6. (A) A trend towards a decrease in absolute amount of lymphocytes 4 days after treatment with GSO-494 was observed, while the absolute numbers of neutrophils, monocyte or eosinophils remained unaltered compared to GSO-control (GSO-ctr). (B) Also, no major changes in systemic cytokine and chemokine levels were observed after GSO-494 treatment.

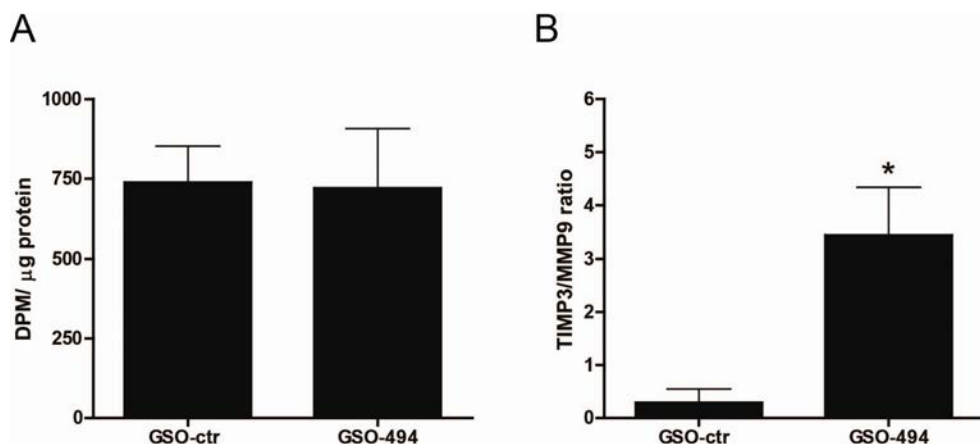


Figure 7. (A) Treatment of smooth muscle cells with GSO-494 did not result in increased collagen synthesis rate. (B) The relative expression of *TIMP3*, a predicted target gene for miR-494, was significantly increased in macrophages after GSO-494 treatment, while *MMP9* expression remained unaltered, resulting in a net increase in *TIMP-MMP* ratio. * $P < 0.05$, compared to GSO-control (GSO-ctr).

Discussion

The current study is the first to report a role for miR-494 from the 14q32 miR-gene cluster in the development of atherosclerosis. We used a unique strategy to identify miR-494, by combining knowledge from our own previous experiments and literature in an *in silico* approach. For this Reversed Target Prediction, we compiled a list of miRs, predicted to either aggravate or ameliorate atherosclerosis. As expected, many of the miRs identified by this approach have been described in literature to affect vascular inflammation. Besides recovering miRs known to be important in atherosclerosis, we were able to identify miRs that have not been investigated yet in this disease, in particular those from the 14q32 cluster. The 14q32 miR gene cluster is highly conserved in mammals and consists of 61 miR genes in mice and 54 in human³⁶. Previously it has been shown that many of the 14q32 miRs are implicated in human disease³⁷ and we here show that miR-494 is abundantly expressed in human atherosclerotic plaques, in particular in unstable lesions. Also, miR-494 was seen to be expressed in the murine vessel wall, as well as in other organs involved in the development of atherosclerosis, such as the liver and the spleen. *In vivo*, inhibition of miR-494 resulted in a marked decrease in atherosclerotic plaque formation, with increased plaque stability. Even though miR-494 was predicted to target more pro- than anti-inflammatory target genes in our RTP, the *in vivo* effects of inhibiting miR-494 revealed a positive effect on atherosclerosis. This may be explained by the fact that some atheroprotective genes, such as *TGFB2*³⁸ or *IL33*³⁹, were *in vivo* upregulated after

GSO-494 treatment. A number of studies have targeted pro-atherogenic genes in order to reduce atherosclerosis, but our data suggest that upregulation of anti-atherogenic genes may be just as, or even more, promising when treating this complex disease.

In our study, we inhibited miR-494 by means of GSOs, as was described previously²⁴. We were able to detect fluorescently labeled GSO-494 in the affected area of the carotid artery in which collars were placed, while we did not detect any fluorescence in control carotids. Moreover, uptake of labeled GSO-494 was observed in the aortic arch, which is known to contain early lesions in apoE^{-/-} mice fed a western type diet for 6 weeks. In patients, atherosclerotic lesions have developed over the years without surgical intervention such as performed in our murine collar model. These data indicate that our GSOs are indeed targeted to the atherosclerotic lesion site, which is highly relevant for future therapeutic applicability as patients that enter the clinic already have established atherosclerosis.

Reduction of cholesterol levels by statins is still the most commonly used treatment of atherosclerosis. Lowering of LDL levels after statin treatment ranges from 20% to 60%, which results in a reduction of cardiovascular events of around 30%⁴⁰. Inhibition of miR-494 reduced plasma cholesterol levels by 13%, mainly by a reduction in VLDL fractions. In order to explain these findings we isolated RNA from the liver of mice treated with GSO-494. However, we could not detect any upregulation of target genes related to lipid or cholesterol metabolism, which may be due to the fact that miR-494 expression is relatively low in the liver. Also, target gene expression in the intestines of GSO treated mice was unaltered. The difficulties to detect pronounced effects on single targets are a common challenge in miR research. As has been suggested by van Rooij *et al*⁹, it is sometimes impossible to ascribe the effects of a miR to the regulation of one or two specific mRNA targets due to a minimal increase (<1.5 fold) in the expression of these targets. The mode of action of miRs is therefore postulated to be caused by the cumulative effect of all the minor changes in target gene expression they induce. However, even though the 13% plasma cholesterol reduction almost certainly contributes, we believe that it is unlikely that the major reduction in plaque size is solely due to this relatively modest decrease. Furthermore, the observed change in plasma lipoproteins does not fully explain the prominent increase in plaque stability seen in our study. Nonetheless, we did observe a significant increase in HDL-mediated efflux *in vitro* in macrophages treated with GSO-494 compared to GSO-control, which suggests that inhibition of miR-494 increases the removal of excess cholesterol from the vessel wall to the liver via HDL, resulting in reduced atherogenesis.

Inhibition of miR-494 proved to be effective in improving atherosclerotic plaque stability as illustrated by a decrease in necrotic core size and an increase in collagen content. Since we detected no differences in smooth muscle cell content,

we looked specifically at the increased amount of collagen and hypothesized that this may be caused by increased collagen homeostasis. No changes in collagen synthesis rate were detected after treating smooth muscle cells *in vitro* with GSO-494. However, the TIMP/MMP ratio was significantly increased, indicative of decreased collagen degradation. *In vivo*, decreased collagen degradation will result in an increased thickness of the fibrous cap, thereby reducing the risk of plaque rupture with concomitant cardiovascular events.

Involvement of miR-494 has not been previously shown in atherosclerosis. However interestingly, our group has recently described a role of miR-494 in therapeutic neovascularization. For patients suffering from ischemia, such as in peripheral artery disease and after myocardial infarction, increasing blood flow to the tissues is crucial. Stimulating arterio- and angiogenesis is always accompanied by an inflammatory reaction, which often leads to an aggravation of the underlying cause of the ischemia: atherosclerosis. This so-called Janus phenomenon⁴¹ is a major drawback in this field of research, especially in translation towards the clinic. Intriguingly, our group showed that inhibition of miR-494 leads to a profound increase in blood flow after hind limb ischemia²⁴. Inhibiting miR-494 may therefore be unique in inducing neovascularization while simultaneously reducing atherosclerosis.

In conclusion, we discovered a role for miR-494 from the 14q32 miR gene cluster in atherosclerosis by utilizing the specific characteristic of miRs to regulate multiple genes and cellular processes. Inhibition of miRs-494 led to a reduction in lesion size and an increase in plaque stability. This makes miR-494 a promising new therapeutic target for patients suffering from cardiovascular disease

Acknowledgements

The authors would like to thank dr. J.F.P. Berbée and dr. G.H.M. van Puijvelde for their technical support.

Sources of funding

This study was supported by grants from the Dutch Heart Foundation (A.W.: 2010B029 and H.M.L.: 2010B244), the Netherlands Organisation for Scientific Research (A.Y.N.: Veni 916.12.041), the Leiden University Fund/Nypels- van der Zee Fund (2219/5-4-12\NZ) and the Netherlands Institute for Regenerative Medicine (S.M.J.W.: NIRM, FES0908). We acknowledge the support from the Netherlands CardioVascular Research Initiative: "the Dutch Heart Foundation, Dutch Federation of University Medical Centres, the Netherlands Organisation for Health Research and Development and the Royal Netherlands Academy of Sciences" for the GENIUS project "Generating the best evidence-based pharmaceutical targets for atherosclerosis" (CVON2011-19).

References

1. Galkina E, Ley K. Immune and inflammatory mechanisms of atherosclerosis. *Annu Rev Immunol*. 2009;27:165-97.
2. Ley K, Miller YI, Hedrick CC. Monocyte and macrophage dynamics during atherogenesis. *Arterioscler Thromb Vasc Biol*. 2011;31:1506-16.
3. Libby P. Inflammation in atherosclerosis. *Arterioscler Thromb Vasc Biol*. 2012;32:2045-51.
4. Keaney JF Jr. Immune modulation of atherosclerosis. *Circulation*. 2011;124:e559-60.
5. Virmani R, Kolodgie FD, Burke AP, Farb A, Schwartz SM. Lessons from sudden coronary death: a comprehensive morphological classification scheme for atherosclerotic lesions. *Arterioscler Thromb Vasc Biol*. 2000;20:1262-75.
6. Shah PK. Mechanisms of plaque vulnerability and rupture. *J Am Coll Cardiol*. 2003;41:15S-22S.
7. Chen K, Rajewsky N. The evolution of gene regulation by transcription factors and microRNAs. *Nat Rev Genet*. 2007;8:93-103.
8. Rajewsky N. MicroRNA target predictions in animals. *Nat Genet*. 2006;38:S8-13.
9. van Rooij E, Olson EN. MicroRNA therapeutics for cardiovascular disease: opportunities and obstacles. *Nat Rev Drug Discov*. 2012;11:860-72.
10. Rayner KJ, Esau CC, Hussain FN, et al. Inhibition of miR-33a/b in non-human primates raises plasma HDL and lowers VLDL triglycerides. *Nature*. 2011;478:404-7.
11. Sun C, Alkhoury K, Wang YI, Foster GA, Radecke CE, Tam K, Edwards CM, Facciotti MT, Armstrong EJ, Knowlton AA, Newman JW, Passerini AG, Simon SI. IRF-1 and miRNA126 modulate VCAM-1 expression in response to a high-fat meal. *Circ Res*. 2012;111:1054-64.
12. Fang Y, Davies PF. Site-specific microRNA-92a regulation of Kruppel-like factors 4 and 2 in atherosusceptible endothelium. *Arterioscler Thromb Vasc Biol*. 2012;32:979-87.
13. Alaiti MA, Orasanu G, Tugal D, Lu Y, Jain MK. Kruppel-like factors and vascular inflammation: implications for atherosclerosis. *Curr Atheroscler Rep*. 2012;14:438-49.
14. Wang YS, Wang HY, Liao YC, Tsai PC, Chen KC, Cheng HY, Lin RT, Juo SH. MicroRNA-195 regulates vascular smooth muscle cell phenotype and prevents neointimal formation. *Cardiovasc Res*. 2012;95:517-26.
15. Nazari-Jahantigh M, Wei Y, Noels H, Akhtar S, Zhou Z, Koenen RR, Heyll K, Gremse F, Kiessling F, Grommes J, Weber C, Schober A. MicroRNA-155 promotes atherosclerosis by repressing Bcl6 in macrophages. *J Clin Invest*. 2012;122:4190-202.
16. Zhu J, Chen T, Yang L, Li Z, Wong MM, Zheng X, Pan X, Zhang L, Yan H. Regulation of microRNA-155 in atherosclerotic inflammatory responses by targeting MAP3K10. *PLoS One*. 2012;7:e46551.
17. Ji R, Cheng Y, Yue J, Yang J, Liu X, Chen H, Dean DB, Zhang C. MicroRNA expression signature and antisense-mediated depletion reveal an essential role of MicroRNA in vascular neointimal lesion formation. *Circ Res*. 2007;100:1579-88.
18. Seo D, Wang T, Dressman H, Herderick EE, Iversen ES, Dong C, Vata K, Milano CA, Rigat F, Pittman J, Nevins JR, West M, Goldschmidt-Clermont PJ. Gene expression phenotypes of atherosclerosis. *Arterioscler Thromb Vasc Biol*. 2004;24:1922-7.
19. Tabibiazar R, Wagner RA, Ashley EA, King JY, Ferrara R, Spin JM, Sanan DA, Narasimhan B, Tibshirani R, Tsao PS, Efron B, Quertermous T. Signature patterns of gene expression in mouse atherosclerosis and their correlation to human coronary disease. *Physiol Genomics*. 2005;22:213-26.
20. Fu S, Zhao H, Shi J, Abzhanov A, Crawford K, Ohno-Machado L, Zhou J, Du Y, Kuo WP, Zhang J, Jiang M, Jin JG. Peripheral arterial occlusive disease: global gene expression analyses suggest a major role for immune and inflammatory responses. *BMC Genomics*. 2008;9:369.
21. Laukkanen J, Ylä-Herttua S. Genes involved in atherosclerosis. *Exp Nephrol*. 2002;10:150-63.
22. Lusis AJ. Genetics of atherosclerosis. *Trends Genet*. 2012;28:267-75.
23. Von der Thüsen JH, van Berkel TJC, Biessen EAL. Induction of rapid atherogenesis by perivascular carotid collar placement in apolipoprotein E-deficient and low-density lipoprotein receptor-deficient mice. *Circulation*. 2001;103:1164-1170.
24. Welten SM, Bastiaansen AJ, de Jong R, de Vries MR, Peters EH, Boonstra M, Sheikh SP, La Monica N, Kandimalla ER, Quax PH, Nossent AY. Inhibition of 14q32 MicroRNAs miR-329, miR-487b, miR-494 and miR-495 Increases Neovascularization and Blood Flow Recovery after Ischemia. *Circ Res*. 2014;115:696-708.
25. Nossent AY, Eskildsen TV, Andersen LB, Bie P, Brønnum H, Schneider M, Andersen DC, Welten SM,

- Jeppesen PL, Hamming JF, Hansen JL, Quax PH, Sheikh SP. The 14q32 MicroRNA-487b Targets the Antiapoptotic Insulin Receptor Substrate 1 in Hypertension-Induced Remodeling of the Aorta. *Ann Surg*. 2013;258:743-53.
26. Bhagat L, Putta MR, Wang D, Yu D, Lan T, Jiang W, Sun Z, Wang H, Tang JX, La Monica N, Kandimalla ER, Agrawal S. Novel oligonucleotides containing two 3'-ends complementary to target mRNA show optimal gene-silencing activity. *J Med Chem*. 2011;54:3027-36.
 27. Zhao Y, Pennings M, Hildebrand RB, Ye D, Calpe-Berdiel L, Out R, Kjerrulf M, Hurt-Camejo E, Groen AK, Hoekstra M, Jessup W, Chimini G, Van Berkel TJ, Van Eck M. Enhanced foam cell formation, atherosclerotic lesion development, and inflammation by combined deletion of ABCA1 and SR-BI in Bone marrow-derived cells in LDL receptor knockout mice on western-type diet. *Circ Res*. 2010;107:e20-31.
 28. Razin E, Marx G. Thrombin-induced degranulation of cultured bone marrow-derived mast cells. *J Immunol* 1984;133:3282-3285.
 29. McGookin R. RNA extraction by the guanidine thiocyanate procedure. *Methods Mol Biol*. 1985;2:113-6.
 30. Boon RA, Hergenreider E, Dimmeler S. Atheroprotective mechanisms of shear stress-regulated microRNAs. *Thromb Haemost*. 2012;108:616-20.
 31. Karagiannis GS, Weile J, Bader GD, Minta J. Integrative pathway dissection of molecular mechanisms of moxLDL-induced vascular smooth muscle phenotype transformation. *BMC Cardiovasc Disord*. 2013;13:4.
 32. Zernecke A, Bot I, Djalali-Talab Y, Shagdarsuren E, Bidzhekov K, Meiler S, Krohn R, Schober A, Sperandio M, Soehnlein O, Bornemann J, Tacke F, Biessen EA, Weber C. Protective role of CXCR4 receptor 4/CXCR4 ligand 12 unveils the importance of neutrophils in atherosclerosis. *Circ Res*. 2008;102:209-17.
 33. Bot I, Daissormont IT, Zernecke A, et al. CXCR4 blockade induces atherosclerosis by affecting neutrophil function. *J Mol Cell Cardiol*. 2014;74C:44-52.
 34. Bot I, de Jager SC, Zernecke A, Lindstedt KA, van Berkel TJ, Weber C, Biessen EA. Perivascular mast cells promote atherogenesis and induce plaque destabilization in apolipoprotein E-deficient mice. *Circulation*. 2007;115:2516-25.
 35. Willems S, Vink A, Bot I, Quax PH, de Borst GJ, de Vries JP, van de Weg SM, Moll FL, Kuiper J, Kovanen PT, de Kleijn DP, Hoefer IE, Pasterkamp G. Mast cells in human carotid atherosclerotic plaques are associated with intraplaque microvessel density and the occurrence of future cardiovascular events. *Eur Heart J*. 2013;34:3699-706.
 36. Seitz H, Royo H, Bortolin ML, Lin SP, Ferguson-Smith AC, Cavaille J. A large imprinted microRNA gene cluster at the mouse Dlk1-Gtl2 domain. *Genome Res*. 2004;14:1741-8.
 37. Benetatos L, Hatzimichael E, Londin E, Vartholomatos G, Loher P, Rigoutsos I, Briasoulis E. The microRNAs within the DLK1-DIO3 genomic region: involvement in disease pathogenesis. *Cell Mol Life Sci*. 2013;70:795-814.
 38. Mallat Z, Gojova A, Marchiol-Fournigault C, Esposito B, Kamaté C, Merval R, Fradelizi D, Tedgui A. Inhibition of transforming growth factor-beta signaling accelerates atherosclerosis and induces an unstable plaque phenotype in mice. *Circ Res*. 2001;89:930-4.
 39. Pei C, Barbour M, Fairlie-Clarke KJ, Allan D, Mu R, Jiang HR. Emerging role of interleukin-33 in autoimmune diseases. *Immunology*. 2014;141:9-17. Hoeber RC, et al. Induction of atherosclerotic plaque rupture in apolipoprotein E-/- mice after adenovirus-mediated transfer of p53. *Circulation*. 2002; 105; 2064-70.
 40. Law MR, Wald NJ, Rudnicka AR. Quantifying effect of statins on low density lipoprotein cholesterol, ischaemic heart disease, and stroke: systematic review and meta-analysis. *BMJ*. 2003;326:1423. stroke statistics--2012 update: a report from the American Heart Association. *Circulation*. 2012; 125:e220.
 41. Epstein SE, Stabile E, Kinnaird T, Lee CW, Clavijo L, Burnett MS. Janus phenomenon: the interrelated tradeoffs inherent in therapies designed to enhance collateral formation and those designed to inhibit atherogenesis. *Circulation*. 2004;109:2826-31.

Table 1A. Reversed target prediction performed by analyzing binding sites in human target genes. MiRs of the 14q32 miR gene cluster are identified with an asterisk (*).

MiR	# of putative target genes
miR-590-3p	65
miR-129-5p/129ab-5p	46
miR-186	46
*miR-495/1192	45
*miR-543	45
miR-24/24ab/24-3p	45
miR-150/5127	44
miR-340-5p	43
miR-203	42
*miR-410/344de/344b-1-3p	42
miR-326/330/330-5p	41
*miR-300/381/539-3p	41
miR-128/128ab	41
miR-149	40
miR-33ab/33-5p	40
miR-181abcd/4262	39
*miR-539/539-5p	39
*miR-494	38
*miR-485-5p/1698/1703/1962	38
*miR-376c/741-5p	37
miR-204/204b/211	37
miR-290-5p/292-5p/371-5p/293	37
miR-384/384-3p	37
miR-93/93a/105/106a/291a3p/294/295/302abcde /372/373/428/519a/520be/520acd-3p/1378/1420ac	36
miR-197	36
*miR-544/544ab/544-3p	36
miR-23abc/23b-3p	35
miR-124/124ab/506	35
miR-185/882/3473/4306/4644	35
miR-874	34
miR-374ab	34
miR-17/17-5p/20ab/20b-5p/93/106ab/427/518a-3p/519d	33
miR-320abcd/4429	33
miR-214/761/3619-5p	33
*miR-134/3118	32
miR-488	32
miR-339b/339-5p/3586-5p	31
miR-15abc/16/16abc/195/322/424/497/1907	31
*miR-329/329ab/362-3p	30
miR-873	30
miR-155	30
miR-125a-5p/125b-5p/351/670/4319	30
miR-9/9ab	29
miR-199ab-5p	29
miR-27abc/27a-3p	29
miR-342-3p	29
miR-34ac/34bc-5p/449abc/449c-5p	29
miR-141/200a	28
miR-103a/107/107ab	28
miR-7/7ab	28

Table 1B. Reversed target prediction performed by analyzing binding sites in murine target genes. MiRs of the 14q32 miR gene cluster are identified with an asterisk (*).

MiR	# of putative target genes
miR-466l-3p	63
miR-694	44
miR-325-3p	43
miR-340-5p	42
miR-875-3p.m	42
*miR-410/344de/344b-1-3p	41
miR-1958	40
miR-335-3p	40
miR-5101	40
miR-677/4276	40
miR-590-3p	39
miR-692/4753-3p	39
*miR-495/1192	37
miR-326/330/330-5p	37
miR-466k/466d-5p	37
miR-181abcd/4262	37
miR-186	36
miR-669f-3p	35
*miR-494	34
*miR-300/381/539-3p	34
miR-450b-3p/3100-5p	34
miR-141/200a	34
miR-452-3p	34
miR-5110	34
miR-5113	34
miR-669m-3p	34
miR-1587/3083/4505	33
miR-1756b/1896	33
miR-33ab/33-5p	33
miR-545/3065/3065-5p	33
miR-125b-2-3p	32
miR-1941-5p	32
miR-207	32
miR-290-5p/292-5p/371-5p/293	32
miR-3057-3p	32
miR-3474	32
miR-466d/466l-5p	32
miR-488	32
miR-5112	32
*miR-543	32
miR-683	32
miR-712	32
miR-1968	31
miR-214/761/3619-5p	31
miR-297b-3p/466ade-3p/467g	31
miR-3090/4726-3p	31
miR-873	31
*miR-377	30
miR-204/204b/211	30
*miR-1906	30

Supplemental data

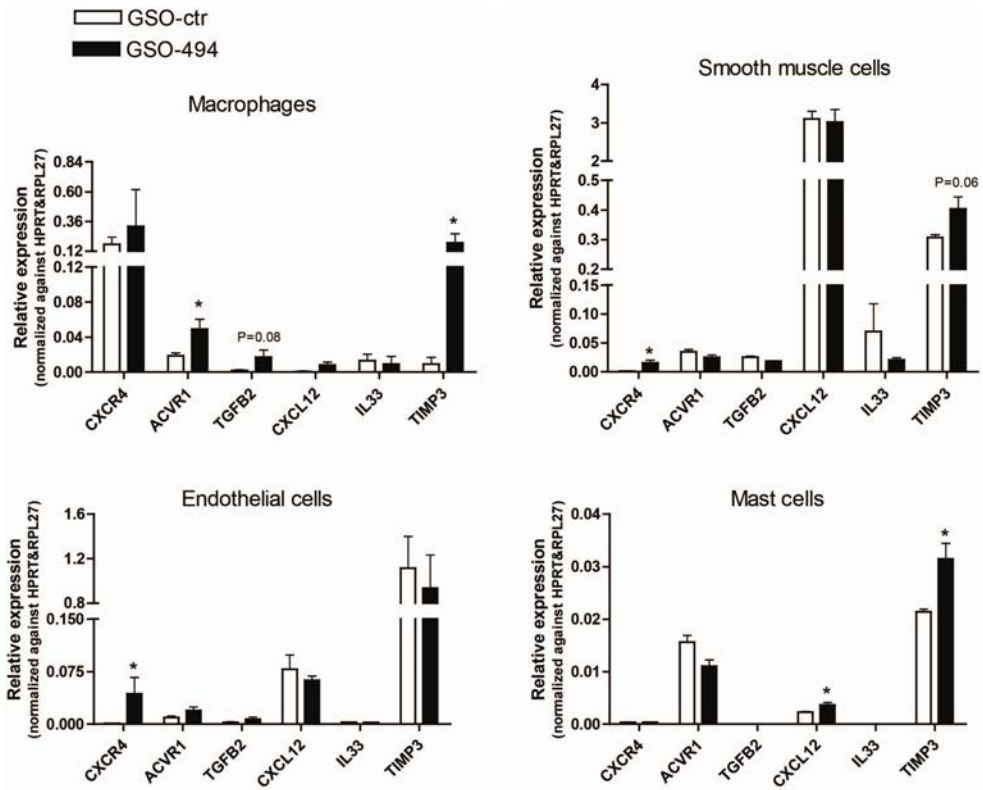
Supplemental table 1. The sequences of miRs and GSOs used for *in vitro* and *in vivo* experiments are listed.

MiR	Sequence
mmu-miR-494	5'-UGAAACAUAACACGGGAAACCUC-3'
mmu-miR-495	5'-AAACAACAUGGUGCACUUCUU-3'
mmu-miR-329	5'-AACACACCCAGCUAACCUUUUU-3'
mmu-miR-122	5'-UGGAGUGUGACAAUGGUGUUUG-3'
mmu/hsa-miR-let7c-5p	5'-UGAGGUAGUAGGUUGUAUGGUU-3'
GSO	Sequence
mmu-GSO-494	3'-ACTTTGTATGTGCCCTTTGGAG-X-GAGGTTTCCCGTGTATGTTTCA-3'
negative control GSO	3'-TGTACGACTCCATAACGGT-X-TGGCAATACCTCAGCATGT-3'

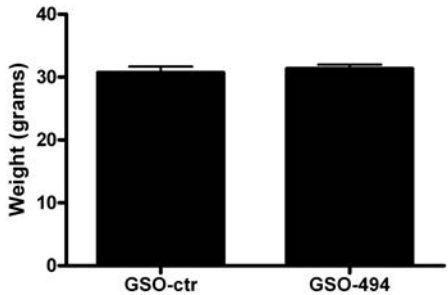
Supplemental table 2. List of all primers used for *in vitro* and *in vivo* experiments.

Gene	Forward primer	Reversed primer
CXCR4	GGTGATCCTGGTCATGGGTT	TGACAGGTGCAGCCGGTA
TIMP3	ACTGTGCAACTTTGTGGAGAGGT	GAGACACTCATTCTTGAGGTCA
CXCL12	TGCATCAGTGACGGTAAACCA	GGCTCTCGAAGAACCAGC
ADIPOR2	CATGTTTGCCACCCCTCAGTATC	AGCCAGCCTATCTGCCCTATG
TGFB2	AGACCCACATCTCCTGCTAATC	AATCAATGTAAAGAGGGCGAAGGC
LRP6	TTTGAACCCACCAACCATCGCCTGCC	GCGGTGCAAAGTGCCGGTAGCTGTA
LDLrap1	CAGCCTCACTAGCCAGCTCATC	CGAACACCTTGTCTGTGCATCTTG
LXRa	TCAGCATCTTCTCTGCAGACC	TCATTAGCATCCGTGGGAACA
SIRT1	ACCTTGAGAGCAGGTTGCAGGAATCCAA	GCACCTAGGGCACCGAGGAAGTACC
ACVR1	GGAAGTCCGCCATTGCCCATC	GGTTGTTTCCCACATCAAGCTGGT
IL33	CCAGGTGCTACTACGCTACTATGAG	AGATGTCTGTGTCTTTGATGGGACT
HPRT	TTGCTCGAGATGTCATGAAGGA	AGCAGGTCAGCAAAGAAGTATAG
RPL27	TGAAAGGTTAGCGGAAGTGC	TTTCATGAAGTTGCCCATCTC

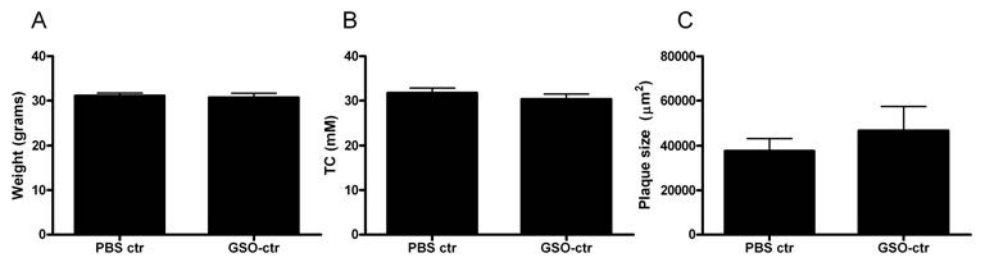
Supplemental Figure 1. *In vitro* target gene expression. Smooth muscle cells, endothelial cells, macrophages, fibroblasts and mast cells were used for *in vitro* assays in order to reflect the involvement of various cell types in atherosclerosis. Upregulation of different target genes is shown after inhibition of miR-494. * $P < 0.05$, compared to GSO-control (GSO-ctr).



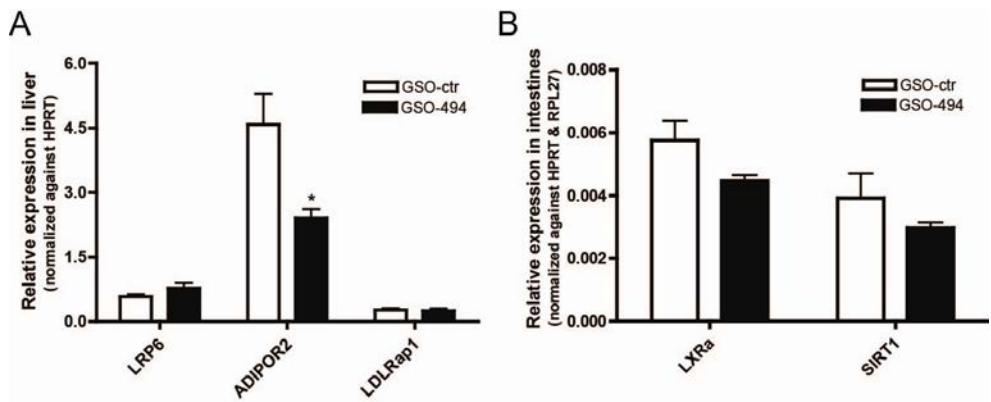
Supplemental Figure 2. No differences between GSO-494 and GSO-control (GSO-ctr) treated mice were detected in weight.



Supplemental Figure 3. No differences between PBS and GSO-control (GSO-ctr) treated mice were detected in weight (A), plasma cholesterol levels (B) or plaque size (C), indicating that GSO-ctr did not exert a-specific effects.



Supplemental Figure 4. No upregulation of target gene expression in the liver is observed 3 days after GSO-494 injection (A). Also, target genes in the intestine were not upregulated 3 days after GSO treatment (B). *P<0.05, compared to GSO-control (GSO-ctr).



Chapter 9

General summary and perspectives

Summary

The general term “cardiovascular disease” (CVD) comprises diseases of the heart and circulation, including myocardial infarction, stroke and peripheral artery disease. The major underlying cause of CVD is atherosclerosis, in which lesions develop over several decades at predisposed areas in the arterial vasculature, influenced by processes involved in cholesterol metabolism and inflammation. Advances in treatment options, including interventions such as bypass or stent placement, lifestyle changes and lipid-lowering or anti-hypertensive drugs, have contributed to a considerably improved prognosis of CVD. However, despite these developments, CVD are still among the leading causes of death worldwide¹. Therefore, investigating the underlying mechanisms of atherosclerosis is crucial to identify new therapeutic leads for the treatment of this disease, in order to prevent acute cardiovascular syndromes (ACS).

The formation of early lesions is initiated by endothelial damage and transmigration of monocytes into the vessel wall, which subsequently differentiate into macrophages and scavenge lipids, transforming them into foam cells. Atherogenesis is further aggravated by the influx and inflammatory actions of other immune cells, such as T cells and mast cells. Research has focused on the prevention of destabilization of advanced atherosclerotic plaques, since at this stage most patients present themselves at the clinic. So-called unstable lesions consist of a large lipid core, covered by a thin fibrous cap depleted of smooth muscle cells and collagen. The inflammatory cell count as well as the intraplaque density of microvessels is high, and luminal erosions may occur². Rupture of the plaque results in thrombus formation, which can lead to distal embolization with subsequent tissue ischemia. Therefore, it is promising to direct therapeutic interventions not only towards lesional growth, but also towards stabilization of the atherosclerotic plaque. Furthermore, problems arise after treatment of patients with acute cardiovascular syndromes. A surgical intervention strategy commonly used to restore blood flow to the ischemic tissue is venous bypass grafting. Unfortunately, the patency of these venous conduits is often poor due to failure of the grafts, which may be the result of intimal hyperplasia. Endothelial damage, excessive smooth muscle cell proliferation and inflammation all play a crucial role in vein graft disease (VGD)³, and more research is necessary to fully elucidate the mechanisms involved in immune responses in this disease.

In this thesis, the involvement and modulation of several components of the innate immune system were investigated in relation to both early atherosclerosis, late stage plaque destabilization and in vein graft disease. In **Chapter 2** the role of mast cell derived mediators in early atherogenesis and advanced atherosclerosis were discussed, as well as ligands capable of mast cell activation in the setting

of atherosclerosis. **Chapter 3** has demonstrated a role for the complement component C5a in the attraction and activation of mast cells in the initiation of vein graft disease. Late stage activation with C5a was seen to result in lesional vein graft disruptions independent of mast cells in **Chapter 4**. In **Chapter 5**, mast cell mediated neutrophil influx in the setting of atherosclerosis was described. Exacerbated vein graft disease accompanied by increased mast cell activation in RP105 deficient mice was observed in **Chapter 6** while the role of the monocyte and RP105 deficiency in early atherogenesis were investigated in **Chapter 7**. Finally, modulation of multiple processes involved in atherosclerosis by use of a microRNA inhibitor was studied in **Chapter 8**.

Mast cells and complement component C5a in atherosclerosis and vein graft disease

Chapter 2 provides a general overview of ligands capable of activating mast cells in the setting of atherosclerosis, as well as the diverse effects that mast cell derived mediators may exert on atherosclerosis. Interestingly, besides an important role for mast cells in atherosclerosis, mast cells were also seen to accumulate in the perivascular tissue of vein grafts during the progression of vein graft disease, as was demonstrated in **Chapter 3**. To establish whether mast cells play a causal role in vein graft disease, venous grafts were placed in mast cell deficient Kit^{W-sh/W-sh} mice and control C57BL/6 mice. Indeed, a significant decrease in vessel wall thickening was observed in mice lacking mast cells. Accordingly, local activation of perivascular mast cells with a DNP hapten resulted in aggravated lesion formation, accompanied by a decrease in the percentage of lesional smooth muscle cells and endothelial cell coverage. We then aimed to elucidate which ligand is mainly responsible for mast cell activation in the setting of vein graft disease. Previously, mast cells have been found to co-localize with C5aR in atherosclerotic plaques⁴. C5a is one of the end products of the complement system, capable of acting as a chemoattractant as well as inducing a potent inflammatory reaction. Mast cells can be activated via the C5aR and therefore we determined whether C5a may act as a mast cell activator in vein graft disease. First, we provided both mRNA and protein expression patterns of C5 and C5aR during vein graft disease. A distinct peak in C5 expression was visible 6 hours after surgery, while the expression of C5aR was maximally increased 1 day after vein graft placement. Next, we investigated the effects of local treatment with C5a at time of vein graft placement, which significantly increased the vessel wall area. In line with these findings, mice treated with the C5a receptor antagonist PMX-205 displayed reduced lesional area. Interestingly, perivascular mast cell numbers in mice treated with PMX-205 were reduced as well. Finally, to test whether C5a affects vein graft disease specifically via mast cell activation, mice were again locally treated with C5a, this time in combination with systemic injections of the mast cell stabilizer cromolyn or PBS

as a control. Intriguingly, the increase in vessel wall thickening after treatment with C5a could significantly be reduced by cromolyn treatment, indeed indicating a mast cell-dependent mechanism.

In addition to lesion formation, mast cells are known to play a crucial role in lesion destabilization. Previously, Bot *et al.* demonstrated that perivascular mast cell activation with DNP increased the frequency of intraplaque hemorrhages as well as the percentage of lesional apoptotic cells, both indicative of reduced atherosclerotic plaque stability⁵. Therefore, we aimed to determine in **Chapter 4** whether late stage exposure to C5a would increase perivascular mast cell activation with subsequent plaque rupture. Investigating plaque ruptures in murine experimental models is a major challenge, since these events do not usually occur in mice similar to the human situation. Interestingly, signs of disruptions accompanied by fibrin layers and intraplaque hemorrhage have been found in the murine vein graft lesions⁶, making this a useful model to study the underlying mechanisms of lesion disruptions. Venous grafts were placed in apoE^{-/-} mice and 24 days after surgery, when advanced plaques were formed, C5a or PBS was focally applied in a pluronic gel at the lesion site. To dissect out potential mast cell mediated effects, C5a treated mice received systemic injections with either cromolyn or PBS. Local application of C5a resulted in a profound increase in the amount of plaque disruptions, with concomitant intraplaque hemorrhage. The observed disruptions were not inhibited by cromolyn treatment, suggesting that at this late stage, C5a does not primarily exert its effects via the mast cell. The contrasting results of C5a activation in early versus advanced lesions can be explained by a difference in the number of cells present in these lesions and the plaque composition. In early lesion formation recruitment of inflammatory cells plays a dominant role, possibly via a range of mast cell derived chemokines such as CXCL2, CCL5 and CCL2. In advanced lesions, the number of immune cells present in the vessel wall is already strongly increased. Therefore, C5a itself may have more direct effects on other cell types involved in plaque stability. Indeed, we observed a dose-dependent increase in cellular apoptosis upon stimulation of both endothelial and smooth muscle cells *in vitro*. This was confirmed by increased lesional cell apoptosis in mice treated with C5a as well, which may contribute to plaque destabilization.

Mast cell mediated leukocyte recruitment

Mast cells excrete a range of mediators upon activation, and for most of these mediators a detrimental role in atherosclerosis has been established. For instance, mast cell specific proteases induce matrix degradation and smooth muscle apoptosis, leading to thinning of the fibrous cap. Basic fibroblast growth factor may increase the frequency of neovessels, while histamine and tryptase contribute to

the leakiness of these vessels. The secreted inflammatory cytokines activate other immune cells and drive the ongoing inflammatory reaction in the vessel wall. However, a definite role for mast cell derived chemokines has not been established yet in atherosclerosis. In **Chapter 5**, we thus investigated whether mast cells can actively recruit inflammatory cells to the plaque by chronic mast cell activation with IgE in μ Chain mice, which lack endogenous IgE. Interestingly, a striking increase was observed in the number of neutrophils in the intima, and in particular in the adventitia where mast cells reside. To dissect out a direct mast cell mediated effect, mast cell deficient $\text{Kit}^{\text{W-sh/W-sh}}$ mice and control mice received intraperitoneal injections with the mast cell activator compound 48/80. No differences were observed in the recruitment of monocyte or lymphocyte populations, however, a profound influx of neutrophils was observed in the control mice, which was absent in mice lacking mast cells. Also, *in vitro* migration of neutrophils was significantly increased after addition of supernatant from activated mast cells to a transwell setup. Thus, these data suggest that mast cell mediated neutrophil influx may be a novel mechanism via which the mast cell can aggravate the ongoing inflammatory process in the setting of atherosclerosis.

Regulatory actions of RP105 in vein graft disease and atherosclerosis

Toll-like receptor 4 is capable of inducing powerful inflammatory signalling; and its detrimental role in atherosclerosis and vein graft disease has previously been established^{7,8}. As with many components of the immune system, excessive activation is prevented by the presence of inhibitory molecules to avoid unnecessary tissue damage. In the case of TLR4, inflammatory signalling in macrophages and dendritic cells is inhibited by the accessory molecule RP105 through a direct extra-cellular interaction. However, RP105 seems to exert a completely different effect on the B cell, leading to its activation rather than inhibition. These dichotomous actions make RP105 a difficult, but even more so an interesting molecule to study. In **Chapter 6** vein grafts were placed in RP105 deficient mice, and we hypothesized that lesion formation would be aggravated due to increased TLR4 signalling. Indeed, vessel wall thickening was markedly increased in mice that lack RP105, moreover, an increased number of plaque disruptions was observed. These findings are in line with a previous study performed by our group, in which damage-induced neointima formation was exacerbated in $\text{RP105}^{-/-}$ mice⁹. As vein graft disease is often accompanied by superimposed atherosclerosis, we also investigated how RP105 affects vein graft disease in a hypercholesterolemic setting. In $\text{LDLR}^{-/-}$ mice fed a western type diet, RP105 deficiency resulted in a less stable plaque phenotype of the vein grafts. Further *in vitro* investigations demonstrated excessive CCL2 secretion by $\text{RP105}^{-/-}$ smooth muscle cells, also, the activation status as well as the proliferative capacity of $\text{RP105}^{-/-}$ mast cells was markedly increased. The observed effects on vein graft lesions may therefore

at least partly be explained by aggravated mast cell activation, which is in line with the findings in chapter 3, where we established that perivascular mast cell activation exacerbates vein graft disease.

Previously, we have shown that transfer of RP105^{-/-} bone marrow into control mice results in a reduction of atherosclerotic lesion formation¹⁰. This was in fact an unexpected finding, taking into consideration the above described effects of RP105 deficiency on vein graft disease and damage-induced neointima formation. The beneficial effects on atherosclerosis were suggested to be caused by alterations in B cells, in particular due to a decrease in activated B2 cells. Since in this study only myeloid cells lacked RP105, we investigated the effect of total body RP105 deficiency on atherosclerosis in **Chapter 7**. Atherosclerotic lesions induced by carotid collars were decreased in RP105 deficient mice compared to control; moreover, lesional macrophage content was significantly reduced. We aimed to further elucidate the mechanisms behind the decrease in macrophages by investigation of the migratory capacity of the monocyte in these mice. Intriguingly, monocyte recruitment to the peritoneum was impaired in RP105^{-/-} mice compared to control mice. *In vitro*, downregulation of the chemokine receptor CCR2 was observed after stimulating monocytes with LPS, which was more profound in monocytes lacking RP105. Therefore, the decreased monocyte recruitment may be caused by exaggerated CCR2 downregulation, possibly contributing to the reduction in lesional macrophages.

Modulating multiple processes involved in atherosclerosis via microRNA inhibition

MicroRNAs (miRs) are short, non-coding RNA strands capable of regulating the expression of multiple genes. It is this specific ability that makes them suitable targets for the treatment of complex diseases involving various processes, such as atherosclerosis. In order to identify miRs that may have a major impact on atherosclerosis, we made use of a unique Reversed Target Prediction in **Chapter 8**. Instead of taking a miR that is differentially expressed in atherosclerosis, we took 164 atherosclerosis-related genes as a starting point. Next, we determined the number of miRs with predicted binding sites for these genes, and counted them manually. We found enrichment of binding sites for multiple miRs from the 14q32 miR gene cluster (chromosome 12Fl in mice). From this cluster, miR-494 was seen to be abundantly expressed in human atherosclerotic plaques, as well as in murine organs involved in the development of atherosclerosis. Therefore, we selected miR-494 for further investigations. To investigate the effect of miR-494 on atherosclerosis, we placed collars in apoE^{-/-} mice fed a western type diet and inhibited miR-494 in these mice by means of gene silencing oligonucleotides (GSOs). Effective uptake of GSOs in the affected areas of the arteries was confirmed using fluorescently labeled GSOs. Interestingly, we observed a marked decrease of lesion formation in mice treated with GSO-494; moreover, lesions

were more stable, as measured by increased collagen content and a reduction of the necrotic core area. Although we were unable to confirm de-repression of some of the target genes, we detected *in vivo* upregulation of a number of the predicted target genes, such as TIMP3, TGFB2, and IL33, in the atherosclerotic plaque. This is in fact a common challenge in miR research; and as van Rooij *et al*¹¹ has previously postulated, it is often impossible to attribute the effects of a miR to the regulation of a few specific mRNA targets due to the minor increase in the expression of these targets. Therefore, the mode of action via which miRs are suggested to act is more likely caused by the accumulation of all delicate changes induced in the expression of their target genes.

Future perspectives

In this thesis, modulation of different components from the innate immune system in atherosclerosis and vein graft disease has been investigated. Our data provide new mechanistic insights, as well as possible therapeutic targets for the treatment of cardiovascular diseases. We have shown that mast cell activation, mediated by C5a, aggravates vein graft lesion development. Also, we demonstrated that mast cell mediated neutrophil influx may aggravate atherosclerosis. These data add to an increasing amount of evidence towards a detrimental role for mast cells in vascular remodelling. As of yet, limited clinical trials in humans with cardiovascular disease have been performed using mast cell stabilizers. The PRESTO trial investigated the use of the anti-allergic drug Tranilast in 10.000 patients undergoing percutaneous coronary intervention¹². A 9-month follow-up period did not show any effect on major adverse cardiovascular events or restenosis. However, since Tranilast exerts effects on fibroblasts and endothelial cells as well, it is difficult to draw any conclusions regarding mast cell specificity. Recently, a patent for the use of mast cell stabilizers in the treatment and prevention of cardiovascular disease has been published (US8445437 B2)¹³. Thus in the near future, research directed at mast cell stabilization in patients with cardiovascular disease may deliver promising results. It should be noted however that mast cells do not only exert harmful effects. Mast cells are of importance in for example wound healing and they play a vital role as sentinels in our bodies, acting as a first line of defense against bacterial and parasite infections. Therefore, care must be taken with complete systemic mast cell inhibition and unwanted side-effects such as infections should be tightly monitored.

Instead of complete mast cell stabilization, a different approach may also be used, for instance via the inhibition of a specific ligand responsible for one route of mast cell activation in the setting of atherosclerosis. One of these ligands which may be advantageous for drug targeting is complement factor C5a. Our

research has demonstrated adverse effects for C5a mediated mast cell activation on vein graft lesion development. Moreover, we have demonstrated that C5a itself has direct effects on late stage lesional disruptions, indeed making C5a a promising therapeutic target. Previous studies have reported increased serum levels of C5a in patients with CVD¹⁴; also, high C5a serum levels directly before stent placement have been correlated with increased in-stent restenosis¹⁵. The therapeutic potential in cardiovascular disease of a C5 inhibitor, the monoclonal antibody Pexelizumab, has already been tested in phase III trials. For instance, patients undergoing coronary artery bypass surgery and reperfusion therapy for myocardial infarction have received treatment with Pexelizumab. Interestingly, a systemic meta-analysis pointed out that Pexelizumab was associated with a 26% reduction in risk of death after coronary artery bypass surgery¹⁶. Taken together, these data indicate that C5a may be a promising therapeutic target in the treatment of cardiovascular disease.

With regard to the accessory protein RP105, we have made some progress in unraveling the mechanisms behind the regulatory effects of RP105 on inflammation and vascular remodelling. We demonstrated that RP105^{-/-} mice develop exacerbated vessel wall thickening and lesion disruptions in an experimental vein graft model. This is in accordance with a previous report by our group, which showed that neointima formation is increased in RP105^{-/-} mice, while overexpression of the RP105-MD1 complex resulted in reduced neointima formation⁹. These data would suggest that RP105 can be used to develop a novel therapeutic strategy to inhibit neointima formation and vein graft disease. However, in this thesis we have also established that deficiency of RP105 decreases atherosclerosis by reducing monocyte influx. It is therefore of high importance to be aware of differences in pathophysiology underlying atherosclerosis versus neointima formation and vein graft disease. In the latter two cases, smooth muscle cell migration and proliferation plays a more predominant role. Smooth muscle cells lacking RP105 display an increased proliferation rate; also, they excrete increased levels of CCL2, thereby aggravating the disease process. In atherosclerosis, monocyte influx is a crucial step in the initiation of the lesion and defects in monocyte recruitment, as observed in RP105^{-/-} mice, may thus attenuate atherosclerosis. In addition, it has also been shown by our group that RP105 deficiency alters B cell activation and proliferation, which may also reduce atherosclerotic lesion formation¹⁰. These contrasting data on vein graft disease and neointima formation versus atherosclerosis make it difficult to conclude on the therapeutic potential of RP105. After all, venous grafts and stents are most often placed in patients suffering from atherosclerosis; and improving one disease process while aggravating the other would not be a desirable treatment option. In conclusion, additional research

into RP105 is necessary to establish its therapeutic potential. For instance, vein grafts are particularly accessible for local or even *ex-vivo* treatment. Site-specific RP105 overexpression may thus attenuate vein graft disease without affecting atherosclerosis elsewhere in the arterial vasculature.

MiRs have a unique ability to regulate the expression of multiple genes; and in this thesis, we have aimed to utilize this particular characteristic in order to single out a miR that may exert a broad effect on atherosclerosis. The profound effects on lesion formation and stability after miR-494 inhibition in our study indicates that miRs indeed may serve as an interesting drug target. Only one miR drug, a miR-122 inhibitor (SPC3649), has been used in clinical studies yet for the treatment of hepatitis C¹⁷. Technical challenges with miR inhibition usually involve delivery, stability and trying to avoid eliciting an immune response. For our studies, we made use of GSOs, which have a modified phosphorothioate backbone to improve stability and linked 5'ends in order to prevent TLR-mediated immune activation. However, additional pre-clinical evaluations of GSOs are required to further investigate their exact mode of action, the time-frame of their inhibitory effects and possible off-target effects. This holds true for the miR we inhibited in our study as well: miR-494. Since we aimed to exert broad effects on atherosclerosis, it is important to exclude the possibility of side-effects. Furthermore, to ensure clinical relevance, it would be interesting to investigate if we could induce plaque regression by inhibiting miR-494. Taken together, miR research is a promising, fast-developing field; and additional studies will have to point out whether their inhibition in patients with cardiovascular disease is a feasible treatment option.

In conclusion, this thesis provides novel insight into the inflammatory and regulatory mechanisms of multiple components from the innate immune system. Furthermore, experimental studies have identified potential therapeutic targets in the setting of atherosclerosis and vein graft disease.

References

1. World Health Organization. The leading causes of death in the world 2012. Fact sheet N°310.
2. Shah, P. K. Mechanisms of plaque vulnerability and rupture. *J. Am. Coll. Cardiol.* 2003;41:15S–22S.
3. Kim, F. Y., Marhefka, G., Ruggiero, N. J., Adams, S. & Whellan, D. J. Saphenous vein graft disease: review of pathophysiology, prevention, and treatment. *Cardiol. Rev.* 2013;21:101–109.
4. Oksjoki R, Laine P, Helske S, Vehmaan-Kreula P, Mäyränpää MI, Gasque P, Kovanen PT, Pentikäinen MO. Receptors for the anaphylatoxins C3a and C5a are expressed in human atherosclerotic coronary plaques. *Atherosclerosis.* 2007;195:90-9.
5. Bot, I. *et al.* Perivascular mast cells promote atherogenesis and induce plaque destabilization in apolipoprotein E-deficient mice. *Circulation* 2007;115:2516–2525.
6. De Vries, M. R. *et al.* Plaque rupture complications in murine atherosclerotic vein grafts can be prevented by TIMP-1 overexpression. *PLoS One* 2012;7:e47134.
7. Lu Z, Zhang X, Li Y, Jin J, Huang Y. TLR4 antagonist reduces early-stage atherosclerosis in diabetic apolipoprotein E-deficient mice. *J Endocrinol* 2013;216:61-71

8. Karper JC, de Vries MR, van den Brand BT, et al. Toll-like receptor 4 is involved in human and mouse vein graft remodeling, and local gene silencing reduces vein graft disease in hypercholesterolemic APOE*3Leiden mice. *Arterioscler Thromb Vasc Biol.* 2011;31:1033-40.
9. Karper JC, Ewing MM, de Vries MR, et al. TLR accessory molecule RP105 (CD180) is involved in post-interventional vascular remodeling and soluble RP105 modulates neointima formation. *PLoS One.* 2013;8:e67923.
10. Karper JC, de Jager SC, Ewing MM, de Vries MR, Bot I, van Santbrink PJ, Redeker A, Mallat Z, Binder CJ, Arens R, Jukema JW, Kuiper J, Quax PH. An unexpected intriguing effect of Toll-like receptor regulator RP105 (CD180) on atherosclerosis formation with alterations on B-cell activation. *Arterioscler Thromb Vasc Biol* 2013;33:2810-7.
11. van Rooij E, Olson EN. MicroRNA therapeutics for cardiovascular disease: opportunities and obstacles. *Nat Rev Drug Discov.* 2012;11:860-72.
12. Holmes DR Jr, Savage M, LaBlanche JM, Grip L, Serruys PW, Fitzgerald P, Fischman D, Goldberg S, Brinker JA, Zeiher AM, Shapiro LM, Willerson J, Davis BR, Ferguson JJ, Popma J, King SB 3rd, Lincoff AM, Tcheng JE, Chan R, Granett JR, Poland M. Results of Prevention of REStenosis with Tranilast and its Outcomes (PRESTO) trial. *Circulation.* 2002;106:1243-50.
13. Guo-ping, Shi. 2013. Treatment and prevention of cardiovascular disease using mast cell stabilizers. U.S. patent 8445437 B2, filed July 24, 2007, and issued May 21, 2013
14. Speidl WS, Exner M, Amighi J, et al. Complement component C5a predicts future cardiovascular events in patients with advanced atherosclerosis. *Eur Heart J.* 2005;26:2294-9
15. Speidl WS, Katsaros KM, Kastl SP, et al. Coronary late lumen loss of drug eluting stents is associated with increased serum levels of the complement components C3a and C5a. *Atherosclerosis.* 2010; 208:285-9.
16. Testa L, Van Gaal WJ, Bhindi R, Biondi-Zoccai GG, Abbate A, Agostoni P, Porto I, Andreotti F, Crea F, Banning AP. Pexelizumab in ischemic heart disease: a systematic review and meta-analysis on 15,196 patients. *J Thorac Cardiovasc Surg.* 2008;136:884-93.
17. Nana-Sinkam SP, Croce CM. Clinical applications for microRNAs in cancer. *Clin Pharmacol Ther.* 2013;93:98-104.

Nederlandse samenvatting

Introductie

De algemene term 'hart- en vaatziekten' omvat aandoeningen aan het hart en het bloedvatenstelsel, waaronder een myocard infarct (hartaanval), cerebro vasculaire aandoeningen (CVA, beroerte) of perifere vaatlijden ('etalegebeneden'). De meest voorkomende oorzaak van hart- en vaatziekten is de ontwikkeling van atherosclerose in de vaatwand, ook wel aderverkalking genoemd. Atherosclerose is een chronisch ziekteproces waarin zich afzettingen, bestaande uit cholesterol en ontstekingscellen, in de vaatwand van slagaders vormen, de zogeheten 'atherosclerotische plaques'. Dit ontstaat al bij jongvolwassenen rond de leeftijd van 20 tot 30 jaar, vaak zonder dat hiervan klinische effecten waarneembaar zijn. De vroege plaques vormen zich doordat op bepaalde plaatsen in het vaatstelsel, voornamelijk bij aftakkingen, de bloedstroom verstoord aanwezig is. Dit kan in combinatie met risicofactoren als roken, erfelijke belasting, een hoog cholesterol gehalte of een verhoogde bloeddruk, leiden tot beschadigingen of activatie van endotheelcellen die de binnenkant van het bloedvat bekleeden. Circulerende monocytten, cellen die behoren tot ons immuunsysteem, reageren op de veranderingen in de endotheelcellen en migreren tussen deze cellen door de wand van het bloedvat in. Daar transformeren monocytten tot macrofagen, die gemodificeerd cholesterol in de vaatwand op kunnen nemen. Vervolgens veranderen de macrofagen in 'schuimcellen', welke het begin vormen van de vroege atherosclerotische 'fatty streaks'. De fatty streaks kunnen in de tijd weer verdwijnen, maar ze kunnen zich ook verder ontwikkelen tot vergevorderde atherosclerotische plaques.

In een vergevorderd stadium van atherosclerose gaat een deel van de schuimcellen in de vaatwand dood; waardoor een 'necrotische kern' bestaande uit celresten en cholesterol ontstaat. Over deze necrotische kern heen ligt een fibreus kapsel van gladde spiercellen en bindweefsel. Een hoog percentage ontstekingscellen, ingroei van nieuwe bloedvaatjes, een grote necrotische kern en een dun fibreus kapsel zijn belangrijke kenmerken van een instabiele atherosclerotische plaque. Ruptuur van een instabiele plaque zorgt ervoor dat de necrotische kern wordt blootgesteld aan het stromende bloed, wat onmiddellijk resulteert in de vorming van een bloedstolsel. Dit bloedstolsel kan verderop in het vaatbed een bloedvat verstoppen, met als mogelijk gevolg een hartaanval of een herseninfarct. Stabiele atherosclerotische plaques hoeven niet per definitie klinische symptomen te geven. Indien de slagader niet dusdanig vernauwd is dat de bloedstroom er door wordt verminderd, kunnen patiënten zonder klachten door leven. Voor therapeutische opties is het daarom van belang om niet alleen de groei van een atherosclerotische plaque te remmen, maar om ook de verandering van stabiele plaque naar onstabiele plaque, zogeheten destabilisatie, te voorkomen. Huidige therapieën bestaan bijvoorbeeld uit gebruik van cholesterol- of bloeddrukverlagende

medicijnen, interventies zoals dotteren of het plaatsen van een stent of bypass, of uit leefstijl veranderingen zoals stoppen met roken. Ondanks verbeteringen in deze behandelmethodes sterft nog steeds 1 op de 4 Nederlanders aan hart- en vaatziekten. Daarom is het van groot belang om de onderliggende mechanismen van het atherosclerotische proces te onderzoeken, zodat aangrijpingspunten voor nieuwe therapieën kunnen worden geïdentificeerd.

Eén van de mogelijke behandelopties bij vernauwing van een slagader is een bypass operatie: het plaatsen van een omleiding met behulp van een vaatsegment. Helaas zijn de lange termijn resultaten hiervan niet altijd positief ten gevolge van 'vein graft disease' of intimale hyperplasie. Vein graft disease kan acuut ontstaan door trombose of op lange termijn door vernauwing van het vaatsegment. De vernauwing wordt veroorzaakt door overmatige ingroei van gladde spiercellen gepaard met instroom van ontstekingscellen, vaak in combinatie met versnelde atherosclerose.

In zowel atherosclerose als vein graft disease speelt ons immuunsysteem een belangrijke rol. Het immuunsysteem wordt over het algemeen ingedeeld in het aspecifieke (aangeboren) afweersysteem en het adaptieve (verworven) afweersysteem. Onder andere monocyten, macrofagen, neutrofielen en mestcellen behoren tot het aangeboren afweersysteem en deze cellen functioneren als primaire verdedigingslinie tegen infecties. In dit proefschrift zijn verschillende componenten van het aspecifieke immuunsysteem onderzocht in relatie tot de ontwikkeling van vroege atherosclerotische plaques en vergevorderde stabiele versus instabiele plaques. Daarnaast is ook onderzoek gedaan naar de rol van bepaalde immuuncellen in het ontstaan van vein graft disease.

Mestcellen en complement component C5a in atherosclerose en vein graft disease.

Mestcellen zijn robuuste ontstekingscellen die voornamelijk bekend staan om hun rol in afweer tegen parasieten en in ziektebeelden als astma en allergieën. Ongeveer tien jaar geleden is echter bekend geworden dat mestcellen ook nadelige effecten kunnen uitoefenen op atherosclerose. Mestcellen zitten vol met granules, welke een scala aan ontstekingsfactoren bevatten. Zodra mestcellen worden geactiveerd door een ligand scheiden ze acuut deze granules uit in het omliggende weefsel. **Hoofdstuk 2** geeft een algemeen overzicht van mogelijke liganden die mestcellen kunnen activeren gedurende de ontwikkeling van atherosclerose en van de effecten van de verschillende ontstekingsfactoren uitgescheiden door mestcellen op zowel vroege als late atherosclerotische plaques. Naast een belangrijke rol in atherosclerose hebben we ook een toename van het aantal mestcellen waargenomen in het weefsel dat de vein grafts omringt, wat beschreven is in **Hoofdstuk 3**. Om vast te stellen of mestcellen daadwerkelijk een oorzakelijke rol spelen in vein graft disease hebben we veneuze grafts geplaatst in Kit^{W-sh/W-sh}

muizen: dit zijn muizen die door een mutatie geen mestcellen hebben. In deze muizen hebben we een significante afname van vaatwanddikte van de vein grafts waargenomen vergeleken met controle muizen. Tevens zijn, in een aparte groep muizen, de lokale mestcellen die vein grafts omringen geactiveerd met een algemene mestcel activator. Dit resulteerde in een sterk toegenomen vaatwanddikte, een lager percentage gladde spiercellen en minder bedekking van endotheelcellen. Vervolgens hebben we onderzocht welk ligand belangrijk is voor mestcel activatie gedurende de ontwikkeling van intinale hyperplasie na een bypass operatie. C5a is een onderdeel van het complement systeem, dat bestaat uit een groep factoren aanwezig in het bloed die sterk betrokken zijn bij de activatie van immuuncellen. Het is eerder aangetoond dat C5a mestcellen kan aantrekken naar de plek van ontsteking en dat mestcellen geactiveerd kunnen worden door C5a via de receptor C5aR. Eerst hebben we in weefsel van vein grafts gekeken naar de expressie van C5 en C5aR, welke beiden toenemen na respectievelijk 6 uur en 1 dag na plaatsing van de vein graft. Vervolgens hebben we de muizen met C5a behandeld, waarna de vaatwanddikte van de vein grafts sterk toenam. In overeenstemming met deze bevindingen, resulteerde remming van de C5a receptor in verminderde vaatwanddikte van de vein grafts. Om tot slot te onderzoeken of C5a zijn effecten daadwerkelijk direct via de mestcel uitoefent, hebben we muizen lokaal behandeld met C5a, in combinatie met de mestcel remmer cromolyn. De toegenomen vaatwanddikte na C5a behandeling kon inderdaad significant geremd worden met cromolyn, wat wijst op een mestcel afhankelijk mechanisme.

Het is eerder aangetoond dat mestcellen, naast het ontstaan van plaques, ook destabilisatie en bloedingen in de plaques beïnvloeden. Daarom hebben we in **Hoofdstuk 4** onderzocht of toediening van C5a aan muizen met bestaande plaques zou leiden tot acute mestcel activatie met als gevolg plaque ruptuur. Het onderzoeken van plaque ruptuur in muizen is uitdagend, omdat dit van nature niet voorkomt in muizen. Het voordeel van het vein graft model waar wij gebruik van maken, is dat hier wel plaquerupturen waargenomen kunnen worden, met aanwezigheid van fibrine en rode bloedcellen in de vaatwand. Daarom hebben wij voor dit experiment eerst veneuze grafts geplaatst in muizen, en vervolgens 24 dagen gewacht tot er vergevorderde plaques waren ontstaan. Op dat moment is C5a lokaal toegediend, in combinatie met cromolyn. Lokale behandeling met C5a resulteerde in een sterk toegenomen aantal plaque rupturen, wat niet geremd kon worden met cromolyn. In een laat stadium heeft C5a dus ook sterke, directe effecten op andere cellen in de vaatwand die belangrijk zijn voor de stabiliteit van de plaque, naast de mestcel. Om te onderzoeken welke cellen belangrijk zijn in plaque ruptuur veroorzaakt door C5a, hebben we *in vitro* gladde spiercellen en endotheelcellen behandeld met C5a. Beide celtypen lieten een dosisafhankelijke toename van celdood zien na toediening van C5a. Ook in de vaatwand hebben

we meer celdood geobserveerd in muizen behandeld met C5a, wat waarschijnlijk geleid heeft tot de toename in het aantal plaque rupturen.

Rekrutering van witte bloedcellen door geactiveerde mestcellen

Na activatie scheiden mestcellen een scala aan ontstekingsmediatoren uit, waarvan voor het grootste deel bekend is wat hun nadelige effect is op atherosclerose. Zo kunnen bepaalde enzymen uitgescheiden door de mestcel zorgen voor afbraak van bindweefsel, wat ervoor zorgt dat het fibreuze kapsel dunner wordt. Ook scheiden mestcellen groeifactoren uit die zorgen voor ingroei van nieuwe vaatjes in de plaque, en inflammatoire 'cytokines' die de ontstekingsreactie verergeren. Een definitieve rol voor chemokinen uitgescheiden door de mestcel is echter nog niet vastgesteld in atherosclerose. Chemokinen zijn moleculen die een gerichte migratie van witte bloedcellen naar de plek van ontsteking kunnen induceren, en mede daardoor spelen ze een belangrijke rol in het immuunsysteem. In **Hoofdstuk 5** hebben we daarom bepaald of chronische mestcel activatie met IgE leidt tot actieve rekrutering van ontstekingscellen naar de atherosclerotische plaque in μ MT muizen, waar endogeen IgE ontbreekt. In deze muizen vonden we een sterk toegenomen aantal neutrofielen in the plaque, en in het bijzonder in het perivascularaire weefsel: het omringende weefsel waar zich ook veel mestcellen bevinden. Om verder te bepalen of dit een mestcel specifiek effect is, hebben we mestcel deficiënte $\text{Kit}^{\text{W-sh/W-sh}}$ muizen en controle muizen geïnjecteerd met een mestcel activator in de buikholte. Geen verschillen werden gevonden in het type witte bloedcellen monocyten of lymphocyten, maar wederom werd een sterke toename gezien in de migratie van neutrofielen in de controle muizen. Neutrofiel migratie was afwezig in de mestcel deficiënte muizen, wat inderdaad wijst op een mestcel afhankelijke effect. *In vitro* hebben we nogmaals bevestigd dat geactiveerde mestcellen zorgen voor een toegenomen migratie van neutrofielen, wat kan bijdragen aan het ontstekingsproces in de atherosclerotische plaque.

Regulerende werking van RP105 in vein graft disease en atherosclerose

Toll-like receptoren zijn de primaire receptoren van het aspecifieke afweersysteem. Van Toll-like receptor 4 (TLR4) in het bijzonder is al bekend dat signalering via deze receptor een krachtige ontstekingsreactie induceert, die een verergering van atherosclerose en vein graft disease veroorzaakt. Signalering van TLR4 wordt gereguleerd door een structureel gelijkend molecuul: RP105. Op macrofagen en dendritische cellen geeft RP105 remming van TLR4 signalering, terwijl RP105 op een andere type immuuncel, de B cel, juist voor meer activatie zorgt. In **Hoofdstuk 6** hebben we veneuze grafts geplaatst in muizen die het molecuul RP105 niet hebben. Onze hypothese was dat de vaatwand sterker verdikt zou zijn in RP105 deficiënte muizen, omdat er door het ontbreken van RP105 een toegenomen signalering, en dus meer ontsteking, zou zijn van TLR4. Inderdaad, analyse van de

vein graft plaques liet een toegenomen vaatwanddikte zien, met meer plaque rupturen. En ook in RP105 deficiënte muizen op een hoog cholesterol dieet werden meer plaque rupturen gezien vergeleken met controle muizen. *In vitro* hebben we aangetoond dat gladde spiercellen die geen RP105 hebben veel meer CCL2, een belangrijk chemokine voor het aantrekken van monocytten, uitscheiden. Ook raken mestcellen die geen RP105 hebben veel sterker geactiveerd via de TLR4 route vergeleken met controle mestcellen. De toename in vein graft disease zou dus deels verklaard kunnen worden door toegenomen CCL2 secretie en verhoogde mestcel activatie, waarvan ook in hoofdstuk 3 al is aangetoond dat dit een belangrijke rol speelt in de versterkte ontwikkeling van vein graft disease.

In eerdere studies hebben we gedemonstreerd dat de transplantatie van RP105 deficiënt beenmerg leidt tot een vermindering van atherosclerose. Dit was een verrassende bevinding, gezien de effecten op vein graft disease die hierboven zijn beschreven. De gunstige effecten op atherosclerose werden deels verklaard doordat B cellen minder geactiveerd waren in de muizen die RP105 deficiënt beenmerg hadden ontvangen. Omdat in deze studie alleen RP105 in cellen afgeleid van het beenmerg ontbrak, bestudeerden we in **Hoofdstuk 7** de effecten van totale RP105 deficiëntie op atherosclerose. In overeenstemming met de vorige studie waren de atherosclerotische plaques afgenomen in muizen deficiënt voor RP105, en tevens observeerden we een afgenomen percentage macrofagen in de plaque. Om het mechanisme achter het verminderde aantal macrofagen te vinden onderzochten we de migratie capaciteit van RP105 deficiënte monocytten. Rekrutering van monocytten naar de buikholte bleek sterk verminderd te zijn in muizen deficiënt voor RP105, vergeleken met controle muizen. *In vitro* observeerden we een afname van de belangrijke chemokine receptor CCR2 na activatie van TLR4, wat veel sterker aanwezig was bij RP105 deficiënte monocytten vergeleken met controle monocytten. De verminderde monocyte rekrutering in de RP105 deficiënte muizen is dus waarschijnlijk veroorzaakt door een versterkte negatieve regulering van CCR2, dat leidt tot een afname van plaque macrofagen en minder atherosclerose.

Modulering van meerdere processen betrokken in atherosclerose via inhibitie van microRNAs

microRNAs (miRs) zijn kleine, niet-coderende RNA-strengen die de expressie van meerdere genen kunnen reguleren. Deze specifieke eigenschap maakt miRs geschikt voor de behandeling van complexe ziektes waarin veel verschillende processen betrokken zijn, zoals atherosclerose. Om miRs te identificeren die mogelijk een groot effect kunnen hebben op de ontwikkeling van atherosclerose, hebben we gebruik gemaakt van een unieke "Reversed Target Prediction" protocol in **Hoofdstuk 8**. In plaats van te kijken naar miRs die hoog tot expressie komen in

atherosclerose, hebben we 164 genen als startpunt genomen waarvan bekend is dat ze een rol spelen in atherosclerose. Vervolgens hebben we het aantal miRs bepaald met een voorspelde bindingsplaats voor deze genen, en deze miRs hebben we handmatig geteld. Voor meerdere miRs van het 14q32 miR cluster hebben we een groot aantal voorspelde atherosclerose gerelateerde targetgenen gevonden, waaronder miR-494. In humane atherosclerotische plaques vonden we een hoge expressie van miR-494, voornamelijk in instabiele plaques. We hebben daarom miR-494 geselecteerd om zijn rol in atherosclerose te onderzoeken, door middel van remming met GSOs (gene silencing oligonucleotides). Remming van miR-494 met GSOs resulteerde in een sterke afname van de atherosclerotische plaque grootte. Daarnaast was ook de stabiliteit van de plaques vergroot door een toename in collageen en een afname van de necrotische kern grootte. Van een aantal van onze voorspelde genen kon inderdaad worden vastgesteld dat hun expressie *in vivo* was toegenomen na remming van miR-494. Het was echter niet mogelijk om een toename voor alle voorspelde targetgenen vast te stellen doordat miRs vaak subtiele veranderingen tot stand brengen. De opsomming van al deze kleine veranderingen in gen expressie is wat uiteindelijk leidt tot het grote effect dat miRs uit kunnen oefenen.

In conclusie levert dit proefschrift nieuw inzicht en kennis in de onderliggende regulerende en ontsteking mechanismen van verschillende componenten van ons aspecifieke immuunsysteem. Daarnaast zijn meerdere experimentele studies uitgevoerd die potentiële therapeutische aangrijpingspunten hebben geïdentificeerd voor de behandeling van atherosclerose en vein graft disease.

Curriculum Vitae

Anouk Wezel werd geboren op 28 november 1986 in Zaanstad. In augustus 2003 is zij voor een 'exchange jaar' naar Canada gegaan, waar zij op de Edward Schreyer School (Beausejour) een Honoury Diploma heeft behaald (juni 2004). Haar VWO diploma heeft zij in 2006 behaald aan de Gemeentelijke Scholen Gemeenschap in Schagen met een 8,4 gemiddeld. Datzelfde jaar is zij Geneeskunde gaan studeren in Leiden. Tijdens haar studie was zij medewerker van het onderzoek 'A comparison of remifentanyl patient-controlled analgesia with epidural analgesia during labor' op de afdeling verloskunde van het Leids Universitair Medisch Centrum. Haar wetenschapstage van 6 maanden heeft zij onder begeleiding van dr. Jan Lindeman voltooid op de afdeling Vaatchirurgie in het LUMC. In deze periode heeft zij 2 maanden onderzoek gedaan op het Cardiovascular Pathology Laboratory (CV-Path) van dr. Renu Virmani (Gaithersburg, Maryland) in de Verenigde Staten. Januari 2011 heeft zij haar doctoraal diploma behaald. Van december 2010 tot december 2014 heeft zij haar promotieonderzoek verricht op de afdeling Biofarmacie van het Leiden Academic Centre for Drug Research en deels op de afdeling Vaatchirurgie van het LUMC, onder leiding van dr. Ilze Bot, prof. Johan Kuiper en prof. Paul Quax. Dit onderzoek maakte deel uit van een door de Nederlandse Hartstichting gefinancierd project. Zij heeft in 2011 de 2e prijs gekregen voor haar presentatie op de cursus 'Vascular Biology' van de Nederlandse Hartstichting. In 2013 heeft zij de prijs voor beste posterpresentatie gekregen op het Rembrandt Institute of Cardiovascular Science Congres, en in 2014 de prijs voor de beste posterpresentatie op het LACDR Spring Symposium. Tijdens haar promotietraject is zij twee jaar actief geweest in het bestuur van de LAP- LUMC Association for PhD candidates, die zich inzet voor de belangen van promovendi binnen het LUMC en diverse lezingen en activiteiten organiseert. In november 2014 startte zij haar co-schappen in het LUMC.

Publications

Full papers

Wezel A, van der Velden D, Maassen JM, Lagraauw HM, de Vries MR, Karper JC, Kuiper J, Bot I, Quax PH. RP105 deficiency attenuates early atherosclerosis via decreased monocyte influx in a CCR2 dependent manner. *Conditionally accepted by Atherosclerosis*.

Wezel A, Quax PH, Kuiper J, Bot I. The role of mast cells in atherosclerosis. *Hämostaseologie*, in press.

Wezel A, de Vries MR, Lagraauw HM, Foks AC, Kuiper J, Quax PH, Bot I. Complement factor C5a induces atherosclerotic plaque disruptions. *J Cell Mol Med*. 2014; 18: 2020-30

Wezel A, Welten SMJ, Razawy W, Lagraauw HM, de Vries MR, Goossens EAC, Boonstra MC, Kandimalla ER, Kuiper J, Quax PH, *Nossent AY, *Bot I. Inhibition of MicroRNA-494 Reduces Atherosclerotic Lesion Development and Increases Plaque Stability. *Submitted for publication*. (*These two authors contributed equally)

*Wezel A, *Lagraauw HM, van der Velden D, de Jager SCA, Quax PH, Kuiper J, Bot I. Mast cells mediate neutrophil recruitment during atherosclerotic plaque progression. *Submitted for publication*. (*These two authors contributed equally)

*Wezel A, *de Vries MR, Maassen HM, Kip P, Karper JC, Kuiper J, Bot I, Quax PH. RP105 deficiency aggravates vein graft disease and lesion instability via increased inflammation and mast cell activation. *Submitted for publication*. (*These two authors contributed equally)

Bastiaansen AJ, Karper JC, Wezel A, de Boer HC, Welten SM, de Jong RC, Peters EA, de Vries MR, van Oeveren-Rietdijk AM, van Zonneveld AJ, Hamming JF, Nossent AY, Quax PH. TLR4 Accessory Molecule RP105 (CD180) Regulates Monocyte-Driven Arteriogenesis in a Murine Hind Limb Ischemia Model. *PLoS One*. 2014; 9: e99882.

Lagraauw HM, Westra MM, Bot M, Wezel A, van Santbrink PJ, Pasterkamp G, Biessen EA, Kuiper J, Bot I. Vascular neuropeptide Y contributes to atherosclerotic plaque progression and perivascular mast cell activation. *Atherosclerosis*. 2014; 235: 196-203.

de Vries MR, Wezel A, Schepers A, van Santbrink PJ, Woodruff TM, Niessen HW, Hamming JF, Kuiper J, Bot I, Quax PH. Complement factor C5a as mast cell activator mediates vascular remodelling in vein graft disease. *Cardiovasc Res*. 2013;97:311-20.

Published abstracts

Bot I, Wezel A, Lagraauw HM, van der Velden D, de Jager SCA, Quax PHA, Kuiper J. Mast cell mediated neutrophil influx enhances plaque progression. *Cardiovascular Research*. 2014;103 Suppl 1:S5.

Wezel A, Welten S, Lagraauw HM, de Vries MR, Kandimalla E, Kuiper J, Quax PHA, Nossent AY, Bot I. 14q32 MicroRNA inhibition reduces atherosclerotic lesion formation, increases plaque stability and lowers cholesterol levels. *Atherosclerosis*. 2014;2:e41.

Wezel A, Welten S, Lagraauw HM, de Vries MR, Kandimalla E, Kuiper J, Quax PHA, Nossent AY, Bot I. 14q32 MicroRNA inhibition reduces atherosclerotic lesion formation, increases plaque stability and lowers cholesterol levels. *Arterioscler Thromb Vasc Biol*. 2014;34:A676.

Wezel A, Lagraauw HM, van der Velden D, de Jager SCA, Quax PHA, Kuiper J, Bot I. Mast cell-mediated neutrophil influx enhances plaque progression. *Arterioscler Thromb Vasc Biol*. 2014;34:A476.

Lagraauw HM, Westra MM, Bot M, Wezel A, van Santbrink PJ, Pasterkamp G, Biesen EAL, Kuiper J, Bot I. Vascular Neuropeptide Y expression contributes to atherosclerotic plaque progression and perivascular mast cell activation. *Arterioscler Thromb Vasc Biol*. 2014;34:A459.

Wezel A, Welten S, Lagraauw HM, de Vries MR, Kandimalla E, Kuiper J, Quax PHA, Bot I, Nossent AY. 14q32 MicroRNA Inhibition Reduces Atherosclerotic Lesion Formation, Increases Plaque Stability and Lowers Cholesterol Levels. *Circulation*. 2013;128:A14484.

de Vries MR, Wezel A, Schepers A, Kuiper J, Bot I, Quax PHA. Mast cell activation via complement factor C5a modulates vein graft remodeling and accelerated atherosclerosis. *Vascular Pharmacology*. 2012;56:372.

Wezel A, de Vries MR, Schepers A, Kuiper J, Bot I, Quax PHA. Complement factor C5a modulates vein graft remodeling and accelerated atherosclerosis via interference in mast cell activation. *Molecular Immunology*. 2011;48:1693.

de Vries MR, Wezel A, Schepers A, Kuiper J, Bot I, Quax PHA. Complement factor C5a modulates vein graft remodeling and accelerated atherosclerosis via interference in mast cell activation. *Atherosclerosis*. 2011;12:367.